CSIC

University of Granada

DOCTORAL THESIS

Doctoral Program
in Fundamental and Sistems Biology

Study of the mechanisms of iron homeostasis in the arbuscular mycorrhizal fungus *Rhizophagus irregularis*

Elisabeth María Tamayo Martínez

Granada, 2017

Editor: Universidad de Granada. Tesis Doctorales
Autora: Elisabeth María Tamayo Martínez
ISBN: 978-84-9163-524-6
URI: http://hdl.handle.net/10481/48322

University of Granada
Consejo Superior de Investigaciones Científicas

Doctoral Program in Fundamental and Sistems Biology

Study of the mechanisms of iron homeostasis in the arbuscular mycorrhizal fungus *Rhizophagus irregularis*

Elisabeth María Tamayo Martínez

DOCTORAL THESIS

Granada, 2017

University of Granada

Consejo Superior de Investigaciones Científicas

Study of the mechanisms of iron homeostasis in the arbuscular mycorrhizal fungus *Rhizophagus irregularis*

Memoria presentada por Dña. Elisabeth María Tamayo Martínez, licenciada en Biología, para optar al grado de Doctor en Ciencias Biológicas por la Universidad de Granada con mención internacional.

Memory presented to aspire to Doctor in Biology
(With mention "International Doctor")

Fdo.: **Elisabeth María Tamayo Martínez**

V° B° de la directora de la Tesis Doctoral/ ***Thesis supervisor***

Fdo.:
Dr. Nuria Ferrol González
Doctor in Chemical Sciences
Scientific Researcher in CSIC

Financiación y publicaciones

Este trabajo de Tesis Doctoral ha sido realizado en el Departamento de Microbiología del Suelo y Sistemas Simbióticos (Grupo de investigación "Micorrizas") de la Estación Experimental del Zaidín (EEZ-CSIC).

Para la realización del siguiente trabajo, la licenciada Elisabeth María Tamayo Martínez fue financiada por las siguientes fuentes:

▫ Beca predoctoral I3P del Consejo Superior de Investigaciones Científicas, disfrutada desde el 1 de Septiembre de 2010 hasta el 31 de agosto de 2014.

▫ Proyectos de Investigación del Plan Nacional AGL2009-08868 y AGL2012-35611 del Ministerio de Economía y Competitividad.

▫ Beca de movilidad I3P para estancias breves del Consejo Superior de Investigaciones Científicas, disfrutada en el Departamento de Medicina de Perelman School of Medicine (Universidad de Pennsylvania, Phyladelphia, PA, USA), bajo la supervisión del Dr. Andrew Dancis. Septiembre-Diciembre de 2012 (15 semanas).

Parte de los resultados presentados en esta Memoria de Tesis Doctoral se han publicado en revistas internacionales o están en vías de publicación:

Ferrol N, **Tamayo E**, Vargas P. 2016. The heavy metal paradox in arbuscular mycorrhiza: from mechanisms to biotechnological applications. Journal of Experimental Botany 67, 6253-6265. doi: 10.1093/jxb/erw403.

Tamayo E, Benabdellah K, Ferrol N. 2016. Characterization of three new glutaredoxin genes in the arbuscular mycorrhizal fungus *Rhizophagus irregularis*: putative role of RiGRX4 and RiGRX5 in iron homeostasis. PLoS One 11: e0149606. doi:10.1371/journal.pone.0149606

Tamayo E, Gómez-Gallego T, Azón-Aguilar C, Ferrol N. 2014.Genome-wide analysis of copper, iron and zinc transporters in the arbuscular mycorrhizal fungus *Rhizophagus irregularis*. Frontiers in Plant Science 5, 547. doi: 10.3389/fpls.2014.00547

Tamayo E, Knight SAB, Dancis A, Ferrol N. Molecular characterization of a high-affinity iron uptake system in *Rhizophagus irregularis*. (En preparación).

Tamayo E, Ferrol N. The *Rhizophagus irregularis* multicopper oxidase family: a search for proteins with potential ferroxidase activity. (En preparación).

La doctoranda / *The doctoral candidate* Elisabeth María Tamayo Martínez y la directora de tesis / *and the thesis supervisor* Nuria Ferrol González:

Garantizamos, al firmar esta tesis doctoral, que el trabajo ha sido realizado por la doctoranda bajo la dirección de la directora de la tesis y hasta donde nuestro conocimiento alcanza, en la realización del trabajo, se han respetado los derechos de otros autores a ser citados, cuando se han utilizado sus resultados o publicaciones.

/

Guarantee, by signing this doctoral thesis, that the work has been done by the doctoral candidate under the direction of the thesis supervisor and, as far as our knowledge reaches, in the performance of the work, the rights of other authors to be cited (when their results or publications have been used) have been respected.

Granada,

Directora de la Tesis / *Thesis supervisor*

Fdo.: Nuria Ferrol González

Doctoranda / *Doctoral candidate*

Fdo.: Elisabeth María Tamayo Martínez

Cover: Designed by Pablo Tamayo Martínez

A mis padres
y hermanos

Miré al cielo. Dije

un sueño espera ser soñado

(Chantal Maillard)

INDEX

ACRONYMS

AM	Arbuscular mycorrhizal
BLAST	Basic local alignment search tool
CDF	Cation diffusion facilitator
CDS	Coding DNA sequence
COPT	Copper transporter
CSM	Complete synthetic medium
DMA	Deoxymugineic acid
EDTA	Ethylenediaminetetraacetic acid
ER	Endoplasmic reticulum
ERM	Extraradical mycelium
FAD	Flavin adenine dinucleotide
FRD	Ferric reductase domain
FRE	Ferric reductase
FTR	Fe transporter
GFP	Green fluorescent protein
GRX	Glutaredoxin
GSH	Glutathione
HM	Heavy metal
IRM	Intraradical mycelium
JGI	Joint Genome Institute
LSD test	Least significant difference test
MAT locus	Mating-type locus
MCO	Multicopper oxidase

MEGA	Molecular evolutionary genetics analysis
NAD(P)H	Nicotinamide adenine dinucleotide (phosphate)
NCBI	National Center for Biotechnology Information
NJ	Neighbor-Joining
NOX	NADPH oxidase
NRAMP	Natural resistance-associated macrophage protein
OD	Optical density
OFet	Oxidase-dependent Fe^{2+} transporter
OPT	Oligopeptide transporter
PMSF	Phenylmethylsulfonyl fluoride
PolyP	Polyphosphate
PPA	Pre-penetration apparatus
PS	Phytosiderophore
RACE	Rapid amplification of cDNA ends
RIA	Reductive iron assimilation
ROS	Reactive oxygen species
RT	Reverse transcriptase
SD	Synthetic dextrose
SIT	Siderophore-iron transporter
SNP	Single nucleotide polymorphism
VIT	Vacuolar iron transporter
YPD	Yeast extract-peptone-dextrose
ZIP	Zinc-iron permease

ABSTRACT

Arbuscular mycorrhizal (AM) symbioses that involve most plants and Glomeromycota (AM) fungi are integral and functional parts of plant roots. In these associations, the fungi not only colonize the root cortex but also maintain an extensive network of hyphae that extend out of the root into the surrounding environment. These external hyphae contribute to plant uptake of low mobility nutrients, such as P, Fe and Zn. Besides improving plant mineral nutrition, AM fungi can alleviate heavy metal (HM) toxicity to their host plants. The HM Fe plays essential roles in many biological processes but is toxic when present in excess, since it can produce toxic free radicals *via* the Fenton reaction. This makes its transport and homeostatic control of particular importance to all living organisms. AM fungi play an important role in modulating plant HM acquisition in a wide range of soil metal concentrations and have been considered to be a key element in the improvement of micronutrient concentrations in crops and in the phytoremediation of polluted soils. Although the main benefit of the AM association is an improved P status of the mycorrhizal plant, AM fungi also play a role in Fe nutrition of their host plants, and direct evidence of the capability of the extraradical mycelium (ERM) to take up Fe from the soil and to transfer it to the host plant has been found. Conversely, other studies have shown that AM fungi play a role in reducing Fe uptake when the soil concentration is high. Nevertheless, little is known about the mechanisms of Fe uptake and homeostasis in arbuscular mycorrhizas.

Within this PhD thesis, several methods have been used to analyze the mechanisms of Fe homeostasis in the model AM fungus *Rhizophagus irregularis*, which is easily grown in monoxenic cultures and whose genome has been recently sequenced. Genome-wide analyses were undertaken in order to identify *R. irregularis* genes involved in Fe transport and homeostasis, by making use of transport databases, genome organism websites and *in silico* bioinformatics tools for sequence analyses, such as software for protein structure predictions and methods for phylogenetic analyses. For experimental studies, *R. irregularis* monoxenic cultures were established in order to obtain exclusively fungal material for the subsequent gene isolation, gene expression analyses or enzymatic assays. Since it is not still possible to

genetically manipulate AM fungi, functional and localization analyses of the newly identified *R. irregularis* genes were performed in a heterologous system: the budding yeast *Saccharomyces cerevisiae*.

As a first approach to get some insights into Fe homeostasis mechanisms, a genome-wide analysis of Fe transporters was performed. This *in silico* analysis allowed the identification of 12 open reading frames in the *R. irregularis* genome, which potentially encode Fe transporters involved in iron acquisition from the soil or iron use and storage in the different subcellular compartments. Phylogenetic comparisons with the genomes of a set of reference fungi showed an expansion of some Fe transporter families. Analysis of the published transcriptomic profiles of *R. irregularis* revealed that some genes were up-regulated in mycorrhizal roots compared to germinated spores and ERM, which suggests that Fe is a metal important for plant colonization. Two components of a reductive pathway of high-affinity Fe transport, *RiFTR1* and *RiFTR2*, were found to be within the full complement of genes encoding Fe transporters identified in the *R. irregularis* genome, showing high homology to the *S. cerevisiae* Fe permease Ftr1.

In the well characterized *S. cerevisiae* system, the first step of the reductive Fe assimilation system is accomplished by the metalloreductases Fre1 and Fre2. Then, the reduced ferrous Fe is rapidly taken up by a high-affinity ferrous-specific transport complex consisting of a plasma membrane multicopper ferroxidase (Fet3) that oxidizes the Fe, which is then transported to the cytosol by a permease (Ftr1). When the ferric reductase activity was assayed *in vivo* on *R. irregularis* mycelia, it was found a basal level of activity in mycelium grown in control plates, which was activated when mycelia was grown in media without Fe. These data indicated that the reductive Fe uptake system is operating in *R. irregularis*. Only one ferric reductase homolog, RiFRE1, was found in the *R. irregularis* genome, but it was not able to restore the poor growth of the *fre1-2* yeast mutant under low-Fe conditions, probably due to the low sequence homology of RiFRE1 and ScFRE1-2. Protein characterization and gene expression analyses of the two other putative components of the reductive pathway of Fe acquisition in *R. irregularis*, RiFTR1 and RiFTR2, indicated that RiFTR1 plays an *in vivo* role in high-affinity reductive Fe acquisition in Fe-limited environments. Nevertheless, the

role of RiFTR2 in *R. irregularis* has not been elucidated in our study, probably because the protein failed to exit the ER, as shown in the yeast localization assays. It was also found that the genes encoding the three components of the reductive Fe assimilation pathway identified (*RiFRE1*, *RiFTR1* and *RiFTR2*) are responsive to Fe, as shown by the gene expression analyses performed by real time RT-PCR.

In order to identify the ferroxidase partner of RiFTR1, a search for candidate genes belonging to the multicopper oxidase (MCO) family was performed. It was concluded that *R. irregularis* has at least nine MCOs (*RiMCO1-9*) in its genome. Intron and similarity analyses defined five gene subfamilies. However, a phylogenetic analysis of MCO sequences of different taxonomic groups revealed that all the RiMCOs belong to the ferroxidase/laccase group and none of them clustered with the Fet3-type ferroxidases. *RiMCO1* was the only *MCO* displaying a gene expression pattern typical of a high-affinity Fe transport component. Furthermore, RiMCO1 enables the *fet3* yeast mutant to take up Fe. These data suggest that RiMCO1 might have a role in the reductive high-affinity Fe uptake system together with the Fe transporter RiFTR1 at the ERM. However, some other member(s) of the RiMCO family could also have ferroxidase activity. Gene expression analyses also revealed that some transcripts were very abundant in the ERM (*RiMCO1* and *RiMCO5*) and others in the intraradical mycelium (*RiMCO2*), suggesting the different RiMCOs have specific functions.

Finally, as an attempt to identify some other elements involved in the regulation of Fe homeostasis in *R. irregularis*, and since the yeast glutaredoxins (GRXs) Grx3-4 and Grx5 have been shown to have a role in Fe homeostasis, the full complement of GRXs in *R. irregularis* (RiGRX1,4,5,6) was identified and characterized (RiGRX1 was previously characterized in our group). Heterologous functional analyses showed that while the four *R. irregularis* GRXs are involved in oxidative stress protection, RiGRX4 and RiGRX5 (homologues of ScGrx3-4 and ScGrx5, respectively) also play a role in Fe homeostasis in yeast. In addition, gene expression data showed that *RiGRX4* was the only *R. irregularis GRX* gene responsive to Fe, suggesting that it might be involved in Fe uptake regulation by interacting with iron-responsive transcription factors, as previously shown for its homologs in other fungi.

Increased expression of *RiGRX1* and *RiGRX6* in the intraradical mycelium suggests that these GRXs could play a key role in oxidative stress protection of *R. irregularis* during its *in planta* phase.

Despite in this PhD thesis only the fungal transporters involved in iron uptake from the soil and the glutaredoxins have been characterized, an integrating model is proposed for regulation of iron homeostasis and transport through the mycorrhizal pathway in a mycorrhizal root.

RESUMEN

Las simbiosis micorrícico arbusculares (MA) que implican a la mayoría de las plantas y los hongos Glomeromycota (MA) son partes integrales y funcionales de las raíces de las plantas. En estas asociaciones, el hongo no sólo coloniza la corteza de la raíz, sino que también mantiene una red extensa de hifas que se extienden fuera de la raíz en el entorno circundante. Estas hifas externas contribuyen a la absorción vegetal de nutrientes de baja movilidad, como P, Fe y Zn. Además de mejorar la nutrición mineral de la planta, los hongos MA alivian de la toxicidad de metales pesados a las plantas hospedadoras. El metal pesado Fe desempeña un papel esencial en muchos procesos biológicos, pero es tóxico cuando está presente en exceso, ya que puede producir radicales libres a través de la reacción de Fenton. Por ello, es de particular importancia el control de su transporte y homeostasis en todos los organismos vivientes. Los hongos MA tienen un papel importante en la modulación de la adquisición de metales pesados por la planta en un amplio rango de concentración del metal en el suelo y se han considerado un elemento clave en la mejora de las concentraciones de micronutrientes de los cultivos y en la fitorremediación de suelos contaminados. Aunque el principal beneficio de la asociación MA es una mejora en el estado del P de la planta micorrizada, los hongos MA también desempeñan una función en la nutrición de Fe de la planta hospedadora, y se han encontrado evidencias directas de la capacidad del micelio extrarradical (ERM, en inglés *extraradical mycelium*) para absorber Fe del suelo y transferirlo a la planta hospedadora. Por el contrario, otros estudios han demostrado que los hongos MA desempeñan un papel reduciendo la absorción de Fe cuando la concentración en el suelo es alta. Sin embargo, se sabe poco acerca de los mecanismos de absorción y homeostasis de Fe en micorrizas arbusculares.

En esta tesis doctoral se han utilizado varios métodos para analizar los mecanismos de homeostasis de Fe en el hongo MA modelo *Rhizophagus irregularis*, fácilmente cultivable en cultivos monoxénicos y cuyo genoma se ha secuenciado recientemente. Se han realizado análisis a genoma completo con el objeto de identificar genes de *R. irregularis* implicados en el transporte y homeostasis de Fe, haciendo uso de bases de datos de transporte, sitios web

de genomas de organismos y herramientas bioinformáticas *in silico* para análisis de secuencias, como software para predicciones de estructura proteica y métodos para análisis filogenéticos. Para los estudios experimentales, se establecieron cultivos monoxénicos de *R. irregularis* con fin de obtener material exclusivamente fúngico para el subsecuente aislamiento génico, análisis de expresión génica o ensayos enzimáticos. Dado que no es posible manipular genéticamente los hongos MA, los análisis funcionales y de localización de los genes recién identificados de *R. irregularis* se llevaron a cabo en un sistema heterólogo: la levadura de gemación *Saccharomyces cerevisiae*.

Como un primer enfoque para entender los mecanismos de homeostasis de Fe, se realizó un análisis a genoma completo de transportadores de Fe. Este análisis *in silico* permitió la identificación de 12 marcos abiertos de lectura en el genoma de *R. irregularis*, que codifican potencialmente transportadores de Fe implicados en la adquisición de hierro desde el suelo o en su uso y almacenamiento en diferentes compartimentos celulares. La comparación filogenética con los genomas de un grupo de hongos de referencia mostró una expansión de algunas familias de transportadores de Fe. El análisis de los perfiles transcriptómicos publicados de *R. irregularis* reveló que algunos genes se regularon al alza en raíces micorrizadas comparados con esporas germinadas y ERM, lo que sugirió que el Fe es un metal importante para la colonización de la planta. Dentro del complemento completo de genes que codifican transportadores de Fe identificados en el genoma de *R. irregularis* se encontraron dos componentes de una vía reductiva de transporte de Fe de alta afinidad, *RiFTR1* y *RiFTR2*, que mostraron una alta homología con la permeasa de Fe Ftr1 de *S. cerevisiae*.

En el sistema bien caracterizado de *S. cerevisiae*, el primer paso del sistema reductivo de asimilación de Fe se realiza por las metalorreductasas Fre1 y Fre2. A continuación, el Fe reducido es absorbido rápidamente por un complejo de transporte de alta afinidad específico de hierro ferroso que consiste en una ferroxidasa multicobre de membrana plasmática (Fet3) que oxida el Fe, el cual es entonces transportado al citosol por una permeasa (Ftr1). Cuando se examinó *in vivo* la actividad reductasa férrica sobre el micelio de *R. irregularis*, se encontró un nivel basal de actividad en el micelio crecido en

placas control, que fue activada cuando el micelio se cultivó en medio sin Fe. Estos datos indicaron que el sistema reductivo de absorción de Fe está funcionando en *R. irregularis*. Sólo se encontró un homólogo de reductasa férrica, RiFRE1, en el genoma de *R. irregularis*, pero no fue capaz de restaurar el pobre crecimiento del mutante de levadura *fre1-2* en condiciones de deficiencia de Fe, probablemente debido a la baja homología de secuencia de RiFRE1 y ScFRE1-2. La caracterización proteica y los análisis de expresión génica de los otros dos componentes putativos de la vía reductiva de adquisición de Fe en *R. irregularis*, RiFTR1 y RiFTR2, indicaron que RiFTR1 juega un papel *in vivo* en la adquisición reductiva de Fe de alta afinidad en ambientes limitantes de Fe. Sin embargo, el papel de RiFTR2 en *R. irregularis* no se ha podido dilucidar en nuestro estudio, probablemente debido a que la proteína no pudo salir del retículo endoplasmático, como se mostró en los ensayos de localización en levadura. También se encontró que los genes que codifican los tres componentes de la vía reductiva de asimilación de Fe identificados (*RiFRE1*, *RiFTR1* y *RiFTR2*) son genes de respuesta a Fe, como se mostró con los análisis de expresión génica realizados por RT-PCR a tiempo real.

Con el fin de identificar el compañero ferroxidasa de RiFTR1, se realizó una búsqueda de genes candidatos pertenecientes a la familia de oxidasas multicobre (MCOs, del inglés *multicopper oxidases*). Con este estudio se concluyó que *R. irregularis* tiene al menos nueve MCOs (*RiMCO1-9*) en el genoma. Los análisis de intrones y de similitud definieron cinco subfamilias génicas. Sin embargo, un análisis filogenético de secuencias MCO de diferentes grupos taxonómicos reveló que todas las RiMCOs pertenecen al grupo de ferroxidasas/lacasas, y ninguna se agrupó con las ferroxidasas tipo Fet3. *RiMCO1* fue el único gen de *MCO* que mostró un patrón de expresión génica típico de un componente del transporte de Fe de alta afinidad. Además, RiMCO1 permite que el mutante *fet3* de levadura absorba Fe. Estos datos sugieren que RiMCO1 podría tener un papel en el sistema reductivo de absorción de Fe de alta afinidad junto con el transportador de Fe RiFTR1 en el ERM. Sin embargo, algún(os) otro(s) miembro(s) de la familia RiMCO también podría(n) tener actividad ferroxidasa. Los análisis de expresión génica también revelaron que algunos transcritos fueron muy abundantes en

el ERM (*RiMCO1* y *RiMCO5*) y otros en el micelio intrarradical (*RiMCO2*), lo que sugiere que las diferentes RiMCOs tienen funciones específicas.

Finalmente, para intentar identificar algunos otros elementos implicados en la regulación de la homeostasis de Fe en *R. irregularis*, y dado que se ha demostrado que las glutarredoxinas (GRXs) Grx3-4 y Grx5 de levadura tienen un papel en la homeostasis de Fe, se identificó y caracterizó el complemento completo de GRXs en *R. irregularis* (RiGRX1,4,5,6) (RiGRX1 se caracterizó previamente en nuestro grupo). Los análisis funcionales en el sistema heterólogo mostraron que mientras que las cuatro GRXs de *R. irregularis* están implicadas en la protección frente a estrés oxidativo, RiGRX4 y RiGRX5 (homólogas a ScGrx3-4 y ScGrx5, respectivamente) también tienen un papel en la homeostasis de Fe en levadura. Además, los datos de expresión génica mostraron que *RiGRX4* fue el único gen de glutarredoxina de respuesta a Fe, lo que sugirió que podría estar implicado en la regulación de la absorción de Fe mediante la interacción con factores de transcripción de respuesta a hierro, como se ha demostrado anteriormente para sus homólogos en otros hongos. El aumento de la expresión de *RiGRX1* y *RiGRX6* en el micelio intrarradical sugiere que estas GRXs podrían tener un papel clave en la protección frente a estrés oxidativo de *R. irregularis* durante su fase *in planta*.

A pesar de que en esta tesis doctoral sólo se han caracterizado los transportadores del hongo implicados en la absorción de hierro del suelo y las glutarredoxinas, se propone un modelo integrador para la regulación de la homeostasis de hierro y su transporte a través de la vía micorrícica en una raíz micorrizada.

INTEREST OF THE STUDY

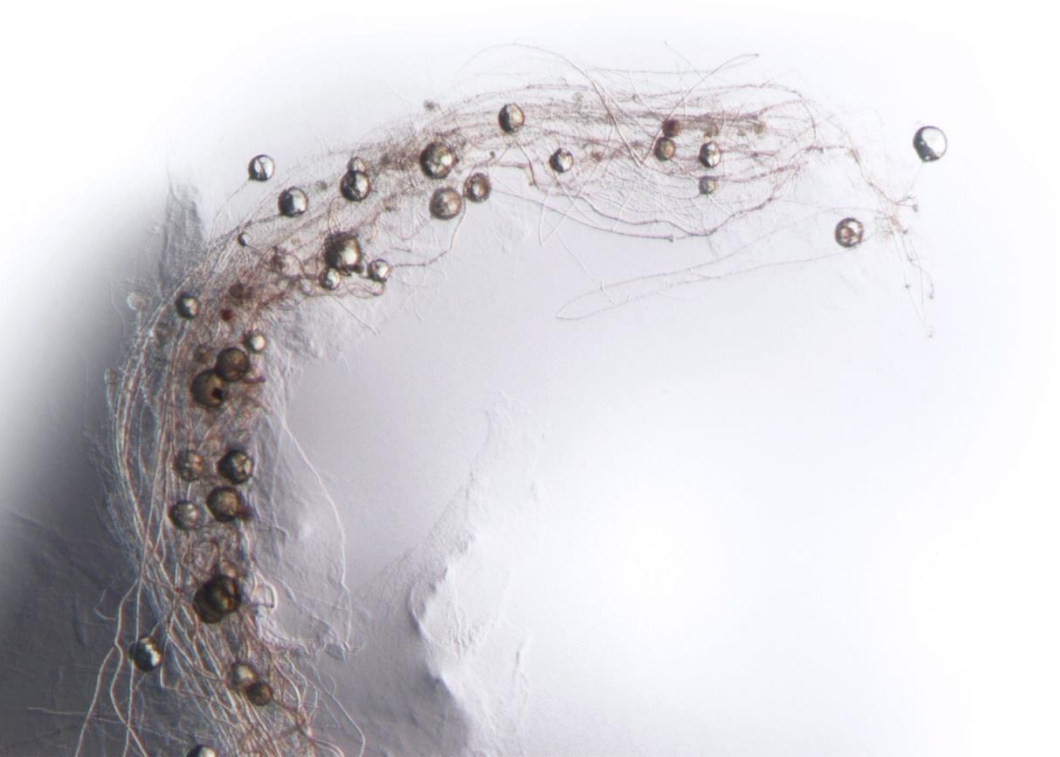

Pollution is increasing with time due to rapid industrialization, mining, combustion of fossil fuels and massive use of fertilizers, among other anthropogenic activities. Heavy metals (HMs) are the main group of inorganic pollutants which are continuously accumulating in our environment, having a deleterious impact on agro-systems and natural ecosystems. As an example, data from the Andalusian administration show that Río Tinto, in Minas de Riotinto (Huelva) presents an acidic pH around 2.5 due to the 16000 tons of equivalent acids, 1300 of copper and 8500 of iron, probably as a result of mining activity. Río Tinto is an unusual ecosystem due to its acidity and high concentration of HMs (Fe, Cu, Zn, As, etc.). Other places damaged by mining activity in Andalucía are Alquife (Granada) or Aznalcollar (Sevilla). Strategies destined to recuperation of metal-polluted ecosystems include bioremediation, that is, the use of living organisms to recover contaminated areas. In the case of metal-contaminated soils, phytoremediation is an especially interesting strategy, which is the use of plants to make soil contaminants non toxic. On the other hand, most ecosystems nowadays present low levels of metals, especially in basic soils, in which metal mobility is reduced. In fact, one of the main factors limiting plant growth and tolerance to stress and reduces crop nutritional value is the deficiency of soils in essential micronutrients such as Fe, Cu or Zn. Accordingly, human diet in many areas of the world does not include the expected metal nutrient requirement, causing from anemia, neurological impairments or minor immunological alterations to death. Many are the strategies by which plants strive to obtain essential metals from soils, such as acidification of the soil or secretion of chelators and considerable effort has been carried out to increase plant metal uptake, such as the development of new crop varieties with improved metal uptake potential or the use of metal fertilizers.

Nevertheless, it is important to take into account that plants do not live alone in natural conditions, but in tight association with a wide variety of microorganisms. In this sense, we have to keep in mind that around 80% of land plants form arbuscular mycorrhiza, symbiotic associations with soil fungi which increase plant nutrient uptake ability and protect the host plant against biotic and abiotic stresses. Arbuscular mycorrhizal (AM) fungi have

been shown on the one hand to increase the uptake of low mobility micronutrients, such as Zn, Cu and Fe, when plants grow in soils deficient in these elements and, on the other, to alleviate metal toxicity in polluted soils. This has led to the hypothesis that AM functions as a "buffer" to protect the plant against damage caused by metals in the soil. Given the central role AM fungi play in modulating plant metal acquisition in a wide range of soil metal concentrations, they have been considered to be a key element in the improvement of micronutrient concentrations in crops and in the phytoremediation of polluted soils.

Despite the importance of the AM symbiosis for plant development in metal polluted and deficient soils, the underlying mechanisms are not completely understood. It is expected that both, the increased tolerance of mycorrhizal plants to HM excess and the increased uptake of transition metals in metal deficient soils are, at least partially, the result of the molecular mechanisms ongoing in the mycorrhizal fungus. However, plants must also accommodate their own metal homeostasis to the presence of the microsymbiont.

With the aim of getting a further understanding of these mechanisms, the main objective of this PhD thesis was to study the mechanisms of Fe homeostasis in the model fungus *Rhizophagus irregularis*. It is expected that an improved knowledge of these mechanisms will help to better pintpoint biological mechanisms contributing to beneficial effects of the symbiosis under Fe toxic and deficient conditions.

INTRODUCTION

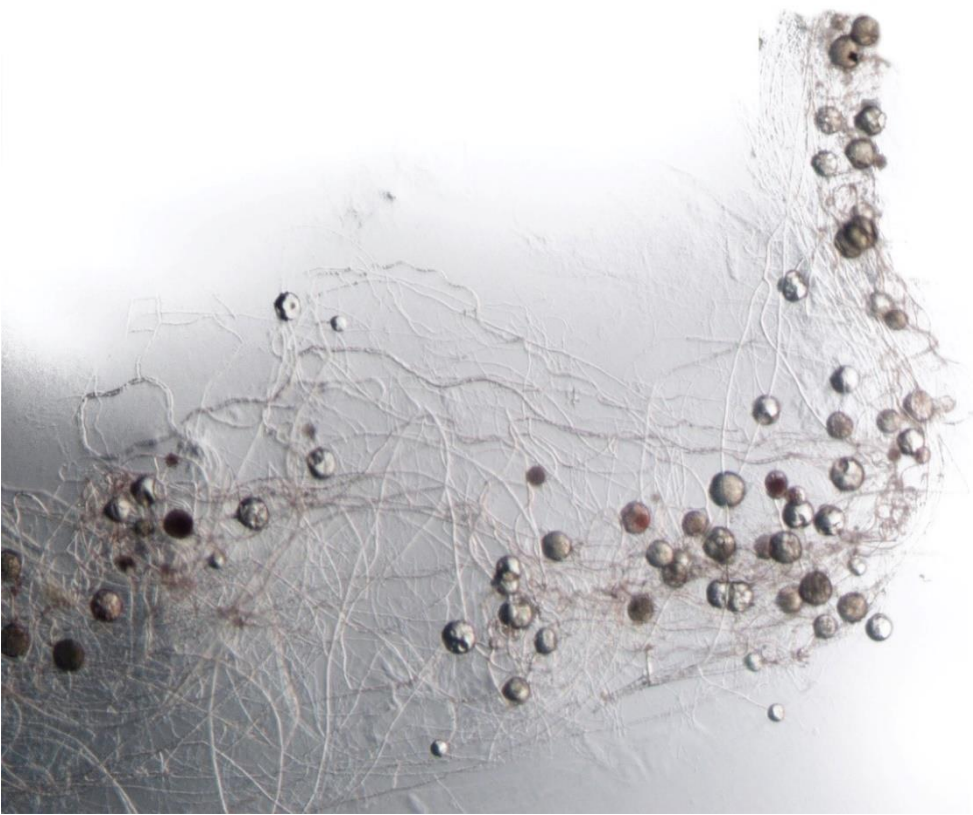

1. Arbuscular mycorrhizal symbiosis: an overview

The word "mycorrhiza", from the Greek *mykós* (fungus) and *riza* (root), describes the mutualistic symbiotic association formed between certain soil fungi and plants. This term was introduced by the German botanist A. Bernhard Frank in 1885. Basically, the host plant receives mineral nutrients *via* the fungal mycelium, while the heterotrophic fungus obtains carbon compounds from the host's photosynthates (Barea and Azcón-Aguilar, 2013). Mycorrhizal fungi colonize the root and develop an extraradical mycelium (ERM) which overgrows the soil surrounding plant roots. This hyphal network is a structure specialized for the acquisition of mineral nutrients from the soil.

There are two main types of mycorrhizas, ecto- and endomycorrizas, which have important differences in structure and in the physiological relationships between symbionts (Smith and Read, 2008).

In ectomycorrhizas, the fungus develops a mantle around the roots. The mycelium penetrates the root and develops between the epidermal and cortical cells forming the "Hartig net" that constitutes the site of nutrient exchange between partners. About 3% of higher plants, mainly forest trees, form ectomycorrhizas with fungi mostly belonging to Basidiomycota and Ascomycota.

In endomycorrhizas, the fungi colonize the root cortex with typical intracellular penetrations. Some endomycorrhizal types are restricted to species in the Ericaceae or Orchidaceae, whilst the most common mycorrhizal type, the **arbuscular mycorrhizas**, is widely distributed throughout the plant kingdom.

In an intermediate mycorrhizal type, the ectendomycorrhiza, the mantle may be reduced or absent, the Hartig net is usually well developed and hyphae penetrate into the plant root cells.

Most of the major plant families (70-80% of extant plant species) form arbuscular mycorrhizal (AM) associations (Brundrett, 2009; Barea and Azcón-Aguilar, 2013). The fungi involved in these associations are members of the phylum Glomeromycota. The host plants for AM fungi includes angiosperms, gymnosperms and sporophytes of pteridophytes, all of which have roots, as well as the gametophytes of some hepatics and pteridophytes which do not (Smith and Read, 2008). This symbiosis is characterized by the tree-like structures termed "arbuscules" that the fungus develops within the root

cortical cells, and where most of the nutrient exchange between partners takes place. AM fungi, by acting as a bridge connecting the root to the surrounding soil microhabitats, contribute to nutrients acquisition and supply to plants, improving therefore plant mineral nutrition. In addition, the AM symbiosis improves plant health through increased protection against hard conditions including biotic or abiotic stresses (Jeffries and Barea, 2012; Jeffries et al., 2003).

AM fungi

AM fungi are ubiquitous soil-borne microscopic fungi that belong to the Glomeromycota phylum. They are strict symbionts, unable to complete their lifecycle in the absence of a host plant. This feature hinders their use and complicates their study. Some important aspects of their phylogeny and biology are outlined below.

Phylogeny of AM fungi

The origin and divergence of the phylum Glomeromycota dates back more than 500 million years, therefore being considered the oldest existent asexual lineage of eukaryotes (Redecker et al. 2000; Schüßler et al., 2001). Since the description of the first AM fungal species, *Glomus macrocarpum* (formerly *Endogone macrocarpus*) by Tulasne and Tulasne (1845), the phylogeny and taxonomy of AM fungi have been subjected to several changes (for an historical review of taxonomy, see Stürmer, 2012). Before the advent of molecular techniques, identification of AM fungi was based on the microscopic examination of spores, which exhibit features with taxonomic value, such as shape, colour, size, wall structure, certain wall component staining, presence of septa and connection to sustaining hypha. However, morphological similarities do not always reflect phylogenetic relationships. Thanks to the availability of molecular data, AM fungi were repositioned in a monophyletic basal fungal group, the Glomeromycota, distinct from the Zygomycota where they had previously been placed (Schüßler et al., 2001). More recently, a total revision of their taxonomy has been performed taking into account the numerous papers published during a decade of molecular systematics of AM fungi (Schüßler and Walker, 2010).

The phylum Glomeromycota is currently represented by about 250 described species, although molecular analyses from environmental samples (i.e. soil and plant roots) suggest a broader diversity (Öpik et al., 2013) and new AM fungal species are frequently described (Redecker et al., 2013; Malbreil et al., 2014; Bonfante and Desirò 2015). Their taxonomy is reorganized at different hierarchical levels (Redecker et al., 2013): until 2001, AM fungi were distributed in 1 class, 1 order, 3 families and 6 genera; but through the use of molecular phylogeny, they were later assigned to 1-3 classes, 4 to 5 orders, 11-15 families, and to 25-29 genera, depending on the scheme of the adopted classification. Fig. 1 represents the overall classification system emerged from several recent studies (Oehl et al., 2011; right panel) and the more recent consensus classification of the Glomeromycota (Redecker et al., 2013; left panel).

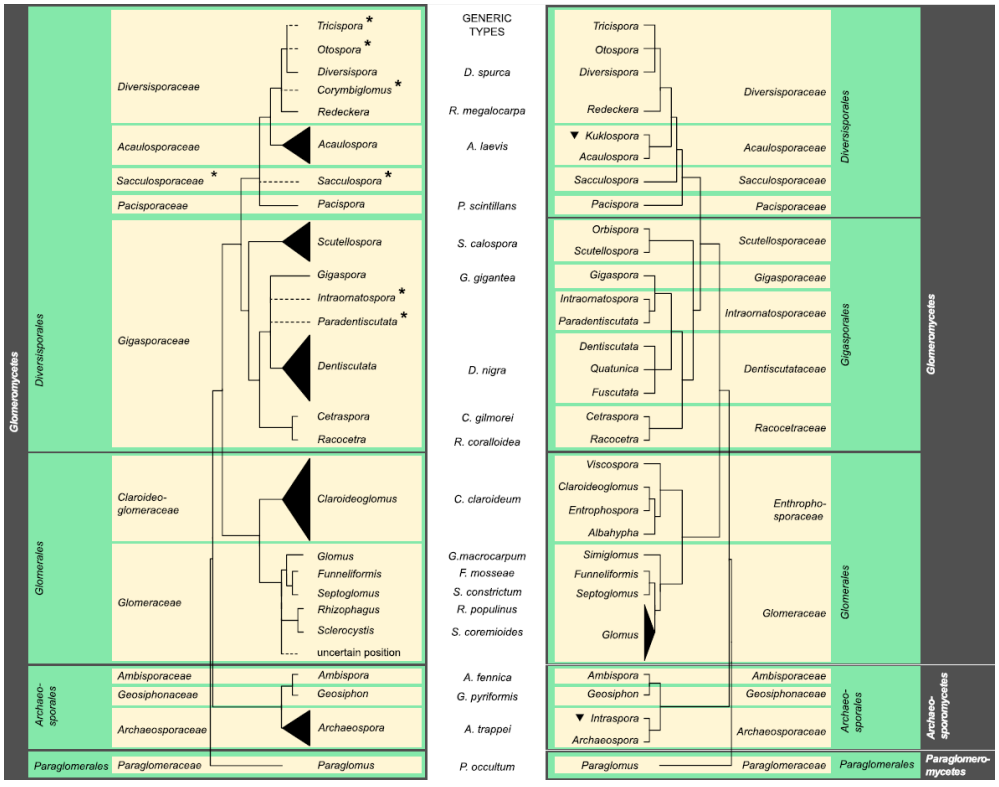

Figure 1. Consensus classification of the Glomeromycota (left panel) in comparison to the system summarized by Oehl et al. (2011) (right panel), including additional taxa proposed by Goto et al. (2012) (family Intraornatosporaceae). Classes, orders, families, and genera are showed. From Redecker et al. (2013).

Redecker et al. (2013) consider that all glomeromycotan orders group into only one class, the Glomeromycetes, while Oehl et al. (2011) consider that the plylum splits into three classes: Glomeromycetes, Archaeosporomycetes, and Paraglomeromycetes.

rDNA-phylogeny from all basal fungal lineages suggested placement of Glomeromycotan fungi as a sister phylum to the Dikarya (i.e., the phyla of Basidiomycota and Ascomycota; Schüβler et al., 2001). However, this placement was challenged by several studies using nuclear or mitochondrial protein-encoding genes (Liu et al., 2009; Lee and Young, 2009), in which AM fungi usually clustered with those belonging to the Mucoromycotina. More recently, on the basis of the complete genome of *R. irregularis* (Tisserant et al., 2013; Lin et al., 2014) and of 118 orthologous genes of *Gigaspora rosea*, *G. margarita* (Diversisporales) and *R. irregularis* (Glomerales) (Tang et al., 2016), Glomeromycota were again phylogenetically placed closer to Mucoromycotina (Fig. 2). The Mucoromycotina, a basal group of fungi also characterized by a coenocytic myceliym, has been proposed to be the sister group of the Glomeromycota (Young, 2015).

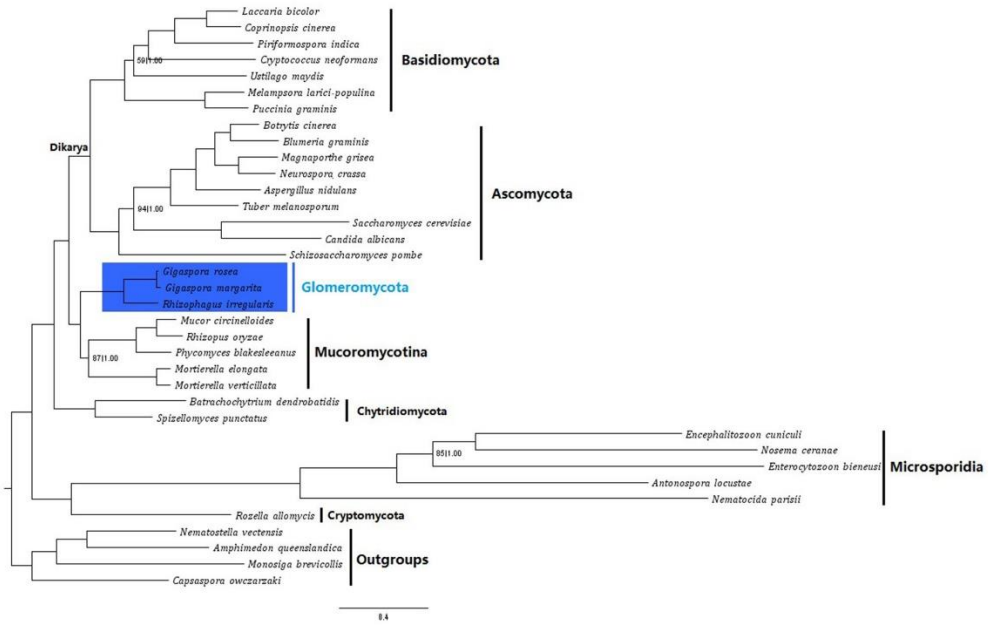

Figure 2. Phylogenetic placement of the Glomeromycota within fungi. From Tang et al. (2016).

General features of AM fungi

Besides being obligate biotrophs, AM fungi display many unusual biological features that make them a fascinating subject of study. AM fungi have no known sexual cycle (Sanders, 1999), and reproduce clonally through large multinucleated spores (Fig. 3), which have abundant storage lipids and resistant thick walls containing chitin (Smith and Read, 2008). AM fungi have multiple nuclei which share a common cytoplasm in their coenocytic hyphae and in the spores. The main mechanism for filling a spore with so many nuclei appears to be a massive influx of nuclei from subtending mycelium into the developing spore (Jany and Pawlowska, 2010). Although they are assumed to only reproduce asexually, recent genome and transcriptome analyses indicate that they do possess genetic information essential for sexual reproduction and meiosis (Tisserant et al. 2012; 2013).

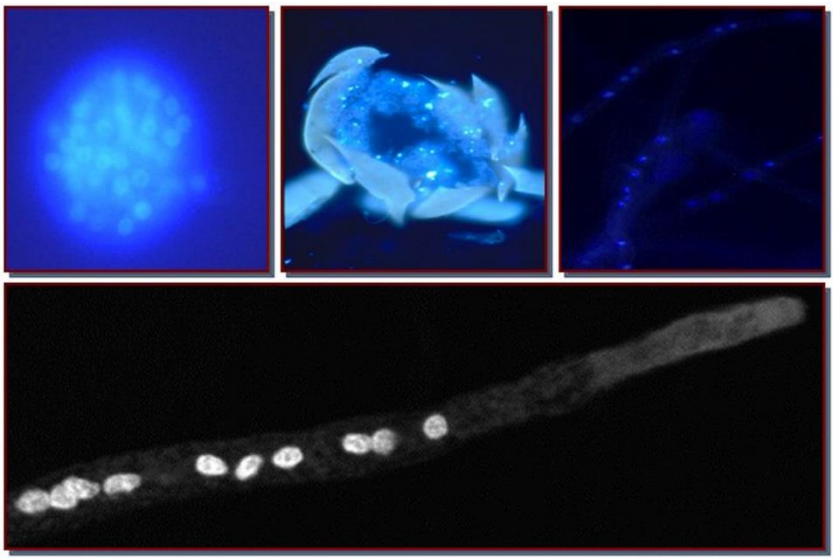

Figure 3. Typical multinucleated asexual spores and extraradical hyphae of *Rhizophagus irregularis*. Courtesy of A. Bago.

These peculiarities introduce limitations in the application of standard techniques like genetic transformation or mutant generation/characterization for the study of these organisms, and they greatly hinder advances in the knowledge about gene function in AM fungi. It is still not possible to obtain stable transformant or mutant lines of AM fungi, but transient expression was reported (Helber and Requena, 2008; Malbreil et al., 2014). Recently,

functional validation of a few *R. irregularis* genes was performed by using host-induced gene silencing (Helber et al., 2011; Tsuzuki et al., 2016) and virus-induced gene silencing (Kikuchi et al., 2016).

The concept of species is poorly defined in this group of organisms, since they show a high degree of genetic variability. The genetic organization of coexisting nuclei in the Glomeromycota has been a major source of debate for the past 15 years, with two opposite main hypotheses: heterokaryosis (Angelard et al., 2014; Boon et al., 2015) and homokaryosis (Pawlowska and Taylor, 2004), which defend the presence or absence of internuclear genetic divergence, respectively (Ropars and Corradi, 2015). Furthermore, it has also been suggested that individual spores contain a uniform population of nuclei characterized by intranuclear polymorphism (Pawloska and Taylor, 2004; Pawlowska, 2005). It has been hypothesized that the heterokaryotic structure has arisen from hyphal anastomosis between genetically different mycelia and by accumulation of mutations (Bever and Wang, 2005). However, anastomosis events have only been observed between hyphae of closely related fungal strains (Croll et al., 2009). Data from the genome sequence of the model fungus *R. irregularis* DAOM197198 (Tisserant et al., 2013), and also at the level of a single fungal nucleus (Lin et al., 2014), strongly support the homokaryotic status. However, the discussion is not still closed. A potential homokaryotic/heterokaryotic lifecycle was reported in *R. irregularis*. Nicolas Corradi's team showed that some strains of this species maintain a balanced population of two genetically divergent haploid nuclei within their single cytoplasm over several generations, and revealed the presence of a putative AM fungal mating-type locus similar to the MAT locus of some Dikarya, suggesting that sexual reproduction might be present in AM fungi (Ropars et al., 2016; Corradi and Brachmann, 2017). While the diversity of nuclear genomes remains unresolved, multiple complete mitochondrial genomes are now available, with no variation within isolates but significant variation between them (Young, 2015).

Finally, many AM fungi contain endobacteria in their cytoplasm, and this leads to an unexpected increase in their genetic complexity (Bianciotto et al., 2003; Desirò et al., 2014).

The first genome project dedicated to an AM fungus

The announcement of the genome-sequencing program for an AM fungus in 2004 posed a real challenge (Martin et al., 2004). First, genomes of AM fungi are among the largest in fungi, ranging from 150 Mb to over 1 Gb depending on the species (Hosny et al., 1998). Second, producing enough tissue to study presents a challenge as they require co-cultivation with a host plant. *Rhizophagus irregularis* DAOM 197198 was chosen as the model fungus because of its relatively small genome size (153 Mb) (Sędzielewska et al., 2011) and the possibility to propagate it efficiently with *in vitro* root organ cultures. Because of their heterokaryotic nature, AM fungi were anticipated to be very difficult to sequence. In fact, such heterokaryotic organization would limit shotgun sequencing strategies, as it impairs assembly procedures.

Taking advantage of the development of next-generation sequencing technologies, two independent studies published genomic sequences for *R. irregularis* DAOM 197198 (Tisserant et al., 2013; Lin et al., 2014). The genome was estimated to be 153 Mb with a high frequency of transposable elements (36-40% of the genome). Thus, 66 and 92% of the deduced genome, respectively, is covered by the two assemblies (genome assembly length: 101 Mb, Tisserant et al., 2013; 141 Mb, Lin et al., 2014). *R. irregularis* DAOM197198 presents a classical haploid fungal genome, atypically A+T rich (A+T content, 72%; Tisserant et al., 2013), and contains 28,232 protein-coding gene models. Gene expansion was observed in several gene families, such as kinases and mating-related genes, whereas, in both assemblies, other genes were strikingly absent, such as glycoside hydrolases, which could damage plant cell walls. The obligate biotrophy of AM fungi is not explained by genome erosion or any related loss of metabolic complexity in central metabolism. *R. irregularis* has a relatively small repertoire of effector-like proteins in comparison to pathogenic fungi, but some of these secreted proteins are unique to *R. irregularis*, which suggests that such effectors play important roles in the symbiosis.

By sequencing individual nuclei, Lin et al. (2014) showed that ribosomal regions are highly variable within each nucleus. Moreover, the rate of single nucleotide polymorphisms (SNPs) found in *R. irregularis* was similar

to that of other genomes of mycorrhizal fungi. The analysis of genomic sequences from different *R. irregularis* ecotypes recently confirmed the low rate of SNPs (Ropars et al., 2016). A similar result was also found for the gene repertoire of another AM species, *Gigaspora rosea* (Tang et al., 2016). Global analyses of the coding gene repertoires obtained at this time indicate that AM fungi exhibit features of a classical genome.

As mentioned above, these genomic advances also drastically changed our views on the lack of sexuality of AM fungi. The finding of genes involved in meiosis and sexuality in several AM fungi and the expansion of mating-related genes suggest that they have a cryptic sexual cycle (Riley and Corradi, 2013; Riley et al., 2014). The comparison of genomic sequences from ecotypes of *R. irregularis* revealed differential allele distributions consistent with the probable existence of homokaryotic and dikaryotic strains (Ropars et al., 2016).

Life cycle of AM fungi

Establishment of the symbiosis is usually described as occurring in three steps: (i) asymbiotic hyphal growth, where the spores can germinate and develop hyphae autonomously but during a limited period; (ii) presymbiotic growth, where hyphal growth is stimulated by host signal perception; and (iii) symbiotic life, where the fungus penetrates the plant root and develops both intraradical mycelium (IRM) (to exchange nutrients) and extraradical hyphae (to recruit nutrients in the soil and form new spores) (Fig. 4).

The spores of AM fungi can germinate in the absence of a host but are capable of only limited growth during this "host-free", **asymbiotic phase**. To date and as mentioned above, no sexual mechanisms have been identified for the formation of such spores. They are dormancy structures that enable the invasion of new plants when climatic conditions are favourable. The establishment of an AM symbiosis proceeds as a series of genetically controlled steps and starts with the **presymbiotic phase**, a presymbiotic molecular crosstalk leading to reciprocal recognition within the rhizosphere (Nadal and Paszkowski, 2013).

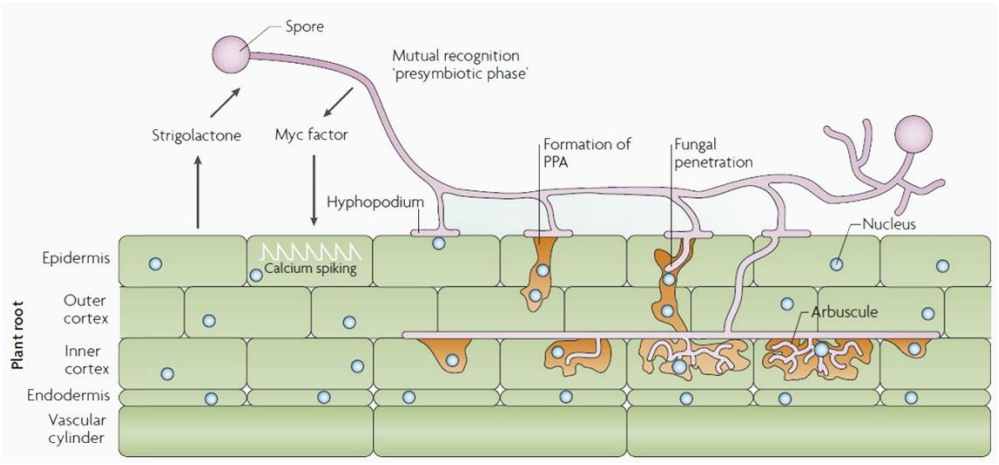

Figure 4. Steps in the development of arbuscular mycorrhizas. From Parniske (2008).

After spore germination, the fungal hyphae explore the soil searching for a compatible host and respond to the perception of a number of chemically unrelated plant metabolites. Certain hydroxy fatty acids exuded by plants stimulate hyphal ramification with low branching at several cm distance from roots (Nagahashi et al., 2010; Nagahashi and Douds, 2011). AM fungi are also able to detect strigolactones in close proximity to roots. Strigolactones are a group of terpenoid lactones that derive from carotenoid metabolism and that are released into the rizosphere by most plant roots (Ruyter-Spira et al., 2013). These compounds trigger intense hyphal branching and increase their mitotic activity, lipid catabolism and mitochondrial respiration (Akiyama et al., 2005; Besserer et al., 2006, 2008). Fungal strigolactone perception is a switch from asymbiosis to presymbiosis, and the fungus becomes irreversibly committed to an anticipation program and presymbiotic responses. The rapid degradation of strigolactones creates a high concentration gradient proximal to the root thus providing positional information about the root's proximity. Recent data suggest that AM fungi might perceive strigolactones through a calcium-mediated pathway (Moscatiello et al., 2014). Nevertheless, fungal strigolactone receptors remain unknown and analysis of the *R. irregularis* genome has not revealed the existence of fungal homologs of the known strigolactone receptors in plants, suggesting that fungal and plant strigolactone receptors likely differ in structure, which opens the possibility that AM fungi independently evolved strigolactone perception mechanisms (Koltai, 2014; Bonfante and Genre, 2015).

Simultaneously, also the fungus produces diffusible factors, often referred as "Myc factors" (from mycorrhization) (Kosuta et al., 2003; Maillet et al., 2011), that include short-chain chitin oligomers which trigger Ca^{2+} spiking in roots (Genre et al., 2013), and lipochitooligosaccharides that induce lateral root formation (Maillet et al., 2011). Although their chemical structure links them to chitin biosynthesis, lipochitooligosaccharides are not known to perform inherent functions in AM fungi and might therefore be specifically produced as signals to the plant host.

The **symbiotic phase** starts when a hyphal tip reaches the surface of a root. After the selection of the root penetration site, the hypha develops a hyphopodium as an anchorage structure (Fig. 4). Plant cells prepare the intracellular environment for AM fungal hyphae. After 4-5 hours of the formation of a hyphopodium, the pre-penetration apparatus (PPA) is formed as a subcellular structure that predetermines the path of fungal growth through the plant cells. Formation of the PPA is preceded by a migration of the plant cell nucleus towards the point of anticipated fungal entry. The nucleus then moves ahead of the developing PPA, as if to guide its growth direction through the cell. The PPA is a thick cytoplasmic bridge across the vacuole of the host cell. It contains cytoskeletal microtubules and microfilaments, which together with dense endoplasmic reticulum cisternae form a hollow tube within the PPA that connects the leading nucleus with the site of appressorial contact (Genre et al., 2005, 2008). Only after this "transcellular tunnel" is completed, the fungal hypha can penetrate the host cell. Intracellular fungal colonization strictly follows the route of the PPA from the epidermis to the inner cortex, always surrounded by a perifungal membrane that allows the fungus to grow inside the plant cell without breaking its integrity (Bonfante and Genre, 2010). As soon as the fungus is approaching the cortical layer it induces the development of a PPA-like structure, and when it is in the inner cortical cells, it produces highly branched structures called arbuscules, assumed to be the preferential zone of exchange between the two symbionts (Fig. 4). Here the periarbuscular membrane does not simply envelope the arbuscule as a whole, but closely surround all the thin branches. Periarbuscular membrane biogenesis, and thus arbuscule growth, requires vesicle transport to the periarbuscular membrane at hyphal

tips (Genre et al., 2012; Ivanov et al., 2012). Arbuscules are ephemeral structures that at some point after maturity, approximately two to three days, collapse and degenerate, while the host cell regains its previous organization can undergo new colonization. Root colonization by AM fungi is not a synchronous event and arbuscules of different ages can exist at the same time in neighboring cells. Simultaneosuly to intraradical colonization, the fungus develops an extensive network of hyphae, the ERM, which explores the soil for nutrient acquisition and becomes competent for the production of a new generation of spores.

AM functioning: Nutrient transport and exchange

As in any mutualistic symbiosis, the two partners obtain a benefit from the other in AM. The plant transfers carbon to the AM fungus and there is a reciprocal movement of mineral nutrients (mainly phosphate, nitrogen, sulphur, potassium and various microelements) from fungus to plant (Smith and Read, 2008; Casieri et al., 2013; Sieh et al., 2013).

Phosphorus nutrition

The main benefit of the AM symbiosis is an improved plant P status. Two pathways contribute to P uptake from the soil in mycorrhizal plants: a direct pathway by root epidermal cells and the mycorrhizal pathway, *via* AM fungi (Bucher, 2007; Smith and Smith, 2012) (Fig. 5). Radiotracer experiments have made possible to assess the relative amount of Pi that enters a plant *via* the AM fungus and by the direct pathway. These studies have shown that depending on the plant and fungal species involved in the association the mycorrhizal pathway can contribute from 20 to 100% of the plant P uptake (Smith et al., 2004; Facelli et al., 2010).

The mycorrhizal pathway first involves the uptake of Pi from the soil solution by the ERM. Several $Pi:H^+$ transporters were identified and characterized in AM fungi: DePT, FmPT and RiPT, in *Diversispora epigaea* (formerly named *Glomus versiforme*), *F. mosseae* and *R. irregularis*, respectively (Harrison and van Buuren, 1995; Maldonado-Mendoza et al., 2001; Benedetto et al., 2005). These fungal transcripts were predominantly expressed in ERM, and their expression was enhanced by low P availability (Maldonado-

Mendoza et al., 2001), suggesting a role in Pi acquisition from the soil solution. The release of the *R. irregularis* genome (Tisserant et al., 2013; Lin et al., 2014) allowed the identification of three putative Pi:Na transporters, *RiPT1-RiPT3*, with questionable function (Casieri et al., 2013).

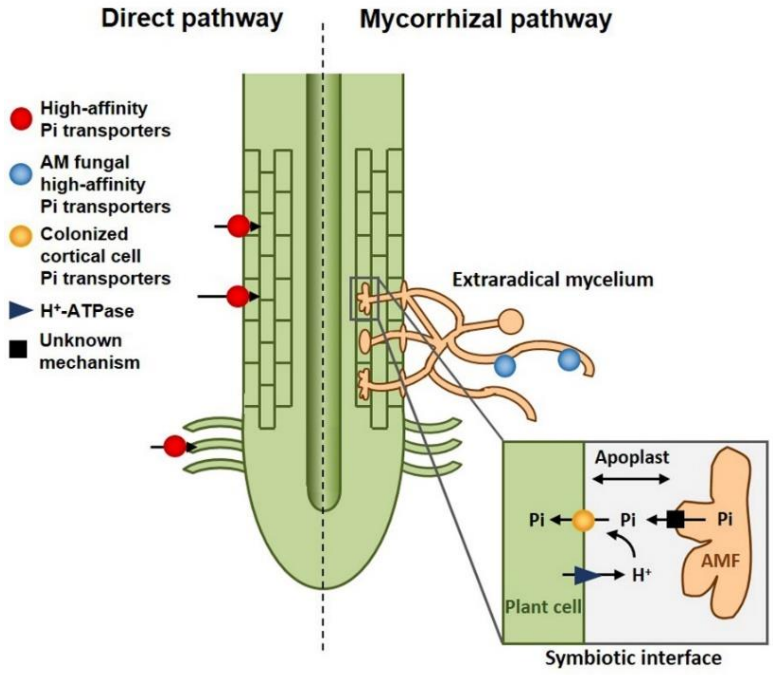

Figure 5. Nutrient uptake pathways in arbuscular mycorrhizal plants. Modified from Smith et al. (2010).

After Pi uptake by the ERM, it first supply the needs of the metabolically active Pi pool in the hyphae while the surplus Pi is rapidly transported into the fungal vacuoles and condensed into polyphosphate (polyP) (Fig. 6), which is the largest P storage and mediator of long distance P translocation in AM fungi (Hijikata et al. 2010). Once in the arbuscules, vacuolar PolyP is hydrolyzed, Pi is transported to the cytosol, and released from the fungus towards the apoplast of the symbiotic interface through unknown mechanisms (Casieri et al., 2013).

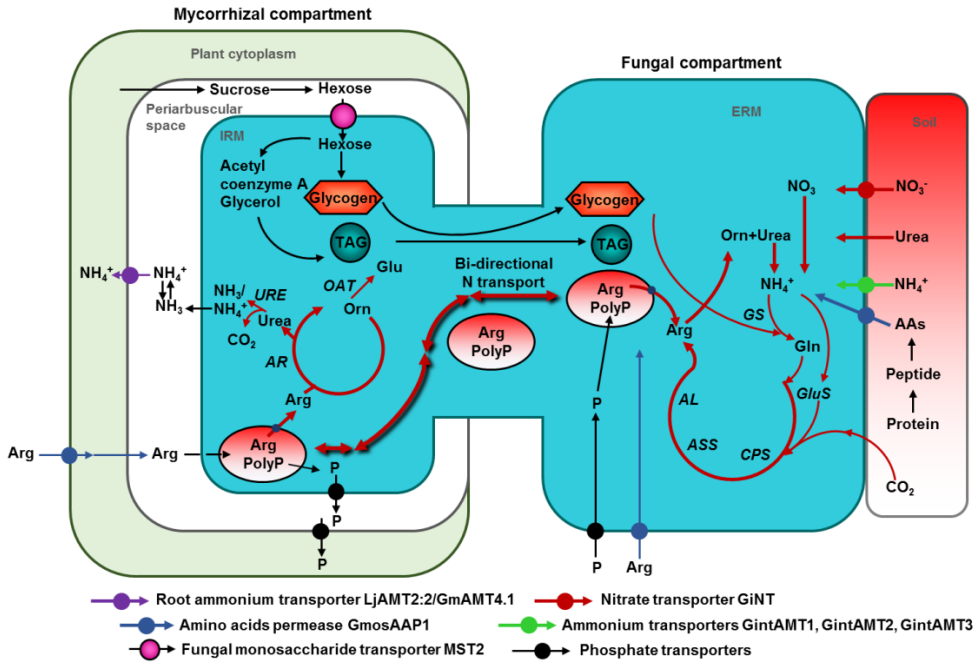

Figure 6. Proposed model of C, N and P uptake, translocation and transfer in arbuscular mycorrhizal fungi. Modified from Jin et al. (2012).

Mycorrhiza-specific plant Pi transporters localized on the periarbuscular membrane are responsible for the uptake of Pi released from arbuscules (Javot et al., 2007). Several mycorrhiza-induced P transporters have been identified in many monocotyledonous and dicotyledonous species, and they have been shown to be essential for Pi uptake *via* the mycorrhizal pathway (Harrison et al., 2002; Walder et al., 2015; Berruti et al., 2016). Moreover, it has been shown that activation of the mycorrhizal Pi uptake pathway induces down-regulation of plant Pht1 transporters located in epidermal root cells and, therefore, of the direct pathway (Liu et al., 1998).

Nitrogen nutrition

Although the role of the AM on plant N nutrition is not as clear as on P nutrition, AM can play a major role in N uptake. In fact, N uptake of the host plant *via* the mycorrhizal pathway can reach up to 42% (Mäder et al., 2000). Extraradical hyphae can take up from the soil both inorganic (NO_3^- and NH_4^+) and organic N compounds (small peptides or amino acids) (Bago et al., 1996; Govindarajulu et al., 2005; Jin et al., 2005; Hawkins et al., 2000), although

a clear preference for NH_4^+, which is energetically less costly, has been observed (Toussaint et al., 2004). The first molecular evidence for N uptake by AM fungi was obtained through the characterization of an ammonium transporter of *R. irregularis* (López-Pedrosa et al., 2006). Afterwards, an amino acid transporter and a nitrate transporter were described in *F. mosseae* and *R. irregularis*, respectively (Cappellazzo et al., 2008; Tian et al., 2010), and more recently, three ammonium transporters in *R. irregularis*. GintAMT1 was characterized as a typical high-affinity ammonium transporter that is mainly expressed in the ERM and mediates NH_4^+ uptake from the soil solution (López-Pedrosa et al., 2006). The other two NH_4^+ transporters, GintAMT2 and GintAMT3, exhibited a lower ammonium transport capability and were expressed at higher levels in the IRM (Pérez-Tienda et al., 2011; Calabrese et al., 2016).

Uptake from the soil by ERM is followed by long-distance transfer to the arbuscules (Fig. 6). Once absorbed, most of the inorganic N is assimilated and incorporated into arginine. N moves as arginine, and that translocation through the hyphae occurs in vacuoles (Cruz et al., 2007; Govindarajulu et al., 2005). The arginine is translocated to the IRM, and it is metabolized in the arbuscule. The free NH_4^+ is then released into the periarbuscular space where it will be taken up by the host plant (Govindarajulu et al., 2005; Tian et al., 2010).

On the plant side, micorrhiza-inducible ammonium transporters (AMT) have been also identified in *Medicago truncatula*, *Lotus japonicus*, *Glycine max*, *Sorghum bicolor* and *Oryza sativa* (Gomez et al., 2009; Guether et al., 2009; Kobae et al., 2010; Koegel et al., 2013; Pérez-Tienda et al., 2014). AMTs have been located in the arbusculated cells of *Lotus*, soybean and *Medicago*, suggesting a role in ammonium transport to the cortical cells (Guether, et al., 2009; Kobae et al., 2010; Breuillin-Sessoms et al., 2015).

Besides inorganic N uptake, AM fungi can obtain N from decomposing organic matter, in particular amino acids (Hodge and Fitter, 2010). This process can involve amino acid permeases (AAP), among other transporters. GmosAPP1, a functional APP from *F. mosseae*, may play a role in the first steps of amino acid acquisition, allowing direct amino acid uptake

from the soil. *GmAPP1* is expressed in the ERM and its activity was observed to increase upon exposure to organic N (Cappellazzo et al., 2008).

Carbon metabolism

As a reward to the improvement in mineral nutrients thanks to the AM fungi, the plant redirects up to 25% of its photosynthates towards the mycorrhizal roots and transfer them to the fungal partner (Casieri et al., 2013). Evidence of the transcriptional regulation of genes involved in sucrose transport have been reported in several plant-AM fungus combinations (Casieri et al., 2013, and references therein), although much work is still needed to understand which plant SUTs (sucrose transporters) or regulatory mechanisms are active in sucrose partitioning in mycorrhizal plants. It has recently been suggested that the SWEET transporters, integral membrane proteins that catalyze both the efflux and uptake of carbohydrates, play a role in sugar downloading processes during AM symbiosis (Manck-Götzenberger and Requena, 2016).

The form in which carbon is provided from the host plant to the AM fungus is still under debate, although most of the experimental evidence suggests that glucose is the main form taken up by the fungus (Shachar-Hill et al., 1995; Solaiman and Saito, 1997; Pfeffer et al., 1999). However, the finding that AM fungi lack the enzyme for *de novo* fatty acid biosynthesis, the type I FAS, (Tisserant et al., 2013; Salvioli et al., 2016; Tang et al., 2016) led to the hypothesis that, in addition to sugars, plants might be providing lipids as a source of carbon to their symbionts (Wewer et al., 2014). Currently, however, there is no experimental evidence on the mechanisms of how fatty acids could be released into the periarbuscular space or taken up into the fungus. In contrast, molecular support for sugar import into the fungus from the apoplastic space was obtained with the identification of the high affinity monosaccharide transporter MST2 from the AM fungus *R. irregularis* (Fig. 6), only expressed in symbiosis at arbuscule-containing cells and intercellular hyphae (Helber et al., 2011). Once incorporated, hexoses are then converted into trehalose, glycogen and lipids (Bago et al, 2000; Shachar-Hill et al., 1995). Trehalose and glycogen synthases genes are present in the *R. irregularis* gene inventory (Tisserant et al., 2012, 2013).

Micronutrients

This point will be addressed in section 2 (page 41).

Tolerance of AM plants to environmental stresses

Besides promoting plant growth through an increased improved mineral nutrition, the AM symbiosis increases plant tolerance to a variety of environmental stresses, either biotic (e.g., pathogen attack) or abiotic (e.g., drought, salinity, extreme temperature, presence of organic pollutants or heavy metal (HM) toxicity).

Although many studies have shown that root colonization by AM fungi improve plant resistance or tolerance to biotic stresses, some of the underlying mechanisms remain largely unknown. This AM-mediated protection seems to result from the combination of multiple mechanisms that operate simultaneously, such as improved plant nutrition, competition for colonization sites and activation of plant defenses (Azcón-Aguilar and Barea, 1997; Goicoechea et al., 2010). During AM establishment, modulation of plant defence responses occurs upon recognition of the AM fungus and a mild activation of the plant immune responses may occur, not only in local but also in systemic tissues. This activation leads to a primed state of the plant that allows a more efficient activation of defense mechanisms in response to attacks by potential adversaries (Pozo et al., 2009, 2010; Jung et al., 2012). In fact, AM symbioses have an important impact on plant interactions with pathogens and insects. The association leads generally to a reduction of damage caused by soil-borne pathogens, but effects on shoot targeting organisms depend on the attacker lifestyle. Mycorrhiza induced resistance in above-ground tissues seems to be effective against necrotrophic pathogens and generalists chewing insects, but not against biotrophs. Mycorrhiza induced resistance is associated with priming for an efficient activation of defence mechanisms upon attack. The spectrum of mycorrhiza induced resistance efficiency correlates with a potentiation of jasmonate-dependent plant defences (Pozo and Azcón-Aguilar, 2007). Furthermore, indirect plant defense mechanisms have been observed to be modulated in AM plants, as

the volatile blends released by AM plants attractive to aphid parasitoids (Guerrieri et al., 2004).

The increased tolerance of mycorrhizal plants to water deficit is also due to the regulation of several physiological processes. One of the main reasons of the improved water status of the mycorrhizal plants is the direct transfer of water that is taken up by the fungal hyphae to the plant roots from water reservoirs in the soil inaccessible for the roots (Ruth et al., 2011). A potential water transport *via* AM fungus to the host plant has been suggested on the basis of the gene expression profiles of three fungal aquaporin genes, thus supporting the existence of a direct AM fungus involvement in plant tolerance to drought (Aroca et al., 2009; Li et al., 2013). On the other hand, to take water efficiently from soils affected by osmotic stress, roots (and AM mycelium) have to decrease their osmotic potential below that of the soil. AM fungi have been shown to ameliorate the plant osmotic adjustment by accumulation of different compounds such as proline and sugars (Sheng et al., 2011; Ruiz-Lozano et al., 2011).

Under osmotic stress conditions, AM symbiosis also regulates host plant aquaporins and root hydraulic properties (Aroca et al., 2007). Bárzana et al. (2014) found that the AM symbiosis regulates the expression of a wide number of aquaporin genes in the host plant, and that it depends on the watering conditions and on the severity of the drought stress imposed. Recently, it has been shown that plant cation transporter genes are regulated in AM plants under saline conditions, as a mechanism for mitigation of ionic imbalance by the AM symbiosis, in maize plants as well as in rice (Estrada et al., 2013*a*; Porcel et al., 2016). In rice, the enhanced tolerance of the mycorrhizal plants to salinity was attributed to a decrease of Na^+ root-to-shoot distribution and an increase of Na^+ accumulation in the roots (Porcel et al., 2016). Finally, it is becoming clear that the AM symbiosis protects the host plant against the detrimental effect of reactive oxygen species (ROS) generated by osmotic stress conditions (Ruiz-Sánchez et al., 2010; Porcel et al., 2012; Estrada et al., 2013*b*).

Mechanisms underlying AM tolerance to HM stress will be addressed in the next section.

2. The heavy metal paradox in arbuscular mycorrhiza: from mechanisms to biotechnological applications

Adapted from:

Ferrol N, Tamayo E*, Vargas P*. 2016.

The heavy metal paradox in arbuscular mycorrhiza:

from mechanisms to biotechnological applications.

Journal of Experimental Botany 67, 6253-6265. doi: 10.1093/jxb/erw403

*These two authors contributed equally to this work.

Abstract

Arbuscular mycorrhizal (AM) symbioses that involve most plants and Glomeromycota fungi are integral and functional parts of plant roots. In these associations, the fungi not only colonize the root cortex but also maintain an extensive network of hyphae that extend out of the root into the surrounding environment. These external hyphae contribute to plant uptake of low mobility nutrients, such as P, Zn and Cu. Besides improving plant mineral nutrition, AM fungi can alleviate heavy metal (HM) toxicity to their host plants. HMs, such as Cu, Zn, Fe and Mn, play essential roles in many biological processes but are toxic when present in excess. This makes their transport and homeostatic control of particular importance to all living organisms. AM fungi play an important role in modulating plant HM acquisition in a wide range of soil metal concentrations and have been considered to be a key element in the improvement of micronutrient concentrations in crops and in the phytoremediation of polluted soils. In the present review, we provide an overview of the contribution of AM fungi to plant HM acquisition and performance under deficient and toxic HM conditions, and summarize current knowledge of metal homeostasis mechanisms in arbuscular mycorrhizas.

Key words: arbuscular mycorrhiza, biofortification, heavy metals, heavy metal homeostasis, micronutrients, phytoremediation

Introduction

Some HMs, such as Cu, Fe, Zn, Co and Mn, are required for the normal growth, development and reproduction of plants. These transition metals are essential and are considered to be mineral micronutrients. Some of these elements (Cu and Fe) are redox-active, which is the basis for their occurrence as catalytically active cofactors in many metalloenzymes. Other metals (like Zn) have, in addition to their catalytic role, a structural function in stabilizing proteins. However, when present in high concentrations, the same redox properties that make metal ions essential elements lead to the formation of reactive oxygen species (ROS) with detrimental consequences for the cell (Palmer and Guerinot, 2009; Puig and Peñarrubia, 2009). Furthermore, plants must deal with other metals (Hg, Cd, Pb) and metalloids (As), which may potentially be harmful.

Plants are challenged by environmental HM concentrations that fluctuate from low to high toxic levels. In addition, plants have to fit the variable demands of different tissues during growth and development or in response to environmental cues. To fulfil their requirements for metabolic processes and to minimize the deleterious effects of the excesses and deficits of essential HMs in the environment, plants have developed flexible and adaptive strategies of HM homeostasis. These homeostatic and detoxification mechanisms, which have been reviewed extensively, involve metal uptake pathways, chelation and/or trafficking within the cell, delivery of metals into cellular compartments, organelles, and enzymes as well as systems for HM storage and efflux and long-distance transport (DalCorso et al., 2013; Viehweger, 2014).

The first important process in plant HM homeostasis is metal acquisition. Even when abundant, HMs can be inaccessible in the soil owing to their tendency to be present predominantly in an insoluble form. To cope with the inaccessibility of these elements, plants use either a reductive or chelation strategy, although probably one of the most important strategies is the association with rhizosphere microorganisms and, in particular, with AM fungi, one of the most prominent groups of soil microorganisms (Barea, 1991).

In addition to nutrient uptake, AM fungi improve plant performance through increased defence against environmental stresses, both biotic and abiotic, such as drought, salinity, HM toxicity and organic pollutants (Smith and Read, 2008). The potential of AM fungi, on the one hand, to increase the uptake of low mobility metal micronutrients when plants grow in soils deficient in these elements and, on the other hand, to alleviate HM toxicity in polluted soils has led to the hypothesis that arbuscular mycorrhizas function as a "buffer" to protect the plant against damage caused by HMs in the soil. In the present review, we provide an overview of the contribution of AM fungi to plant HM acquisition and performance under deficient and toxic HM conditions and summarize current knowledge of HM homeostasis mechanisms in arbuscular mycorrhizas.

Contribution of arbuscular mycorrhizas to plant micronutrient nutrition

Although the main benefit of arbuscular mycorrhizas is an improved plant P status, root colonization by AM fungi often results in enhanced uptake of micronutrients when plants grow in deficient soils (Li et al., 1991; Liu et al., 2000; Ryan and Angus, 2003). Since Zn, Cu, Fe and Mn are poorly mobile in soil, improvements in micronutrient nutrition by AM fungi are mainly due to the capability of the external mycelium to explore and exploit larger volumes of soil.

Using a compartmented pot system with separate soil zones for hyphal growth where the micronutrient was only supplied to the hyphal compartment, Li et al. (1991) demonstrated, in white clover and later, Lee and George (2005) in cucumber, that *Glomus mosseae*- renamed as *Funneliformis mosseae* (Schüßler and Walker, 2010) and henceforth called *F. mosseae*- contributed up to 62 and 75 % of total Cu uptake, respectively. While this contribution was shown to be independent of the effects of mycorrhizal colonization on P nutrition, Cu partitioning between roots and shoots was strongly affected by P (Li et al., 1991). Increased Cu uptake in mycorrhizal plants has been confirmed for a number of plant-fungus combinations (Manjunath and Habte, 1988; Lambert and Weidensaul, 1991). A recent meta-analysis of studies reporting the contribution of arbuscular mycorrhizas to

crop metal micronutrient nutrition shows that AM fungi exert a significant generally positive effect on Cu nutrition (Lehmann and Rillig, 2015).

The importance of AM fungi in plant Zn nutrition has long been recognized and extensively reviewed (Thompson, 1990; Cavagnaro, 2008, 2014). However, the contribution of the mycorrhizal pathway to plant Zn uptake was difficult to demonstrate because of the strong relationship between P and Zn nutrition in most plant species. Zn uptake in mycorrhizal plants has been shown to be dependent on soil Zn and P concentrations (Chen et al., 2003; Ryan and Angus, 2003; Watts-Williams et al., 2013). Under low P fertilization, the uptake of P, Zn and other micronutrients increases in mycorrhizal plants. However, at higher soil P concentrations, mycorrhizal colonisation was usually lower; and the potential for arbuscular mycorrhizas to take up Zn and other nutrients may be reduced (Watts-Williams et al., 2013; Watts-Williams and Cavagnaro, 2014). Direct evidence of Zn uptake by AM fungi comes from studies using ^{65}Zn as a tracer in compartments only accessible by the external hyphae. Using an agar plate system, Cooper and Tinker (1978) demonstrated that ^{65}Zn was translocated along the hyphae of *F. mosseae* into *Trifolium repens* and that the rate of ^{65}Zn translocation was lower than the rate of translocation of P. Bürkert and Robson (1994) showed that Zn uptake is influenced by the distribution and length of the ERM in soil. These observations were corroborated by Jansa et al. (2003), who demonstrated that the external mycelium of *Glomus intraradices* -renamed as *Rhizophagus irregularis* (Schüßler and Walker, 2010) and henceforth called *R. irregularis*- was able to take up both ^{65}Zn and ^{33}P from distances of up to 14 cm, although a much higher proportion of ^{33}P than ^{65}Zn was transported to the plant. These studies provide clear evidence of the capability of the external hyphae to transfer Zn to the plant, but they provide little information on the relative importance of the mycorrhizal uptake pathway. Recently, Watts-Williams et al. (2015) reported that the contribution to shoot Zn via the mycorrhizal pathway in tomato plants colonized by *R. irregularis* depends on soil Zn concentrations, with a maximum contribution (24%) found to be at the lowest level of Zn in the soil. Increasing the level of Zn in soil significantly decreased the contribution of the mycorrhizal pathway, while the contribution of the direct uptake by roots increased.

Data on the effect of mycorrhizal colonisation on Fe concentration in plant tissues and on total plant Fe uptake are variable and inconsistent. The meta-analysis, mentioned above, of >200 studies reporting the contribution of arbuscular mycorrhizas to micronutrient concentrations in crops shows that AM fungi have an overall positive effect on crop Fe nutrition, although this effect is only significant in roots (Lehmann and Rillig, 2015). Direct evidence of the contribution of the mycorrhizal uptake pathway to shoot Fe content was provided by Caris et al. (1998) using ^{59}Fe as a tracer in compartmented pots. These authors observed that *F. mosseae* hyphae were able to take up ^{59}Fe from labelled soil and to transfer it to sorghum but not to peanut plants. This difference in ^{59}Fe acquisition may be due to the fact that these two plant species use different strategies for Fe acquisition (Kim and Guerinot, 2007). Peanut is a dicotyledoneous and activates a reduction-based Strategy I when starved of Fe (enhanced net excretion of protons from the roots and increased Fe-reducing capacity), while sorghum is a graminaceous and activates a chelation-based Strategy II (enhanced release of phytosiderophores from the roots). More recently, Fe uptake via the mycorrhizal pathway in maize, another Strategy II plant, has also been reported (Kobae et al., 2014). Further tracer studies need to be carried out on other plant species to determine if AM fungi also contribute to Fe uptake in Strategy I plants.

Uptake of other micronutrients via external hyphae is not so well established (Marschner and Dell, 1994). The uptake of Mn has repeatedly been found to be lower in mycorrhizal plants (Liu et al., 2000; Corrêa et al., 2014), although, in some cases, Mn uptake was observed to be higher (Eivazi and Weir, 1989; Lehmann and Rillig, 2015). The negative effect of arbuscular mycorrhizas on Mn uptake has been attributed to a shift in the composition and activity of rhizosphere microorganisms caused by inoculation with AM fungi which decreased the abundance of Mn-reducers (Kothari et al., 1991).

Contribution of arbuscular mycorrhizas to plant metal tolerance

HM toxicity in plants can be caused by excessive uptake of both essential and non-essential metals from the soil. Although arbuscular mycorrhizas usually increase plant HM tolerance, the effects of AM fungi on

plant performance in metal-contaminated soils depend on the fungal isolate, plant species and HM involved in the association.

Alleviation of plant HM toxicity by AM fungi is not necessarily associated with a reduced HM uptake. Large effects of AM fungi in increasing plant HM accumulation have been reported (Joner and Leyval, 2001; Carvalho et al., 2006; de Andrade et al., 2008; de Souza et al., 2012). In many cases, the potentially toxic effects decreased because the actual metal concentrations were reduced as a consequence of the improvement in P nutrition and growth of the mycorrhizal plant (Joner and Leyval, 2001; Chen et al., 2003). However, growth stimulation induced by inoculation with AM fungi is not always connected with lower metal concentrations in plant tissues. For example, alleviation of Cu and Zn phytotoxicity was found in a white poplar clone colonized by either *F. mosseae* or *R. irregularis* despite the higher Cu and Zn concentrations of the mycorrhizal plants (Lingua et al., 2008).

Arbuscular mycorrhizas often results in increased concentrations of HMs in roots but lower shoot metal partitioning (Joner and Leyval, 1997; Chen et al., 2005; Sheikh-Assadi et al., 2015; Wu et al., 2016). A pioneering study by Joner and Leyval (1997), using ^{109}Cd and compartmented pots in *Trifolium subterraneum*, reveals that AM fungi can transport Cd from soil and that a large proportion of the Cd content of the mycorrhizal plants was sequestered in roots. Metal stabilization in mycorrhizal roots and their preferential accumulation in intraradical fungal structures rather than in root cells have been confirmed in element localization studies in mycorrhizal roots using spectroscopic techniques (Turnau et al., 1993; Turnau, 1998; Wu et al., 2016).

In other cases, AM fungi have been shown to reduce plant HM uptake (Heggo et al., 1990; Li and Christie, 2001; Tullio et al., 2003). For example, a decrease in Zn uptake and in root and shoot concentrations were found in red clover (Li and Christie, 2001) and tomato (Watts-Williams et al., 2013) mycorrhizal plants grown under high Zn conditions. In addition to metal immobilization in the ERM, reduced metal uptake in mycorrhizal plants may be attributed to changes in metal solubility mediated by changes in the soil solution of the mycorrhizal treatments. Similarly to Zn, reduced uptake of the metalloid As by mycorrhizal roots has been shown in several studies

(Gonzalez-Chavez et al., 2002; Ultra et al., 2007; Christophersen et al., 2012; Chen et al., 2013). In this case, given that plant arsenate tolerance involves constitutive suppression of the high-affinity phosphate uptake system (which also transports arsenate), increased tolerance of mycorrhizal plants to arsenate could be due to the involvement of arbuscular mycorrhizas in compensating for the inhibition of high-affinity phosphate uptake systems and low growth caused by arsenate toxicity. In fact, a higher P/As molar ratio was found in *Holcus lanatus* (Gonzalez-Chavez et al., 2002), *Medicago truncatula* (Christophersen et al., 2012) and rice (Chen et al., 2013) mycorrhizal plants. Furthermore, the pioneering work of Gonzalez-Chavez et al (2002) shows that enhanced arsenate tolerance of mycorrhizal plants is due to the ability of AM fungi to further suppress arsenate influx into the host.

The frequency of AM fungi (determined by spore counts or root colonization) is generally lower in HM contaminated soils than in non-polluted soils. However, propagules of AM fungi never disappear and these indigenous fungi are often more tolerant to high HM concentrations and more efficient at enhancing plant HM tolerance. For example, the *R. irregularis* Br1 ecotype isolated by Hildebrandt et al. (1999) from the rhizosphere of the metallophyte species *Viola calaminaria* was consistently shown to be more effective in conferring HM tolerance on a variety of plants (tomato, maize and *M. truncatula*) than an ecotype of the same species isolated from a non-contaminated soil (Kaldorf et al., 1999).

Mechanisms of HM homeostasis in arbuscular mycorrhizas

To balance transition metal requirements and to avoid their potential toxic excess, cellular concentrations of these elements are tightly controlled. Due to the essential roles played by some metals in living organisms, a lack or excess of these elements should have a profound effect not only on the plant but also on the fungus and, by extension, in their interaction. Interest in fundamental biological questions of HM homeostasis in arbuscular mycorrhizas has increased during the last 10-15 years. During this period, several potential HM tolerance factors have been identified. Their key elements are chelation and sequestration, which result in inactivation and

removal of toxic HMs from sensitive sites, and metal transport systems, which control HM acquisition and efflux.

Metal uptake systems

Uptake of essential and non-essential HMs from the soil in arbuscular mycorrhizas occurs through specific transport proteins localized in the plant and fungal plasma membranes. In recent decades, large families of metal transporters have been identified in plant genomes (Mäser et al., 2001; Benedito et al., 2010; Kiranmayi et al., 2014; Vatansever et al., 2016) and, more recently, in the genome of *R. irregularis* (Tisserant et al., 2013). However, only a limited number of metal transporters have so far been characterized in arbuscular mycorrhizas. In this section, we focus on plant and fungal transporters putatively involved in the mycorrhizal uptake of essential metal micronutrients and of non-essential HMs.

(i) Fungal metal transporters

Movement of essential metals through the mycorrhizal uptake pathway begins with their uptake through the plasma membrane of the ERM (Fig. 1A).

Most of the metals taken up by the fungus may be used to maintain fungal functioning while surplus metal is transferred to the plant. Irrespective of the metal´s final destination, once it reaches the fungal cytoplasm it has to be delivered to its specific targets. Since free HMs in the cytosol could represent a serious threat, organisms have developed mechanisms to sequester and deliver them in a bound-form. In the case of Cu, the Cu chaperones collect the metal from the influx transporters and deliver it to efflux transporters or to apometalloproteins. In the *R. irregularis* genome, three genes encoding putative chaperones have been identified: RiATOX1, RiSco1 and RiSSC that deliver Cu to the ATPases, the cytochrome C oxidase synthesis and the Cu, Zn superoxide dismutase, repectively.

Metal supply to the plant requires metal translocation through hyphae from the ERM to the arbuscules, the fungal structures involved in nutrient transfer to the plant.

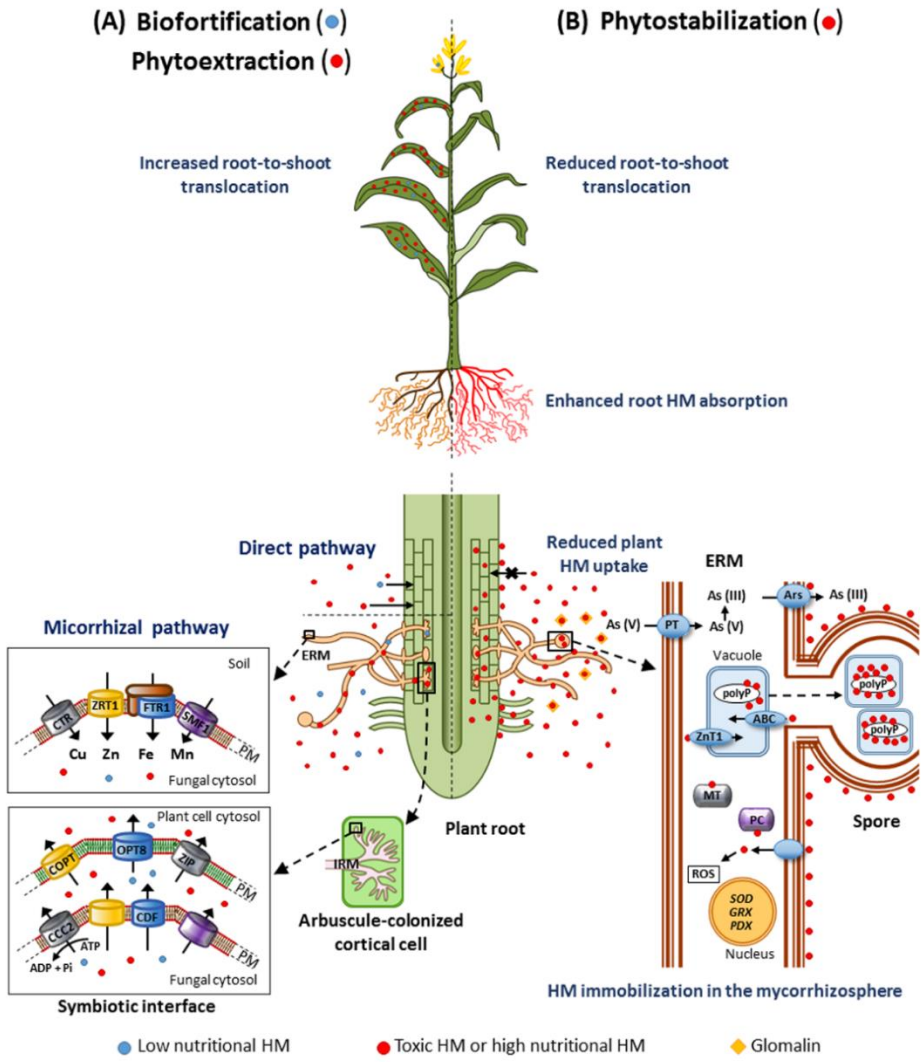

Figure 1. Schematic representation of arbuscular mycorrhizas contribution to plant heavy metal (HM) acquisition and distribution.

(A) Enhanced uptake and shoot transfer.

Under metal deficient conditions, metals are taken up through the direct pathway and the mycorrhizal pathway, with arbuscular mycorrhizas thus contributing to metal biofortification. The direct pathway involves high-affinity metal transporters located in root hairs and epidermal cells. The mycorrhizal pathway involves high-affinity metal transporters located at the extraradical mycelium (ERM), followed by metal translocation along the hyphae to intracellular structures (IRM) and then transfer to the root at the symbiotic interface. The putative fungal and plant metal transporters involved in the mycorrhizal pathway are

illustrated (panels in lower left corner). CTR: Fungal Cu transporter, CCC2: Cu-ATPase, CDF: Cation diffusion facilitator, COPT: Plant Cu transporter, FTR1: Fe permesase, OPT: Oligopeptide transporter, SMF1: Mn transporter, ZRT1: Zn transporter, ZIP: Zn-Fe permease (some ZIP members transport Mn).

Under toxic HM conditions, increased biomass of mycorrhizal plants resulting from enhanced P nutrition leads to increased removal of HMs from the soil, with arbuscular mycorrhizas thus contributing to HM phytoextraction.

(B) Soil HM immobilization.

HMs are stabilised in the AM fungal structures, with arbuscular mycorrhizas thus contributing to HM phytostabilisation. Mechanisms of HM tolerance in the fungus are illustrated in the lower right hand corner of the diagram. These mechanisms include: HM binding to cell wall, chelation by glomalin, decreased uptake and/or increased efflux to the exterior, chelation of metal ions in the cytosol, HM compartmentalization in the vacuoles and activation of antioxidant defences. In the vacuoles, HMs are stabilised with polyP and some of these vacuoles are translocated to the spores.

ABC: ABC transporter, Ars: Arsenite pump, GRX: Glutaredoxin, MT: Metallothionein, PC: Phytochelatin, PDX: Pyridoxine synthase, PT: P transporter, ROS: Reactive oxygen species, SOD: Superoxide dismutase, ZnT1: Zn transporter.

Taking into account that vacuoles are considered to be major sites for provisional HM storage for later remobilization when nutritional demand increases, that polyP accumulated in the fungal vacuoles play a central role in the long-distance translocation of P through hyphae (Cox et al., 1980; Hijikata et al., 2010) and that metals co-localize with polyP in the fungal vacuoles (González-Guerrero et al., 2008; Nayuki et al., 2014), long-distance translocation is likely to occur in the fungal vacuoles.

Once they reach the IRM, release from the fungus in the apoplast of the symbiotic interface could be facilitated by a yet uncharacterized ion-specific carrier, pump or channel, such as a plasma membrane Cu-ATPase or a member of the Cation Diffusion Facilitator (CDF) family. As previously reported for the fungal phosphate and ammonium transporters (Benedetto et al., 2005; Pérez-Tienda et al., 2011; Calabrese et al., 2016), two metal uptake transporters, the Zn transporter RiZRT1 (Hildebrandt et al., 2007) and the Fe permease RiFTR1 (Tisserant et al., 2013), are highly expressed in mycorrhizal roots, which suggests that the plant and the fungus compete for these metals at places of close contact. Due to the importance of metals for life, it is not surprising that organisms compete for them when in short supply and that

they activate the transport systems enabling the uptake of metals required for their development.

Since non-essential HMs are toxic, specific transporters for their uptake and transport are unlikely to exist in AM fungi. Their transport is thus probably accomplished by transport systems for the essential elements Cu, Zn, Fe and Mn, or even through phosphate transporters, as it has been shown for the uptake of the metalloid arsenate that occurs via the high-affinity phosphate transporter GiPT (González-Chávez et al., 2011).

(ii) Plant metal transporters

Metals released by the fungus at the symbiotic interface are likely to be taken up by specific plant transporters expressed in the periarbuscular membrane (Fig. 1A). Up-regulation of genes encoding putative metal transporters in mycorrhizal roots has been observed in several transcriptomic analyses aimed at identifying plant genes induced in arbuscular mycorrhizas (Table 1). For example, Gomez et al. (2009) described induction of putative Zn (7.6 fold) and Cu (50 fold) transporters in *M. truncatula* mycorrhizal roots. Induction of four Zn transporters and of some Fe transport related proteins, such as a vacuolar Fe transporter and a ferric-chelate reductase, have also been reported in sorghum mycorrhizal roots (Handa et al., 2015). Genome-wide analyses of transcription patterns in laser microdissected cortical cells colonized by arbuscules revealed that the Cu transporter previously described by Gomez et al. (2009) was specifically expressed in arbuscule-containing cortical cells, suggesting that it might be involved in Cu acquisition by the periarbuscular membrane (Hogekamp et al., 2011; Gaude et al., 2012). However, since some transporters, such as a putative Zn transporter and the Mn transporter MtZIP7, were expressed both in arbuscule-colonized and in adjacent non-colonized cortical cells, metal uptake seems not to be restricted to the arbuscules.

Table 1. List of plant metal transporters identified in different transcriptomic analysis with enhanced expression in mycorrhizal roots.

Transport Family	Plant	Gen ID/ Probe Set	Proposed substrate	Reference
Zinc (Zn^{2+})-Iron (Fe^{2+}) Permease (ZIP)	*L. japonicus*	LjSGA_035191.1	Zn	Handa *et al.*, 2015
		CM0019.90.r2.m	Zn	Handa *et al.*, 2015
		LjSGA_021647.2	Zn	Handa et al., 2015
		CM1826.100.r2.m	Zn	Handa *et al.*, 2015
	M. truncatula	Msa.2748.1.S1_at	Zn	Hogekamp *et al.*, 2011
		AJ499771	Zn	Gomez *et al.*, 2009
		Medtr3g058630.1[a]	Mn (MtZip7)	Hogekamp *et al.*, 2011
Copper Transporter (COPT)	*M. truncatula*	Medtr7g066070.1[b]	Cu	Gomez *et al.*, 2009; Gaude *et al.*, 2012; Hogekamp *et al.*, 2011
		Medtr3g105330.1	Cu	Hogekamp and Küster, 2013
Vacuolar iron transporter (VIT)	*L. japonicus*	CM0337.610.r2.m	Fe	Handa *et al.*, 2015
Oligopeptide Transporter (OPT)	*M. truncatula*	Mtr.7741.1.S1_at	Metal complexes[d]	Hogekamp *et al.*, 2011 ; Gomez *et al.*, 2009
		Mtr.4863.1.S1_at	Metal complexes	Hogekamp *et al.*, 2011 ; Gomez *et al.*, 2009
		Medtr2g017750.1	Metal complexes	Hogekamp *et al.*, 2011
		Medtr8g087780.1[c]	Metal complexes	Gaude *et al.*, 2012
	Zea mays	OPT8a	Fe-NA	Kobae *et al.*, 2014
		OPT8b	Fe-NA	Kobae *et al.*, 2014

[a, b, c] New loci associated to the Affymetrix probe sets: Mtr.40995.1.S1_at[a], Mtr.37110.1.S1_at[b], and Mtr.17764.1.S1_at[c], in the *M. truncatula* Genome Project v4.0 http://jcvi.org/medicago/)

[d] OPTs transport a broad range of substrates (peptides, GSH, GSH-Cd, PC_n-Cd, Fe-NA complexes).

In maize, a plant that uses a Strategy II for Fe uptake, based on the biosynthesis and secretion into the rhizosphere of the phytosiderophore deoxymugineic acid (DMA) and further uptake of the DMA-Fe(III) complexes through a YELLOW STRIPE 1 (YS1) protein, arbuscular mycorrhizas did not affect the expression of a gene encoding the DMA synthase or the ZmYS1 transporter despite the fungal contribution to Fe uptake. However, arbuscular mycorrhizas up-regulated two nicotinianamine synthase isoforms, enzymes that synthesize an immediate precursor of DMA, and of two oligopeptide transporters (ZmOPT8a and ZmOPT8b) (Kobae et al., 2014). Since nicotianamine plays a dominant role in intracellular and intercellular Fe transport (Zhou et al., 2013), it was suggested that it might chelate the Fe delivered by the fungus. Substrate specificity of the OPT family is broad, but since some OPTs transport free metals (Wintz et al., 2003) and Fe-nicotianamine conjugates (Vasconcelos et al., 2008), ZmOPT8 might be involved either in Fe uptake by the periarbuscular membrane or in long-distance transport in mycorrhizal roots. In this respect, two, so far uncharacterized, oligopeptide transporters have been specifically found to be expressed in arbuscule-colonized cells (Gomez et al., 2009; Hogekamp et al., 2011; Gaude et al., 2012). However, further studies are needed to confirm these hypotheses.

Responses to HM imbalances

The primary response of living organisms to an insufficient supply of essential transition metals is to activate uptake systems to efficiently incorporate the micronutrient. Conversely, under excess HM conditions, non-specific metal uptake seems unavoidable, and organisms activate intracellular chelation and compartmentalization mechanisms. Moreover, since high intracellular concentrations of HMs generate ROS, activation of antioxidant defences also occurs under HM excess conditions. Recently reported strategies evolved by AM fungi to survive in HM polluted soils and how plant responses to HM toxicity are modulated by the symbiosis are described below.

(i) Fungal strategies for dealing with HM toxicity

(i) Restriction of HM entry

Two common strategies used by soil microorganisms to prevent HMs from entering the cytoplasm are the release of HM complexing agents into the surrounding soil and precipitation or binding of the metal onto the cell surface. The effect of AM fungal exudates on HM bioavailability has received little attention. However, AM fungi produce glomalin (glomalin-related protein), initially believed to be a secreted hydrophobin and later identified as a spore and cell wall localized 60 kDa heat shock protein (Wright and Upadhyaya, 1996), which appears to play a role in HM immobilization. Several studies have demonstrated the capability of these glomalin soil related proteins to sequester Cu, Cd, Fe, Pb, Zn and Cr, and to reduce HM bioavailability (González-Chávez et al., 2004; Cornejo et al., 2008; Gil-Cardeza et al., 2014).

The importance of the fungal wall in HM retention has been shown in several studies (Galli et al., 1994; Joner et al., 2000; Gonzalez-Chavez et al., 2002). Joner et al. (2000) found that the fungal wall is responsible for 50 % of the metal retained by AM fungi and that this adsorption is extremely fast. Accumulation of HMs in the hyphae and spore cell walls has been corroborated using transmission electron microscopy connected to an energy dispersive X-ray spectrometer (Gonzalez-Chavez et al., 2002; González-Guerrero et al., 2008) and synchrotron micro X-ray fluorescence (Nayuki et al., 2014). The affinity of the wall for HMs is not surprising given the significant HM-binding abilities of the major constituents of fungal cell walls (e.g., chitin, melanin, and, in the case of AM fungi, glomalin). In general, it was found that the spore wall retained a higher concentration of HMs than the hyphal wall (González-Guerrero et al., 2008) and that HM retention differs between species (Gonzalez-Chavez et al., 2002). These variations might be due to differences in cell wall composition and/or structure of hyphae and spores and of different fungal species.

(ii) Intracellular chelation

Chelation of HMs in the cytosol by high-affinity ligands is potentially a very important mechanism of HM detoxification and tolerance. Potential ligands include amino acids and organic acids, and two classes of peptides, phytochelatins and metallothioneins (Hall, 2002). In AM fungi, the only chelators characterized so far are metallothioneins, short cytosolic cysteine-rich proteins capable of tightly binding metals. A gene encoding a metallothionein has been identified in *Gigaspora margarita* (Lanfranco et al., 2002) and in *R. irregularis* (González-Guerrero et al., 2007). Although both genes were constitutively expressed, they were able to restore Cu tolerance to a metallothionein deficient yeast, and their expression was up-regulated under Cu stress, indicating that metallothioneins play a role in metal stress protection. Glutathione (GSH) and GSH oligomers, such as phytochelatins, are also likely to be associated with HM resistance in AM fungi. In this respect, a yet uncharacterized gene putatively encoding a phytochelatin synthase is present in the *R. irregularis* genome (Shine et al., 2015).

(iii) HM compartmentalization

Metal sequestration in the vacuolar compartment is also an important cellular mechanism of HM tolerance in AM fungi. An accumulation of Zn, Cu and Cd was observed in the vacuoles when the ERM of *R. irregularis* grown in association with carrot root organ cultures was exposed to these metals (González-Guerrero et al., 2008). Vacuolar accumulation of Cd was also observed in the Cd-exposed ERM of *R. irregularis* in symbiosis with clover (Yao et al., 2014) and in the ERM of *Gigaspora margarita* in symbiosis with *Lotus japonicus* (Nayuki et al., 2014). Since these studies revealed metal co-localization with polyP, it was suggested that polyP acts as a counter ion that stabilizes the metal in the fungal vacuoles. Analysis of transport systems at the tonoplast has provided further evidence of the importance of the vacuolar mechanism of tolerance in AM fungi. González-Guerrero et al. (2005) proposed that GintZnT1, a homolog of the yeast vacuolar Zn transporter zrt1, is involved in Zn detoxification in *R. irregularis*. GintZnT1 was shown to decrease Zn cytosolic levels in yeast and its expression pattern in response to Zn correlated with the accumulation pattern of Zn in the vacuoles (González-

Guerrero et al., 2005, 2008). The *R. irregularis* ABC transporter *GintABC1*, putatively encoding a homolog of the yeast Cd factor that transports bis-GSH-Cd complexes across the tonoplast (Li et al., 1996), has also been proposed to be involved in Cd and Cu internalization in vacuoles (González-Guerrero et al., 2010*a*).

Besides vacuolar compartmentalization, AM fungi can compartmentalize excess metal in the spores. Cornejo et al. (2013) reported the presence of green-blue spores of *Claroideoglomus claroideum* in a Cu-polluted soil and of *R. irregularis* grown monoxenically and exposed to Cu. The blue-green colour was associated with an accumulation of Cu in the cytoplasm. Since these spores were metabolically inactive, it was suggested that another fungal strategy for survival in Cu-polluted environments is metal compartmentalization in some spores. An accumulation of Al in *R. irregularis* spores has also been observed (Aguilera et al., 2011).

(iv) HM efflux

An alternative way of controlling intracellular HM levels involves the active efflux of metal ions. Since most of these cations are essential, complete exclusion is not possible and selective efflux would be more likely. The only example of HM efflux as an adapted tolerance mechanism in AM fungi is in relation to As toxicity. As discussed above, uptake of arsenate by *R. irregularis* occurs via the high-affinity phosphate transporter GiPT (González-Chávez et al., 2011). By using microspectroscopic X-ray fluorescence and microespectroscopic X-ray absorption near edge structure, González-Chávez et al. (2014) found that arsenate taken up by the hyphae was rapidly reduced to arsenite. These authors also found a time-concerted induction of *GiPT* expression followed by *GiArsA*, a putative arsenite efflux pump, and suggested that As tolerance in AM fungi involves a rapid reduction of arsenate to arsenite and subsequent efflux, probably via the arsenite efflux pump GiArsA.

(v) Antioxidant defences

HMs partially cause cell damage by inducing oxidative stress. This is particularly true for redox-active metals, such as Cu or Fe, which generate

ROS (Halliwell and Gutteridge, 1989). The effect of oxidative stress on AM fungi has been assessed by analysing alterations induced by Cu in some redox metabolic components of *R. irregularis*. As expected, Cu stress induces ROS accumulation and oxidative damage to the fungal membranes (Benabdellah et al., 2009b; González-Guerrero et al., 2010*b*). To deal with this imbalanced redox status and to repair the damage caused by Cu, the fungus activates the expression of genes encoding some components of its antioxidant network, such as *GintSOD1* encoding a superoxide dismutase (González-Guerrero et al., 2010*b*), *GintGRX1* encoding a multifunctional protein displaying oxidoreductase, peroxidase and glutathione S-transferase activity (Benabdellah et al., 2009*b*) and *GintPDX1*, encoding an enzyme involved in vitamin B6 biosynthesis (Benabdellah et al., 2009*a*). Since superoxide dismutases directly act as ROS detoxifiers, GintSOD1 is probably involved in scavenging ROS resulting from redox Cu activity (González-Guerrero et al., 2010*b*). However, GintGRX1 is likely to play a role in protecting the fungus against Cu-induced oxidative damage, given that glutaredoxins act as redox regulators of protein thiols and are involved in maintaining the cell redox balance.

In addition to these enzymatic systems, AM fungi possess small molecules, such as GSH and vitamins B6, C and E, which act as antioxidants. The contribution of GSH to mitigating the redox imbalance caused by toxic metals has not been directly assessed. However, since toxic HMs induce the expression of genes encoding proteins that use GSH as a cofactor (glutaredoxins) or as a substrate (glutathione-S-transferases; (Waschke et al., 2006; Hildebrandt et al., 2007), tolerance of AM fungi to toxic HMs should also be dependent on GSH metabolism.

The fungal mechanisms of HM tolerance described above are summarized in Fig. 1B.

(ii) Regulation of plant HM responses

Since AM fungi usually reduce plant HM availability, down-regulation of pathways involved in stress responses and HM detoxification is expected to occur in mycorrhizal plants. In this respect, several studies have shown that plant HM responses are modulated by the symbiosis. For

example, Repetto et al. (2003), using a proteomic approach, observed that mycorrhizal establishment modulated the expression of proteins involved in Cd-responses in the roots of a Cd-sensitive pea genotype. In *M. truncatula*, it was also observed that the proteomic changes induced by Cd in non-mycorrhizal roots were absent or inverse in mycorrhizal roots, including down-accumulation of Cd stress-responsive proteins (Aloui et al., 2009).

Several studies have addressed the impact of AM fungi on specific molecular players of plant HM tolerance, but the results are sometimes controversial. Special attention has been paid to the study of the role of antioxidant enzymes, metallothioneins and phytochelatins. Transcript analysis of stress defence genes in a poplar clone grown in a polluted soil showed that AM fungi reduced transcript abundance of genes involved in antioxidant defence in roots and leaves and induced the expression of a gene encoding a phytochelatin synthase in leaves (Pallara et al., 2013). Reduction or no change in the activity of antioxidant enzymes, such as superoxide dismutase, GSH reductase and peroxidase, has also been observed in the tissues of mycorrhizal plants grown under HM toxic conditions and has been attributed to their lower metal content (Meier et al., 2011; Garg and Kaur, 2013; Kumar et al., 2015). However, other studies have reported that these enzymes are activated in mycorrhizal plants. For example, Garg and Aggarwal (2012) reported that colonization of *Cajanus cajan* by *F. mosseae* in a polluted soil increased superoxide dismutase, catalase and peroxidase activities, despite the lower tissue metal concentrations of the mycorrhizal plants.

Concerning HM chelators, Ouziad et al. (2005) observed in tomato that under HM toxic conditions arbuscular mycorrhizas induced down-regulation of metallothionein gene expression, which was attributed to the lower HM concentration of the mycorrhizal plants. By contrast, in poplar, AM fungi considerably up-regulated the expression of several metallothionein isoforms. Since mycorrhizal poplar plants accumulated more metals than their non-mycorrhizal counterparts, it was suggested that metallothioneins afford protection against HM induced stress (Cicatelli et al., 2010, 2012). However, in other cases, metallothionein gene expression patterns did not correlate with the metal concentration of plant tissues (Rivera-Becerril et al., 2005; Dabrowska et al., 2012). The contribution of phytochelatins to metal tolerance

in arbuscular mycorrhizas has also been addressed in different plant-fungus-metal combinations (Christophersen et al., 2012; Cicatelli et al., 2012; Degola et al., 2015; Jiang et al., 2016). Most of these studies have revealed that, under HM toxic conditions, arbuscular mycorrhizas induced up-regulation of phytochelatin synthase gene expression and an accumulation of phytochelatins. Polyamines have been also involved in HM stress recovery in mycorrhizal plants (Lingua et al., 2008).

Increased HM tolerance of mycorrhizal plants may also be related to changes in gene expression and protein synthesis induced by the symbiosis itself. Upon mycorrhizal colonization, a significant transcriptomic reprogramming occurs in the plant, leading to important changes in the plant primary and secondary metabolism and regulation of the plant defence mechanisms (Harrison, 1999; Hause and Fester, 2005). These changes usually have a major impact on plant physiology, altering the plant's ability to cope with biotic and abiotic stresses (Jung et al., 2012). Aloui et al. (2009), using a proteomic approach to study the mechanisms of Cd stress alleviation in *M. truncatula* by *R. irregularis*, observed that the symbiotic proteome displayed low sensitivity to Cd and suggested that part of the symbiotic program may be used to counteract Cd toxicity through the mycorrhiza-dependent synthesis of proteins putatively involved in alleviating oxidative damage.

Arbuscular mycorrhizas have been also shown to modulate transcriptomic and proteomic leaf responses to HM stress (Aloui et al., 2011; Cicatelli et al., 2012; Lingua et al., 2012). A proteomic study aimed at understanding how aboveground tissues of *M. truncatula* mycorrhizal plants cope with Cd stress revealed that, in the absence of Cd, establishment of the symbiosis led both to an increase in photosynthesis-related proteins and to a reduction in gluconeogenesis/glycolysis and antioxidant processes. However, the opposite response was found in the shoots of mycorrhizal plants grown with Cd (Aloui et al., 2011). It was suggested that the shoots of *M. truncatula* mycorrhizal plants are unaffected by Cd stress through a metabolic shift involving a glycolysis-mediated mobilization of defence mechanisms at the expense of the photosynthesis-dependent symbiotic sucrose sink. This conclusion supports the Audet and Charest´s hypothesis according to which avoidance of HM toxicity in the shoots of mycorrhizal plants is not mediated

by an intrinsic tolerance mechanism but by the use of antioxidant proteins at the expense of the symbiotic sucrose sink (Audet and Charest, 2008).

Biotechnological applications

The potential of AM fungi, on the one hand, to increase the uptake of low mobility micronutrients when plants grow in soils deficient in these elements and, on the other hand, to alleviate HM toxicity in polluted soils has promoted research on the contribution of AM fungi to plant biotechnological strategies that alleviate two important agronomical and environmental problems, such as micronutrient deficiency and HM excess in soils.

Biofortification

Micronutrient deficiency is a major issue affecting the health of billions of people around the world. Plant biofortification through plant breeding, genetic engineering and the use of certain agronomic practices has emerged as an important approach to increasing the uptake and accumulation of mineral micronutrients in agricultural food products and is considered as a promising strategy to increase human dietary nutrient intake and therefore to tackle micronutrient malnutrition, especially in developing countries (White and Broadley, 2009). Given the importance of the ERM of AM fungi in nutrient acquisition and crop production processes, they have been proposed as a key element in biofortification (He and Nara, 2007). Although very little is known about the impact of AM fungi on micronutrient concentrations in edible parts of the plant, AM fungi appear to be effective in improving the nutritional value of plant-derived food. For example, inoculation with AM fungi has been shown to increase grain Fe and Zn concentrations in chickpea (Pellegrino and Bedini, 2014) and maize (Subramanian et al., 2013). It was also found that the indigenous AM fungi were more efficient in increasing Zn and Fe concentrations of maize grains and that grains from mycorrhizal plants had a lower phytic acid concentration. Since phytic acid is an anti-nutritional compound that binds micronutrients in the intestine, preventing micronutrient uptake while enhancing excretion, inoculation with AM fungi might contribute to grain biofortification not only by increasing soil micronutrient uptake but also by overcoming the impact of anti-nutritional

factors. The optimal design of arbuscular mycorrhizas-assisted biofortification strategies requires further understanding of the effectiveness of different AM fungal isolates and plant varieties to increase metal micronutrient accumulation in different crops and soil conditions.

Phytoremediation

Throughout the word, soils exist that are almost vegetation-free because of their high HM content. Phytoremediation is a promising technology to make soil contaminants non toxic based on the synergic action of plants and microorganisms (Chaney et al., 1997; Denton, 2007). Initial colonizers of HM-contaminated soils are metal tolerant plant species, which are frequently characterized by their ability to hyperaccumulate HMs. Due to the ability of AM fungi to survive in extremely contaminated soils and to increase plant HM tolerance, much attention has been paid over recent decades to the study of the potential contribution of arbuscular mycorrhizas to soil HM phytoremediation (reviewed in Göhre and Paszkowski, 2006; Meier et al., 2012; Cabral et al., 2015). Although many hyperaccumulators belong to plant families that tend to be non-mycorrhizal or to develop low colonization levels, such as Brassicaceae and Caryophyllaceae, several *Thlaspi* species of the Brassicaceae have been reported to harbor AM fungi under field and experimental conditions, though the degree of colonization is generally low (Regvar et al., 2003; Vogel-Mikuš et al., 2005; Pongrac et al., 2009). High levels of mycorrhizal colonization were also reported in *Berkheya coddii* from Ni-ultramafic soils (Turnau and Mesjasz-Przybyłowicz, 2003), *Phyllanthus favieri* from metal-rich lateric soils (Perrier et al., 2006), in As hyperaccumulating Pterydophyta (Agely et al., 2005; Liu et al., 2005) and in the ornamental plants *V. calaminaria* (Hildebrandt et al., 1999) and *Limonium sinuatum* (Sheikh-Assadi et al., 2015). The outcome of the symbiosis established with these metallophytes has been shown to depend on the fungal isolate, the plant species and the nutritional status of the contaminated soils. For example, in *Thlaspi praecox*, *V. calaminaria*, *L. sinuatum* and *P. favieri*, mycorrhizal colonization was shown to decrease plant metal concentrations. In these cases, AM fungi could be important in projects to stabilize HM-contaminated soils against erosion. In contrast, inoculation of the As

hyperaccumulator *Pteris vittata* with indigienous AM fungi from an As-contaminated site resulted in increased As uptake (Agely et al., 2005), suggesting the potential of this symbiosis to increase the efficiency of phytoextraction. However, more data on mycorrhizal colonization of metallophytes and hyperaccumulating plants are needed to fully understand the potential of arbuscular mycorrhizas in phytoremediation strategies.

OBJECTIVES

The importance of the AM symbiosis in improving plant metal micronutrient nutrition and in alleviating metal toxicity has been well established. However, the mechanisms by which AM fungi protect plants on metal polluted soils and increase plant micronutrient uptake on metal deficient soils are not completely understood.

With the aim of getting further insights into these mechanisms, and since very little is known about the mechanisms of iron homeostasis in the symbiosis, the overall goal of this PhD thesis was to study the mechanisms of iron homeostasis in the AM fungus *Rhizophagus irregularis*.

To achieve the general aim of this PhD thesis, the following **specific objectives** were established:

1. Identification of the iron transport systems operating in the AM fungus *R. irregularis* (Chapter 1).

2. Molecular characterization of the *R. irregularis* high-affinity iron reductive uptake system (Chapters 2 and 3).

3. Assessment of the putative roles of monothiol glutaredoxins on iron homeostasis in *R. irregularis* (Chapter 4).

MATERIALS AND METHODS

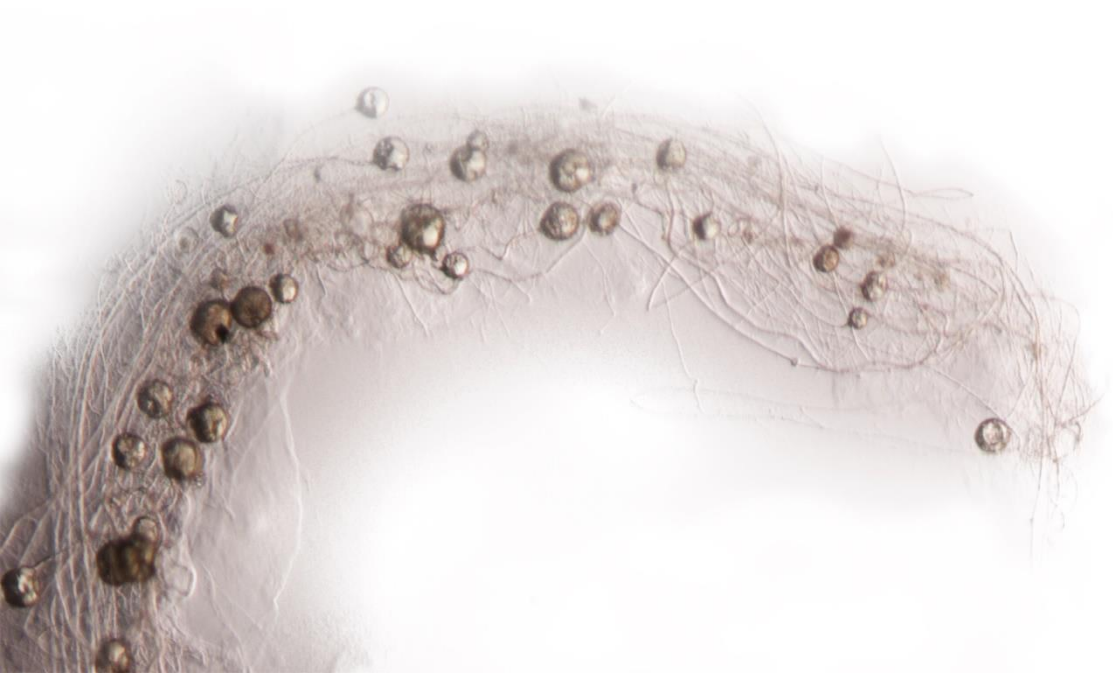

1. Biological materials

The AM fungus used for the study was *Rhizophagus irregularis* DAOM 197198, the most successful species in *in vitro* root organ cultures and whose genome has been recently sequenced.

Monoxenic cultures

Given the obligate symbiont character of AM fungi, and in order to obtain exclusively fungal material, free of plant material or other microorganisms, the monoxenic culture system was used, that is, double cultures of the AM fungus with roots grown *in vitro*, under conditions of complete sterility. *R. irregularis* monoxenic cultures were established as described by St-Arnaud et al. (1996), with some modifications. Briefly, clone DC2 of carrot (*Daucus carota* L.) Ri-T DNA transformed roots (transformed with *Agrobacterium rhizogenes*) were cultured with the AM fungus *R. irregularis* Schenck and Smith DAOM 197198 in two-compartment Petri dishes, allowing the separation of mycorrhizal roots (root compartment) from the ERM (hyphal compartment) (Fig. 1). Cultures were initiated in one compartment of each plate containing M medium (Chabot et al., 1992) by placing several non-mycorrhizal carrot root segments and a piece of fungal inoculum containing ERM, fragments of mycorrhizal roots and spores. Fungal hyphae and roots were allowed to grow over to the other compartment containing the same M medium. Plates were incubated in the dark at 24°C for 7–8 weeks until the second compartment was profusely colonized by the fungus and the roots. Then, depending on the final purpose of the culture, contents of the older compartment remains like that or was removed and refilled with liquid (modified without Phytagel™) M medium (15 ml) without sucrose (M-C medium), containing the rest of the components at double concentration and the supplements for the experimental condition to test. Fungal hyphae, but not roots, were allowed to grow over to this hyphal compartment. Plates were incubated in the dark at 24°C for 2–3 additional weeks. The control plates received 15 ml of liquid M-C medium (without any additional reagent or component).

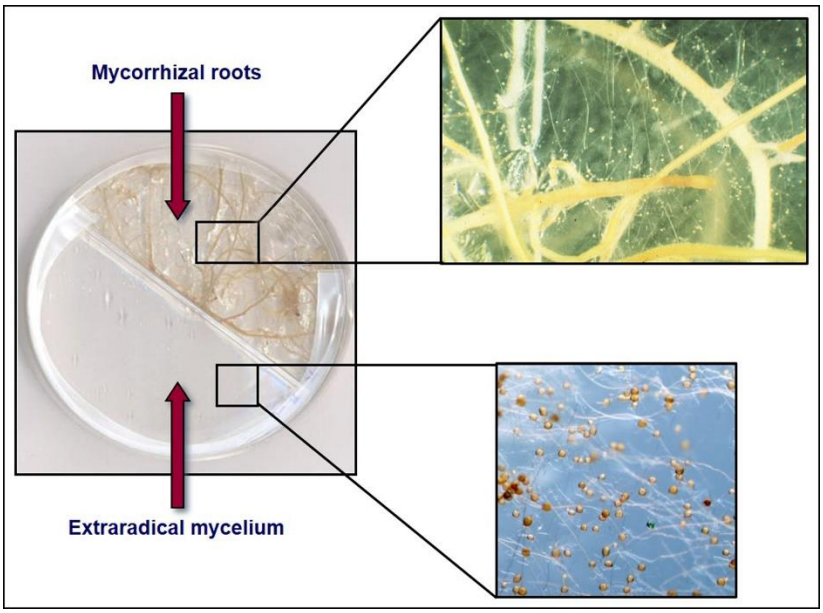

Figure 1. Experimental system: mycorrhizal Ri T-DNA transformed *Daucus carota* roots. Modified from St-Arnaud et al. (1996).

ERM from the different hyphal compartments was periodically examined and plates were opened to remove roots attempting to move to the hyphal compartment. After the 2-3 weeks, ERM was directly recovered under sterile conditions by using a pair of tweezers, washed with sterile water and dried on filter paper. The mycelium was immediately frozen in liquid nitrogen and stored at -80°C until used.

To analyze intraradical gene expression, hyphae growing in the hyphal compartment were used as a source of mycorrhizal inoculum. Carrot roots were placed on top of a densely colonized hyphal compartment (around 6 weeks after the start of the cultures) and collected 15 days later. Extraradical hyphae attached to the roots were removed with forceps under a binocular microscope. Roots were then washed with sterile water, dried on filter paper and immediately frozen in liquid N and stored at -80°C until used.

2. Molecular biology methods

Nucleic acids extraction and cDNA synthesis

R. irregularis genomic DNA was extracted from around 30 mg ERM developed in the hyphal compartment of control plates using the DNeasy Plant Mini Kit (Qiagen), according to the manufacturer's instructions.

Total plant RNA was isolated from 0.5 g (fresh weight) plant roots using the phenol/SDS method followed by LiCl precipitation as described by García-Rodríguez et al. (2007). Total fungal RNA from ERM from the different treatments of *R. irregularis* and mycorrhizal carrot roots, was extracted using the RNeasy Plant Mini Kit (QIAGEN, Maryland), following manufacturer's instructions. DNAse treatment was performed using the RNA-free DNase set (QIAGEN, Maryland) following the manufacturer's instructions. cDNAs were obtained from 1 μg of total DNase-treated RNA in a 20 μl reaction containing 200 units of Super-Script III Reverse Transcriptase (Invitrogen) and 50 pmol oligo $(dT)_{20}$ (Invitrogen), according to the manufacturer's instructions.

Gene expression analyses

R. irregularis gene expression was studied by real-time RT-PCR using an iQ™5 Multicolor Real-Time PCR Detection System (Bio-Rad). Each 20 μl reaction contained 1 μl of a 1:10 dilution of the cDNA, 200 nM each primer, 10 μl of iQ™ SYBR Green Supermix 2x (Bio-Rad). The PCR program consisted in a 3 min incubation at 95°C, followed by 36 cycles of 30 s at 95°C, 30 s (58°C for fungal genes and 60 °C for plant genes) and 30 s at 72°C, where the fluorescence signal was measured. The specificity of the PCR amplification procedure was checked with a heat-dissociation protocol (from 58 to 95°C) after the final cycle of the PCR. The efficiency of the different primer sets was evaluated by performing real-time PCR on several dilutions of cDNA. Because RNA extracted from mycorrhizal roots contains plant and fungal RNAs, specificity of the primer pairs was also analyzed by PCR amplification of genomic DNA isolated from non-mycorrizal carrot roots and plant leaves and of cDNA from non-colonized carrot and plant roots. The results obtained for the different treatments were standardized to the elongation factor 1-alpha

gene levels (GenBank Accession No. DQ282611), which were amplified with the primers GintEFfw and GintEFrev. RT-PCR determinations were performed on at three independent biological samples from three replicate experiments. Real-time PCR experiments were carried out three times for each biological sample, with the threshold cycle (Ct) determined in triplicate. The relative levels of transcription were calculated by using the $2^{-\Delta CT}$ method or the $2^{-\Delta\Delta CT}$ method (Schmittgen and Livak, 2008), and the standard error was computed from the average of the ΔCT values for each biological sample.

Gene isolation

Genomic clones and full-length cDNAs of *R. irregularis* were obtained by PCR amplification of *R. irregularis* genomic DNA and cDNA, respectively, using the corresponding primer pairs. PCR products were cloned in the pCR2.1 vector (Invitrogen, Carlsbad, CA, USA) or in the pGEM-T easy vector (Promega, Madison, USA).

All plasmids were amplified by transformation of *Escherichia coli* following standard procedures and purified by using the Qiagen Miniprep Kit (Qiagen, Maryland, USA). All sequences and constructs were checked by sequencing before further use. Nucleotide sequences were determined by Taq polymerase cycle sequencing by using an automated DNA sequencer (ABI Prism 3130xl Genetic Analyzer, Applied Biosystems, Carlsbad, USA).

3. Yeast methods

Heterologous expression

For heterologous *R. irregularis* protein expression analyses, the full length cDNAs were cloned into the yeast expression vector pFL61 (Minet et al., 1992) or pDR195 (Rentsch et al., 1995). The full length cDNAs of *S. cerevisiae* proteins were also cloned into the expression vector and used as positive controls in the complementation analyses of the corresponding yeast strains.

Yeast strains used in this PhD thesis were grown on YPD (Yeast extract-Peptone-Dextrose) rich medium, or on a defined minimal yeast medium, named as synthetic dextrose (SD) medium or complete synthetic

medium (CSM), the latest used for the selective growth of yeasts according to the auxotrophy of the strain to grow. *S. cerevisiae* mutant strains were transformed with the corresponding constructs, the empty vector (negative control), or the corresponding positive controls using a lithium acetate-based method (Schiestl and Gietz, 1989), and yeast transformants were selected on minimal medium by autotrophy to uracil.

Protein localization analyses

Localization of the *R. irregularis* proteins in *S. cerevisiae* was performed with C-terminal fusions of the respective genes to the enhanced green fluorescent protein (GFP) gene in the pertinent yeast strains. GFP fusion proteins were imaged using a 450–490 nm filter. Image sets were processed and overlapped using Adobe Photoshop™.

4. Bioinformatics analyses

Gene identification

Amino acid sequences of fungal transporters were retrieved from the freely accessible transport databases TCDB (http://www.tcdb.org/) and TransportDB (http://www.membranetransport.org/). Amino acid sequences of *S. cerevisiae* were retrieved from the freely accessible *S. cerevisiae* genome database (http://www.yeastgenome.org/). These sequences were used to search for orthologous sequences in the filtered model dataset of *R. irregularis* on the JGI website (http://genome.jgi-psf.org/Gloin1) via a protein BLAST. A second search was performed via a keyword search directly. Since many of the fungal reference proteins were phylogenetically distant from *R. irregularis*, manually curated *Laccaria bicolor* (http://genome.jgi-psf.org/Lacbi2), *Tuber melanosporum* (http://genome.jgi.doe.gov/Tubme1) and *Rhizopus oryzae* (http://genome.jgi.doe.gov/Rhior3) databases were used to look for additional orthologous sequences in the filtered model dataset of *R. irregularis*. This was also done via a BLASTp, run with the standard program settings. Amino acid sequences of *R. irregularis* were retrieved from JGI website or from Lin et al. (2014).

Sequence management

Management and first sequence alignments were performed using the bioinformatics DNAstar package version 7.0 (Lasergene).

Sequences analyses

Predictions of putative transmembrane domains were made using the TMHMM Server v.2.0 (http://www.cbs.dtu.dk/services/TMHMM/) and SMART software (http://smart.embl-heidelberg.de/). Predictions of subcellular localizations were made using the TargetP 1.1 Server (http://www.cbs.dtu.dk/services/TargetP/), PSORTII (http://psort.hgc.jp/form2.html) and WoLF PSORT (http://www.genscript.com/wolf-psort.html).

For the phylogenetic studies, full-length amino acid sequences were aligned with the orthologous sequences of a number of fungi representatives of distinct taxonomic groups by ClustalW (Version 2.1; http://www.ebi.ac.uk/Tools/msa/clustalw2/; Larkin et al., 2007) or by CLUSTAL Omega (http://www.ebi.ac.uk/Tools/msa/clustalo/). Alignments were imported into the Molecular Evolutionary Analysis (MEGA) package version 6 (Tamura et al., 2013). Phylogenetic analyses were performed using the Neighbor-Joining (NJ) method implemented in MEGA using the Poisson correction model and pairwise deletion of gaps option for distance computation. Bootstrap analyses were carried out with 1000 replicates. The evolutionary tree was drawn to scale.

5. Statistical methods

Statgraphics Centurion XVI software was used for the statistical analysis of the means and standard deviation determinations. ANOVA, followed by a Fisher's LSD test ($p<0.05$) when possible, was used for the comparison of the treatments based on at least 3 biological replicates for each treatment.

A more detailed description of the procedures used can be found at the Materials and Methods section of each chapter.

RESULTS

CHAPTER I

Genome-wide analysis of iron and zinc transporters in the arbuscular mycorrhizal fungus *Rhizophagus irregularis*

Adapted from:

Tamayo E, Gómez-Gallego T, Azón-Aguilar C, Ferrol N. 2014. Genome-wide analysis of copper, iron and zinc transporters in the arbuscular mycorrhizal fungus *Rhizophagus irregularis*. Frontiers in Plant Science 5, 547. doi: 10.3389/fpls.2014.00547

Abstract

Arbuscular mycorrhizal (AM) fungi, belonging to the Glomeromycota, are soil microorganisms that establish mutualistic symbioses with the majority of higher plants. The efficient uptake of low mobility mineral nutrients by the fungal symbiont and their further transfer to the plant is a major feature of this symbiosis. Besides improving plant mineral nutrition, AM fungi can alleviate heavy metal toxicity to their host plants and are able to tolerate high metal concentrations in the soil. Nevertheless, we are far from understanding the key molecular determinants of metal homeostasis in these organisms. To get some insights into these mechanisms, a genome-wide analysis of Fe and Zn transporters was undertaken, making use of the recently published whole genome of the AM fungus *Rhizophagus irregularis*. This *in silico* analysis allowed identification of 23 open reading frames in the *R. irregularis* genome, which potentially encode metal transporters. Phylogenetic comparisons with the genomes of a set of reference fungi showed an expansion of some metal transporter families. Analysis of the published transcriptomic profiles of *R. irregularis* revealed that a set of genes were up-regulated in mycorrhizal roots compared to germinated spores and extraradical mycelium, which suggests that metals are important for plant colonization.

Keywords: arbuscular mycorrhizal fungi, iron, metal transporters, *Rhizophagus irregularis*, symbiosis, zinc.

Introduction

The transition metals Fe and Zn play essential and catalytic roles throughout the cell in various subcellular compartments. These metal cofactors are critical for processes such as transcription, translation, the production of ATP in the mitochondria and the scavenging of toxic free radicals (van Ho et al., 2002; Schaible and Kaufmann, 2004; Kim et al., 2008). However, these metals are a highly reactive group of elements and are toxic at high concentrations (Valko et al., 2005). Therefore, their biological concentrations are finely regulated in living cells. To maintain micronutrient homeostasis, all organisms have developed a complex network of metal uptake, chelation, trafficking and storage processes (Festa and Thiele, 2011). Transporters represent the first line of defence to perturbations of cellular and subcellular metal homeostasis and constitute an important component of this network. When metal reserves are depleted, transporters contribute to the specific supply and distribution of the needed cofactor before deficiency symptoms appear. However, when the concentration of metal within the cell exceeds the cell´s buffering capacity, transporters provide the route to expel excess cofactors before toxicity occurs (Nies, 2007). The toxic heavy metals (HMs), such as cadmium, lead, mercury and nickel, have no physiological function but compete with the transporters of the essential biological metals. Therefore, the activity and specificity of the transporters of physiologically important HMs also control the lethality of the toxic metals.

Arbuscular mycorrhizal (AM) fungi are soil microorganisms that establish symbiotic mutualistic associations with most land plants. These fungi provide their host plants an efficient supply of low mobility mineral nutrients, mainly phosphorus and some micronutrients such as Cu and Zn. Thanks to the hyphal network they develop in the soil, AM fungi acquire nutrients not only for their own needs, but also for delivering them to the host plant. In return, the plant supplies the fungus with carbon compounds (Smith and Read, 2008). Besides improving plant mineral nutrition, AM fungi can alleviate HM toxicity to their host plants (Lingua et al., 2008; Göhre and Paszkowski, 2006). HM tolerant AM fungi ecotypes have been isolated from polluted soils and these indigenous populations cope better with HM-toxicity

than those isolated from unpolluted soils (del Val et al., 1999). To persist in environments with high HM content, AM fungi have evolved a series of strategies to avoid the damage produced by the metal, such as compartmentalization of the metal excess in some spores (González-Guerrero et al., 2008; Cornejo et al., 2013) and highly efficient homeostatic mechanisms (Ferrol et al., 2009; González-Guerrero et al., 2009). Despite the central role of metal transporters in HM homeostasis, only a gene encoding a Zn transporter has been characterized in AM fungi to date (González-Guerrero et al., 2005).

With the genome of *Rhizophagus irregularis* available (Tisserant et al., 2013), we have the unique opportunity to identify and present a global view of proteins involved in HM transport in an AM fungus. In this work we have taken advantage of the recently released genome sequence of *R. irregularis* to establish a repertoire of candidate genes potentially involved in the transport of Fe and Zn in this fungus and to interpret them in light of its extremely adaptable character to grow in conditions of HM deficiency or toxicity. This *R. irregularis* repertoire has been compared with that present in some reference fungi. To get some clues about the expression profiles of these genes throughout the fungal life cycle, we explored the published transcriptomic profiles in the extraradical mycelium (ERM) and symbiotic roots (IRM) obtained using the *R. irregularis* expression oligoarray (Tisserant et al., 2012) and the RNA-Seq reads obtained from germinating spores and *Medicago*-colonized roots (Tisserant et al., 2013).

Materials and Methods

Gene identification

Amino acid sequences of fungal Fe and Zn transporters were retrieved from the freely accessible transport databases TCDB (http://www.tcdb.org/) and TransportDB (http://www.membranetransport.org/). These sequences were used to search for orthologous sequences in the filtered model dataset of *R. irregularis* on the JGI website (http://genome.jgi-psf.org/Gloin1) via a protein BLAST. A second search was performed via a keyword search directly.

Since many of the fungal reference proteins were phylogenetically distant from *R. irregularis*, manually curated *Laccaria bicolor* (http://genome.jgi-psf.org/Lacbi2), *Tuber melanosporum* (http://genome.jgi.doe.gov/Tubme1) and *Rhizopus oryzae* (http://genome.jgi.doe.gov/Rhior3) databases were used to look for additional orthologous sequences in the filtered model dataset of *R. irregularis*. This was also done via a BLASTp, run with the standard program settings.

Sequences analyses

Searches for conserved domains in the orthologous proteins found in *R. irregularis* were performed using the Conserved Domain Database at NCBI (http://www.ncbi.nlm.nih.gov/cdd). Predictions of putative transmembrane domains were made using the TMHMM Server v.2.0 (http://www.cbs.dtu.dk/services/TMHMM/) and SMART software (http://smart.embl-heidelberg.de/). Full-length amino acid sequences were aligned with the orthologous sequences of a number of fungi representatives of distinct taxonomic groups by CLUSTALW (http://www.ebi.ac.uk/Tools/msa/clustalw2/). Alignments were imported into the Molecular Evolutionary Analysis (MEGA) package version 6. Phylogenetic analyses were performed using the neighbour-joining (NJ) method implemented in MEGA using the Poisson correction model and pairwise deletion of gaps option for distance computation. Bootstrap analyses were carried out with 1000 replicates.

Results and Discussion

The release of the *R. irregularis* genome (Tisserant et al., 2013; Lin et al., 2014) allowed making a genome-wide inventory of genes coding for Fe and Zn transporters. This *in silico* analysis allowed identification of 23 open reading frames in the *R. irregularis* genome, which potentially encode HM transporters. These candidate genes belong to several multigene families. Table 1 lists the six phylogenetic families to which these proteins belong and the major HM substrate for each transporter. These HM transport families are described in the following sections.

Table 1. Overview of the putative metal transporters identified in the *Rhizophagus irregularis* genome. Columns 1 to 5 contain protein name, protein JGI identification (JGI ID) number, predicted major metal transported, ratio of expression levels in *M. truncatula* symbiotic roots (IRM) to 2 d germinated spores (calculated from the RNA-seq reads in Tisserant et al., 2013), and ratio of expression levels in IRM to extraradical mycelium (ERM) (from Tisserant et al., 2012). SIT, siderophore-iron (Sid.-Fe) transporter; OFet, oxidase-dependent Fe^{2+} transporter; VIT, vacuolar iron transporter; ZIP, zinc-iron permease; CDF, cation diffusion facilitator; NRAMP, natural resistance-associated macrophage protein. Modified from Tamayo et al. (2014).

Protein name	JGI ID	Major substrate	Ratio IRM/spore	Ratio IRM/ERM
SIT family				
SIT1	305535	Sid.-Fe	0.6	-
SIT2	193231	Sid.-Fe	1.9	1.9
SIT3	71812	Sid.-Fe	1	-
OFet family				
FTR1	347887	Fe	10	-
FTR2	34848	Fe	1.5	-
VIT family				
CCC1.1	278480	Fe/Mn	0.9	3.4
CCC1.2	57183	Fe/Mn	0.04	0.1
CCC1.3	340222	Fe/Mn	2.7	-
ZIP family				
ZRT1	327155	Zn	420	8
YKE4	337446	Zn	0.9	-
ATX2	80864	Mn	1.2	-
ZRT3.1	13899	Zn	3.5	-
ZRT3.2	336612	Zn	3	14
CDF family				
ZnT1	70407	Zn	100	-
ZnT2	286233	Zn	1	-
MMT1	85722	Fe	2	-
MSC2	340453	Zn	0.9	0.9
ZRG17	67256	Zn	1	0.9
MnT1	232215	Mn	0.8	0.8
NRAMP family				
SMF1	136431	Mn/Fe	3	0.9
SMF2	89717	Mn	6	-
SMF3.1	313253	Fe	1.9	-
SMF3.2	337501	Fe	0.7	1

IRON

Iron uptake

Although Fe is abundant in nature, this metal has a low availability because it is most commonly found as ferric hydroxide, which is a rather stable and poorly soluble compound. A common strategy engaged by fungi to efficiently get the metal involves "sequestering" of Fe through the production and subsequent uptake of siderophores, which are small molecules that act as high-affinity Fe chelators (Haas et al., 2008). Another important Fe uptake mechanism involves a group of specialized membrane proteins that are part of the reductive iron assimilation (RIA) system. In this high-affinity uptake machinery, the metal is reduced from Fe^{3+} to Fe^{2+} (in order to increase Fe solubility) by membrane-bound ferrireductases, and then it is rapidly internalized by the concerted action of a ferroxidase and a permease that form a plasma membrane protein complex (Kosman, 2010).

A number of fungi harbour both types of high affinity systems, examples are *Ustilago maydis*, *Schizosaccharomyces pombe*, *Aspergillus fumigatus* and *Fusarium graminearum* (Askwith and Kaplan, 1997; Eichhorn et al., 2006; Greenshields et al., 2007; Mei et al., 1993; Roman et al., 1993; Schrettl et al., 2004; Schwecke et al., 2006). Others, such as *Saccharomyces cerevisiae*, *Candida albicans* and *Cryptococcus neoformans* (Howard, 1999; Lesuisse and Labbe, 1989; Schwyn and Neilands, 1987), are unable to synthesize siderophores but can utilize those produced by other organisms.

The siderophore pathway

AM fungi are assumed to play a key role in Fe uptake and delivery to their associated host plants. However, it is still unknown whether AM fungi produce siderophores. The majority of fungal siderophores are hydroxamates. The first committed step in the biosynthesis of fungal hydroxamate siderophores is the *N5*-hydroxylation of ornithine catalysed by ornithine-*N5*-monooxygenase (named *Sid1*/*SidA*). The absence of a *Sid1*/*SidA* ortholog in a fungal genome is generally taken as a strong evidence of no siderophore production. Inspection of the *R. irregularis* genome indicates that it does not contain *Sid1*/*SidA* orthologs. Similarly, the genomes of

Saccharomycotina and Mucoromycotina and some Basidiomycota lack genes coding for this enzyme, which is in agreement with the observed lack of siderophore production by these fungi (Lesuisse and Labbe, 1989; Plattner and Diekmann, 1994). Interestingly, although the *L. bicolor* genome also lacks *Sid1*/*SidA* orthologous genes, production of a set of different hydroxamate siderophores by *L. bicolor* has been recently reported (Haselwandter et al., 2013).

A gene encoding a putative bifunctional iucA/iucC siderophore biosynthetic protein (RiSid1) that is highly expressed in mycorrhizal roots was found in the genome of *R. irregularis*. IucA and iucC catalyse discrete steps in the biosynthesis of the siderophore aerobactin from N epsilon-acetyl-N epsilon-hydroxylysine and citrate. The C-terminal region of RiSid1 is related to the bacterial ferric iron reductase FhuF-like transporter. The genomes of the reference fungi used in this study also contain orthologs of this gene. Therefore, the production of siderophores by *R. irregularis* remains uncertain.

Irrespective of their ability to produce siderophores, fungi have siderophore transporters that allow them to uptake different types of these small chelators, including bacterial ones like coprogen or enterobactin. This allows several fungi to take advantage of the siderophores produced by other organisms, securing in such manner their own iron needs (Haas et al., 2008; Saha et al., 2013). This type of siderophore transporters belong to the SIT (siderophore-iron transporter) subfamily (2.A.1.16) of the major facilitator superfamily, a protein subfamily present exclusively in fungi (and not in other eukaryotes or prokaryotes). SITs are secondary transporters with 12-14 predicted transmembrane domains, which likely function as proton symporters energized by the plasma membrane potential (Haas et al., 2003; Philpott and Protchenko, 2008). Searches in the *R. irregularis* genome using as query the SIT genes of *S. cerevisiae* and *S. pombe* allowed identification of three putative siderophore transporters (RiSIT1, RiSIT2 and RirSIT3), which are expressed in all fungal structures (Table 1). Detailed characterization of these transporters is needed to determine their substrate specificity.

The reductive iron assimilation (RIA) pathway

The RIA pathway starts with reduction of ferric iron sources to the more soluble ferrous iron Fe^{2+} by plasma membrane-localized ferrireductases.

Reduced Fe is then specifically taken up by a high-affinity transport complex consisting of a ferroxidase and a Fe permease, the oxidase-dependent Fe^{2+} transporter (OFeT), or non-specifically through other plasma membrane divalent cation transporters, as it will be discussed below. In *S. cerevisiae*, Fe^{2+} can be also taken up by the low-affinity Fe transporter Fet4 (Dix et al., 1994). This low-affinity system seems to be absent in *R. irregularis* as well as in the other reference fungi used in this study, except the ascomycetes *S. cerevisiae*, *Aspergillus niger* and *Botrytis cinerea* (Table 2).

Table 2. Number and classification of the putative Fe and Zn transporters identified in the genome of *Rhizophagus irregularis* and in the genomes of the reference fungi used in this study. SIT, siderophore-iron (Sid.-Fe) transporter; OFet, oxidase-dependent Fe^{2+} transporter; VIT, vacuolar iron transporter; ZIP, zinc-iron permease; CDF, cation diffusion facilitator; NRAMP, natural resistance-associated macrophage protein. Modified from Tamayo et al. (2014).

	Basidiomycota							Ascomycota					Glomeromycota	Mucoromycotina
	Puccinia graminis	*Ustilago maydis*	*Laccaria bicolor*	*Coprinopsis cinerea*	*Cryptococcus neoformans*	*Piriformospora indica*	*Suillus luteus*	*Saccharomyces cerevisiae*	*Tuber melanosporum*	*Aspergillus niger*	*Neurospora crassa*	*Botrytis cinerea*	***Rhizophagus irregularis***	*Rhizopus oryzae*
OFet (Ftr1)	1	1	3	0	3	1	1	2	1	3	1	1	2	1
Low affinity Fe^{2+}transporter	0	0	0	0	0	0	0	1	0	1	0	1	0	0
NRAMP	3	1	1	1	1	0	2	3	0	1	2	1	4	4
ZIP	2	3	7	4	4	3	5	5	7	8	8	7	5	7
VIT	4	1	1	1	1	1	2	1	1	2	1	1	3	2
CDF	2	5	9	5	5	5	7	6	4	6	5	6	6	4

The oxidase-dependent Fe2+transporter (OFeT) family

In *S. cerevisiae*, the ferroxidation/permeation pathway is mediated by the ferroxidase FET3 and the iron permease FTR1. This bipartite complex operates with an apparent *Km* of 0.2 μM. The Fe^{2+} to be transported is first oxidized by FET3, and then transported into the cytosol as Fe^{3+} by FTR1 via a channelling mechanism (Kwok et al., 2006). The advantage gained by redox coupling of this transport mechanism is unclear, although it possibly imparts specificity to transport. FET3 contains a single transmembrane domain and an extracellular multicopper oxidase domain, showing remarkable similarity to other multicopper oxidases, such as laccases and ascorbate oxidases. Searches in the *R. irregularis* genome for ferroxidases retrieved several genes putatively encoding multicopper oxidases. Characterization of these genes is presented in Chapter 3.

Two putative orthologs of yeast *FTR1*, named *RiFTR1* and *RiFTR2*, have been found in the *R. irregularis* genome. RiFTR1 and RiFTR2 were more similar to the FTR1 homolog of the Bryophyte *Physcomitrella patens* (43% identity, 66% similarity and 37% identity, 60% similarity, respectively) than to fungal FTRs. Phylogenetic analyses of the FTR protein sequences of the reference fungi used in this study revealed that RiFTR1 and RiFTR2 clustered together and separated from the other sequences (Fig. 1).

Functional characterization of RiFTR1 and RiFTR2 is described in next chapter.

Expression analysis of the genes putatively involved in the ferroxidation/permeation pathway in the available transcriptomic data of *R. irregularis* revealed that the two Fe permeases identified in the genome are expressed in germinated spores and mycorrhizal roots (Table 1) and that some of the putative multicopper oxidases are expressed in all fungal structures (data not shown), which suggest that the Fe reductive assimilation pathway operates in AM fungi. Interestingly, the Fe permease gene *RiFTR1* was up-regulated (10-fold) during the symbiotic phase of the fungus (Table 1).

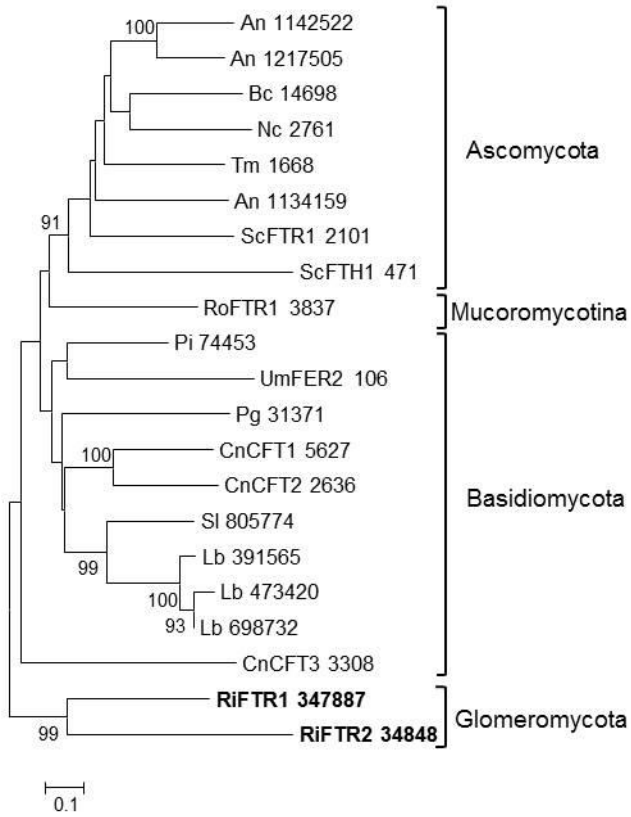

Figure 1. Phylogenetic relationships of the *Rhizophagus irregularis* iron permeases (FTR) with homologous sequences from selected species representative of the major fungal phyla. The Neighbour-Joining tree was created with MEGA 6. Protein JGI identification numbers are indicated. *R. irregularis* genes are shown in bold. Organisms: An, *Aspergillus niger*; Bc, *Botrytis cinerea*; Cc, *Coprinopsis cinerea*; Cn, *Cryptococcus neoformans*; Lb, *Laccaria bicolor*; Nc, *Neurospora crassa*; Pi, *Piriformospora indica* Pg, *Puccinia graminis*; Sc, *Saccharomyces cerevisiae*; Sl, *Suillus luteus*; Tb, *Tuber melanosporum;* Ri, *Rhizophagus irregularis*; Ro, *Rhizopus oryzae*; Um, *Ustilago maydis*. Bootstrap values above 70 and supporting a node used to define a cluster are indicated.

Vacuolar iron transport

Several studies have highlighted the importance of the AM fungal vacuoles for storage and detoxification of HMs (Turnau et al., 1993; González-Guerrero et al., 2007; Nayuki et al., 2014). Iron is likely stored in the fungal vacuoles in the ferric form as polyphosphate. In yeast, Fe is loaded into the vacuole by CCC1, a member of the vacuolar iron transporter (VIT) family (Li et al., 2001). Homologs are found in eukaryotes, bacteria and archaea. Most

fungal species encode one CCC1 protein and some others, such as *Aspergillus* and *Rhizopus* species, encode two paralogs (Gsaller et al., 2012). In contrast, three putative paralogs have been found *in R. irregularis*, named *RiCCC1.1*, *RiCCC1.2* and *RiCCC1.3*. As shown in the phylogenetic tree of fungal VITs, the three putative *R. irregularis* paralogs are closely related and cluster together with the *R. oryzae* homologs, clearly separated from sequences of Ascomycota and Basidiomycota (Fig. 2). The three paralogs were differentially expressed in the different fungal structures. *RiCCC1.1* was the most highly expressed paralog in the ERM. While *RiCCC1.2* was down-regulated in mycorrhizal roots, *RiCCC1.3* was up-regulated (Table 1).

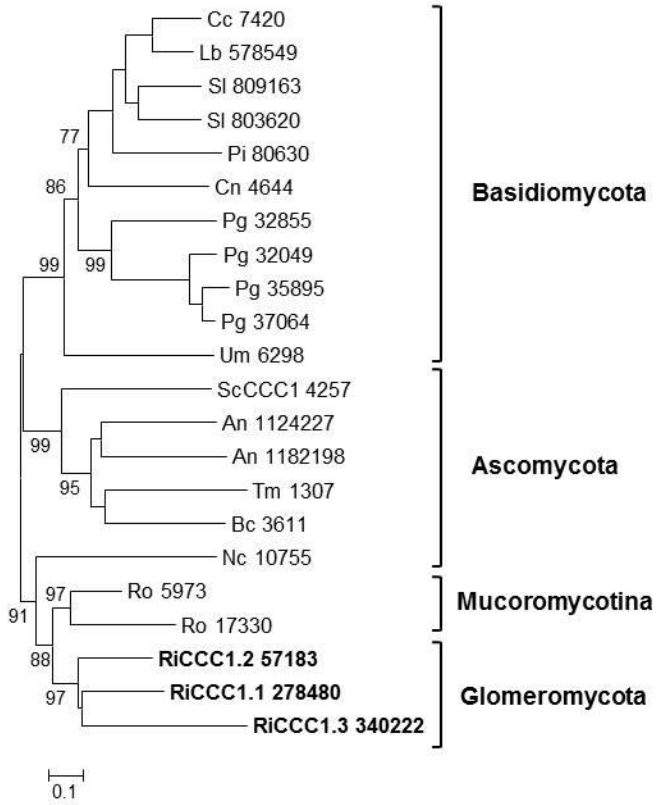

Figure 2. Phylogenetic relationships of the *Rhizophagus irregularis* vacuolar iron transporters (VIT) with homologous sequences from selected species representative of the major fungal phyla. The Neighbour-Joining tree was created with MEGA 6. Protein JGI identification numbers are indicated. *R. irregularis* genes are shown in bold. Organisms: An, *Aspergillus niger*; Bc, *Botrytis cinerea*; Cc, *Coprinopsis cinerea*; Cn, *Cryptococcus neoformans*; Lb, *Laccaria bicolor*; Nc, *Neurospora crassa*; Pi, *Piriformospora indica* Pg, *Puccinia graminis*; Sc, *Saccharomyces cerevisiae*; Sl, *Suillus luteus*; Tb, *Tuber melanosporum;* Ri, *Rhizophagus irregularis*; Ro,

Rhizopus oryzae; Um, *Ustilago maydis*. Bootstrap values above 70 and supporting a node used to define a cluster are indicated.

When Fe is low, mobilization of the vacuolar Fe stores should be mediated by a Fe permease/oxidase complex, as it was discussed in the former section, and/or by a homolog of the *S. cerevisiae* NRAMP family member SMF3 that exports Fe from the vacuole into the cytosol (see the NRAMP family section).

ZINC

In eukaryotes, Zn homeostasis is largely attributed to the coordinated action of two transporter families: the ZIP (zinc-iron permease or ZRT-IRT-like Protein) and the CDF (Cation Diffusion Facilitator) families (Eide, 2006). Only three Zn transporters of the CDF family have been characterized so far in mycorrhizal fungi. The first one was identified in *R. irregularis* (González-Guerrero et al., 2005), the second in *Hebeloma cylindrosporum* (Blaudez and Chalot, 2011) and more recently a new one has been reported in the ericoid fungus *Oidiodendrom maius* (Khouja et al., 2013).

The zinc-iron permease (ZIP) family

The name of the ZIP family refers to the first members that were functionally characterized, the *S. cerevisiae* Zn transporter ZRT1 and the *Arabidopsis thaliana* Fe transporter IRT1. A key feature of the ZIP family is that, without any yet known exceptions, these proteins transport Zn and/or other metal ion substrates from the extracellular space or organellar lumen into the cytoplasm. ZIP transporters are found at all phylogenetic levels including bacteria, fungi, plants and mammals (Eide, 2006). Most ZIP proteins have eight predicted transmembrane domains and similar predicted topologies with the N- and C-termini of the protein located on the extracytoplasmic face of the membrane. A histidine-rich region present between transmembrane regions three and four is necessary for Zn selectivity (Nishida et al., 2008).

The number of ZIP genes in the genomes of the reference fungi ranges from two to eight (Table 2). In *S. cerevisiae*, five ZIP family members have been described: ZRT1, ZRT2, ZRT3, ATX2 and YKE4. The *R. irregularis* ZIP family also includes five candidate genes, which have been named according to their

closest yeast orthologs. The fungal ZIP family is divided into four distinct subfamilies. One of the *R. irregularis* paralogs clusters with the plasma membrane high- and low-affinity Zn transporters ZRT1 and ZRT2 of *S. cerevisiae* in the ZRT1/ZRT2-like group (Zhao and Eide, 1996). Two paralogs were grouped in the ZRT3-like cluster and are closely related to the *S. cerevisiae* ZRT3, which mediates Zn release from the vacuole to the cytosol (Simm et al., 2007). The ATX2-like and YKE-like subfamilies including, respectively, the yeast ATX2 protein involved in Mn trafficking (Lin and Culotta, 1996) and the bidirectional Zn transporter YKE4 (Kumánovics et al., 2006), also comprised one *R. irregularis* gene each (Fig. 3). ZIP member distribution in the phylogenetic tree was not related to organism taxonomy, but rather to substrate specificity or subcellular location suggesting ancient duplication events followed by subfunctionalization in a common ancestor.

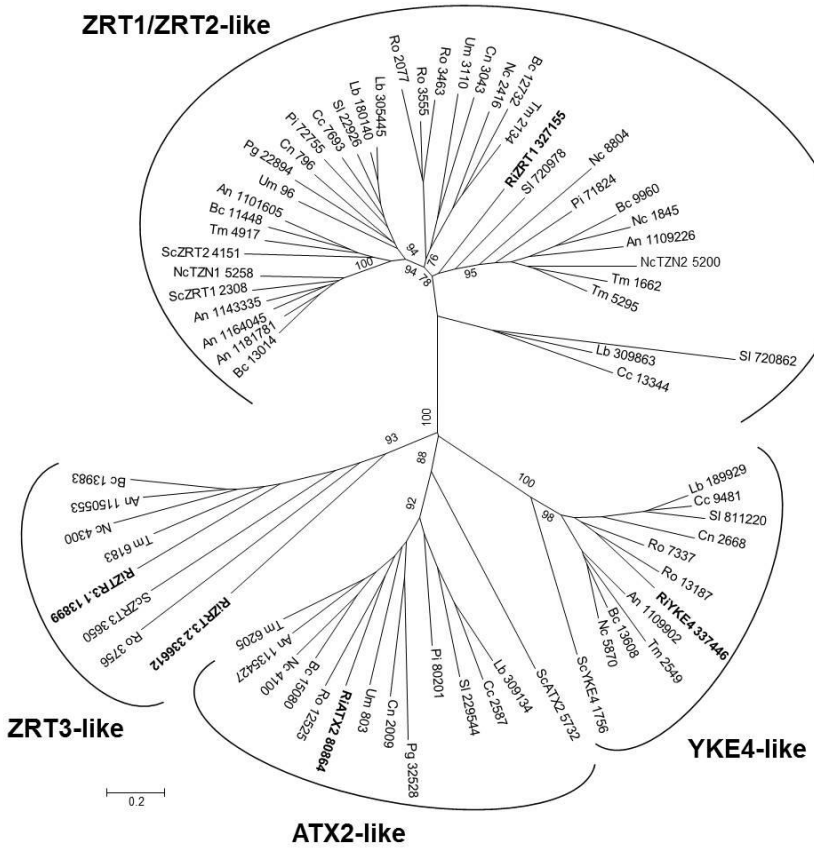

Figure 3. Phylogenetic relationships of the *Rhizophagus irregularis* zinc-iron permeases (ZIPs) with homologous sequences from selected species representative of the major fungal

phyla. The Neighbour-Joining tree was created with MEGA 6. Protein JGI identification numbers are indicated. *R. irregularis* genes are shown in bold. Organisms: An, *Aspergillus niger*; Bc, *Botrytis cinerea*; Cc, *Coprinopsis cinerea*; Cn, *Cryptococcus neoformans*; Lb, *Laccaria bicolor*; Nc, *Neurospora crassa*; Pi, *Piriformospora indica* Pg, *Puccinia graminis*; Sc, *Saccharomyces cerevisiae*; Sl, *Suillus luteus*; Tb, *Tuber melanosporum;* Ri, *Rhizophagus irregularis*; Ro, *Rhizopus oryzae*; Um, *Ustilago maydis*. Bootstrap values above 70 and supporting a node used to define a cluster are indicated.

Expression analyses revealed that all the *R. irregularis* paralogs were expressed in all the fungal structures tested. *RiZRT1* was highly up-regulated in mycorrhizal roots relative to the expression levels detected in germinated spores (420-fold) and in the ERM (8-fold). The two homologs of the yeast vacuolar Zn transporter, *RiZTR3.1* and *RiZTR3.2*, were also up-regulated (3-fold) in mycorrhizal roots (Table 1). These expression data suggest that the fungus takes up Zn from the apoplast of the symbiotic interface and that a mobilization of the vacuolar Zn stores occurs in the IRM.

The cation diffusion facilitator (CDF) family

The key feature of this family is that they transport Zn and/or other metal ions from the cytoplasm into the lumen of intracellular organelles or to the outside of the cell. Thus, CDF proteins work in opposition to the ZIP transporters. CDF transporters are also found at all phylogenetic levels. Most members of this family have six predicted transmembrane domains with the N- and C-termini predicted to be cytoplasmic. A notable exception to this rule is the yeast MSC2 protein that forms a heteromeric CDF complex with ZRG17 to transport Zn into compartments of the secretory pathway. Like the ZIP proteins, many CDF family members have histidine rich motifs, in this case usually in the cytoplasmic loop between transmembrane domains 4 and 5. The majority of CDF family members are classified into three groups, each containing characterised members that share the same specificity towards the principally transported metal, Zn, Fe/Zn or Mn. An additional group is the ZRG17-like subfamily, which is very distant from the Zn-CDF but with similar biochemical characteristics (Montanini et al., 2007). Six genes putatively encoding CDFs were identified in *R. irregularis*, which have been named according to their closest yeast orthologs. Three were included in the Zn-CDF subfamily, two in the ZRC1-like cluster and one in the MSC2-like

cluster (Fig. 4). The ZRC1-like cluster comprises the yeast vacuolar Zn transporters ZRC1 and COT1 (MacDiarmid et al., 2002) and the *R. irregularis* CDF GiZnT1 (González-Guerrero et al., 2005, renamed here as RiZnT1). These transporters mediate Zn uptake into the vacuole and are involved in Zn tolerance. Members of the MSC2-cluster also transport Zn, but into the ER. Another *R. irregularis* CDF, named RiMMT1, was grouped together with the *S. cerevisiae* mitochondrial Fe transporters MMT1 and MMT2 in the Fe-CDF subfamily and it is likely to mediate the transport of Fe. The other two homologs found, RiMnT1 and RiZRG17, were grouped in the Mn-CDF and ZRG17-like subfamilies, respectively, and are proposed to be involved in the transport of Mn and Zn (Montanini et al., 2007; Diss et al., 2011).

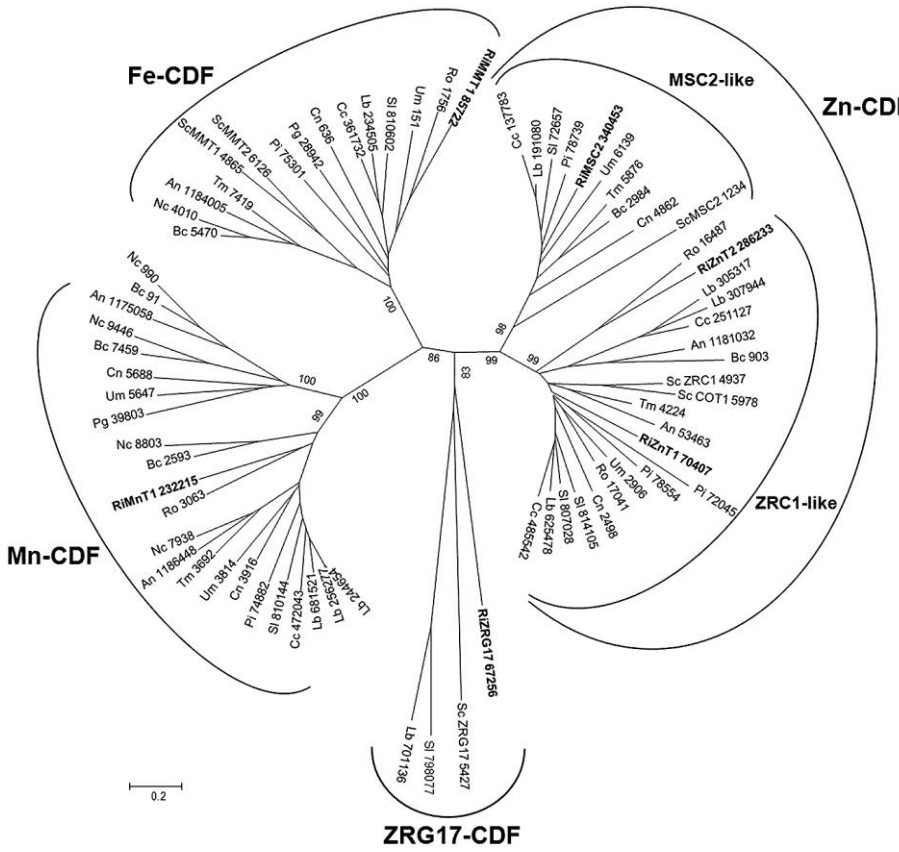

Figure 4. Phylogenetic relationships of the *Rhizophagus irregularis* cation diffusion facilitators (CDFs) with homologous sequences from selected species representative of the major fungal phyla. The Neighbour-Joining tree was created with MEGA 6. Protein JGI identification numbers are indicated. *R. irregularis* genes are shown in bold. Organisms: An, *Aspergillus niger*; Bc, *Botrytis cinerea*; Cc, *Coprinopsis cinerea*; Cn, *Cryptococcus neoformans*; Lb,

Laccaria bicolor; Nc, *Neurospora crassa*; Pi, *Piriformospora indica* Pg, *Puccinia graminis*; Sc, *Saccharomyces cerevisiae*; Sl, *Suillus luteus*; Tb, *Tuber melanosporum;* Ri, *Rhizophagus irregularis*; Ro, *Rhizopus oryzae*; Um, *Ustilago maydis*. Bootstrap values above 70 and supporting a node used to define a cluster are indicated.

Although the metal specificity of the newly identified CDF transporters of *R. irregularis* has been inferred from their distribution in the phylogenetic tree, an exhaustive functional characterization of these transporters is needed to confirm the transport processes mediated by the different isoforms.

Expression analyses of the CDF family members revealed that the different orthologs are expressed in all fungal structures analysed, except *RiZnT1* that was expressed at very low levels in germinated spores (Table 1).

The natural resistance-associated macrophage proteins (NRAMP) family of divalent metal transporters

The NRAMP family constitutes a class of divalent metal transporters that are highly conserved from bacteria to mammals. These transporters use the transmembrane proton gradient to facilitate transport of a broad range of divalent cations towards the cytosol. *S. cerevisiae* has three homologs of this family in its genome, *SMF1*, *SMF2* and *SMF3*. SMF1 and SMF2 mainly transport Mn, although SMF1 also transports Fe. While SMF1 operates at the plasma membrane in the uptake of either Mn or Fe (Portnoy et al., 2000; Chen et al., 1999), SMF2 is localized on membranes of intracellular Golgi vesicles, being involved in transport of Mn out of the vesicles (Reddi et al., 2009). SMF3 exports iron from the vacuole to the cytosol (Diffels et al., 2006), and together with CCC1, is responsible for Fe homeostasis in this organelle.

Searches in the *R. irregularis* genome led to the identification of four putative NRAMP homologs, all of them having the signature sequence DPGN. The sequences from Basidiomycota clearly separated from those of Ascomycota in the phylogenetic tree. The *R. oryzae* and *R. irregularis* homologs were grouped together in two different clades (Fig. 5). Analysis of the available gene expression profiles of R. irregularis revealed that *RiSMF1* and *RiSMF3.1* are expressed in all fungal structures and that *RiSMF1* and *RiSMF2* are expressed at very low levels in germinated spores (Tisserant et al., 2012).

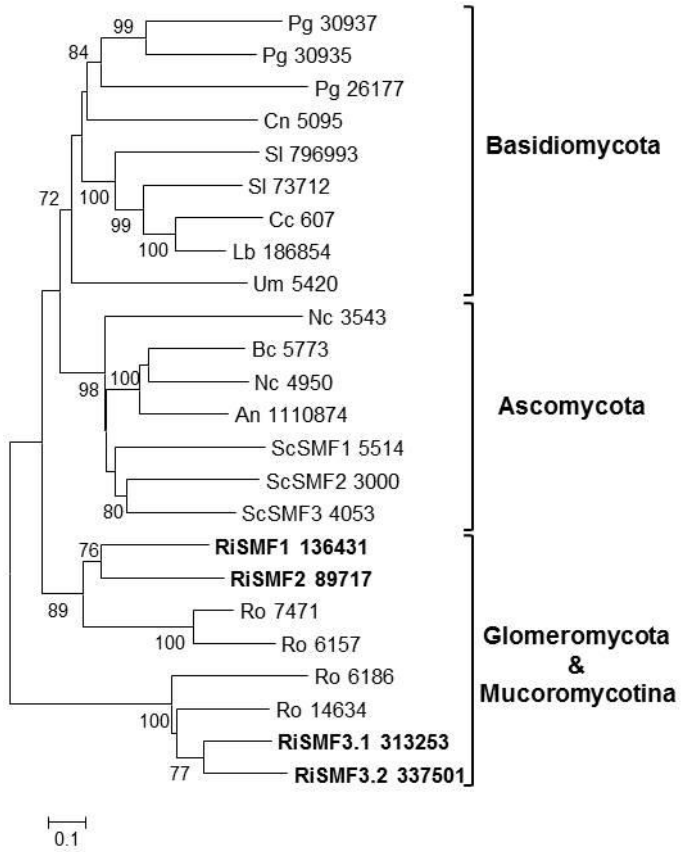

Figure 5. Phylogenetic relationships of the *Rhizophagus irregularis* natural resistance-associated macrophage proteins (NRAMPs) with homologous sequences from selected species representative of the major fungal phyla. The Neighbour-Joining tree was created with MEGA 6. Protein JGI identification numbers are indicated. *R. irregularis* genes are shown in bold. Organisms: An, *Aspergillus niger*; Bc, *Botrytis cinerea*; Cc, *Coprinopsis cinerea*; Cn, *Cryptococcus neoformans*; Lb, *Laccaria bicolor*; Nc, *Neurospora crassa*; Pi, *Piriformospora indica* Pg, *Puccinia graminis*; Sc, *Saccharomyces cerevisiae*; Sl, *Suillus luteus*; Tb, *Tuber melanosporum;* Ri, *Rhizophagus irregularis*; Ro, *Rhizopus oryzae*; Um, *Ustilago maydis*. Bootstrap values above 70 and supporting a node used to define a cluster are indicated.

Concluding remarks

The present analysis aimed at establishing a repertoire of candidate genes that represent the genetic potential for transport of Fe and Zn in *R. irregularis*. We have revealed the presence of at least 23 genes encoding putative transition metal transporters, showing all of them detectable transcript levels in the fungal structures analysed. Fig. 6 summarizes the

candidate genes identified in this genomic survey. The sequences and expression information reported herein will be useful for further investigation of the roles of these transport proteins in Fe and Zn homeostasis in AM fungi and in the symbiosis. A comprehensive physiological analysis of the current dataset needs detailed characterization of the encoded proteins. However, we would like to highlight two features that stood out in this *in silico* analysis: (i) expansion of some families of metal transporters, specifically of VITs and NRAMPs, and (ii) up-regulation of a certain number of genes putatively encoding transport proteins mediating the influx of Fe/Zn (RiFTR1, RiZRT1) and the mobilization of the vacuolar Zn stores (RiZRT3) in the intraradical phase of the fungus. Since these transporters are unlikely to be involved in metal transfer to the plant, they should play a role in maintaining Fe and Zn homeostasis in the IRM. The challenge now is to functionally characterize these transporters and to identify their location and roles in the symbiosis.

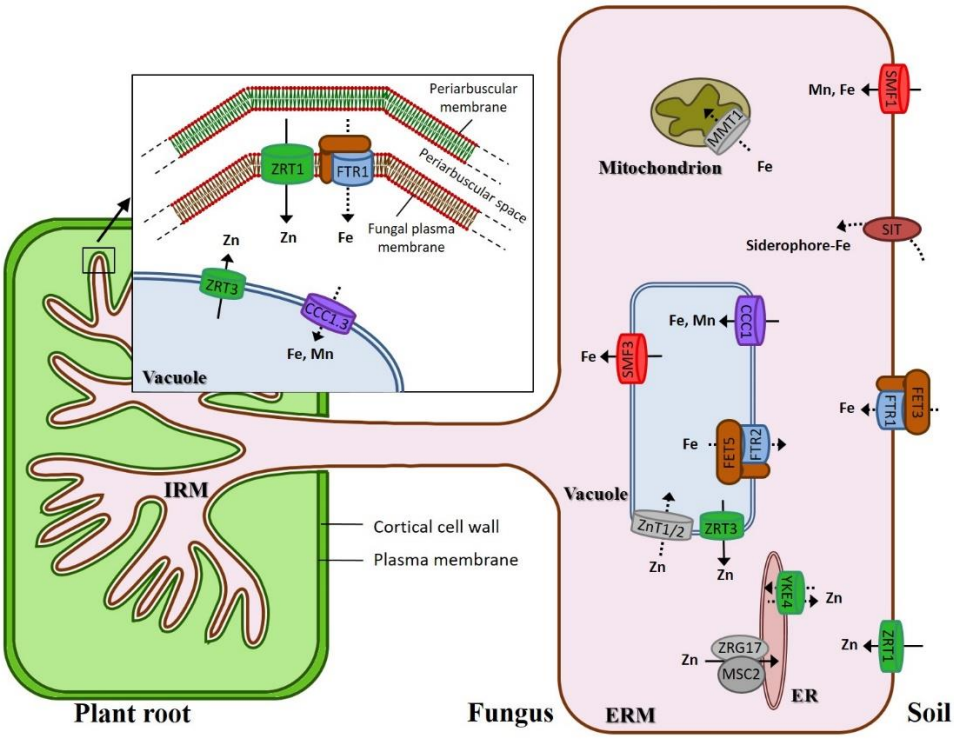

Figure 6. Schematic representation of the putative Fe and Zn transport systems in *Rhizophagus irregularis*. Transcripts for all these transporters have been detected in symbiotic roots and germinated spores. Discontinuous arrows refer to transporters whose transcript levels in the extraradical mycelium (ERM) have not been determined yet. Transcripts up-

regulated by more than 2.5-fold in the symbiotic roots are shown in the intraradical mycelium (IRM), except ZnT1 that was expressed at very low levels in germinated spores and SMF1 that was only up-regulated in the symbiotic roots relative to germinated spores but not to the ERM. The oxidase-dependent Fe^{2+}transporter (OFeT) family members are in brown (ferroxidases) and blue (permeases); zinc-iron permeases (ZIPs) in green; cation diffusion facilitators (CDFs) in grey, natural resistance-associated macrophage proteins (NRAMPs) in red and vacuolar iron transporters (VITs) in purple. ER, endoplasmic reticulum. Modified from Tamayo et al. (2014).

References

Askwith C, Kaplan J. 1997. An oxidase-permease-based iron transport system in *Schizosaccharomyces pombe* and its expression in *Saccharomyces cerevisiae*. The Journal of Biological Chemistry 272, 401–405. doi: 10.1074/jbc.272.1.401

Blaudez D, Chalot M. 2011. Characterization of the ER-located zinc transporter ZnT1 and identification of a vesicular zinc storage compartment in *Hebeloma cylindrosporum*. Fungal Genetics and Biology 48, 496–503. doi: 10.1016/j.fgb.2010.11.007

Chen X-Z, Peng J-B, Cohen A, Nelson H, Nelson N, Hediger MA. 1999. Yeast SMF1 mediates H^+-coupled iron uptake with concomitant uncoupled cation currents. The Journal of Biological Chemistry 274, 35089–35094. doi: 10.1074/jbc.274.49.35089

Cornejo P, Pérez-Tienda J, Meier S, Valderas A, Borie F, Azcón-Aguilar C, Ferrol N. 2013. Copper compartmentalization in spores as a survival strategy of arbuscular mycorrhizal fungi in Cu-polluted environments. Soil Biology and Biochemistry 57, 925–928. doi: 10.1016/j.soilbio.2012.10.031

del Val C, Barea JM, Azcón-Aguilar C. 1999. Diversity of arbuscular mycorrhizal fungus populations in heavy-metal-contaminated soils. Applied and Environmental Microbiology 65, 718–723.

Diffels JF, Seret M-L, Goffeau A, Baret PV. 2006. Heavy metal transporters in Hemiascomycete yeasts. Biochimie 88, 1639–1649. doi: 10.1016/j.biochi.2006.08.008

Diss L, Blaudez D, Gelhaye E, Chalot M. 2011. Genome-wide analysis of fungal manganese transporters, with an emphasis on *Phanerochaete chrysosporium*. Environmental Microbiology Reports 3, 367–382. doi: 10.1111/j.1758-2229.2010.00235.x

Dix DR, Bridgham JT, Broderius MA, Byersdorfer CA, Eide DJ. 1994. The *FET4* gene encodes the low affinity Fe(II) transport protein of *Saccharomyces cerevisiae*. The Journal of Biological Chemistry 269, 26092–26099.

Eichhorn H, Lessing F, Winterberg B, Schirawski J, Kämper J, Müller P, Kahmann R. 2006. A ferroxidation/permeation iron uptake system is required for virulence in *Ustilago maydis*. The Plant Cell 18, 3332–3345. doi: 10.1105/tpc.106.043588

Eide DJ. 2006. Zinc transporters and the cellular trafficking of zinc. Biochimica et Biophysica Acta 1763, 711–722. doi: 10.1016/j.bbamcr.2006.03.005

Ferrol N, González-Guerrero M, Valderas A, Benabdellah K, Azcón-Aguilar C. 2009. Survival strategies of arbuscular mycorrhizal fungi in Cu-polluted environments. Phytochemistry Reviews 8, 551–559. doi: 10.1007/s11101-009-9133-9

Festa RA, Thiele DJ. 2011. Copper: an essential metal in biology. Current Biology 21, R877-R883. doi: 10.1016/j.cub.2011.09.040

Göhre V, Paszkowski U. 2006. Contribution of the arbuscular mycorrhizal symbiosis to heavy metal phytoremediation. Planta 223, 1115–1122. doi: 10.1007/s00425-006-0225-0

González-Guerrero M, Azcón-Aguilar C, Mooney M, Valderas A, MacDiarmid CW, Eide DJ, Ferrol N. 2005. Characterization of a *Glomus intraradices* gene encoding a putative Zn transporter of the cation diffusion facilitator family. Fungal Genetics and Biology 42, 130–140. doi: 10.1016/j.fgb.2004.10.007

González-Guerrero M, Cano C, Azcón-Aguilar C, Ferrol N. 2007. *GintMT1* encodes a functional metallothionein in *Glomus intraradices* that responds to oxidative stress. Mycorrhiza 17, 327–335. doi: 10.1007/s00572-007-0108-7

González-Guerrero M, Hong D, Argüello JM. 2009. Chaperone-mediated Cu^{+} delivery to Cu^{+} transport ATPases: requirement of nucleotide binding. The Journal of Biological Chemistry 284, 20804–20811. doi: 10.1074/jbc.M109.016329

González-Guerrero M, Melville LH, Ferrol N, Lott JNA, Azcón-Aguilar C, Peterson RL. 2008. Ultrastructural localization of heavy metals in the extraradical mycelium and spores of the arbuscular mycorrhizal fungus *Glomus intraradices*. Canadian Journal of Microbiology 54, 103–110. doi: 10.1139/w07-119

Greenshields DL, Liu G, Feng J, Selvaraj G, Wei Y. 2007. The siderophore biosynthetic gene *SID1*, but not the ferroxidase gene *FET3*, is required for full *Fusarium graminearum* virulence. Molecular Plant Pathology 8, 411–421. doi: 10.1111/j.1364-3703.2007.00401.x

Gsaller F, Eisendle M, Lechner BE, Schrettl M, Lindner H, Müller D, Geley S, Haas H. 2012. The interplay between vacuolar and siderophore-mediated iron storage in *Aspergillus fumigatus*. Metallomics 4, 1262–1270. doi: 10.1039/c2mt20179h

Haas H, Eisendle M, Turgeon BG. 2008. Siderophores in fungal physiology and virulence. Annual Review of Phytopathology 46, 149–187. doi: 10.1146/annurev.phyto.45.062806.094338

Haas H, Schoeser M, Lesuisse E, Ernst JF, Parson W, Abt B, Winkelmann G, Oberegger H. 2003. Characterization of the *Aspergillus nidulans* transporters for the siderophores enterobactin and triacetylfusarinine C. The Biochemical Journal 371, 505–513. doi: 10.1042/BJ20021685

Haselwandter K, Häninger G, Ganzera M, Haas H, Nicholson G, Winkelmann G. 2013. Linear fusigen as the major hydroxamate siderophore of the ectomycorrhizal Basidiomycota *Laccaria laccata* and *Laccaria bicolor*. Biometals 26, 969–979. doi: 10.1007/s10534-013-9673-8

Howard DH. 1999. Acquisition, transport, and storage of iron by pathogenic fungi. Clinical Microbiology Reviews 12, 394–404.

Khouja HR, Abbà S, Lacercat-Didier L, et al. 2013. OmZnT1 and OmFET, two metal transporters from the metal-tolerant strain Zn of the ericoid mycorrhizal fungus *Oidiodendron maius*, confer zinc tolerance in yeast. Fungal Genetics and Biology 52, 53–64. doi: 10.1016/j.fgb.2012.11.004

Kim BE, Nevitt T, Thiele DJ. 2008. Mechanisms for copper acquisition, distribution and regulation. Nature Chemical Biology 4, 176–185. doi: 10.1038/nchembio.72

Kosman D J. 2010. Redox cycling in iron uptake, efflux, and trafficking. The Journal of Biological Chemistry 285, 26729–26735. doi: 10.1074/jbc.R110.113217

Kumánovics A, Poruk KE, Osborn KA, Ward DM, Kaplan J. 2006. *YKE4* (YIL023C) encodes a bidirectional zinc transporter in the endoplasmic reticulum of *Saccharomyces cerevisiae*. The Journal of Biological Chemistry 281, 22566–22574. doi: 10.1074/jbc.M604730200

Kwok EY, Severance S, Kosman DJ. 2006. Evidence for iron channeling in the Fet3p-Ftr1p high-affinity iron uptake complex in the yeast plasma membrane. Biochemistry 45, 6317–6327. doi: 10.1021/bi052173c

Lesuisse E, Labbe P. 1989. Reductive and non-reductive mechanisms of iron assimilation by the yeast *Saccharomyces cerevisiae*. Journal of General Microbiology 135, 257–263. doi: 10.1099/00221287-135-2-257

Li L, Chen OS, McVey Ward D, Kaplan J. 2001. CCC1 is a transporter that mediates vacuolar iron storage in yeast. The Journal of Biological Chemistry 276, 29515–29519. doi: 10.1074/jbc.M103944200

Lin K, Limpens E, Zhang Z, et al. 2014. Single nucleus genome sequencing reveals high similarity among nuclei of an endomycorrhizal fungus. PLoS Genetics 10, e1004078. doi: 10.1371/journal.pgen.1004078

Lin S, Culotta VC. 1996. Suppression of oxidative damage by *Saccharomyces cerevisiae ATX2*, which encodes a manganese-trafficking protein that localizes to Golgi-like vesicles. Molecular and Cellular Biology 16, 6303-6312.

Lingua G, Franchin C, Todeschini V, Castiglione S, Biondi S, Burlando B, Parravicini V, Torrigiani P, Berta G. 2008. Arbuscular mycorrhizal fungi differentially affect the response to high zinc concentrations of two registered poplar clones. Environmental Pollution 153, 137–147. doi: 10.1016/j.envpol.2007.07.012

MacDiarmid CW, Milanick MA, Eide DJ. 2002. Biochemical properties of vacuolar zinc transport systems of *Saccharomyces cerevisiae*. The Journal of Biological Chemistry 277, 39187–39194. doi: 10.1074/jbc.M205052200

Mei B, Budde AD, Leong SA. 1993. *sid1*, a gene initiating siderophore biosynthesis in *Ustilago maydis*: molecular characterization, regulation by iron, and role in phytopathogenicity. Proceedings of the National Academy of Sciences 90, 903–907. doi: 10.1073/pnas.90.3.903

Montanini B, Blaudez D, Jeandroz S, Sanders D, Chalot M. 2007. Phylogenetic and functional analysis of the Cation Diffusion Facilitator (CDF) family: improved signature and prediction of substrate specificity. BMC Genomics 8, 107. doi: 10.1186/1471-2164-8-107

Nayuki K, Chen B, Ohtomo R, Kuga Y. 2014. Cellular imaging of cadmium in resin sections of arbuscular mycorrhizas using synchrotron micro X-ray

fluorescence. Microbes and Environments 29, 60–66. doi: 10.1264/jsme2.ME13093

Nies DH. 2007. How cells control zinc homeostasis. Science 292, 2488-2492. doi: 10.1126/science.1149048

Nishida S, Mizuno T, Obata H. 2008. Involvement of histidine-rich domain of ZIP family transporter TjZNT1 in metal ion specificity. Plant Physiology and Biochemistry 46, 601–606. doi: 10.1016/j.plaphy.2008.02.011

Philpott CC, Protchenko O. 2008. Response to iron deprivation in *Saccharomyces cerevisiae*. Eukaryotic Cell 7, 20–27. doi: 10.1128/EC.00354-07

Plattner HJ, Diekmann H. 1994. Enzymology of siderophore biosynthesis. pp. 99-116 In: *Metal Ions in Fungi*. Eds. Winkelmann, G. and Winge, D.R. (New York, NY: M. Dekker, Inc.), 99-116.

Portnoy ME, Liu XF, Culotta VC. 2000. *Saccharomyces cerevisiae* expresses three functionally distinct homologues of the nramp family of metal transporters. Molecular and Cellular Biology 20, 7893–7902. doi: 10.1128/MCB.20.21.7893-7902.2000

Reddi AR, Jensen LT, Naranuntarat A, Rosenfeld L, Leung E, Shah R, Culotta VC. 2009. The overlapping roles of manganese and Cu/Zn SOD in oxidative stress protection. Free Radical Biology and Medicine 46, 154–162. doi: 10.1016/j.freeradbiomed.2008.09.032

Roman DG, Dancis A, Anderson GJ, Klausner RD. 1993. The fission yeast ferric reductase gene *frp1*$^{+}$ is required for ferric iron uptake and encodes a protein that is homologous to the gp91-*phox* subunit of the human NADPH phagocyte oxidoreductase. Molecular and Cellular Biology 13, 4342–4350. doi: 10.1128/MCB.13.7.4342

Saha R, Saha N, Donofrio RS, Bestervelt LL. 2013. Microbial siderophores: a mini review. Journal of Basic Microbiology 53, 303–317. doi: 10.1002/jobm.201100552

Schaible UE, Kaufmann SH. 2004. Iron and microbial infection. Nature Reviews. Microbiology 2, 946–953. doi: 10.1038/nrmicro1046

Schrettl M, Winkelmann G, Haas H. 2004. Ferrichrome in *Schizosaccharomyces pombe*-an iron transport and iron storage compound. Biometals 17, 647–654. doi: 10.1007/s10534-004-1230-z

Schwecke T, Göttling K, Durek P, Dueñas I, Käufer NF, Zock-Emmenthal S, Staub E, Neuhof T, Dieckmann R, von Döhren H. 2006. Nonribosomal peptide synthesis in *Schizosaccharomyces pombe* and the architectures of ferrichrome-type siderophore synthetases in fungi. Chembiochem 7, 612–622. doi: 10.1002/cbic.200500301

Schwyn B, Neilands JB. 1987. Universal chemical assay for the detection and determination of siderophores. Analytical Biochemistry 160, 47–56. doi: 10.1016/0003-2697(87)90612-9

Simm C, Lahner B, Salt D, LeFurgey A, Ingram P, Yandell B, Eide DJ. 2007. *Saccharomyces cerevisiae* vacuole in zinc storage and intracellular zinc distribution. Eukaryotic Cell 6, 1166–1177. doi: 10.1128/EC.00077-07

Smith SE, Read DJ. 2008. *Mycorrhizal Symbiosis*. Academic Press, London, UK.

Tisserant E, Kohler A, Dozolme-Seddas P, et al. 2012. The transcriptome of the arbuscular mycorrhizal fungus *Glomus intraradices* (DAOM 197198) reveals functional tradeoffs in an obligate symbiont. New Phytologist 193, 755–769. doi: 10.1111/j.1469-8137.2011.03948.x

Tisserant E, Malbreil M, Kuo A, et al. 2013. Genome of an arbuscular mycorrhizal fungus provides insight into the oldest plant symbiosis. Proceedings of the National Academy of Sciences 110, 20117–20122. doi: 10.1073/pnas.1313452110

Turnau K, Kottke I, Oberwinkler F. 1993. Element localization in mycorrhizal roots of *Pteridium aquilinum* (L.) Kuhn collected from experimental plots treated with cadmium dust. New Phytologist 123, 313-324. doi: 10.1111/j.1469-8137.1993.tb03741.x

Valko M, Morris H, Cronin MT. 2005. Metals, toxicity and oxidative stress. Current Medicinal Chemistry 12, 1161–1208. doi: 10.2174/0929867053764635

van Ho A, Ward DM, Kaplan J. 2002. Transition metal transport in yeast. Annual Review of Microbiology 56, 237–261. doi: 10.1146/annurev.micro.56.012302.160847

Zhao H, Eide D. 1996. The *ZRT2* gene encodes the low affinity zinc transporter in *Saccharomyces cerevisiae*. The Journal of Biological Chemistry 271, 23203–23210. doi: 10.1074/jbc.271.38.23203

CHAPTER II

Molecular characterization of a high-affinity iron uptake system in *Rhizophagus irregularis*

A manuscript containing this work is in preparation:

Tamayo E, Knight SAB, Dancis A, Ferrol N.

Molecular characterization of a high-affinity iron uptake system in *Rhizophagus irregularis*.

In preparation.

Abstract

Arbuscular mycorrhizal fungi (AM fungi) have been shown to improve iron (Fe) acquisition of their host plants. However, underlying mechanisms remain unknown to date. Here, we report a characterization of two components of the high-affinity reductive Fe uptake system of *Rhizophagus irregularis*, the ferric reductase and the high affinity iron permease. In the extraradical mycelia, Fe deficiency induced activation of a plasma membrane-localized ferrireductase, an enzyme that reduces ferric iron sources to the more soluble ferrous iron. By using a yeast expression system, we observed that out of the two iron permeases genes described in the *R. irregularis* genome, only RiFTR1 partially reverted the inability of the *ScFtr1* yeast mutant to grow on Fe-limited medium and its Fe transport activity. In the heterologous system, RiFTR1 was expressed in the plasma membrane while RiFTR2 was expressed in the endomembranes. Gene expression analyses revealed that *RiFTR1* expression increased in Fe-deficient extraradical mycelia and that *RiFRE1*, a gene putatively encoding a ferrireductase, *RiFTR1* and *RiFTR2* expression decreased when the fungus was grown under high Fe conditions. *RiFTR1* is highly expressed in the intraradical mycelia. Furthermore, *RiFTR2* expression was shown to be up-regulated in the IRM of maize plants grown under low Fe conditions. These data suggest that the Fe permease RiFTR1 plays a major role in Fe acquisition in Fe-limiting conditions and that maintenance of Fe homeostasis in the IRM might be essential for a successful symbiosis.

Introduction

Iron (Fe) is an essential micronutrient for the survival and function of plants and of almost every organism. Iron´s ability to gain and lose electrons makes this metal a cofactor of choice for numerous important enzymes involved in a variety of oxidation-reduction reactions. Despite its absolute requirement, Fe reacts in cells with oxygen and generates noxious reactive oxygen species that are deleterious for growth and development. Cellular and whole-organism Fe homeostasis must, therefore, be strictly balanced. Although abundant in nature, Fe is often available in limited amounts to plants because it is mostly found in rather insoluble Fe(III) complexes in soils (Guerinot and Yi, 1994). To overcome this problem, plants have evolved highly efficient strategies to acquire Fe from the rhizosphere (Grotz and Guerinot, 2006). Nongrasses use Strategy I, which utilizes proton release to help solubilize Fe(III), a membrane-bound Fe(III) chelate reductase to convert Fe(III) to the more soluble Fe(II), and a Fe(II)-specific transporter for uptake across the plasma membrane. Grasses release phytosiderophores (PSs) that chelate Fe(III); the PS-Fe(III) complexes are then transported into root cells via a plasma membrane transporter in a mechanism known as Strategy II (Römheld and Marschner, 1986; Kobayashi and Nishizawa, 2012). In addition to these strategies, a widespread and evolutionary ancient strategy evolved by plants to increase their nutrient supply is the establishment of arbuscular mycorrhizal (AM) symbioses with some soil-borne fungi belonging to the Glomeromycota phylum (Smith and Read, 2008). The fungus, thanks to the hyphal network it develops in the soil, contribute to the acquisition of low mobility nutrients in the soil, particularly P, N and some micronutrients (Smith and Read, 2008). In return, the plant provides the fungus, which is an obligate symbiont, with the carbohydrates it needs to complete its life cycle.

Although the main benefit of the AM association is an improved P status of the mycorrhizal plant, AM fungi also play a role in Fe nutrition of their host plants (Clark and Zeto, 1996; Liu et al., 2000; Chorianopoulou et al., 2015). Direct evidence of the capability of the extraradical mycelium (ERM) to take up Fe from the soil and to transfer it to the host plant comes from studies using ^{59}Fe as a tracer in compartments only accessible by the external hyphae

(Caris et al., 1998; Kobae et al., 2014). Conversely, other studies have shown that AM fungi play a role in reducing Fe uptake when the soil concentration is high (Liu et al., 2000; Juwarkar and Jambhulkar, 2008). While the role of AM symbiosis on P and N molecular physiology has been extensively studied (Smith and Read, 2008; Miransari, 2011; Smith and Smith, 2011; Casieri et al., 2013), little is known about the mechanisms of Fe uptake.

On the plant side, up-regulation of two genes encoding iron transport proteins, a vacuolar iron transporter and a ferric-chelate reductase, has been reported in a transcriptomic study aimed to identify sorghum genes induced in mycorrhizal roots (Handa et al., 2015). The effect of the AM symbiosis on Fe transport related genes has been addressed in maize, a plant that uses a Fe uptake Strategy II (Kobae et al., 2014; Chorianopoulou et al., 2015). Despite the fungal contribution to Fe uptake, expression of the ZmYS1 encoding a transporter that mediates the uptake of PS–Fe(III) complexes from the rhizosphere was not affected in mycorrhizal roots. However, two oligopeptide transporter genes that were proposed to mediate the transport of Fe or Fe-complexes were highly induced in mycorrhizas (Kobae et al., 2014).

Under iron limited conditions, fungi also employ two high-affinity iron uptake systems: a reductive iron assimilation (RIA) system and a siderophore-mediated iron uptake system (Johnson, 2008). For ferric iron to be available for the reductive pathway it must first be reduced to ferrous. In the well characterized *Saccharomyces cerevisiae* system, this reduction is completed by the metalloreductases Fre1 and Fre2 (Fig. 1). Then, the reduced ferrous iron is rapidly taken up by a high-affinity ferrous-specific transport complex consisting of a plasma membrane multicopper ferroxidase (Fet3) that oxidizes the iron in a copper- and oxygen dependent reaction, which is then transported to the cytosol by a permease (Ftr1) (Eide *et al*., 1992, Askwith *et al*., 1994, De Silva *et al*., 1995; Stearman et al., 1996). As in plants, the second iron uptake system involves the secretion of siderophores and uptake of siderophore-iron complexes by specific high-affinity siderophore transporters (Haas et al., 2008; Philpott and Protchenko, 2008; Saha et al., 2013). The mechanisms of Fe transport in AM fungi have not been characterized yet, but a recent genome-wide analysis of metal transporters in the AM fungus *Rhizophagus irregularis* indicated that Fe uptake occurs through a reductive

pathway since two genes, *RiFTR1* and *RiFTR2*, showing high homology to the *S. cerevisiae* Fe permeases were found in its genome (Tamayo et al., 2014; previous chapter). With the aim to get some insights into the mechanisms of Fe transport in AM fungi, in this study we have characterized three *R. irregularis* genes encoding putative components of the high-affinity reductive iron uptake system: a ferric reductase and the iron permeases RiFTR1 and RiFTR2. Our results indicate that the iron transport reductive pathway is operating in *R. irregularis*, and that the iron permease RiFTR1 plays a major role in Fe acquisition in iron-limiting environments and that it might be important in the *in planta* phase of the fungus.

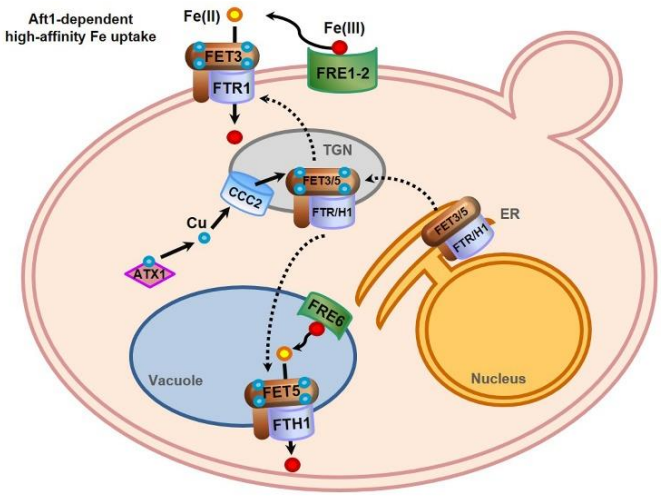

Figure 1. High affinity Fe transport in *Saccharomyces cerevisiae*. Formation of a stable ferroxidase-permease complex is performed in the ER, being a prerequisite for exit from the ER. Then, ferroxidase is loaded with Cu, which takes place in the trans-Golgi network (TGN). The Cu chaperone Atx1 and the post-Golgi Cu-ATPase Ccc2 are required for Cu insertion. After copper loading, the complex Fet3-Ftr1 moves to plasma membrane, where Fe(III) is reduced by Fre1 and Fre2 that constitute the majority (>90%) of the cell surface reductase activity, and the complex Fet5-Fth1 moves to vacuolar membrane where transports Fe(II) into the cytosol. Modified model from Cyert and Philpott (2013).

Materials and methods

Biological materials and growth conditions

R. irregularis monoxenic cultures were established as described by St-Arnaud et al. (1996), with some modifications. Briefly, clone DC2 of carrot

(*Daucus carota* L.) Ri-T DNA transformed roots were grown with the AM fungus *R. irregularis* Schenck and Smith DAOM 197198 in two-compartment Petri dishes. Cultures were initiated in one compartment of each plate containing M medium (Chabot *et al*., 1992) by placing several non-mycorrhizal carrot root segments and a piece of fungal inoculum containing ERM, fragments of mycorrhizal roots and spores. Fungal hyphae and roots were allowed to grow over the plastic wall to the other compartment containing the same M medium. Plates were incubated in the dark at 24 °C for 7–8 weeks until the second compartment was profusely colonized by the fungus and the roots. Then, the older compartment was removed and refilled with liquid M medium without sucrose (M-C medium) containing different Fe concentrations: 0.045 mM (control), 4.5 mM or 45 mM EDTA iron(III) sodium salt. Fungal hyphae, but not roots, were allowed to grow in this compartment (hyphal compartment). Plates were incubated in the dark at 24 °C for 2–3 additional weeks. To induce Fe-deficient conditions, fungal hyphae grown in liquid M-C medium without iron were exposed 3 d to 0.5 mM ferrozine (Sigma). This was done by replacing the liquid medium by a freshly prepared liquid medium without Fe but containing 0.5 mM ferrozine, which was previously prepared in 50 mM MES pH 6.1 (Ferrozine M media). Control plates received the same buffered medium without ferrozine. Plates were incubated in the dark at 24 °C for 3 additional days.

ERM from the different hyphal compartments was directly recovered under sterile conditions using a pair of tweezers, washed with sterilized water and dried on filter paper. The mycelium was immediately frozen in liquid nitrogen and stored at -80 °C until used.

For gene expression analyses, mycorrhizal carrot roots were obtained by placing several non-mycorrhizal carrot root segments on top of a densely colonized hyphal compartment. Plates were incubated at 24 °C and roots were collected 15 days later. Extraradical hyphae attached to the roots were removed with forceps under a binocular microscope. Roots were then frozen in liquid N and stored at -80 °C until used. Furthermore, maize roots colonized by *R. irregularis* and fertilized with or without of Fe were used. Surface-sterilized maize seedlings were germinated in autoclaved vermiculite and seedlings were transplanted into pots containing 1 l of a sterile mixture

of sand:vermiculite (1:1, v:v) and 100 g of a sepiolite-vermiculite based inoculum of *R. irregularis* containing spores, hyphae and fragments of AM roots. Plants were grown in a growth chamber with 25/20 °C day/night temperature, 60 % relative humidity and 16/8 light/dark photoperiod. The pots were watered every other day with half-strength (0.5 X) Hoagland nutrient solution or with a modified nutrient solution without Fe. Roots were harvested 8 weeks after inoculation, gently washed under tap water, frozen in liquid nitrogen and stored at -80 °C until used. Mycorrhizal root colonization was estimated after trypan blue staining according to the grid-line intersect method using a stereomicroscope (Giovannetti & Mosse, 1980).

The *S. cerevisiae* strains used in this study were all isogenic derivatives of YPH499 and YPH252 wild type strains (Table 1). Strains were grown on YPD or complete synthetic medium (CSM), supplemented with appropriate amino acids.

Table 1. *Saccharomyces cerevisiae* strains used in this work.

Strain	Relevant genotype	Reference
YPH499	*MATα ura3-52 lys2-801 ade2-101 trp1-Δ63 his3-Δ200 leu2-Δ1*	Sikorski and Hieter, 1989
499*Δ1Δ2*	As YPH499 but *Δfre1::LEU2 Δfre2::HIS3*	Finegold et al., 1996
Δ1Δ2 pDR195	499*Δ1Δ2* transformed with pDR195	This work
Δ1Δ2 pDR195-*RiFRE1*	499*Δ1Δ2* transformed with pDR195-*RiFRE1*	This work
Δ1Δ2 pDR195-*ScFre1*	499*Δ1Δ2* transformed with pDR195-*ScFre1*	This work
YPH252	*MATα ura3-52 lys2-801 ade2-101 trp1-Δ1 his3-Δ200 leu2-Δ1*	Sikorski and Hieter, 1989
42B *ftr1Δ-1*	As YPH252 but *Δftr1::TRP1*	Stearman et al., 1996
Δftr1 pDR195	42B *ftr1Δ-1* transformed with pDR195	This work
Δftr1 pDR195-*RiFTR1*	42B *ftr1Δ-1* transformed with pDR195-*RiFTR1*	This work
Δftr1 pDR195-*RiFTR2*	42B *ftr1Δ-1* transformed with pDR195-*RiFTR2*	This work
Δftr1 pDR195-*ScFtr1*	42B *ftr1Δ-1* transformed with pDR195-*ScFtr1*	This work
Δftr1 pBL106	42B *ftr1Δ-1* transformed with pBL106	This work
Δftr1 pBL106-*RiFTR1*	42B *ftr1Δ-1* transformed with pBL106-*RiFTR1*	This work
Δftr1 pBL106-*RiFTR2*	42B *ftr1Δ-1* transformed with pBL106-*RiFTR2*	This work

Ferric reductase assays

The ferric reductase activity of the *R. irregularis* ERM was determined following the protocol of Knight et al. (2005) with some modifications. To induce the ferric reductase activity, fungal hyphae grown in the hyphal compartment of a split Petri dish in liquid M-C medium without iron were incubated at 24 °C for 24 h in Ferrozine M media without microelements. For control mycelia with no induction of ferric reductase activity, plates with fungal hyphae grown in liquid M-C control medium were incubated at 24 °C for an additional 24 h after replacing the medium by liquid M-C medium with 50 mM MES buffer added. The ferric reductase assay solution consisted of 50 mM citrate buffer (pH 6.6)-5% D-glucose containing 1 mM bathophenanthrolinedisulfonate (BPS) and 1 mM ferric ammonium sulfate. Before proceeding to the ferric reductase assay, mycelia was washed with ice-cold 50 mM citrate buffer (pH 6.6)-5% D-glucose. For the quantitative assay, excised mycelia were embedded in the ferric reductase assay solution in an Eppendorf tube and incubated in the dark at 24 °C for up to 1 h (until clearly visible red color), and ferric reductase activity was quantified by measuring absorbance at 515 nm. Assay mixtures containing no mycelia were used to determine blank values, which were subtracted from values obtained in assays with ERM.

To analyze *in vivo* localization of *R. irregularis* ferric reductase activity, excised mycelia were embedded in the ferric reductase assay solution solidified with 0.15% (w/v) agar in a 5.5 cm diameter Petri dish (according to Jin et al. (2011) with modifications). Mycelia were incubated overnight at 24 °C, and observed under the dissecting microscope.

Yeast transformants were assayed for ferric reductase activity as described by Knight et al. (2005). Briefly, cells in the exponential growth phase were washed three times with ice-cold 50 mM citrate buffer (pH 6.6)-5% D-glucose and, after measuring optical densities at 720 nm, incubated in the same buffer but prewarmed and containing 1 mM BPS and 1 mM ferric ammonium sulfate for up to 10 min (until clearly visible red color) at 30 °C in low light conditions. Ferric reductase activity was then quantified as described above.

Nucleic acids extraction and cDNA synthesis

R. irregularis genomic DNA was extracted from ERM developed in the hyphal compartment of control plates using the DNeasy Plant Mini Kit (Qiagen), according to the manufacturer's instructions.

Total plant RNA was isolated from maize roots using the phenol/SDS method followed by LiCl precipitation as described by García-Rodríguez et al. (2007). RNA from ERM from the different treatments and from mycorrhizal roots was extracted using the RNeasy Plant Mini Kit (QIAGEN, Maryland), following manufacturer´s instructions. DNAse treatment was performed using the RNA-free DNase set (QIAGEN, Maryland) following the manufacturer's instructions. cDNAs were obtained from 1 μg of total DNase-treated RNA in a 20 μl reaction containing 200 units of Super-Script III Reverse Transcriptase (Invitrogen) and 50 pmol oligo $(dT)_{20}$ (Invitrogen), according to the manufacturer's instructions.

Identification of **FRE** *genes in the* **R. irregularis** *genome and sequences analyses*

Amino acid sequences of *S. cerevisiae* ferric reductases (Fre1-8) were retrieved from the freely accessible *Saccharomyces* genome database (http://www.yeastgenome.org/). These sequences were used to search for orthologous sequences in the filtered model dataset of *R. irregularis* on the JGI website (http://genome.jgi.doe.gov/Gloin1/Gloin1.home.html; Tisserant *et al*., 2012 and 2013) using the Basic Local Alignment Search Tool (BLAST) algorithm (Altschul *et al*., 1990) via a protein BLAST. A second search was performed via a keyword search directly. All amino acid orthologous sequences of a number of fungi representatives of distinct taxonomic groups used in the phylogenetic analysis were retrieved from FGI website (http://www.broadinstitute.org/science/projects/fungal-genome-initiative/fungal-genome-initiative), except for *S. cerevisiae* (http://www.yeastgenome.org/) and *Laccaria bicolor* (http://genome.jgi-psf.org/). Amino acid sequences of *R. irregularis* were retrieved from JGI website or from Lin et al. (2014).

Full-length of FRE-Nox amino acid orthologous sequences were aligned by ClustalW (Version 2.1; Larkin *et al*., 2007; http://www.ebi.ac.uk/Tools/msa/clustalw2/). Alignments were imported into the Molecular Evolutionary Genetics Analysis (MEGA) package version 6 (Tamura et al., 2013). A phylogenetic analysis was conducted by the neighbour-joining (NJ) method, implemented in MEGA, with a pair-wise deletion of gaps and the Poisson model for distance calculation. Bootstrap analyses were carried out with 1000 replicates. The evolutionary tree was drawn to scale. Predictions of putative transmembrane domains were made using the TMHMM Server v.2.0 (http://www.cbs.dtu.dk/services/TMHMM/) and SMART software (http://smart.embl-heidelberg.de/). Predictions of subcellular localizations were made using the TargetP 1.1 Server (http://www.cbs.dtu.dk/services/TargetP/), PSORTII (http://psort.hgc.jp/form2.html) and WoLF PSORT (http://wolfpsort.org/).

Gene isolation

Genomic clones and full-length cDNAs of *RiFRE1*, *RiFTR1* and *RiFTR2* were obtained by PCR amplification of *R. irregularis* genomic DNA and cDNA, respectively, using the corresponding primer pairs (S1 Table). PCR products were cloned in the pGEM-T easy vector (Promega, Madison, USA).

All plasmids were amplified by transformation of *Escherichia coli* following standard procedures and purified by using the Qiagen Miniprep Kit (Qiagen, Maryland, USA). All sequences and constructs were checked by sequencing before further use. Nucleotide sequences were determined by Taq polymerase cycle sequencing by using an automated DNA sequencer (ABI Prism 3130xl Genetic Analyzer, Applied Biosystems, Carlsbad, USA).

Heterologous expression and growth assays

For heterologous gene expression analyses, the full length cDNAs were cloned into the yeast cDNA-cloning vector pDR195, which contains a fragment of the plasma membrane ATPase promoter (Rentsch et al., 1995). To obtain pDR195-*RiFRE1*, pDR195-*RiFTR1* and pDR195-*RiFTR2*, the respective full-length cDNAs were isolated from the pGEM-T easy vector by *Not*I digestion and ligated into the *Not*I- digested pDR195 vector. The full-lenght

cDNAs of *Fre1* and *Ftr1* yeast genes were also cloned into pDR195 and used as positive controls in the complementation analyses of the *Δfre1Δfre2* and *Δftr1* mutant strains.

Yeasts were transformed with the corresponding constructs using a lithium acetate-based method (Schiestl and Gietz, 1989), and transformants (Table 1) were selected in CSM medium by autotrophy to uracil.

For the complementation assay, a specially designed medium was used (Knight et al., 2002). To avoid iron contamination, new plastic or acid washed glassware was used for all media preparation. Briefly, the assay medium consisted of CSM made with a yeast nitrogen base lacking iron and copper (Bio-101), supplemented with 1 μM copper sulfate and 50 mM MES pH 6.1. The iron-limited medium was the assay medium with 1 mM ferrozine (0.1 M stock) and different concentrations of $(NH_4)_2Fe(SO_4)_2$ (ferrous ammonium sulfate) up to 200 μM. The medium supplemented with 1 mM ferrozine and 250 μM ferrous ammonium sulfate was taken as iron-sufficient control media. For the plating assay, the medium contained 2% Bacto agar (Difco). Stationary yeast cultures grown in CSM liquid culture were washed with ice-cold distilled water, resuspended in iron-limited medium supplemented with 50 μM ferrous ammonium sulfate and grown to saturation overnight. These cultures were then washed twice and diluted to an optical density at 600 nm of 5. Serial 1:5 dilutions were spotted (5 μl) onto plates containing the assay media supplemented with ferrozine and different iron concentrations.

High-affinity iron uptake assays in yeast

To induce the high-affinity Fe uptake system, stationary yeast cultures grown in CSM liquid medium were washed with ice-cold distilled water, resuspended in iron-limited medium supplemented with 50 μM ferrous ammonium sulfate and grown to saturation overnight. These cultures were then washed twice and diluted 1:5 in iron-limited medium supplemented with 200 μM ferrous ammonium sulfate, and grown for 3-4 additional hours until exponential growth phase is reached. After washing twice and resuspension in CSM liquid medium without Fe nor ferrozine, we proceeded with the iron uptake assay. High-affinity iron uptake was measured after

being washed three times in citrate-glucose buffer and resuspended in the same buffer. Citrate buffer containing 1 μM ferrous (^{55}Fe)-ascorbate was added to the suspended cells and incubated at 30 °C for 2 hours. At this point, the optical densities at 600 nm of cultures were measured. The cells were then harvested and washed free of ^{55}Fe label by using a cell harvester (PHD Cambridge Technologies) and iron uptake was measured by liquid scintillation counting (Beckman LS6500). Assay mixtures containing no cells were used to calculated blank values for correction.

Protein localization analyses

Localization of *R. irregularis* FTR1 and FTR2 proteins in *S. cerevisiae* was analyzed by fusion of the respective genes with the enhanced green fluorescent protein (GFP) gene. Gene-specific primer pairs containing *Sfi*IA (GGCCATTACGGCC) and *Sfi*IB (GGCCGAGGCGGCC) overhangs, respectively (S1 Table), were used to clone the two iron permease cDNAs into the *Sfi*I sites of the plasmid pBL106, a pDR196sfi vector derivative carrying *GFP* (Ellerbeck et al., 2013). The *Δftr1* yeast mutant strain was transformed with the resulting plasmids pBL106-*RiFTR1*, pBL106-*RiFTR2*, which harbour the fusion genes, or the pBL106 vector. Stationary yeast cultures grown in CSM were washed twice with ice-cold distilled water, diluted in iron-limited medium supplemented with 50 μM ferrous ammonium sulfate, and grown to saturation overnight. These cultures were then washed twice with water, diluted in iron-limited medium supplemented with 300 μM ferrous ammonium sulfate and grown for several hours in this medium to an OD_{600} between 0.8 and 1.6, using acid-treated flasks. Vacuolar membrane staining with FM 4-64 (Molecular Probes) was performed as previously described by Vida and Emr (1995), with some modifications. Briefly, exponential yeast cells were harvested at 3000 rpm for 3 min, washed twice and resuspended at 20-40 OD_{600} /ml in iron-limited medium supplemented with 300 μM iron. Cells were washed three times and resuspended in water before visualization. The fluorescence signal was visualized with a Nikon Eclipse 50i fluorescent microscope. A 510-560 nm filter was used for FM 4-64 fluorescence, and GFP fusion proteins were imaged using a 450-490 nm filter. Image sets were processed and overlapped using Adobe Photoshop™.

Gene expression analyses

R. irregularis gene expression was studied by real-time RT-PCR by using an iQ™5 Multicolor Real-Time PCR Detection System (Bio-Rad). Each 20 µl reaction contained 1 µl of a 1:10 dilution of the cDNA, 200 nM each primer, 10 µl of iQ™ SYBR Green Supermix 2x (Bio-Rad). The PCR program consisted in a 3 min incubation at 95 °C to activate the hot-start recombinant Taq DNA polymerase, followed by 36 cycles of 30 s at 95 °C, 30 s at 58 °C and 30 s at 72 °C, where the fluorescence signal was measured. The specificity of the PCR amplification procedure was checked with a heat-dissociation protocol (from 58 to 95 °C) after the final cycle of the PCR. The primer sets used are listed in S1 Table. The efficiency of the primer set was evaluated by performing real-time PCR on several dilutions of cDNA. Because RNA extracted from mycorrhizal roots contains plant and fungal RNAs, specificity of the primer pairs was also analyzed by PCR amplification of carrot and maize genomic DNA and cDNA from non-mycorrhizal maize roots. The results obtained for the different treatments were standardized to the elongation factor 1-alpha gene levels (GenBank Accession No. DQ282611), which were amplified with the following primers: GintEFfw and GintEFrev. RT-PCR determinations were performed on at least three independent biological samples from three replicate experiments. Real-time PCR experiments were carried out three times for each biological sample, with the threshold cycle (Ct) determined in triplicate. The relative levels of transcription were calculated by using the $2^{-\Delta\Delta CT}$ method (Schmittgen and Livak, 2008), and the standard error was computed from the average of the ΔCT values for each biological sample.

Statistical analyses

Statgraphics Centurion XVI software was used for the statistical analysis of the means and standard deviation determinations. ANOVA, followed by a Fischer's LSD test ($p<0.05$) when possible, was used for the comparison of the treatments based on at least 3 biological replicates for each treatment ($n \geq 3$).

Results

Evidence of ferric reductase activity in R. irregularis

As a first step to determine whether a RIA system operates in *R. irregularis*, an *in vivo* reductase activity assay was carried out in *R. irregularis* ERM grown in monoxenic cultures. A basal level of ferric reductase activity was observed in micelia grown in M medium containing 0.045 mM Fe (control plates). This activity was strongly activated when mycelia was grown in media without Fe and supplemented with ferrozine (Fig. 2A). Activation of the ferric reductase activity by Fe-deficient conditions was also visualized by changes in colour around the *R. irregularis* hyphae due to the formation of Fe (II)-ferrozine complex, as shown by the redish colour observed of the ERM grown in Fe-limiting conditions (Fig. 2B and C).

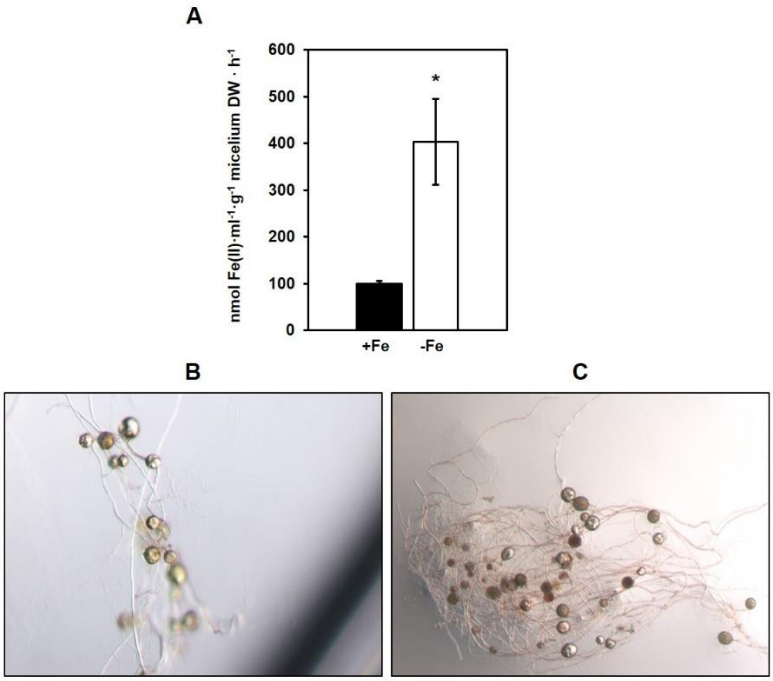

Figure 2. I*n vivo* ferric reductase activity of *Rhizophagus irregularis*. A. Quantitative ferric reductase assay was carried out in *R. irregularis* mycelia grown in liquid M-C medium (+Fe) or under Fe-limiting conditions and incubated for 24 h in buffered M-C medium with ferrozine (-Fe). Ferric reductase activity was visualized in *R. irregularis* mycelia grown in control M-C media (B) or under Fe-limiting conditions (C) and incubated overnight in a semisolid ferric reductase assay solution.

To further characterize this ferric reductase activity, the *R. irregularis* genome was searched for ferric reductase (FRE) homologs. Ferric reductases are membrane-bound oxidoreductases that transfer electrons from cytosolic NADPH to FAD and then, through the heme groups in the reductase, to electron acceptors on the extracellular surface. They are highly similar to NADPH oxidases (Nox) and belong to the ferric reductase domain (FRD) superfamily (Takemoto et al., 2007). One FRE homolog, named *RiFRE1*, was found in the *R. irregularis* genome (GenBank Accession No. ESA06884, JGI ID 349676). Since alignment of RiFRE1 with the *S. cerevisiae* homologs revealed that RiFRE1 had a ~140 amino acids deletion at the N-terminus (Fig. 3), 5´RACE was performed to get sequence upstream of the predicted start codon. A 685 nucleotide-long 5´untranslated sequence containing several in-frame stop codons before the assumed start codon was obtained, confirming that the open reading frame of *RiFRE1* is 1626 bp long. *RiFRE1* contains only one intron flanked by the canonical GT/AG splicing sequence and encodes a protein of 541 amino acids that was predicted to be located at the plasma membrane and to have seven transmembrane domains (Fig. 4). RiFRE1 contains the four canonical heme-coordinating histidines characteristic of the FRD superfamily, several NAD(P)H binding motifs and a FAD binding motif (Fig. 3), but lacks the His-119 and Thr-178 residues that are conserved in the NADPH oxidase proteins of all organisms (Zhang et al., 2013), including the *R. irregularis* NOX genes.

RiFRE1 displays the highest similarity (42%) to the FRE homolog of *R. oryzae* RO3G_05460 (GenBank Accession No. EIE80755). A phylogenetic analysis of fungal FRE proteins revealed that the *R. irregularis* FRE homolog, clustered together with the *Rhizopus oryzae* homologs (Fig. 5).

Figure 3. Alignment of the amino acid sequence of RiFRE1 with the sequences of the *Saccharomyces cerevisiae* ferric reductases FRE1 and FRE2. Putative canonical heme-coordinating histidines (H in bold), NAD(P)H binding motifs (GPYG and CGP) and FAD binding motifs (HPXXXXS) are underlined.

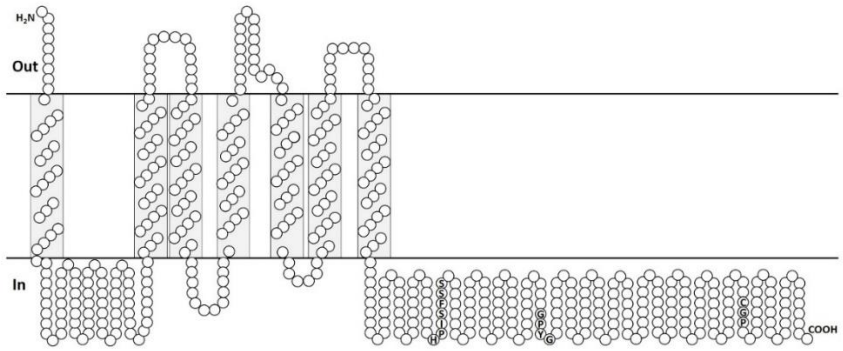

Figure 4. Topological model of RiFRE1. This model was generated at SOSUI (http://harrier.nagahama-i-bio.ac.jp/sosui/sosui_submit.html), but also considering TMHMM and SMART results. Sequence elements identified are indicated (HPXXXXS, GPYG and CGP motifs in C-tail).

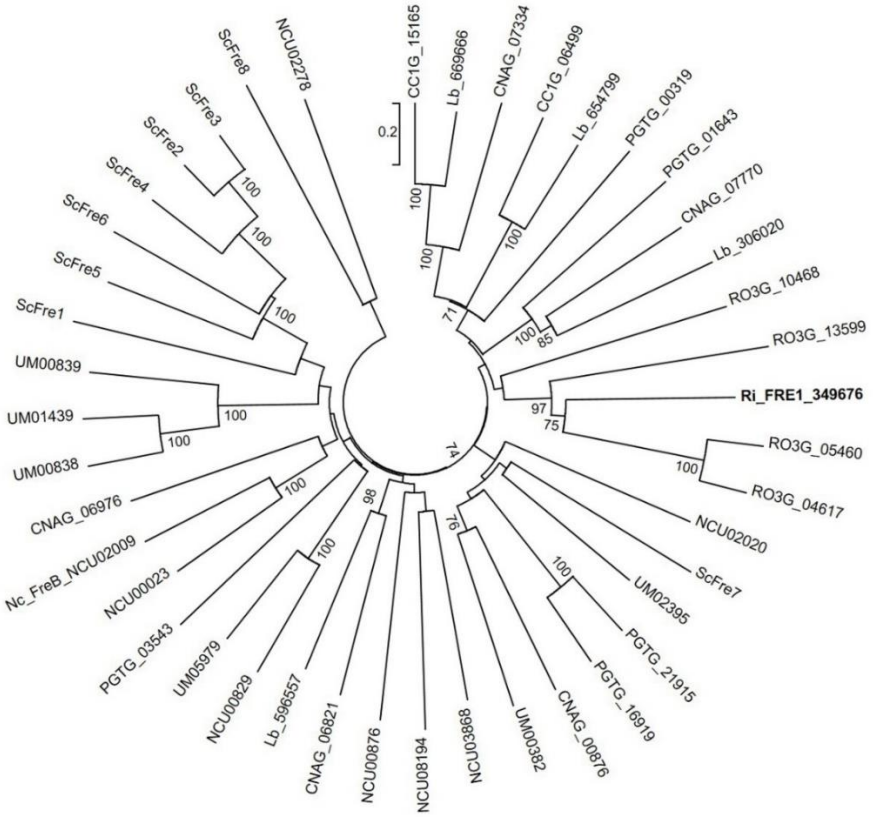

Figure 5. Phylogenetic relationships of the *Rhizophagus irregularis* FRE1 candidate with homologous sequences from selected species representative of the major fungal phyla. The unrooted Neighbor-Joining tree was created with MEGA6. Protein identification numbers from FGI, JGI or SGD are indicated. *R. irregularis* FRE1 is shown in bold. Organisms: Cc, *Coprinopsis*

cinerea; Cn, *Cryptococcus neoformans*; Lb, *Laccaria bicolor*; Nc, *Neurospora crassa*; Pg, *Puccinia graminis*; Ri, *Rhizophagus irregularis*; Ro, *Rhizopus oryzae*; Sc, *Saccharomyces cerevisiae*; Um, *Ustilago maydis*. Bootstrap values above 70 and supporting a node used to define a cluster are indicated.

In silico *analyses of the* R. irregularis *iron permeases*

The *R. irregularis* Ftr1 and Ftr2 full-length cDNA sequences putatively encoding iron permeases were obtained using gene-specific primers based on the sequences described by Tamayo et al. (2014). Comparison of the full-length cDNA and genomic sequences revealed that *RiFTR1* and *RiFTR2* have 2 introns. *RiFTR1* and *RiFTR2* encode proteins of 317 amino acids that are highly homologous to each other (64% similarity) and were predicted to have seven transmembrane helixes and the two REXXE motifs typical of Fe transporters (Fig. 6). RiFTR1 also has a putative iron-channeling EATE motif in loop 6 (Fig. 6A).

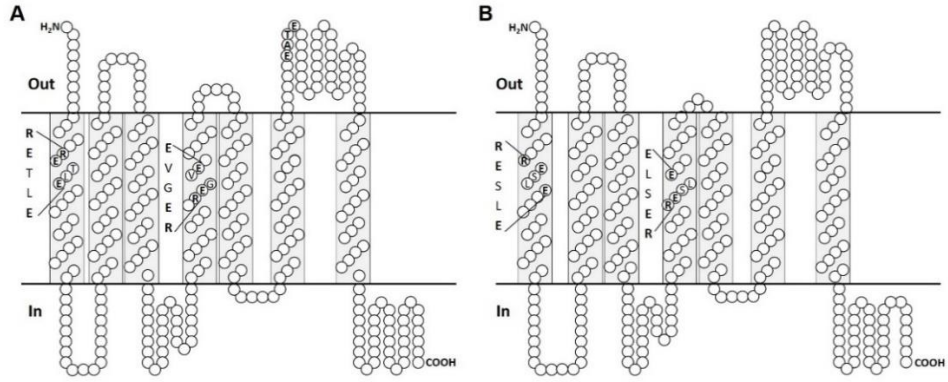

Figure 6. Topological models of RiFTR1 (A) and RiFTR2 (B). These models were generated at SOSUI (http://harrier.nagahama-i-bio.ac.jp/sosui/sosui_submit.html), but also considering TMHMM and SMART results. Sequence elements identified are indicated (REXXE motifs in transmembrane domains 1 and 4 of RiFTR1 and RiFTR2; and a possible iron-channeling EATE motif in loop 6 of RiFTR1).

Functional characterization of the R. irregularis *components of the iron reductase pathway in yeast*

To get further insights into the reductive Fe assimilation system of *R. irregularis* and since no stable transformation protocols exist for AM fungi,

RiFRE1, and RiFTR1 and RiFTR2, two putative orthologs of the yeast plasma membrane Fe transporter FTR1 whose genes were previously found in the *R. irregularis* genome (Tamayo et al., 2014), were functionally characterized in yeast.

The putative iron reductase gene *RiFRE1* was tested for complementation of the iron reductase-deficient mutant yeast *Δfre1Δfre2* (Finegold et al., 1996), and *RiFTR1* and *RiFTR2* of the *Δftr1* disruption mutant of *S. cerevisiae* lacking the plasma membrane Fe permease (Stearman et al., 1996). The *S. cerevisiae Fre1* and *Ftr1* genes were included as positive controls. Cells were transformed with variants of the plasmid pDR195 containing the full length cDNAs of different genes or with the empty vector. The genes were constitutively expressed under the *PMA1* promoter (Rentsch et al., 1995). Unfortunately, RiFRE1 did not restore the poor growth of *Δfre1Δfre2* on low-Fe conditions (Fig. 7A). Moreover, the iron reductase activity of the *RiFRE1*-expressing cells did not significantly differ from the basal level observed in the control cells transformed with the empty vector (Fig. 7B). The inability of RiFRE1 to restore the *Δfre1Δfre2* ferric reductase activity might be due to the low sequence homology of RiFRE1 and ScFRE1-2 (20% and 21% amino acid identity, respectively; Fig. 3).

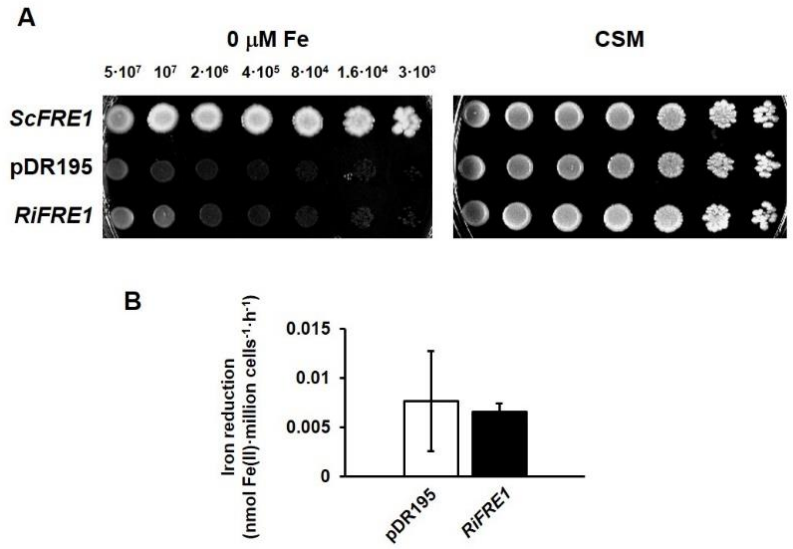

Figure 7. Analysis of the *in vivo* ferric reductase activity of RiFRE1 in yeast. A. *Δfre1Δfre2* cells transformed with the empty vector or expressing *RiFRE1* were plated on specially designed

CSM medium with ferrozine added *versus* regular CSM medium. Plates were incubated at 30 °C for 3 days. B. Ferric reductase activity was determined in exponentially-growing *Δfre1Δfre2* cells transformed with the empty vector or expressing *RiFRE1*. Data are means +/- standard error.

In the case of RiFTR1 and RiFTR2, they were tested for their ability to revert the growth defect in low-iron conditions of the *Δftr1* mutant of *S. cerevisiae*.

Although less efficiently than yeast *FTR1*, expression of *RiFTR1* in the *Δftr1* yeast mutant cells reverted their inability to grow on iron-limited medium supplemented with 150 μM ferrous ammonium sulfate. Nevertheless, *RiFTR2*-transformed *Δftr1* mutant cells were not able to grow on that medium (Fig. 8A). These data indicate that RiFTR1 plays at least in the heterologous system an *in vivo* role in iron transport in iron-limited environments and that RiFTR2 might be the ortholog of the yeast vacuolar Fe permease Fth1.

To test this hypothesis, we examined subcellular location of RiFTR1 and RiFTR2 in the heterologous system by expressing C-terminal green fluorescent protein (GFP)-tagged FTR fusion proteins. For this purpose, *RiFTR1* and *RiFTR2* full length cDNAs were cloned into the yeast expression vector pBL106 and these constructs were expressed in the *Δftr1* cells. As observed for the non-tagged proteins, RiFTR1 complemented the growth defect of the *Δftr1* mutant yeast (Fig. 8A). However, cells transformed with the empty vector (soluble GFP) or with *RiFTR2::GFP* were unable to grow on iron-limited media. RiFTR1-GFP fusion protein was localized to the yeast plasma membrane, but none of them co-localized with the vacuolar membrane marker FM4-64 (Fig. 8B). In the *RiFTR2-GFP* expressing cells the fluorescence signal was distributed in a pattern typical of a secreted protein with putative ER and Golgi localization (Huang and Shusta, 2005), probably as an artefact of the heterologous system.

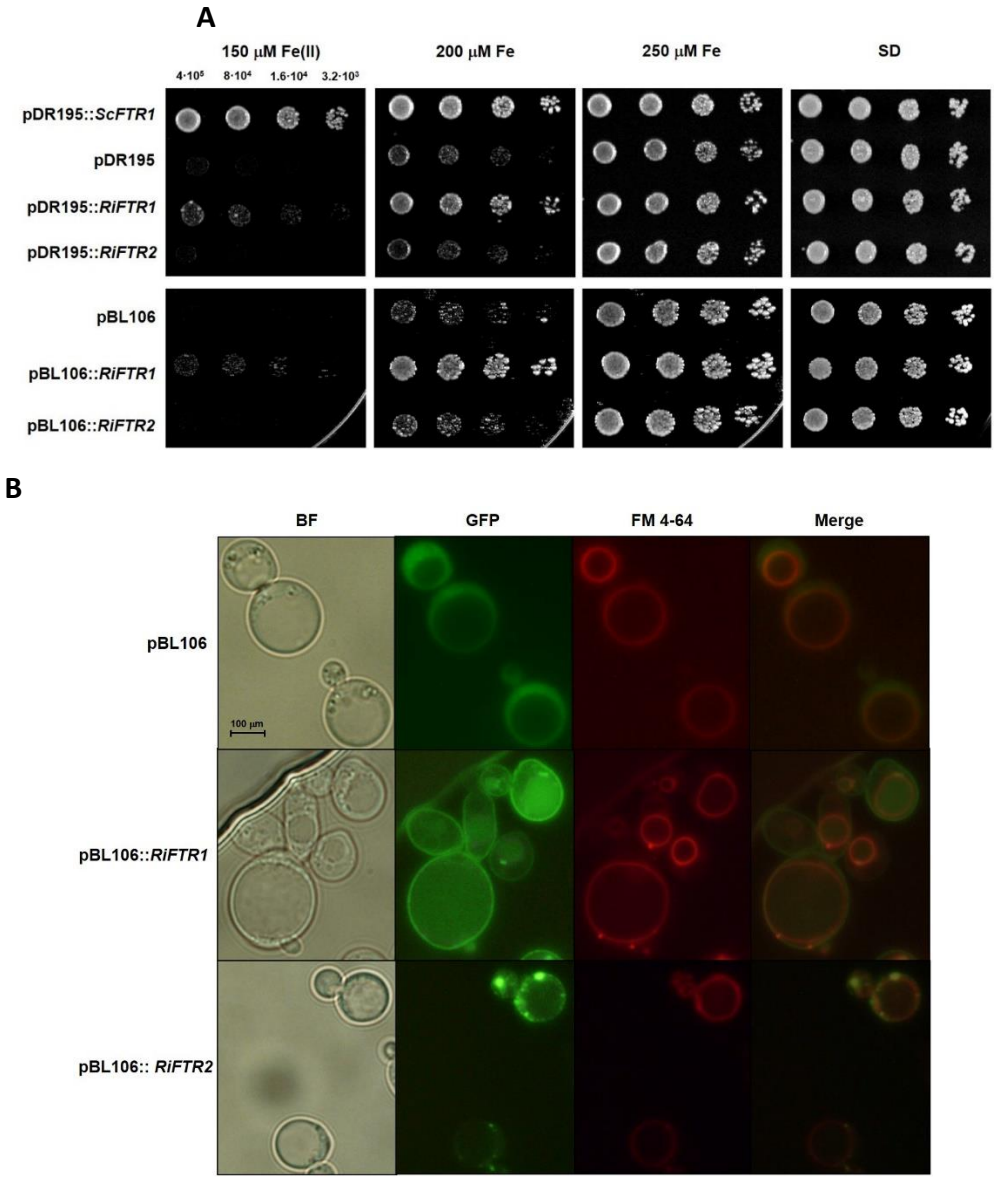

Figure 8. Analysis of the *in vivo* role of RiFTR1 and RiFTR2 in high-affinity iron transport and their *in vivo* localization in yeast. A. *Δftr1* cells transformed with the empty vector or expressing *ScFTR1*, *RiFTR1* or *RiFTR2* (upper panel), or with the vector expressing *GFP* (pBL106), *RiFTR1-GFP* or *RiFTR2-GFP* (lower panel), were plated on specially designed CSM medium supplemented with ferrozine and Fe (150, 200 or 250 μM) or in standard CSM medium. Plates were incubated at 30 °C for 3 days. B. *Δftr1* cells transformed with the vector expressing *GFP* (first row), *RiFTR1-GFP* (second row) or *RiFTR2-GFP* (third row) were visualized with a Nikon Eclipse 50i fluorescent microscope after labelling with FM 4-64 for vacuolar membrane staining. BF, bright field (first column); GFP, green channel (second column); FM 4-64, red channel (third column); Merge, combination of green and red channels (fourth column).

Fe transport assays

To confirm that RiFTR1 indeed transports Fe, *Δftr1* transformants were assayed for ferrous iron transport activity. Expression of *RiFTR1* in the *Δftr1* cells resulted in a 2.9-fold increase in the iron uptake activity of the controls (empty vector-transformants) (Fig. 9).

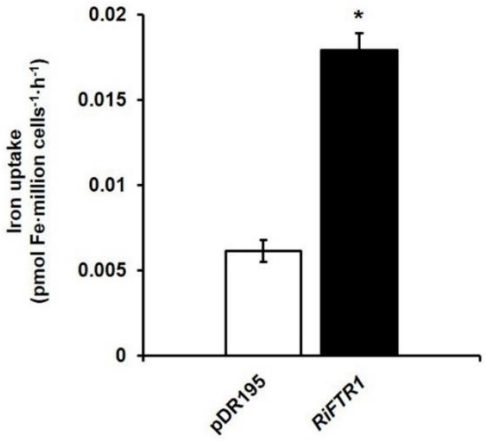

Figure 9. Iron transport assay in yeast. *Δftr1* cells transformed with the empty vector or expressing *RiFTR1* were examined for Fe uptake. Data are means +/- standard error. Asterisks show statistically significant differences ($p<0.05$) relative to the activities of the strain transformed with the empty vector.

Gene expression patterns

The expression of the high-affinity iron transport systems is usually induced in iron-limited environments and repressed in iron-sufficient environments. To assess whether *RiFRE1*, *RiFTR1* and *RiFTR2* expression is dependent on iron availability, their gene expression was analyzed by real-time RT-PCR in the ERM that had been exposed to different Fe concentrations (Fig. 10). Relative to the ERM control grown in M media containing 0.045 mM Fe, a 2.8-fold up-regulation of *RiFTR1* expression was observed in the ERM grown under Fe-limiting conditions. However, expression levels of *RiFRE1* and *RiFTR2* were not significantly affected. As expected for the components of a high affinity transport system, development of the fungus in the presence of 45 mM Fe induced down-regulation of *RiFRE1*, *RiFTR1* and *RiFTR2* gene

expression. An 11.6-fold down-regulation of *RiFTR1* was observed when the fungus was grown in a media supplemented with 4.5 mM Fe.

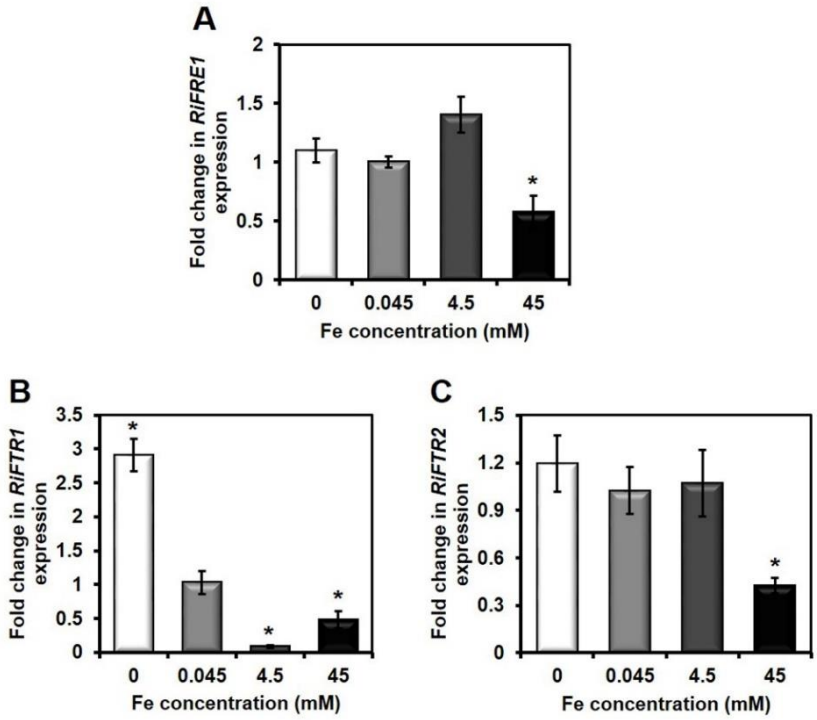

Figure 10. Effect of iron on the expression of the *Rhizophagus irregularis RiFRE1* and *RiFTR* genes. *R. irregularis* was grown in M-C media without Fe, containing 0.045 mM Fe (control) or supplemented with 4.5 mM Fe or 45 mM Fe medium for 2 weeks. ERM grown in media without Fe was exposed for 3 d to ferrozine. *RiFRE1* (A), *RiFTR1* (B) and *RiFTR2* (C) gene expression. Data were normalized using the housekeeping gene *RiTEF*. Relative expression levels were calculated by the $2^{-\Delta\Delta CT}$ method. Data are means +/- standard error. Asterisks show statistically significant differences ($p<0.05$) compared to the control value.

As an additional step to get insights into the role of the RiFRE1 and RiFTR1-2 in *R. irregularis*, quantitative gene expression analysis was performed by real-time RT-PCR on ERM collected from the hyphal compartment of *R. irregularis* monoxenic cultures and on mycorrhizal roots developed in a densely colonized hyphal compartment and devoid of external hyphae and in maize mycorrhizal roots grown in pot cultures. As a control, expression of *RiMST2*, a hexose transporter that is highly expressed in the intraradical phase of the fungus (Helber *et al*., 2011), was also determined. As expected, *RiMST2* was expressed during the *in planta* phase of the fungus and

was barely detected in the ERM (data not shown). Transcript levels of *RiFTR1* were 40- and 80-fold higher in the IRM of the carrot and maize roots, respectively, than in the ERM. Depending on the plant species, *RiFTR2* expression levels were similar or slightly lower in the IRM than in the ERM. No significant differences were observed between the expression levels of *RiFRE1* in both fungal structures (Fig. 11).

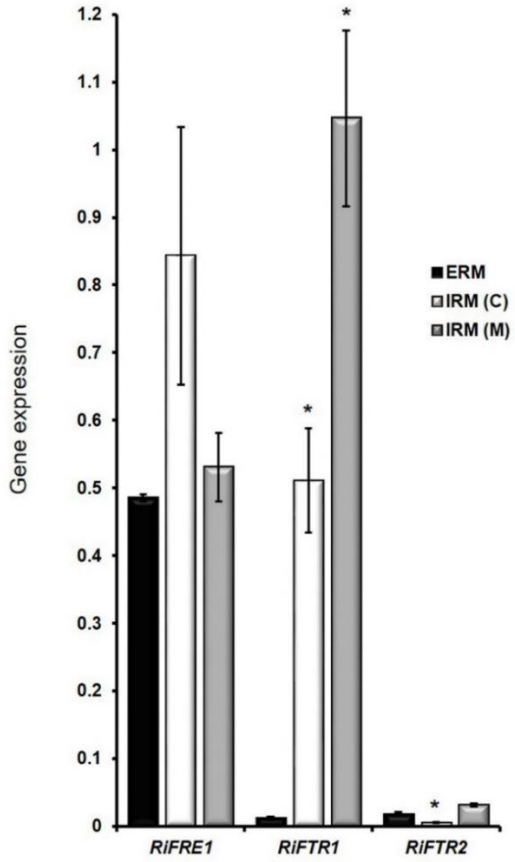

Figure 11. Relative expression of the *RiFRE1* and *RiFTR* genes in extraradical mycelia (ERM) and intraradical mycelia (IRM) of *Rhizophagus irregularis*. Samples were normalized using the housekeeping gene *RiTEF*. Relative expression levels were calculated by the $2^{-\Delta CT}$ method. Data for each condition are presented as mean +/- standard error. Asterisks show statistically significant differences ($p<0.05$) between ERM and IRM. C, carrot; M, maize.

RiFRE1 and *RiFTRs* gene expression was also analyzed in mycorrhizal maize roots developed in pot cultures and fertilized with or without Fe. Mycorrhizal colonization levels were similar in plants fed with the Hoagland nutrient solution containing or not Fe (Fig. 12A). This result was confirmed

by analyzing the expression of the *R. irregularis* elongation factor 1α (*RiEF1α*) gene by qRT-PCR in AM root samples (Fig. 12B). Expression analysis of the mycorrhiza-specific phosphate transporter gene *ZmPT6* also showed that mycorrhizal activity was similar in plants fertilized with and without Fe (Fig. 12C). Transcripts of *RiFRE1*, *RiFTR1* and *RiFTR2* were detected in RNA isolated from mycorrhizal roots but not in RNA from non-mycorrhizal plants. While Fe fertilization did not affect the expression levels of *RiFRE1* and *RiFTR1*, a 2.1-fold increase in *RiFTR2* expression was observed in the roots of the mycorrhizal plants fertilized without Fe (Fig. 12D).

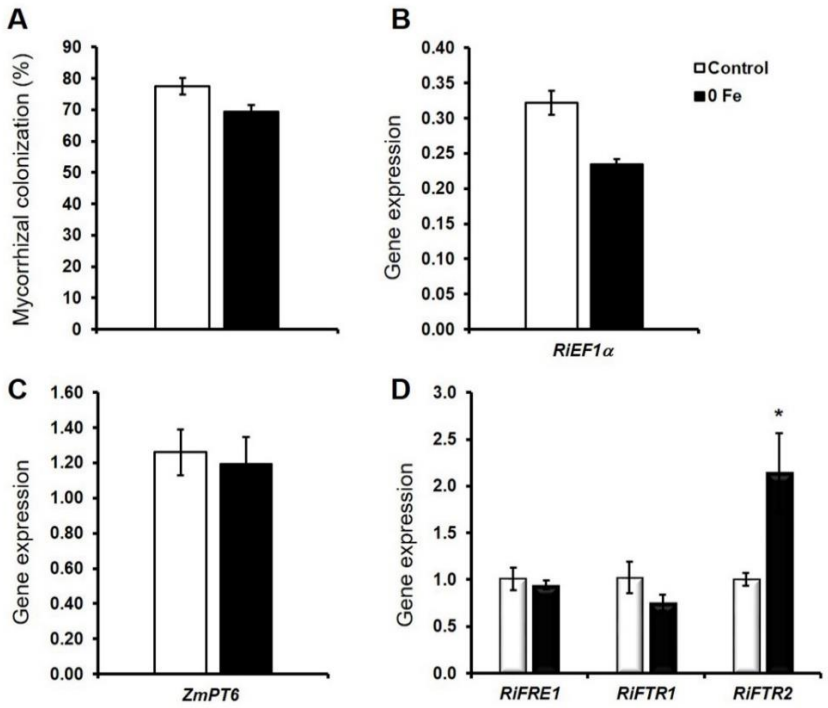

Figure 12. Effect of Fe starvation on *RiFRE1*, *RiFTR1* and *RiFTR2* expression in maize mycorrhizal plants. A. Colonization rates determined by using the gridline intersection method after histochemical staining (n=8). B. qRT-PCR analysis of the *Rhizophagus irregularis* elongation factor 1α (*RiEF1α*) (n=3). C. Relative expression of the mycorrhiza-specific *Zea mays* phosphate transporter *ZmPT6* (n=3). The relative expressions of *RiEF1α* and *ZmPT6* were calculated using the $2^{-\Delta CT}$ method with *ZmEF1α* as housekeeping gene to normalize values. D. *RiFRE1* and *RiFTRs* gene expression was assessed in IRM developed in maize roots grown in control conditions (Control) or without Fe (0 Fe). Data were normalized using the housekeeping gene *RiTEF*. Relative expression levels were calculated by the $2^{-\Delta\Delta CT}$ method. Data are means +/- standard error. Asterisks show statistically significant differences ($p<0.05$) compared to the control value.

Discussion

AM fungi have been shown to improve Fe acquisition of their host plants, but mechanisms underlying Fe acquisition by AM fungi remain unknown. Our results show for the first time that the ERM of *R. irregularis* acquires Fe from the soil through the activity of a high-affinity reductive pathway. We have demonstrated that Fe deficiency induces activation of a plasma membrane-localized ferrireductase, an enzyme that reduces ferric iron sources to the more soluble ferrous iron. Functional characterization of the two Fe permease genes present in the genome of *R. irregularis*, *RiFTR1* and *RiFTR2*, indicates that *RiFTR1* encodes an iron transporter that appear to be largely responsible for *R. irregularis* iron uptake.

In vivo induction of the ferric reductase activity in the ERM of *R. irregularis* grown in iron-depleted media agrees with previous observations in *S. cerevisiae* (Dancis et al., 1990) and in several plant species (Robinson et al., 1999; Waters et al., 2002) that iron reductases are induced under Fe-deficent conditions. Since organics compounds of either plant or microbial origin that retain Fe(III) in the soil solution have a lesser affinity for Fe(II), it is likely that ferric reductase activity releases free iron from organic compounds, generating free iron for fungal uptake. In contrast with what happens in other organisms, a single gene putatively encoding a single ferric reductase, *RiFRE1*, was found in the genome of *R. irregularis*. For example, eight ferric reductase genes are present in the genome of *S. cerevisiae*, each of which carries out specific functions (Singh et al., 2007; Grissa et al., 2010). Although some other members of the FRD superfamily were found in the *R. irregularis* genome, they were more closely related to NADPH oxidases. Unfourtunately, the *RiFRE1* gene product was not functional in the heterologous system, but *in silico* analysis of *RiFRE1* strongly suggests that it encodes a ferric reductase. Support for the role of RiFRE1 in iron uptake by the ERM comes from the correlation of whole ERM Fe(III) reduction and RiFRE1 mRNA accumulation in response to Fe availability in the culture media. Repression of *RiFRE1* expression in the *R. irregularis* ERM grown in high-iron conditions indicates that this protein is regulated by Fe at the transcriptional level and agrees with

previous observations in *S. cerevisiae* (Dancis et al., 1992), *Schizosaccharomyces pombe* (Roman et al., 1993), *Candida albicans* (Knight et al., 2002) and *Aspergillus nidulans* (Oberegger et al., 2002).

Once that Fe(III) is reduced to Fe(II) in the soil solution, it has to be imported into the fungal hyphae. The identification in the *R. irregularis* genome of two genes, *RiFTR1* and *RiFTR2*, highly homologous to the Fe permeases of the high-affinity ferrous-specific transport complex characterized in other fungi suggests that iron transport into the ERM cytosol is mediated by a ferroxidase-permease complex (Eichhorn et al., 2006; Larrondo et al., 2007). Both RiFTR1 and RiFTR2 possess the two RE*X*XE motifs within transmembrane domains 1 and 4 that are essential for Ftr1p iron-uptake function in *S. cerevisiae* (Severance et al., 2004). However, several lines of evidence indicate that RiFTR1 rather than RiFTR2 plays a major role in high-affinity reductive iron acquisition in *R. irregularis*. First, RiFTR1 was able to partially complement the growth defect and the iron transport activity of the *Δftr1* yeast mutant in low-iron conditions. Since RiFTR1 function requires interaction with a ferrous oxidase, partial complementation of the mutant phenotype might be due to an inefficient interaction of RiFTR1 with the *S. cerevisiae* oxidase FET3, the ScFTR1 partner. Second, RiFTR1 has been shown to be targeted to the plasma membrane in the heterologous system. Finally, *RiFTR1* expression was observed to be up-regulated under Fe deficient conditions but down-regulated at high iron concentrations, a typical feature of high-affinity iron transporters (Stearman et al., 1996).

Unfourtunately, the role of RiFTR2 in *R. irregularis* has not been elucidated in this study. The transport activity of RiFTR2 could not be demonstrated because, as shown in the yeast localization assays, *RiFTR2* was expressed exclusively in intracellular compartments, suggesting that the protein failed to exit the ER. Since the ferroxidase-permease complex that mediates the Fe high-affinity transport is formed in the ER (Fig. 1), failure of RiFTR2 to exit the ER might be due to its inability to assemble and traffic with the endogenous ferroxidase ScFET3. In the ERM, *RiFTR2* expression was not regulated by the Fe-limiting conditions used in this study, but decreased at the highest Fe concentration. Since RiFTR1 has been shown to be located at the plasma membrane, it is likely that RiFTR2 is the orthologous of the

vacuolar iron permeases Fth1, FgFtr2 and *Ca*Ftr2 of *S. cerevisiae*, *F. graminearum* and *C. albicans*, that transport stored iron to the cytoplasm (Urbanowski and Piper, 1999; Park et al., 2007; Ziegler et al., 2011). Alternatively, as it has been observed for the *Cryptococcus neoformans* plasma membrane iron permeases CFT2 and CFT1 (Han et al., 2012), there might exist functional redundancy. Unfortunately, since it is not still possible to genetically manipulate AM fungi to generate mutants, it is neither possible to discriminate between these possibilities.

The function of RiFRE1, RiFTR1 and RiFTR2 was also addressed by analysing their expression in the IRM developed in carrot root organ cultures and in maize pot cultures. The finding that *RiFTR1* is highly expressed in the IRM indicates that this protein also plays a key role in Fe uptake during the *in planta* phase of the fungus. As it has been proposed for P and N (Balestrini et al., 2007; Pérez-Tienda et al., 2011; Kiers et al., 2011; Fiorilli et al., 2013), the fungus might exert some control over the amount of Fe that is transferred to the plant. Since Fe is essential for plant and fungal metabolism, both partners can compete for the acquisition of Fe present in the symbiotic interface. The observation that *RiFTR2* expression was up-regulated in the IRM of the maize plants grown under low Fe conditions, suggests that under these limiting conditions the fungus needs to mobilize their vacuolar Fe reserves to support its intraradical growth.

These data suggest that maintenance of Fe homeostasis in the IRM might be essential for root colonization and for the development of a successful symbiosis. In this respect, high-affinity iron uptake systems have been shown to be required for colonization and virulence of several phytopathogenic fungi (Eichhorn et al., 2006; Oide et al., 2006; Albarouki et al., 2014) and for maintenance of mutualism in the *Epichloë festucae*/perennial ryegrass interaction (Johnson et al., 2013). However, further studies are needed to unravel the importance of the high-affinity iron system in the AM symbiosis.

In conclusion, this study shows that the AM fungus *R. irregularis* possesses at least one type of high-affinity iron acquisition systems: the

reductive iron uptake system. Further detailed research is necessary to identify the ferroxidase partners of the iron permeases RiFTR1 and RiFTR2 and to fully understand the specific roles of the different components of the reductive pathway in *R. irregularis*.

References

Albarouki E, Schafferer L, Ye F, von Wirén N, Haas H, Deising HB. 2014. Biotrophy-specific downregulation of siderophore biosynthesis in *Colletotrichum graminicola* is required for modulation of immune responses of maize. Molecular Microbiology 92, 338–355. doi: 10.1111/mmi.12561

Altschul SF, Gish W, Miller W, Myers EW, Lipman DJ. 1990. Basic local alignment search tool. Journal of Molecular Biology 215, 403–410. doi: 10.1016/S0022-2836(05)80360-2

Askwith C, Eide D, Van Ho A, Bernard PS, Li L, Davis-Kaplan S, Sipe DM, Kaplan J. 1994. The *FET3* gene of *S. cerevisiae* encodes a multicopper oxidase required for ferrous iron uptake. Cell 76, 403–410. doi: 10.1016/0092-8674(94)90346-8

Balestrini R, Gómez-Ariza J, Lanfranco L, Bonfante P. 2007. Laser microdissection reveals that transcripts for five plant and one fungal phosphate transporter genes are contemporaneously present in arbusculated cells. Molecular Plant-Microbe Interactions 20, 1055–1062. doi: 10.1094/MPMI-20-9-1055

Caris C, Hördt W, Hawkins H-J, Römheld V, George E. 1998. Studies of iron transport by arbuscular mycorrhizal hyphae from soil to peanut and sorghum plants. Mycorrhiza 8, 35–39. doi: 10.1007/s005720050208

Casieri L, Ait Lahmidi N, Doidy J, et al. 2013. Biotrophic transportome in mutualistic plant-fungal interactions. Mycorrhiza 23, 597–625. doi: 10.1007/s00572-013-0496-9

Chabot S, Bécard G, Piché Y. 1992. Life cycle of *Glomus intraradix* in root organ culture. Mycologia 84, 315–321. doi: 10.2307/3760183

Chorianopoulou SN, Saridis YI, Dimou M, Katinakis P, Bouranis DL. 2015. Arbuscular mycorrhizal symbiosis alters the expression patterns of three key iron homeostasis genes, *ZmNAS1*, *ZmNAS3* and *ZmYS1*, in S deprived maize plants. Frontiers in Plant Science 6. doi: 10.3389/fpls.2015.00257

Clark RB, Zeto SK. 1996. Mineral acquisition by mycorrhizal maize grown on acid and alkaline soil. Soil Biology and Biochemistry 28, 1495–1503. doi: 10.1016/S0038-0717(96)00163-0

Cyert MS, Philpott CC. 2013. Regulation of cation balance in *Saccharomyces cerevisiae*. Genetics 193, 677–713. doi: 10.1534/genetics.112.147207

Dancis A, Klausner RD, Hinnebusch AG, Barriocanal JG. 1990. Genetic evidence that ferric reductase is required for iron uptake in *Saccharomyces cerevisiae*. Molecular and Cellular Biology 10, 2294–2301. doi: 10.1128/MCB.10.5.2294

Dancis A, Roman DG, Anderson GJ, Hinnebusch AG, Klausner RD. 1992. Ferric reductase of *Saccharomyces cerevisiae*: molecular characterization, role in iron uptake, and transcriptional control by iron. Proceedings of the National Academy of Sciences 89, 3869–3873. doi: 10.1073/pnas.89.9.3869

De Silva DM, Askwith CC, Eide D, Kaplan J. 1995. The *FET3* gene product required for high affinity iron transport in yeast is a cell surface ferroxidase. The Journal of Biological Chemistry 270, 1098–1101. doi: 10.1074/jbc.270.3.1098

Eichhorn H, Lessing F, Winterberg B, Schirawski J, Kämper J, Müller P, Kahmann R. 2006. A ferroxidation/permeation iron uptake system is required for virulence in *Ustilago maydis*. The Plant Cell 18, 3332–3345. doi: 10.1105/tpc.106.043588

Eide D, Davis-Kaplan S, Jordan I, Sipe D, Kaplan J. 1992. Regulation of iron uptake in *Saccharomyces cerevisiae*. The Journal of Biological Chemistry 267, 20774–20781.

Ellerbeck M, Schüßler A, Brucker D, Dafinger C, Loos F, Brachmann A. 2013. Characterization of three ammonium transporters of the Glomeromycotan fungus *Geosiphon pyriformis*. Eukaryotic Cell 12, 1554–1562. doi: 10.1128/EC.00139-13

Finegold AA, Shatwell KP, Segal AW, Klausner RD, Dancis A. 1996. Intramembrane bis-heme motif for transmembrane electron transport conserved in a yeast iron reductase and the human NADPH oxidase. The Journal of Biological Chemistry 271, 31021–31024. doi: 10.1074/jbc.271.49.31021

Fiorilli V, Lanfranco L, Bonfante P. 2013. The expression of *GintPT*, the phosphate transporter of *Rhizophagus irregularis*, depends on the symbiotic status and phosphate availability. Planta 237, 1267–1277. doi: 10.1007/s00425-013-1842-z

García-Rodríguez S, Azcón-Aguilar C, Ferrol N. 2007. Transcriptional regulation of host enzymes involved in the cleavage of sucrose during arbuscular mycorrhizal symbiosis. Physiologia Plantarum 129, 737–746. doi: 10.1111/j.1399-3054.2007.00873.x

Giovannetti M, Mosse B. 1980. An evaluation of techniques for measuring vesicular arbuscular mycorrhizal infection in roots. New Phytologist 84, 489–500. doi: 10.1111/j.1469-8137.1980.tb04556.x

Grissa I, Bidard F, Grognet P, Grossetete S, Silar P. 2010. The Nox/Ferric reductase/Ferric reductase-like families of Eumycetes. Fungal Biology 114, 766–777. doi: 10.1016/j.funbio.2010.07.002

Grotz N, Guerinot ML. 2006. Molecular aspects of Cu, Fe and Zn homeostasis in plants. Biochimica et Biophysica Acta 1763, 595–608. doi: 10.1016/j.bbamcr.2006.05.014

Guerinot ML, Yi Y. 1994. Iron: nutritious, noxious, and not readily available. Plant Physiology 104, 815–820. doi: 10.1104/pp.104.3.815

Haas H, Eisendle M, Turgeon BG. 2008. Siderophores in fungal physiology and virulence. Annual Review of Phytopathology 46, 149–187. doi: 10.1146/annurev.phyto.45.062806.094338

Han K, Do E, Jung WH. 2012. A human fungal pathogen *Cryptococcus neoformans* expresses three distinct iron permease homologs. Journal of Microbiology and Biotechnology 22, 1644–1652. doi: 10.4014/jmb.1209.09019

Handa Y, Nishide H, Takeda N, Suzuki Y, Kawaguchi M, Saito K. 2015. RNA-seq transcriptional profiling of an arbuscular mycorrhiza provides insights into regulated and coordinated gene expression in *Lotus japonicus* and *Rhizophagus irregularis*. Plant and Cell Physiology 56, 1490–1511. doi: 10.1093/pcp/pcv071

Helber N, Wippel K, Sauer N, Schaarschmidt S, Hause B, Requena N. 2011. A versatile monosaccharide transporter that operates in the arbuscular mycorrhizal fungus *Glomus* sp is crucial for the symbiotic relationship with plants. The Plant Cell 23, 3812–3823. doi: 10.1105/tpc.111.089813

Huang D, Shusta EV. 2005. Secretion and surface display of green fluorescent protein using the yeast *Saccharomyces cerevisiae*. Biotechnology Progress 21, 349–357. doi: 10.1021/bp0497482

Jin CW, Du ST, Shamsi IH, Luo BF, Lin XY. 2011. NO *synthase*-generated NO acts downstream of auxin in regulating Fe-deficiency-induced root branching that enhances Fe-deficiency tolerance in tomato plants. Journal of Experimental Botany 62, 3875–3884. doi: 10.1093/jxb/err078

Johnson L. 2008. Iron and siderophores in fungal-host interactions. Mycological Research 112, 170–183. doi: 10.1016/j.mycres.2007.11.012

Johnson LJ, Koulman A, Christensen M, Lane GA, Fraser K, Forester N, Johnson RD, Bryan GT, Rasmussen S. 2013. An extracellular siderophore is required to maintain the mutualistic interaction of *Epichloë festucae* with *Lolium perenne*. PLoS Pathogens 9, e1003332. doi: 10.1371/journal.ppat.1003332

Juwarkar AA, Jambhulkar HP. 2008. Phytoremediation of coal mine spoil dump through integrated biotechnological approach. Bioresource Technology 99, 4732–4741. doi: 10.1016/j.biortech.2007.09.060

Kiers ET, Duhamel M, Beesetty Y, et al. 2011. Reciprocal rewards stabilize cooperation in the mycorrhizal symbiosis. Science 333, 880–882. doi: 10.1126/science.1208473

Knight SAB, Lesuisse E, Stearman R, Klausner RD, Dancis A. 2002. Reductive iron uptake by *Candida albicans*: role of copper, iron and the *TUP1* regulator. Microbiology 148, 29–40. doi: 10.1099/00221287-148-1-29

Knight SAB, Vilaire G, Lesuisse E, Dancis A. 2005. Iron acquisition from transferrin by *Candida albicans* depends on the reductive pathway. Infection and Immunity 73, 5482–5492. doi: 10.1128/IAI.73.9.5482-5492.2005

Kobae Y, Tomioka R, Tanoi K, Kobayashi NI, Ohmori Y, Nishida S, Fujiwara T. 2014. Selective induction of putative iron transporters, *OPT8a* and *OPT8b*, in maize by mycorrhizal colonization. Soil Science and Plant Nutrition 60, 843–847. doi: 10.1080/00380768.2014.949854

Kobayashi T, Nishizawa NK. 2012. Iron uptake, translocation, and regulation in higher plants. Annual Review of Plant Biology 63, 131–152. doi: 10.1146/annurev-arplant-042811-105522

Larkin MA, Blackshields G, Brown NP, et al. 2007. Clustal W and Clustal X version 2.0. Bioinformatics 23, 2947–2948. doi: 10.1093/bioinformatics/btm404

Larrondo LF, Canessa P, Melo F, Polanco R, Vicuña R. 2007. Cloning and characterization of the genes encoding the high-affinity iron-uptake protein

complex Fet3/Ftr1 in the basidiomycete *Phanerochaete chrysosporium*. Microbiology 153, 1772–1780. doi: 10.1099/mic.0.2006/003442-0

Lin K, Limpens E, Zhang Z, et al. 2014. Single nucleus genome sequencing reveals high similarity among nuclei of an endomycorrhizal fungus. PLoS genetics 10, e1004078. doi: 10.1371/journal.pgen.1004078

Liu A, Hamel C, Hamilton RI, Ma BL, Smith DL. 2000. Acquisition of Cu, Zn, Mn and Fe by mycorrhizal maize (*Zea mays* L.) grown in soil at different P and micronutrient levels. Mycorrhiza 9, 331–336. doi: 10.1007/s005720050277

Miransari M. 2011. Arbuscular mycorrhizal fungi and nitrogen uptake. Archives of Microbiology 193, 77–81. doi: 10.1007/s00203-010-0657-6

Oberegger H, Schoeser M, Zadra I, Schrettl M, Parson W, Haas H. 2002. Regulation of *freA*, *acoA*, *lysF*, and *cycA* expression by iron availability in *Aspergillus nidulans*. Applied and Environmental Microbiology 68, 5769–5772. doi: 10.1128/AEM.68.11.5769-5772.2002

Oide S, Moeder W, Krasnoff S, Gibson D, Haas H, Yoshioka K, Turgeon BG. 2006. *NPS6*, encoding a nonribosomal peptide synthetase involved in siderophore-mediated iron metabolism, is a conserved virulence determinant of plant pathogenic ascomycetes. The Plant Cell 18, 2836–2853. doi: 10.1105/tpc.106.045633

Park Y-S, Kim J-H, Cho J-H, Chang H-I, Kim S-W, Paik H-D, Kang C-W, Kim T-H, Sung H-C, Yun C-W. 2007. Physical and functional interaction of FgFtr1-FgFet1 and FgFtr2-FgFet2 is required for iron uptake in *Fusarium graminearum*. The Biochemical journal 408, 97–104. doi: 10.1042/BJ20070450

Pérez-Tienda J, Testillano PS, Balestrini R, Fiorilli V, Azcón-Aguilar C, Ferrol N. 2011. GintAMT2, a new member of the ammonium transporter family in the arbuscular mycorrhizal fungus *Glomus intraradices*. Fungal Genetics and Biology 48, 1044–1055. doi: 10.1016/j.fgb.2011.08.003

Philpott CC, Protchenko O. 2008. Response to iron deprivation in *Saccharomyces cerevisiae*. Eukaryotic Cell 7, 20–27. doi: 10.1128/EC.00354-07

Rentsch D, Laloi M, Rouhara I, Schmelzer E, Delrot S, Frommer WB. 1995. *NTR1* encodes a high affinity oligopeptide transporter in *Arabidopsis*. FEBS Letters 370, 264–268. doi: 10.1016/0014-5793(95)00853-2

Robinson NJ, Procter CM, Connolly EL, Guerinot ML. 1999. A ferric-chelate reductase for iron uptake from soils. Nature 397, 694-697. doi: 10.1038/17800

Roman DG, Dancis A, Anderson GJ, Klausner RD. 1993. The fission yeast ferric reductase gene *frp1*$^{+}$ is required for ferric iron uptake and encodes a protein that is homologous to the gp91-*phox* subunit of the human NADPH phagocyte oxidoreductase. Molecular and Cellular Biology 13, 4342–4350. doi: 10.1128/MCB.13.7.4342

Römheld V, Marschner H. 1986. Evidence for a specific uptake system for iron phytosiderophores in roots of grasses. Plant Physiology 80, 175–180. doi: 10.1104/pp.80.1.175

Saha R, Saha N, Donofrio RS, Bestervelt LL. 2013. Microbial siderophores: a mini review. Journal of Basic Microbiology 53, 303–317. doi: 10.1002/jobm.201100552

Schiestl RH, Gietz RD. 1989. High efficiency transformation of intact yeast cells using single stranded nucleic acids as a carrier. Current Genetics 16, 339–346. doi: 10.1007/BF00340712

Schmittgen TD, Livak KJ. 2008. Analyzing real-time PCR data by the comparative C_T method. Nature Protocols 3, 1101–1108. doi: 10.1038/nprot.2008.73

Severance S, Chakraborty S, Kosman DJ. 2004. The Ftr1p iron permease in the yeast plasma membrane: orientation, topology and structure–function relationships. Biochemical Journal 380, 487–496. doi: 10.1042/bj20031921

Sikorski RS, Hieter P. 1989. A system of shuttle vectors and yeast host strains designed for efficient manipulation of DNA in *Saccharomyces cerevisiae*. Genetics 122, 19–27.

Singh A, Kaur N, Kosman DJ. 2007. The metalloreductase Fre6p in Fe-efflux from the yeast vacuole. The Journal of Biological Chemistry 282, 28619–28626. doi: 10.1074/jbc.M703398200

Smith SE, Read DJ. 2008. *Mycorrhizal symbiosis* (Third edition). London: Academic Press.

Smith SE, Smith FA. 2011. Roles of arbuscular mycorrhizas in plant nutrition and growth: new paradigms from cellular to ecosystem scales. Annual Review of Plant Biology 62, 227–250. doi: 10.1146/annurev-arplant-042110-103846

St-Arnaud M, Hamel C, Vimard B, Caron M, Fortin JA. 1996. Enhanced hyphal growth and spore production of the arbuscular mycorrhizal fungus *Glomus intraradices* in an *in vitro* system in the absence of host roots. Mycological Research 100, 328–332. doi: 10.1016/S0953-7562(96)80164-X

Stearman R, Yuan DS, Yamaguchi-iwai Y, Klausner RD, Dancis A. 1996. A permease-oxidase complex involved in high-affinity iron uptake in yeast. Science 271, 1552–1557. doi: 10.1126/science.271.5255.1552

Takemoto D, Tanaka A, Scott B. 2007. NADPH oxidases in fungi: Diverse roles of reactive oxygen species in fungal cellular differentiation. Fungal Genetics and Biology 44, 1065–1076. doi: 10.1016/j.fgb.2007.04.011

Tamayo E, Gómez-Gallego T, Azcón-Aguilar C, Ferrol N. 2014. Genome-wide analysis of copper, iron and zinc transporters in the arbuscular mycorrhizal fungus *Rhizophagus irregularis*. Frontiers in Plant Science 5, 547. doi: 10.3389/fpls.2014.00547

Tamura K, Stecher G, Peterson D, Filipski A, Kumar S. 2013. MEGA6: Molecular evolutionary genetics analysis version 6.0. Molecular Biology and Evolution 30, 2725–2729. doi: 10.1093/molbev/mst197

Tisserant E, Kohler A, Dozolme-Seddas P, et al. 2012. The transcriptome of the arbuscular mycorrhizal fungus *Glomus intraradices* (DAOM 197198) reveals functional tradeoffs in an obligate symbiont. New Phytologist 193, 755–769. doi: 10.1111/j.1469-8137.2011.03948.x

Tisserant E, Malbreil M, Kuo A, et al. 2013. Genome of an arbuscular mycorrhizal fungus provides insight into the oldest plant symbiosis. Proceedings of the National Academy of Sciences 110, 20117–20122. doi: 10.1073/pnas.1313452110

Urbanowski JL, Piper RC. 1999. The iron transporter Fth1p forms a complex with the Fet5 iron oxidase and resides on the vacuolar membrane. The Journal of Biological Chemistry 274, 38061–38070. doi: 10.1074/jbc.274.53.38061

Vida TA, Emr SD. 1995. A new vital stain for visualizing vacuolar membrane dynamics and endocytosis in yeast. The Journal of Cell Biology 128, 779–792. doi: 10.1083/jcb.128.5.779

Waters BM, Blevins DG, Eide DJ. 2002. Characterization of FRO1, a pea ferric-chelate reductase involved in root iron acquisition. Plant Physiology 129, 85–94. doi: 10.1104/pp.010829

Zhang X, Krause KH, Xenarios I, Soldati T, Boeckmann B. 2013. Evolution of the ferric reductase domain (FRD) superfamily: modularity, functional diversification, and signature motifs. PLoS ONE 8, e58126. doi: 10.1371/journal.pone.0058126

Ziegler L, Terzulli A, Gaur R, McCarthy R, Kosman DJ. 2011. Functional characterization of the ferroxidase, permease high-affinity iron transport complex from *Candida albicans*. Molecular Microbiology 81, 473–485. doi: 10.1111/j.1365-2958.2011.07704.x

Supporting Information

S1 Table. Oligonucleotides used in this study. [a] Overhangs are underlined.

Primer	Sequence (5' - 3')[a]	Application
GiFREbF	ATTATTACGAGGCCGGACAA	Real-time PCR
GiFREbR	GTTTTTCCATAAGGCCCATC	Real-time PCR
GiFREb.fF	ATGTTGGAATCAGGAGACTTC	Cloning of *RiFRE1* CDS into pDR195
GiFREb.fR	TTATAATTCGAATGTTTCACAATG	Cloning of *RiFRE1* CDS into pDR195
GiFTRbF	AGGATCGCATAGGATGTCAA	Real-time PCR
GiFTRbR	AGAAAAGACCAGCGGCAAC	Real-time PCR
GiFTRb.fF	CCATGGTTTATTTATTCGATGTTCC	Cloning of *RiFTR1* CDS into pDR195
GiFTRb.fR	TTAAGCTGCATTCACAATAGC	Cloning of *RiFTR1* CDS into pDR195
FTR2.qF	TCACGGGGATTGAAGCTAAAG	Real-time PCR
FTR2.qR	AAGCCTGCTCCCATAAAGAG	Real-time PCR
FTR2.fF	ATGTCAACTAATTTGTTCAATTTC	Cloning of *RiFTR2* CDS into pDR195
FTR2.fR	TTATAATAATAAAGAAACTTCTAAATTTTC	Cloning of *RiFTR2* CDS into pDR195
ScFre1.fF	ATGGTTAGAACCCGTGTATTATTCTG	Cloning of *ScFRE1* CDS into pDR195
ScFre1.fR	TTACCATGTAAAACTTTCTTCTTCTAGTTC	Cloning of *ScFRE1* CDS into pDR195
ScFre1b	CTGGATTGTTTGGATCACG	Sequencing of internal *ScFre1* region
ScFtr1.fF	ATGCCTAACAAAGTGTTTAACGTG	Cloning of *ScFTR1* CDS into pDR195
ScFtr1.fR	TCAAAGAGAGTCGGCTTTAACGTG	Cloning of *ScFTR1* CDS into pDR195
RiFTR1-sfi-F	CAAGGCC**ATTAC**GGCCATGGTTTATTTATTCGATGTTCC	Cloning of *RiFTR1* CDS into pBL106
RiFTR1-sfi-R	GATGGCC**GAGGC**GGCC*GA*AGCTGCATTCACAATAGCC	Cloning of *RiFTR1* CDS into pBL106
RiFTR2-sfi-F	CAAGGCC**ATTAC**GGCCATGTCAACTAATTTGTTCAATTTCC	Cloning of *RiFTR2* CDS into pBL106
RiFTR2-sfi-R	GATGGCC**GAGGC**GGCC*GA*TAATAATAAAGAAACTTCTAAATTTTCTTGC	Cloning of *RiFTR2* CDS into pBL106
GintEFfw	GCTATTTTGATCATTGCCGCC	Real-time PCR
GintEFrev	TCATTAAAACGTTCTTCCGACC	Real-time PCR

CHAPTER III

The *Rhizophagus irregularis* multicopper oxidase family: a search for proteins with potential ferroxidase activity

A manuscript containing this work is in preparation:

Tamayo E, Ferrol N.

The *Rhizophagus irregularis* multicopper oxidase family: a search for proteins with potential ferroxidase activity.

In preparation.

Abstract

The contribution of arbuscular mycorrhizal fungi (AM fungi) to plant iron (Fe) acquisition has been demonstrated in several studies. Recently, it has been showed that AM fungi use a high-affinity Fe reductive pathway for Fe uptake, and two main components of this pathway have been characterized in the AM fungus *Rhizophagus irregularis*, the ferric reductase RiFRE1 and the Fe permease RiFTR1. In an attempt to identify the third component of the reductive iron uptake pathway in *R. irregularis*, a genome-wide approach has been used to find genes encoding ferroxidases of the multicopper oxidase (MCO) gene family. Nine genes putatively encoding MCOs (*RiMCO1-9*) were identified. A phylogenetic analysis of MCO sequences of different taxonomic groups revealed that all RiMCOs clustered together in the ferroxidase/laccase group, and none with the Fet3-type ferroxidases. *In silico* analyses also suggested that *R. irregularis* does not have any Fet3-type ferroxidase. *RiMCO1* was the only *MCO* gene displaying a gene expression pattern typical of a high-affinity Fe transport system. Moreover, RiMCO1 enables the *Fet3* yeast mutant to take up Fe. These data indicate that *R. irregularis* has at least nine MCO members in its genome and that RiMCO1 might have a role in the reductive high-affinity Fe uptake system together with the Fe transporter RiFTR1 at the ERM.

Introduction

Iron (Fe) is an essential metal element, however, it can become extremely toxic at high concentrations. Therefore, its biological levels are finely regulated in living cells. To maintain Fe homeostasis, all organisms have evolved sophisticated tools to cope with their requirements for this metal. Although Fe is abundant in nature, this metal has a low availability because it is most commonly found as ferric hydroxide, which is a rather stable and poorly soluble compound (Kosman, 2003). For this reason, high affinity iron uptake systems are required to take up Fe.

Plants have evolved an evolutionary ancient strategy to increase their nutrient supply, the establishment of arbuscular mycorrhizal (AM) symbioses with fungi belonging to the Glomeromycota. AM fungi are obligate biotrophs that form mutualistic symbiotic associations with most flowering plants. The extensive external mycelium developed by AM fungi in the soil can absorb nutrients beyond the depletion zone that develops around the roots, providing a new pathway for the uptake and transport of low mobility nutrients in soil, specially P, N, but also some micronutrients such as Fe, Cu and Zn (Smith and Read, 2008). In return, the plant provides carbohydrates to the fungus.

The contribution of AM fungi to plant Fe uptake has been shown in several studies (Caris et al., 1998; Kobae et al., 2014) and we recently showed that AM fungi use a high-affinity iron reductive pathway to take up Fe from the soil solution (Tamayo et al., previous chapter). In the well characterized yeast *Saccharomyces cerevisiae*, the high-affinity reductive iron uptake system requires reduction of Fe(III) to Fe (II) by membrane-bound ferrireductases, which is then rapidly internalized by the concerted action of a ferroxidase (FET3) and an iron permease (FTR1) that form a plasma membrane protein complex (Askwith et al., 1994; Stearman et al., 1996; Kosman, 2010). Fe^{2+} is first oxidized by FET3, and then transported into the cytosol as Fe^{3+} by FTR1 via a channeling mechanism (Kwok et al., 2006). In our previous work, we identified two components of this high-affinity iron uptake system in the AM fungus *R. irregularis*, the ferric reductase RiFRE1 and the Fe permease RiFTR1

(Tamayo et al., previous chapter). However, the ferroxidase partner of RiFTR1 remains to be identified.

Fungal ferroxidases (Fe(II): oxygen oxidoreductase, EC 1.16.3.1) are plasma membrane proteins with a single transmembrane domain and an extracellular multicopper oxidase domain responsible for the ferroxidase activity. They belong to the family of multicopper oxidases (MCOs), proteins that have the ability to couple the oxidation of a variety of substrates with the reduction of molecular oxygen to water using four copper atoms (Rydén and Hunt, 1993). Other members of this family are laccases, ascorbate oxidases, bilirubin oxidases and potential ferroxidases/laccases exhibiting either one or both enzymatic functions (Hoegger et al., 2006).

Fungal Fet3-ferroxidases have been characterized in many fungi including *Schizosaccharomyces pombe*, *Pichia pastoris*, *Arxula adeninivorans*, *Aspergillus fumigatus*, *Ustilgo maydis*, *Fusarium graminearum*, *Phanerochaete chrysosporium*, *Cryptococcus neoformans*, *Candida albicans* and *Colletotrichum graminicola* (Askwith and Kaplan, 1997; Paronetto et al., 2001; Wartmann et al., 2002; Schrettl et al., 2004; Eicchorn et al., 2006; Greenshields et al., 2007; Larrondo et al., 2007; Jung et al., 2009; Ziegler et al., 2011; Albarouki and Deising, 2013). Ferroxidases/laccases have been characterized in the fungi *P. chrysosporium* (Larrondo et al. 2003) and *C. neoformans* (Liu et al., 1999).

With the aim of identifying the ferroxidase partner of the iron permease RiFTR1 of *R. irregularis*, a genome-wide approach has been used to find the candidate genes belonging to the MCO gene family. Nine genes putatively encoding MCOs were identified. Phylogenetic analyses revealed that all RiMCOs were grouped in the ferroxidase/laccase cluster of MCOs. *In silico* and expression analyses indicate that RiMCO1 might be the RiFTR1 ferroxidase partner.

Materials and methods

Identification of MCO *genes in* R. irregularis *genome and sequences analyses*

Amino acid sequences of fungal MCOs were retrieved from the freely accessible transport database TCDB (http://www.tcdb.org/). These sequences were used to search for orthologous sequences in the filtered model dataset of *R. irregularis* on the JGI website (http://genome.jgi-psf.org/Gloin1) using Basic Local Alignment Search Tool (BLAST) algorithm (Altschul et al., 1990) via a protein BLAST. A second search was performed via a keyword search directly using "multicopper oxidase", "laccase", "ascorbate oxidase", "ferroxidase", "bilirubin oxidase" and "Fet3" as keywords. Since some of the fungal reference proteins were phylogenetically distant from *R. irregularis*, manually curated *Laccaria bicolor* (http://genome.jgi-psf.org/Lacbi2), *Tuber melanosporum* (http://genome.jgi.doe.gov/Tubme1) and *Rhizopus oryzae* (http://genome.jgi.doe.gov/Rhior3) databases were used to look for additional orthologous sequences in the filtered model dataset of *R. irregularis*. This was also done via a BLASTp, run with the standard program settings. Finally, a keyword search for putative multicopper oxidases was performed on the functional annotation collection from Lin et al. (2014).

Predictions of putative transmembrane domains were made using the TMHMM Server v.2.0 (http://www.cbs.dtu.dk/services/TMHMM/) and SMART software (http://smart.embl-heidelberg.de/). Predictions of subcellular localizations were made using the TargetP 1.1 Server (http://www.cbs.dtu.dk/services/TargetP/).

Full-length amino acid sequences were aligned with the orthologous sequences of a number of fungi representatives of distinct taxonomic groups by ClustalW (Version 2.1; Larkin *et al*., 2007; http://www.ebi.ac.uk/Tools/msa/clustalw2/) with default setting. Alignments were imported into the Molecular Evolutionary Genetics Analysis (MEGA) package version 6 (Tamura et al., 2013). Phylogenetic analyses were conducted by the Neighbor-Joining (NJ) method, implemented in MEGA, with a pair-wise deletion of gaps and the Poisson model for distance

calculation. Bootstrap analyses were carried out with 1000 replicates. The evolutionary tree was drawn to scale.

Biological materials and growth conditions

Rhizophagus irregularis monoxenic cultures were established as described by St-Arnaud et al. (1996), with some modifications. Briefly, clone DC2 of carrot (*Daucus carota* L.) Ri-T DNA transformed roots were cultured with the AM fungus *R. irregularis* Schenck and Smith DAOM 197198 in two-compartment Petri dishes. Cultures were initiated in one compartment of each plate containing M medium (Chabot *et al*., 1992) by placing several non-mycorrhizal carrot root segments and a piece of fungal inoculum containing extraradical mycelium (ERM), fragments of mycorrhizal roots and spores. Fungal hyphae and roots were allowed to grow over to the other compartment containing the same M medium. Plates were incubated in the dark at 24 °C for 7–8 weeks until the second compartment was profusely colonized by the fungus and the roots. Then, the older compartment was removed and refilled with liquid M medium without sucrose (M-C medium) containing different iron concentrations: 45 μM (control), 4.5 mM or 45 mM EDTA iron(III) sodium salt. Fungal hyphae, but not roots, were allowed to grow over to this compartment (hyphal compartment). Plates were incubated in the dark at 24 °C for 2–3 additional weeks. For induction of iron deficiency conditions, after allowing to grow the fungal hyphae over to the compartment filled with control liquid M-C medium, medium was replaced by liquid M-C medium without iron and with 0.5 mM ferrozine and 50 mM MES buffer (pH 6.1) added. Plates were incubated in the dark at 24 °C for 3 additional days.

ERM from the different hyphal compartments was directly recovered under sterile conditions by using a pair of tweezers, washed with sterile water and dried on filter paper. The mycelium was immediately frozen in liquid nitrogen and stored at -80 °C until used.

To analyze intraradical gene expression, hyphae growing in the hyphal compartment were used as a source of mycorrhizal inoculum. Carrot roots were placed on top of a densely colonized hyphal compartment and collected 15 days later. Extraradical hyphae attached to the roots were

removed with forceps under a binocular microscope. Roots were then frozen in liquid N and stored at -80°C until used.

The *S. cerevisiae* strain used in this study was an isogenic derivative of YPH252 wild type strain, the *Δfet3* mutant. This strain and the vector containing *S. cerevisiae Fet3* were kindly provided by Drs. Andrew Dancis and Simon Knight (Department of Medicine, University of Pennsylvania, Philadelphia, Pennsylvania, EEUU). Strains were grown on YPD or complete synthetic medium (CSM), supplemented with appropriate amino acids.

Nucleic acids extraction and cDNA synthesis

Total fungal RNA from ERM from the different treatments of *R. irregularis* and mycorrhizal carrot roots, was extracted using the RNeasy Plant Mini Kit (QIAGEN, Maryland), following manufacturer´s instructions. DNAse treatment was performed using RNA-free DNase Set (QIAGEN, Maryland) following the manufacturer's instructions. cDNAs were obtained from 1 μg of total DNase-treated RNA in a 20 μl reaction containing 200 units of Super-Script III Reverse Transcriptase (Invitrogen) and 50 pmol oligo $(dT)_{20}$ (Invitrogen), according to the manufacturer's instructions.

Gene isolation

The 5′ end of *RiMCO1* was verified by rapid amplification of cDNA ends (RACE) using the SMART RACE cDNA amplification kit (Clontech, Palo Alto, CA, USA), the *RiMCO1*-specific primer GiFETa.rR and 1 μg total RNA from ERM grown in control plates. The full-length cDNA of *RiMCO1* was obtained by PCR amplification of *R. irregularis* cDNA, using the corresponding primer pairs: FETa.fF and FETa.fR (S1 Table). The full-length cDNA of *RiMCO3* was obtainted by RACE using the *RiMCO3*-specific primers FETc.rF and FETc.rR for the 3′ and 5′RACE reactions, respectively, designed based on the sequence GenBank Accesion No. AUPC01010373, and 1 μg total RNA from ERM grown in control plates. Full-length cDNAs of other *RiMCOs* were obtained by PCR amplification of *R. irregularis* cDNA, using the corresponding primer pairs. PCR products were cloned in the pGEM-T easy vector (Promega, Madison, USA).

All plasmids were amplified by transformation of *E. coli* following standard procedures and purified by using the Qiagen Miniprep Kit (Qiagen, Maryland, USA). All sequences and constructs were checked by sequencing before further use. Nucleotide sequences were determined by Taq polymerase cycle sequencing by using an automated DNA sequencer (ABI Prism 3130xl Genetic Analyzer, Applied Biosystems, Carlsbad, USA).

Heterologous expression

For heterologous gene expression analyses, the *RiMCO1* full-length cDNA was cloned into the yeast cDNA-cloning vector pDR195, which contains a fragment of the plasma membrane ATPase promoter (Rentsch et al., 1995). To obtain pDR195-*RiMCO1*, the full-length cDNA was isolated from the pGEM-T easy vector by *Not*I digestion and ligated into the *Not*I- digested pDR195 vector. The full lenght cDNA of yeast *Fet3* gene was also cloned into pDR195 and used as positive control in the complementation analyses of the *Δfet3* mutant strain.

The *S. cerevisiae* mutant strain *Δfet3* was transformed with the construct pDR195-*RiMCO1*, the empty vector (negative control), or the positive control using a lithium acetate-based method (Schiestl and Gietz, 1989). Yeast transformants were selected in CSM medium by autotrophy to uracil.

High-affinity iron uptake assays in yeast

High-affinity iron uptake was measured on exponential yeast cells which were washed three times in citrate-glucose buffer and resuspended in the same buffer. Citrate buffer containing 1 μM ferrous (^{55}Fe)-ascorbate was added to the suspended cells and incubated at 30 °C for 2 hours. At this point, the optical densities of cultures were measured. The cells were then harvested and washed free of ^{55}Fe label by using a cell harvester (PHD Cambridge Technologies) and iron uptake was measured by liquid scintillation counting (Beckman LS6500). Assay mixtures containing no cells were used to calculated blank values for correction.

Gene expression analyses

RiMCOs gene expression was studied by real-time RT-PCR by using an iQ™5 Multicolor Real-Time PCR Detection System (Bio-Rad). Each 20 µl reaction contained 1 µl of a 1:10 dilution of the cDNA, 200 nM each primer, 10 µl of iQ™ SYBR Green Supermix 2x (Bio-Rad). The PCR program consisted in a 3-min incubation at 95 °C to activate the hot-start recombinant Taq DNA polymerase, followed by 36 cycles of 30 s at 95 °C, 30 s at 58 °C and 30 s at 72 °C, where the fluorescence signal was measured. The specificity of the PCR amplification procedure was checked with a heat-dissociation protocol (from 58 to 95 °C) after the final cycle of the PCR. Primer specificity was checked by sequencing the amplicons obtained with each primer pair. The primer sets used are listed in S1 Table. The efficiency of the primer sets was evaluated by performing real-time PCR on several dilutions of cDNA. Because RNA extracted from mycorrhizal roots contains plant and fungal RNAs, specificity of the primer pairs was also analyzed by PCR amplification of genomic DNA isolated from non-mycorrizal carrot roots and of cDNA from non-colonized carrot roots. The results obtained for the different treatments were standardized to the elongation factor 1-alpha gene levels (GenBank Accession No. DQ282611), which were amplified with the following primers: GintEFfw and GintEFrev. RT-PCR determinations were performed on three independent biological samples from three replicate experiments. Real-time PCR experiments were carried out three times for each biological sample, with the threshold cycle (Ct) determined in triplicate. The relative levels of transcription were calculated by using the $2^{-\Delta\Delta CT}$ method (Schmittgen and Livak, 2008), and the standard error was computed from the average of the ΔCT values for each biological sample.

Statistical analyses

Statgraphics Centurion XVI software was used for the statistical analysis of the means and standard deviation determinations. ANOVA, followed by a Fisher's LSD test ($p<0.05$) when possible, was used for the comparison of the treatments based on at least 3 biological replicates for each treatment ($n \geq 3$).

Results

R. irregularis *has at least nine multicopper oxidases in its genome*

A search for putative MCOs in the *R. irregularis* genome (*R. irregularis* DAOM 181602) led to the identification of nine genes putatively encoding MCOs. Since the length of the RiMCO1, RiMCO3, RiMCO8 and RiMCO9 protein sequences found in the *R. irregularis* JGI database was shorter than expected, we attempted to obtain the full-length cDNAs by RACE. The open reading frames and number of introns of *RiMCO4*, *RiMCO5* and *RiMCO6* were also confirmed by cloning and sequencing the respective cDNA sequences. The coding sequences of *RiMCO2*, *RiMCO7*, *RiMCO8* and *RiMCO9* could not be experimentally confirmed because they were not expressed or expressed below the detection levels in the *R. irregularis* ERM. The length of the nucleotide coding sequences of the nine *RiMCO* genes ranged from 1554 to 2127 bp, while the length of the nucleotide genomic sequences varied from 2159 to 2816 bp (Table 1). Comparison between the cDNA and genomic sequences revealed that the number of introns in the individual *RiMCOs* varies from 4 to 11 (Table 1 and Fig. 1).

Table 1. Protein accession number, predicted nucleotide and amino acid sequence length, introns and transmembrane domains of the *Rhizophagus irregularis* MCOs.

Name	NCBI ID	Nucleotide sequence length (bp)	Amino acid sequence length (aa)	Predicted intron number	Predicted transmembrane domains
RiMCO1	ESA08327	2730	606•	9	1
RiMCO2	ESA02114	2189	622	4	0
RiMCO3	EXX63927	2816	540•	11	0
RiMCO4	EXX65257	2593	623	9	1
RiMCO5	EXX55101	2159	608	4	1
RiMCO6	EXX61193	2739	708	7	1
RiMCO7	EXX71299	2614	621	9	0
RiMCO8	ESA00015	2429	517	9	2
RiMCO9	EXX72417	2672	530	11	0

•NCBI sequences are shorter. Sequences were experimentally determined by using RACE technology.

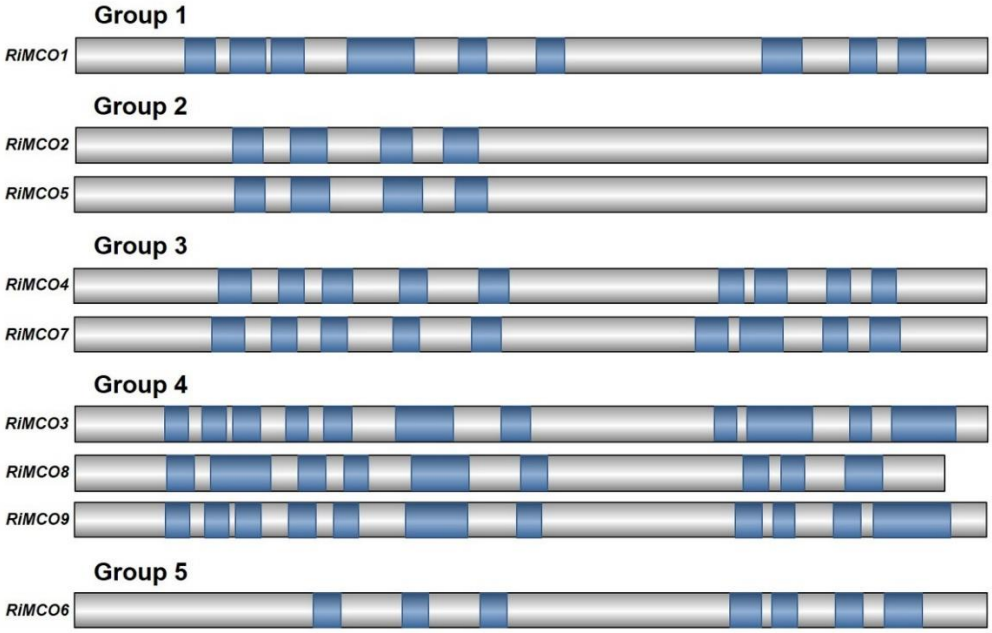

Figure 1. Comparison of exon/intron organization in the *Rhizophagus irregularis MCO* genes. Depicted intron positions were based on GenBank genomic sequence annotations. Blue boxes indicate introns and grey boxes indicate exons.

The length of the predicted amino acid RiMCO sequences ranges from 517 to 708 amino acids (Table 1). Sequence identities among the deduced amino acid sequences of RiMCO1-9 ranges from 24 to 80%, with RiMCO6 having the lowest identity to the others (≤29%) (Fig. 2A). RiMCO4 and RiMCO7 showed the highest degree of identity (80%). Relationships between the nine *R. irregularis* MCOs are also reflected in the phylogenetic tree based on their amino acid similarities (Fig. 2B). Based on the similarity of the RiMCO gene products and on the intron positions, five gene subfamilies were defined (Fig. 1 and 2B).

A

MCO	RiMCO1	RiMCO2	RiMCO3	RiMCO4	RiMCO5	RiMCO6	RiMCO7	RiMCO8	RiMCO9
RiMCO1		44	38	43	46	25	41	33	37
RiMCO2			35	43	66	27	41	33	35
RiMCO3				37	38	29	35	66	75
RiMCO4					44	25	80	32	36
RiMCO5						27	40	34	36
RiMCO6							24	25	27
RiMCO7								30	34
RiMCO8									61
RiMCO9									

B

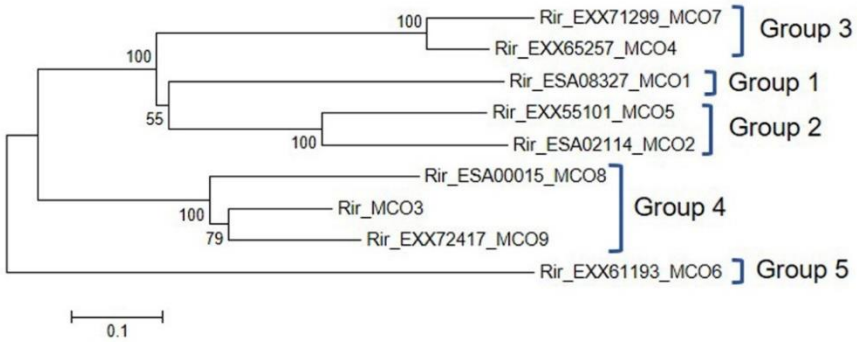

Figure 2. A. Percent sequence identity matrix of putative amino acid sequences of MCOs in *Rhizophagus irregularis*. B. Unrooted Neighbor-Joining tree of the deduced amino acid sequences of the *R. irregularis* MCOs. Rir, *R. irregularis*. Protein NCBI identification numbers are indicated.

A phylogenetic analysis of MCO sequences of different taxonomic groups revealed that all RiMCOs clustered together in the ferroxidase/laccase group (Fig. 3A and B). In contrast with what happens for the MCOs of other fungi, none of the RiMCOs clustered with the Fet3-type ferroxidases (Fig. 3B).

A

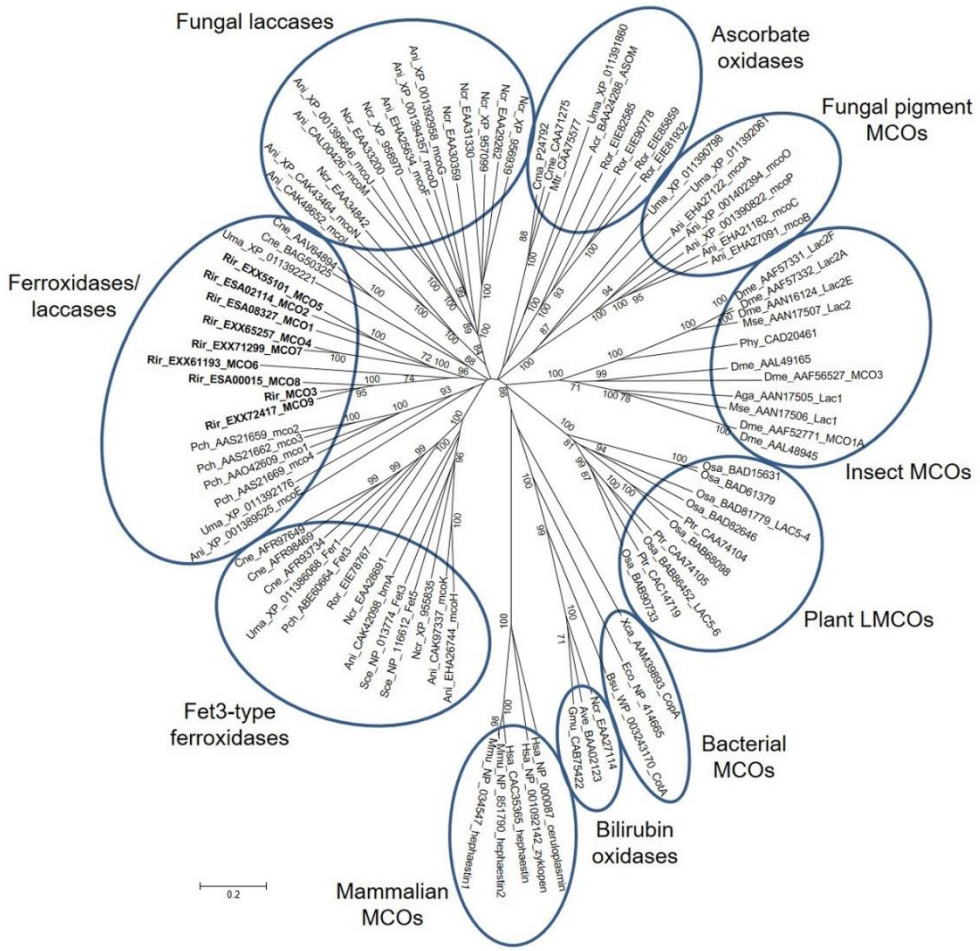

B

	Rir	Ror	Sce	Ani	Ncr	Pch	Uma	Cne
Laccases *sensu stricto*	–	–	–	7	8	–	–	–
Ferroxidases/laccases	9	–	–	1	–	4	2	2
Fet3-type ferroxidases	–	1	2	3	2	1	1	3
Fungal pigment MCOs	–	–	–	5	–	–	2	–
Fungal ascorbate oxidases	–	4	–	–	–	–	1	–
Bilirubin oxidases	–	–	–	–	1	–	–	–
Total MCOs	9	5	2	16	11	5	6	5

Figure 3. A. Unrooted Neighbor-Joining tree of the MCO gene family. Organisms: Acr, *Acremonium* sp.; Aga, *Anopheles gambiae*; Ani, *Aspergillus niger*; Ave, *Albifimbria verrucaria*; Bsu, *Bacillus subtilis*; Cma, *Cucurbita maxima*; Cme, *Cucumis melo*; Cne, *Cryptococcus neoformans*; Dme, *Drosophila melanogaster*; Eco, *Escherichia coli*; Gmu, *Gliomastix murorum*; Hsa, *Homo sapiens*; Mmu, *Mus musculus*; Mse, *Manduca sexta*; Mtr, *Medicago truncatula*; Ncr, *Neurospora crassa*; Osa,

Oryza sativa; Pch, *Phanerochaete chrysosporium*; Phy, *Pimpla hypochondriaca*; Ptr, *Populus trichocarpa*; Rir, *Rhizophagus irregularis*; Ror, *Rhizopus oryzae*; Sce, *Saccharomyces cerevisiae*; Uma, *Ustilgo maydis*; Xca, *Xanthomonas campestris*. *Rhizophagus irregularis* MCOs are emphasized in bold. Protein NCBI identification numbers are indicated. Bootstrap values above 70 and supporting a node are indicated. **B. Number and classification of MCOs in fungal genomes.** Organisms: Ani, *Aspergillus niger*; Cne, *Cryptococcus neoformans*; Ncr, *Neurospora crassa*; Pch, *Phanerochaete chrysosporium*; Rir, *Rhizophagus irregularis*; Ror, *Rhizopus oryzae*; Sce, *Saccharomyces cerevisiae*; Uma, *Ustilgo maydis*.

In silico *characterization of the predicted proteins*

Alignment of the deduced amino acid sequences of RiMCO1-9 with other fungal MCOs revealed that the nine RiMCOs have the four conserved regions that contain the residues involved in copper coordination, a characteristic signature of all MCOs (Fig. 4). However, they lack the cysteine in signature sequence S2, which is always present in *sensu stricto* lacasses but not in Fet3-type ferroxidases (Kumar et al., 2003). RiMCO1, RiMCO3, RiMCO6, RiMCO8 and RiMCO9 have at least one of the four residues (E185, D283, Y354 and D409) that in *S. cerevisiae* have been shown to be essential for Fe oxidation (Wang et al., 2003; Stoj et al., 2006; Fig. 5), a characteristic of ferroxidases and ferroxidases/laccases with a main ferroxidase activity (Kües and Rühl, 2011).

MCO	S1	S2	S3	S4
RiMCO1	108 SVIHWHGMFQRGT	151 GTFWYHAHTHGQYM	468 AIHPIHMHGHNF	521 PGVWSIHCHIEWHVE
RiMCO2	127 AAVHWHGVFQHGT	170 GTFWYHSHFMAQYA	487 DEHPFHMHGHVF	541 PGIWAFHCHIEWHVE
RiMCO3	93 TSIHSHGMFQRGT	136 GTYWYHSHAMTQYV	444 GDHPFHMHGHQF	497 PGVFGIHCHMEWHLQ
RiMCO4	116 TTIHWHGIFQRGT	159 GTYWWHSHFRSQYV	476 ATHPFHLHGHNF	529 PGVWAFHCHIEWHVE
RiMCO5	126 ATIHWHGMFQHGT	169 GTYWYHSHFFAQYV	485 ADHPFHMHGHVF	539 PGVWAFHCHIEWHVE
RiMCO6	193 TTIHVHGMIHKET	235 GTYWYYSHYETQRA	580 LDQVFYLHGHKF	633 PGIWTFSNPIVWHQN
RiMCO7	111 TTIHWHGIFQKGT	154 GTYWWHSNFGSQYV	475 ATHPFHFHGHNF	528 PGIWAFYSHIEWLIE
RiMCO8	85 TAMHAHGMLQRGT	122 GTHWYHAHETMQYV	417 GEHPFHIHGYQF	470 PGAWGIHCHMICYRF
RiMCO9	89 TAIHSHGIFQRGT	132 GTYWYHSHATTQYV	440 GEHPFHIHGHQF	493 PG---------WHLQ
ScFet3	78 TSMHFHGLFQNGT	121 GTYWYHSHTDGQYE	411 GTHPFHLHGHAF	475 PGVWFFHCHIEWHLL
	: :* **:::. *	**.*:::. * •	: :::**: *	**

Figure 4. Sequence alignment of the four copper-binding sites (signature motifs S1 to S4) of the nine *Rhizophagus irregularis* MCOs and the *Saccharomyces cerevisiae* ferroxidase Fet3. Histidine (H) and cysteine (C) copper ligands are indicated. [The conserved 10 histidines and a cysteine residue involved in the coordination of copper are shown]. A black circle denotes a residue in signature sequence S2 that is always a cysteine (C) in classical laccases, but not in Fet3 ferroxidases.

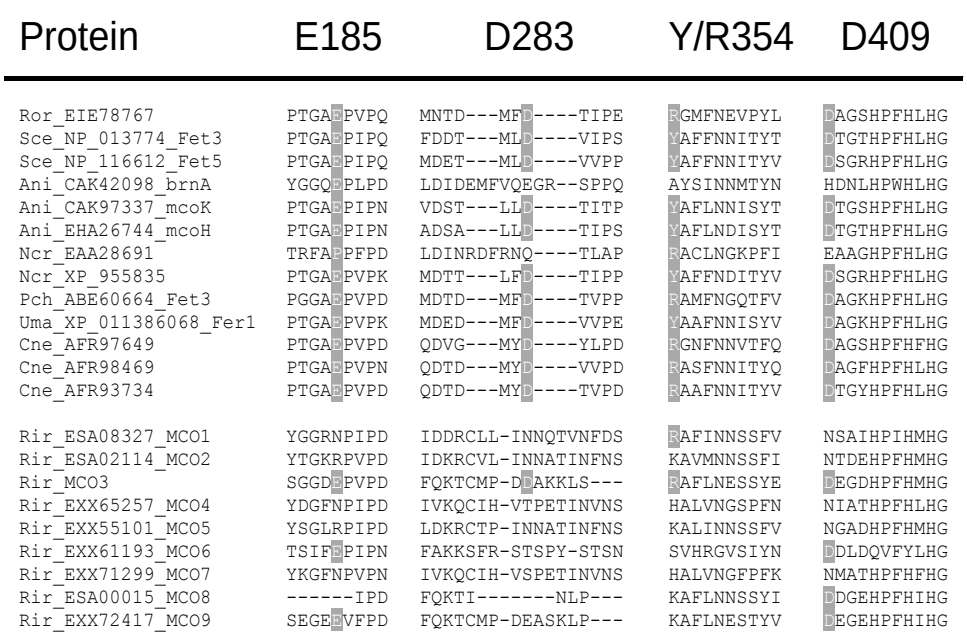

Figure 5. Alignment of the four regions of the *Saccharomyces cerevisiae* ferroxidase Fet3 with the residues E185, D283, Y354, D409 known to function in oxidation of Fe^{2+} to Fe^{3+} with the corresponding sequence regions of Fet3-type ferroxidases from fungi and *Rhizophagus irregularis* MCOs. The upper block presents the cluster of Fet3-like enzymes following the order of the figure 3B and the lower block the cluster of *R. irregularis* ferroxidases/laccases. The residues involved in ferroxidase activity (E185, D283, Y/R354 and D409) are emphasized in grey. Organisms: Ani, *Aspergillus niger*; Cne, *Cryptococcus neoformans*; Ncr, *Neurospora crassa*; Pch, *Phanerochaete chrysosporium*; Rir, *Rhizophagus irregularis*; Ror, *Rhizopus oryzae*; Sce, *Saccharomyces cerevisiae*; Uma, *Ustilgo maydis*. Protein NCBI identification numbers are indicated.

RiMCO1, RiMCO4, RiMCO5 and RiMCO6 were predicted to have an N-terminal transmembrane domain, but lack the C-terminal transmembrane domain typical of ferroxidases. Recently, an N-terminal transmembrane domain was also identified in a novel *Acidomyces acidophilus* MCO oxidase that displays ferroxidase activity (Boonen et al., 2014). RiMCO8 was predicted to have two, one at the N-terminus and the other at the C-terminus (Table 1).

Regulation of RiMCO *gene expression by Fe*

In an attempt to identify the potential *R. irregularis* ferroxidase that interact with the Fe permease RiFTR1, *RiMCOs* transcript levels were analyzed in ERM grown in the presence of different iron concentrations (Fig. 6). Relative to the ERM grown in M media containing 0.045 mM Fe, a 2-fold

up-regulation of *RiMCO1* gene expression was observed when the ERM was grown in a media lacking Fe and exposed for 3 d to the Fe chelator ferrozine. On the other hand, development of the fungus in the presence of 45 mM Fe induced a slight but statistically significant down-regulation of *RiMCO1* gene expression, and a 3.5-fold up-regulation of *RiMCO4* gene expression. Transcript levels of *RiMCO3*, *RiMCO5* and *RiMCO6* were not significantly affected by the amount of Fe present in the culture medium. *RiMCO2*, *RiMCO7*, *RiMCO8* and *RiMCO9* were not expressed in our experimental conditions or were below the detection limit. *RiMCO1* was the only *MCO* gene displaying a gene expression pattern typical of a high-affinity Fe transport system, suggesting that RiMCO1 might be partner of the iron permease RiFTR1.

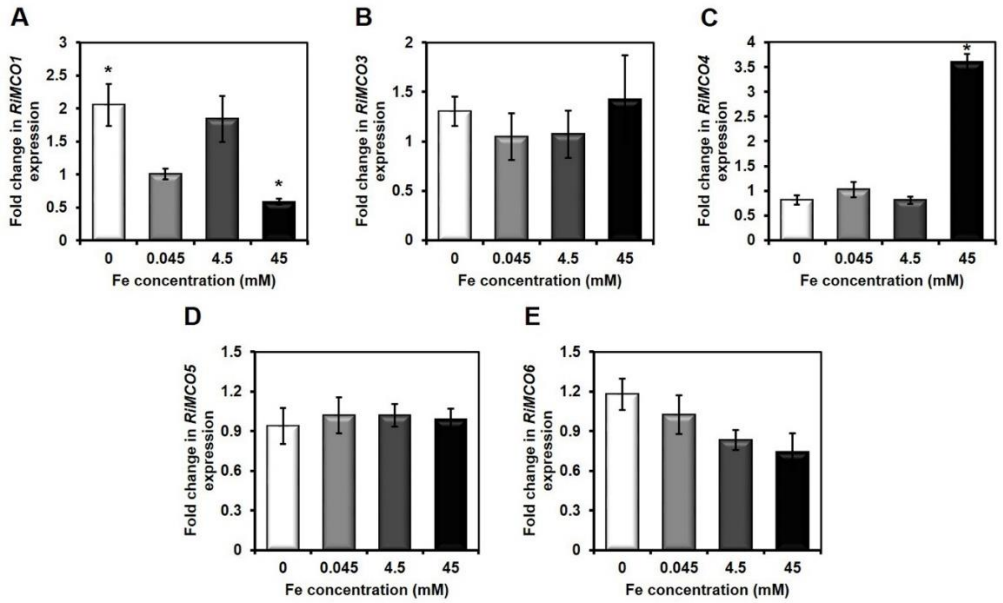

Figure 6. Effect of iron on the expression of the *Rhizophagus irregularis MCO* genes. *R. irregularis* was grown in M-C media containing 0 mM Fe, 0.045 mM Fe (control) or supplemented with 4.5 mM Fe or 45 mM Fe medium for 2 weeks. ERM grown in a media without Fe was exposed for 3 d to ferrozine. *RiMCO1* (A), *RiMCO3* (B), *RiMCO4* (C), *RiMCO5* (D) and *RiMCO6* (E) gene expression. Data were normalized using the housekeeping gene *RiTEF*. Relative expression levels were calculated by the $2^{-\Delta\Delta CT}$ method. Data are means +/- standard error. Asterisks show statistically significant differences ($p<0.05$) compared to the control value, according to the Fisher's LSD test.

RiMCO1 enables the yeast mutant to take up iron

To determine if RiMCO1 could have a Fe-related function, we assessed whether RiMCO1 could restore the inability of the *Δfet3* mutant of *S. cerevisiae* lacking Fet3 ferroxidase activity to take up iron. For this purpose, the *RiMCO1* full length cDNA was cloned into the yeast expression vector pDR195 and the capability of the *RiMCO1*-expressing mutant yeast to transport iron was determined. Relative to the empty vector-transformed cells, a 2-fold increase in iron uptake was observed in the *RiMCO1*-expressing *Δfet3* cells (Fig. 7). Therefore, RiMCO1 enables the yeast mutant to take up iron.

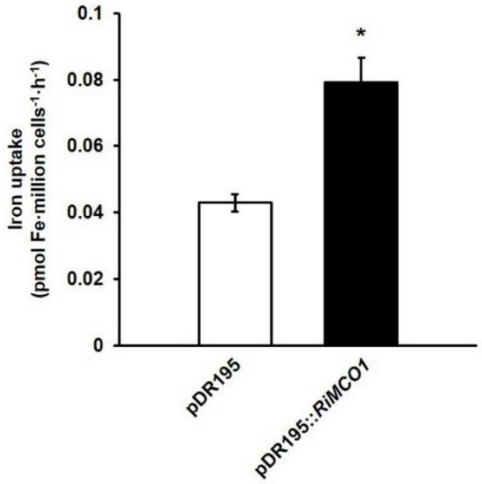

Figure 7. Analysis of the *in vivo* role of RiMCO1 in high-affinity iron transport in yeast. *Δfet3* cells transformed with empty vector or expressing *RiMCO1* were examined for uptake of 1 μM ^{55}Fe(II)-ascorbate. Data are means +/- standard error. Asterisk show statistically significant differences ($p<0.05$).

RiMCOs *are differentially expressed in the intraradical and extraradical mycelium*

To compare *RiMCOs* gene expression in the IRM and ERM, quantitative gene expression analysis was performed by real-time RT-PCR on ERM collected from the hyphal compartment of *R. irregularis* monoxenic cultures and on carrot mycorrhizal roots developed in a densely colonized hyphal compartment of the split Petri dishes lacking ERM. In the ERM, *RiMCO1, RiMOC4* and *RiMCO5* were the most highly expressed genes, followed by *RiMCO3*. *RiMCO6* expression was barely detected in the ERM.

As mentioned above, *RiMCO2*, *RiMCO7*, *RiMCO8* and *RiMCO9* were not expressed in the ERM or were below the detection limit. However, *RiMCO2* was the *RiMCO* most highly expressed in the IRM. Transcript levels of *RiMCO1* and *RiMCO5* were, respectively, more than 100- and-10-fold higher in the ERM than in the IRM of the monoxenically grown carrot roots. No significant differences were observed between the expression levels of *RiMCO3*, *RiMCO4*, *RiMCO6*, *RiMCO7*, *RiMCO8* and *RiMCO9* in both fungal structures (Fig. 8).

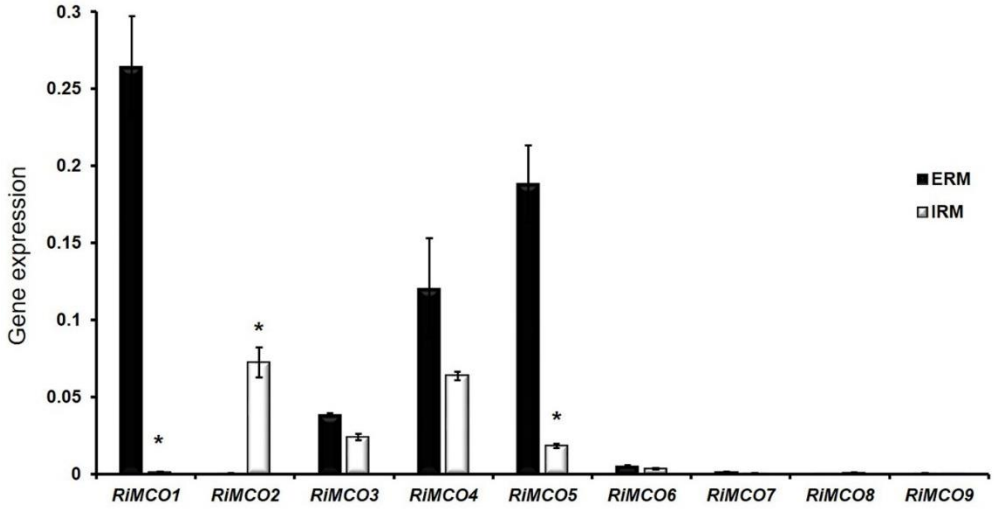

Figure 8. Relative expression of the *MCO* genes in extraradical mycelia (ERM) and intraradical (IRM) mycelia of *Rhizophagus irregularis*. *RiMCO* gene expression was assessed in ERM developed in monoxenic cultures (ERM) and *R. irregularis*-colonized carrot roots grown in monoxenic cultures and lacking ERM (IRM). Samples were normalized using the housekeeping gene *RiTEF*. Relative expression levels were calculated by the $2^{-\Delta CT}$ method. Data are means +/- standard error. Asterisks show statistically significant differences ($p<0.05$) relative to the ERM, according to the Fisher's LSD test.

Discussion

Nine full-length sequences putatively encoding MCOs were identified in the genome of *R. irregularis*. Our *in silico* analysis suggests that *R. irregularis* does not have any *sensu stricto* ferroxidase. *RiMCO1* encodes a protein with ferroxidase activity that is highly expressed in the ERM and is transcriptionally regulated by Fe availability in the culture media.

The number of *R. irregularis MCO* genes is higher than those of *S. cerevisiae* (three MCOs; Hoegger et al., 2006), the basidiomycetes *P. chrysosporium* (five MCOs, Larrondo et al., 2004; Fernandez-Fueyo et al., 2012), *U. maydis* (six MCOs; Hoegger et al., 2006), *C. neoformans* (five MCOs; Kües and Rühl, 2011), and the mucoromycotina *R. oryzae* (five MCOs; Hoegger et al., 2006), but lower than those of the ascomycetes *Aspergillus niger* (sixteen MCOs, Tamayo-Ramos et al., 2011) and *Neurospora crassa* (eleven MCOs; Pöggeler, 2011). The number of introns in the *MCO* sequences ranged between four and eleven and is lower than in basidiomycete *MCO* genes. For example, the *P. chrysosporium MCO* genes have 14-19 introns (Larrondo et al., 2004; Courty et al., 2009). Based on the phylogenetic tree and on intron distributions of the *R. irregularis* MCOs, the protein RiMCO6 seems to have an evolutionary origin different from the eight other MCOs of the species. Intron positions of the *R. irregularis MCO* sequences defined five gene subfamilies, and it is remarkable that one gene of each subfamily is well-expressed in the ERM.

Phylogenetic analyses of the MCO protein sequences of the reference fungi used in this study, including three basidiomycetes, three ascomycetes, one mucoromycotina and the glomeromycotan fungus *R. irregularis* revealed that the nine RiMCOs clustered together in the ferroxidases/lacasses clade. This distribution might be related to organism taxonomy, since *R. irregularis* is the only glomeromycotan fungus used to construct the phylogram.

Based on sequence alignments, it seems that *R. irregularis,* despite using a reductive pathway for iron uptake (Tamayo et al., previous chapter), does not have any ferroxidase *sensu stricto* in its genome. Genomes of all the fungi used in the phylogenetic study, except of *R. irregularis*, contain orthologs of FET3-type ferroxidases. To date, ferroxidase genes (coding Fet3-type ferroxidases or ferroxidases/laccases) have been found in all sequenced basidiomycetes except *Coprinopsis cinerea* (Kües and Rühl, 2011), whose genome also lacks *FTR1* homologs, but has a *sid1*/*sidA* gene involved in the biosynthesis of an iron-chelating siderophore involved in iron acquisition under conditions of low soil iron availability (Hoegger et al., 2006). On the other hand, the lack the RiMCOs of the cysteine (C) in signature S2 that is shared in fungal lacasses (Kumar et al., 2003), suggests that *R. irregularis* might not need a laccase activity.

The finding that out of the nine *RiMCO* genes only *RiMCO1* displays in response to iron availability in the culture media a similar expression pattern than the iron permease RiFTR1 (Fig. 10B, previous chapter) suggests that RiMCO1 might act as the RiFTR1 partner in *R. irregularis*. This hypothesis is supported by the capability of RiMCO1 to enable the *Δfet3* mutant yeast to take up Fe. Our gene expression data also revealed that *RiMCO4* is induced when the ERM was exposed to the highest Fe concentration. Since the ERM exposed to 45 mM Fe presented a brownish colour (data not shown), as suggested for some MCOs of the white rot fungus *Lentinula edodes* (Sakamoto et al., 2015), RiMCO4 might be involved in fungal senescence. Even though *RiMCO1* was the only *RiMCO* candidate gene of the high-affinity Fe transport system, expression of some other(s) gene(s) might be regulated by Fe in a post-transcriptional manner.

Our gene expression analyses also revealed that the *RiMCOs* are differentially expressed in the IRM and the ERM. As it has been reported in *L. edodes*, they might be involved in hyphal morphogenesis and cell wall synthesis (Nakade et al., 2011). However, the function of these MCOs has to be ascertained.

In conclusion, this study shows that the AM fungus *R. irregularis* has at least nine MCO members in its genome and that at the ERM RiMCO1 might play a role in the reductive high-affinity Fe uptake pathway together with the Fe permease RiFTR1.

References

Albarouki E, Deising HB. 2013. Infection structure-specific reductive iron assimilation is required for cell wall integrity and full virulence of the maize pathogen *Colletotrichum graminicola*. Molecular Plant-Microbe Interactions 26, 695–708. doi: 10.1094/MPMI-01-13-0003-R

Altschul SF, Gish W, Miller W, Myers EW, Lipman DJ. 1990. Basic local alignment search tool. Journal of Molecular Biology 215, 403–410. doi: 10.1016/S0022-2836(05)80360-2

Askwith C, Eide D, Van Ho A, Bernard PS, Li L, Davis-Kaplan S, Sipe DM, Kaplan J. 1994. The *FET3* gene of *S. cerevisiae* encodes a multicopper oxidase required for ferrous iron uptake. Cell 76, 403–410. doi: 10.1016/0092-8674(94)90346-8

Askwith C, Kaplan J. 1997. An oxidase-permease-based iron transport system in *Schizosaccharomyces pombe* and its expression in *Saccharomyces cerevisiae*. The Journal of Biological Chemistry 272, 401–405.

Boonen F, Vandamme A-M, Etoundi E, Pigneur L-M, Housen I. 2014. Identification and characterization of a novel multicopper oxidase from *Acidomyces acidophilus* with ferroxidase activity. Biochimie 102, 37–46. doi: 10.1016/j.biochi.2014.02.009

Caris C, Hördt W, Hawkins H-J, Römheld V, George E. 1998. Studies of iron transport by arbuscular mycorrhizal hyphae from soil to peanut and sorghum plants. Mycorrhiza 8, 35–39. doi: 10.1007/s005720050208

Chabot S, Bécard G, Piché Y. 1992. Life cycle of *Glomus intraradix* in root organ culture. Mycologia 84, 315–321. doi: 10.2307/3760183

Courty PE, Hoegger PJ, Kilaru S, Kohler A, Buée M, Garbaye J, Martin F, Kües U. 2009. Phylogenetic analysis, genomic organization, and expression analysis of multi-copper oxidases in the ectomycorrhizal basidiomycete *Laccaria bicolor*. New Phytologist 182, 736–750. doi: 10.1111/j.1469-8137.2009.02774.x

Eichhorn H, Lessing F, Winterberg B, Schirawski J, Kämper J, Müller P, Kahmann R. 2006. A ferroxidation/permeation iron uptake system is required for virulence in *Ustilago maydis*. The Plant Cell 18, 3332–3345. doi: 10.1105/tpc.106.043588

Fernandez-Fueyo E, Ruiz-Dueñas FJ, Ferreira P, et al. 2012. Comparative genomics of *Ceriporiopsis subvermispora* and *Phanerochaete chrysosporium* provide insight into selective ligninolysis. Proceedings of the National Academy of Sciences 109, 5458–5463. doi: 10.1073/pnas.1119912109

Greenshields DL, Liu G, Feng J, Selvaraj G, Wei Y. 2007. The siderophore biosynthetic gene *SID1*, but not the ferroxidase gene *FET3*, is required for full *Fusarium graminearum* virulence. Molecular Plant Pathology 8, 411–421. doi: 10.1111/J.1364-3703.2007.00401.X

Hoegger PJ, Kilaru S, James TY, Thacker JR, Kües U. 2006. Phylogenetic comparison and classification of laccase and related multicopper oxidase protein

sequences. The FEBS Journal 273, 2308–2326. doi: 10.1111/j.1742-4658.2006.05247.x

Jung WH, Hu G, Kuo W, Kronstad JW. 2009. Role of ferroxidases in iron uptake and virulence of *Cryptococcus neoformans*. Eukaryotic Cell 8, 1511–1520. doi: 10.1128/EC.00166-09

Kobae Y, Tomioka R, Tanoi K, Kobayashi NI, Ohmori Y, Nishida S, Fujiwara T. 2014. Selective induction of putative iron transporters, *OPT8a* and *OPT8b*, in maize by mycorrhizal colonization. Soil Science and Plant Nutrition 60, 843–847. doi: 10.1080/00380768.2014.949854

Kosman DJ. 2003. Molecular mechanisms of iron uptake in fungi. Molecular Microbiology 47, 1185–1197. doi: 10.1046/j.1365-2958.2003.03368.x

Kosman DJ. 2010. Redox cycling in iron uptake, efflux, and trafficking. The Journal of Biological Chemistry 285, 26729–26735. doi: 10.1074/jbc.R110.113217

Kües U, Rühl M. 2011. Multiple multi-copper oxidase gene families in basidiomycetes – what for? Current Genomics 12, 72–94. doi: 10.2174/138920211795564377

Kumar SVS, Phale PS, Durani S, Wangikar PP. 2003. Combined sequence and structure analysis of the fungal laccase family. Biotechnology and Bioengineering 83, 386–394. doi: 10.1002/bit.10681

Kwok EY, Severance S, Kosman DJ. 2006. Evidence for iron channeling in the Fet3p-Ftr1p high-affinity iron uptake complex in the yeast plasma membrane. Biochemistry 45, 6317–6327. doi: 10.1021/bi052173c

Larkin MA, Blackshields G, Brown NP, et al. 2007. Clustal W and Clustal X version 2.0. Bioinformatics 23, 2947–2948. doi: 10.1093/bioinformatics/btm404

Larrondo LF, Canessa P, Melo F, Polanco R, Vicuña R. 2007. Cloning and characterization of the genes encoding the high-affinity iron-uptake protein complex Fet3/Ftr1 in the basidiomycete *Phanerochaete chrysosporium*. Microbiology 153, 1772–1780. doi: 10.1099/mic.0.2006/003442-0

Larrondo LF, González B, Cullen D, Vicuña R. 2004. Characterization of a multicopper oxidase gene cluster in *Phanerochaete chrysosporium* and evidence of altered splicing of the *mco* transcripts. Microbiology 150, 2775–2783. doi: 10.1099/mic.0.27072-0

Larrondo LF, Salas L, Melo F, Vicuña R, Cullen D. 2003. A novel extracellular multicopper oxidase from *Phanerochaete chrysosporium* with ferroxidase activity. Applied and Environmental Microbiology 69, 6257–6263. doi: 10.1128/AEM.69.10.6257-6263.2003

Lin K, Limpens E, Zhang Z, et al. 2014. Single nucleus genome sequencing reveals high similarity among nuclei of an endomycorrhizal fungus. PLoS genetics 10, e1004078. doi: 10.1371/journal.pgen.1004078

Liu L, Tewari RP, Williamson PR. 1999. Laccase protects *Cryptococcus neoformans* from antifungal activity of alveolar macrophages. Infection and Immunity 67, 6034–6039.

Nakade K, Watanabe H, Sakamoto Y, Sato T. 2011. Gene silencing of the *Lentinula edodes lcc1* gene by expression of a homologous inverted repeat sequence. Microbiological Research 166, 484–493. doi: 10.1016/j.micres.2010.09.004

Paronetto MP, Miele R, Maugliani A, Borro M, Bonaccorsi di Patti MC. 2001. Cloning of *Pichia pastoris* Fet3: insights into the high affinity iron uptake system. Archives of Biochemistry and Biophysics 392, 162–167. doi: 10.1006/abbi.2001.2425

Pöggeler S. 2011. Evolution of multicopper oxidase genes in coprophilous and non-coprophilous members of the order Sordariales. Current Genomics 12, 95–103. doi: 10.2174/138920211795564368

Rentsch D, Laloi M, Rouhara I, Schmelzer E, Delrot S, Frommer WB. 1995. NTR1 encodes a high affinity oligopeptide transporter in *Arabidopsis*. FEBS letters 370, 264–268. doi: 10.1016/0014-5793(95)00853-2

Rydén LG, Hunt LT. 1993. Evolution of protein complexity: the blue copper-containing oxidases and related proteins. Journal of Molecular Evolution 36, 41–66. doi: 10.1007/BF02407305

Sakamoto Y, Nakade K, Yoshida K, Natsume S, Miyazaki K, Sato S, van Peer AF, Konno N. 2015. Grouping of multicopper oxidases in *Lentinula edodes* by sequence similarities and expression patterns. AMB Express 5, 63. doi: 10.1186/s13568-015-0151-2

Schiestl RH, Gietz RD. 1989. High efficiency transformation of intact cells using single stranded nucleic acids as a carrier. Current genetics 16, 339–346. doi: 10.1007/BF00340712

Schmittgen TD, Livak KJ. 2008. Analyzing real-time PCR data by the comparative C_T method. Nature Protocols 3, 1101–1108. doi: 10.1038/nprot.2008.73

Schrettl M, Bignell E, Kragl C, Joechl C, Rogers T, Arst HN, Haynes K, Haas H. 2004. Siderophore biosynthesis but not reductive iron assimilation is essential for *Aspergillus fumigatus* virulence. The Journal of Experimental Medicine 200, 1213–1219. doi: 10.1084/jem.20041242

Smith SE, Read DJ. 2008. *Mycorrhizal symbiosis* (Third edition). London: Academic Press.

St-Arnaud M, Hamel C, Vimard B, Caron M, Fortin JA. 1996. Enhanced hyphal growth and spore production of the arbuscular mycorrhizal fungus *Glomus intraradices* in an *in vitro* system in the absence of host roots. Mycological Research 100, 328–332. doi: 10.1016/S0953-7562(96)80164-X

Stearman R, Yuan DS, Yamaguchi-iwai Y, Klausner RD, Dancis A. 1996. A permease-oxidase complex involved in high-affinity iron uptake in yeast. Science 271, 1552–1557. doi: 10.1126/science.271.5255.1552

Stoj CS, Augustine AJ, Zeigler L, Solomon EI, Kosman DJ. 2006. Structural basis of the ferrous iron specificity of the yeast ferroxidase, Fet3p. Biochemistry 45, 12741–12749. doi: 10.1021/bi061543

Tamayo Ramos JA, Barends S, Verhaert RMD, de Graaff LH. 2011. The *Aspergillus niger* multicopper oxidase family: analysis and overexpression of laccase-like encoding genes. Microbial Cell Factories 10, 78. doi: 10.1186/1475-2859-10-78

Tamura K, Stecher G, Peterson D, Filipski A, Kumar S. 2013. MEGA6: Molecular evolutionary genetics analysis version 6.0. Molecular Biology and Evolution 30, 2725–2729. doi: 10.1093/molbev/mst197

Wang T-P, Quintanar L, Severance S, Solomon EI, Kosman DJ. 2003. Targeted suppression of the ferroxidase and iron trafficking activities of the multicopper oxidase Fet3p from *Saccharomyces cerevisiae*. JBIC Journal of Biological Inorganic Chemistry 8, 611–620. doi: 10.1007/s00775-003-0456-5

Wartmann T, Stephan UW, Bube I, Böer E, Melzer M, Manteuffel R, Stoltenburg R, Guengerich L, Gellissen G, Kunze G. 2002. Post-translational modifications of the *AFET3* gene product: a component of the iron transport system in budding cells and mycelia of the yeast *Arxula adeninivorans*. Yeast 19, 849–862. doi: 10.1002/yea.880

Ziegler L, Terzulli A, Gaur R, McCarthy R, Kosman DJ. 2011. Functional characterization of the ferroxidase, permease high-affinity iron transport complex from *Candida albicans*. Molecular Microbiology 81, 473–485. doi: 10.1111/j.1365-2958.2011.07704.x

Supporting Information

S1 Table. Oligonucleotides used in this study.

Primer	Sequence 5' - 3'	Application
GiFETa.rR	TGCAGGTCCAGGAATTTGTTGAGG	5’ RACE of *RiMCO1*
FETc.rF	ACTTTAGCCCCGGATGGATTTACTCG	3’ RACE of *RiMCO3*
FETc.rR	GAGATTGTCCTGCCACCCCGTCAA	5’ RACE of *RiMCO3*
GiFETaF	CTCAACCAGTTGGTCCGTATTT	Real-time PCR of *RiMCO1*
GiFETaR	TACCCATTTCAACATGCCACTC	Real-time PCR of *RiMCO1*
FETb.qF	CATTTCATATGCACGGACAC	Real-time PCR of *RiMCO2*
FETb.qR	CCAGGAACGGTCACATTATC	Real-time PCR of *RiMCO2*
RiFETc.qF	GCATTTGCAATCTGGTCTTT	Real-time PCR of *RiMCO3*
RiFETc.qR	TACACAAGCTTTTCGGCATT	Real-time PCR of *RiMCO3*
RiFETd.qF	CCATTCCCATCATGTCAAAT	Real-time PCR of *RiMCO4*
RiFETd.qR	CCTTGTTTGTTTTCCCTCCT	Real-time PCR of *RiMCO4*
FETe.qF	CCGATCAACATGGTGCCTACT	Real-time PCR of *RiMCO5*
FETe.qR	AGCGTCCTGAAGTGGTAAGAGA	Real-time PCR of *RiMCO5*
FETf.qF	TCAATCCCCTCAGAATCACCAGA	Real-time PCR of *RiMCO6*
FETf.qR	GGTTTTGTCGTTTCAGGTTGTG	Real-time PCR of *RiMCO6*
RiFETg.qF	ACAGGGCAGAATTGTTTCAA	Real-time PCR of *RiMCO7*
RiFETg.qR	TTTCTTGACGCTTTTCGAGT	Real-time PCR of *RiMCO7*
RiFETh.qF	AAAAAGGGCAACAATCACAC	Real-time PCR of *RiMCO8*
RiFETh.qR	ATATACCCCCGGTTCAAAAT	Real-time PCR of *RiMCO8*
RiFETi.qF	CTGCAGAAATGCAAGAGACC	Real-time PCR of *RiMCO9*
RiFETi.qR	CATATGCACGGACATTTTGA	Real-time PCR of *RiMCO9*
GintEFfw	GCTATTTTGATCATTGCCGCC	Real-time PCR of *RiEF1α*
GintEFrev	TCATTAAAACGTTCTTCCGACC	Real-time PCR of *RiEF1α*
FETa.fF	ATGGGGGAACAGGATAAGG	Cloning of *RiMCO1* CDS
FETa.fR	CTATACTTTTATTCTTTTCATATCAGTATT	Cloning of *RiMCO1* CDS

CHAPTER IV

Characterization of three new glutaredoxin genes in the arbuscular mycorrhizal fungus *Rhizophagus irregularis*: putative role of RiGRX4 and RiGRX5 in iron homeostasis

Reprinted from:

Tamayo E, Benabdellah K, Ferrol N. 2016.

Characterization of three new glutaredoxin genes in the arbuscular mycorrhizal fungus *Rhizophagus irregularis*: putative role of RiGRX4 and RiGRX5 in iron homeostasis.

PLoS One 11: e0149606. doi:10.1371/journal.pone.0149606

Abstract

Glutaredoxins (GRXs) are small ubiquitous oxidoreductases involved in the regulation of the redox state in living cells. In an attempt to identify the full complement of GRXs in the arbuscular mycorrhizal (AM) fungus *Rhizophagus irregularis*, three additional GRX homologs, besides the formerly characterized GintGRX1 (renamed here as RiGRX1), were identified. The three new GRXs (RiGRX4, RiGRX5 and RiGRX6) contain the CXXS domain of monothiol GRXs, but whereas RiGRX4 and RiGRX5 belong to class II GRXs, RiGRX6 belongs to class I together with RiGRX1. By using a yeast expression system, we observed that the newly identified homologs partially reverted sensitivity of the GRX deletion yeast strains to external oxidants. Furthermore, our results indicated that RiGRX4 and RiGRX5 play a role in iron homeostasis in yeast. Gene expression analyses revealed that *RiGRX1* and *RiGRX6* were more highly expressed in the intraradical (IRM) than in the extraradical mycelium (ERM). Exposure of the ERM to hydrogen peroxide induced up-regulation of *RiGRX1*, *RiGRX4* and *RiGRX5* gene expression. *RiGRX4* expression was also up-regulated in the ERM when the fungus was grown in media supplemented with a high iron concentration. These data indicate the two monothiol class II GRXs, RiGRX4 and RiGRX5, might be involved in oxidative stress protection and in the regulation of fungal iron homeostasis. Increased expression of *RiGRX1* and *RiGRX6* in the IRM suggests that these GRXs should play a key role in oxidative stress protection of *R. irregularis* during its *in planta* phase.

Introduction

Arbuscular mycorrhizal (AM) fungi are soil microorganisms belonging to the Glomeromycota phylum that establish mutualistic symbioses, called arbuscular mycorrhizas, with the roots of the majority of higher plants. In this symbiosis, the fungus provides the plant with mineral nutrients of low mobility in the soil and in return the fungus receives carbon supplies from the plant (Smith and Read, 2008). The AM symbiosis benefits plants not only promoting growth but also enhancing plant tolerance to biotic and abiotic stresses (Barea et al., 2013). In the course of the symbiosis, roots are colonized by fungal hyphae that ultimately form intracellular tree-like structures termed arbuscules in the inner-cortical cells, facilitating nutrient exchange between the two partners. The establishment of such an intimate interaction, allowing the fungus to grow intracellularly in the host cells, requires its recognition as a symbiotic partner and a tight regulation of processes leading to the accommodation of the beneficial fungus. At the molecular level, this process is only partly understood, and the precise function of most plant genes known to be regulated during fungal colonization remains elusive (Requena et al., 2007; Gutjahr and Paszkowski, 2013; Bucher et al., 2014; Bonfante and Genre, 2015). On the fungal side, knowledge of the mechanisms underlying adaptation to the symbiotic mode is even more limited. This is mainly due to the fact that research on AM fungi is hampered by their obligate biotrophic life style and that they are so far not amenable to genetic manipulation. However, the recently published genome and genome-wide transcriptomic data of an AM fungus open new opportunities (Tisserant et al., 2012, 2013; Lin et al., 2014).

The AM association shares several common features with those of plant-fungal pathogens, including local and transient production of reactive oxygen species (ROS) (Fester and Hause, 2005; Nanda et al., 2010), induction of plant defence genes (Jung et al., 2012) and the use of effector proteins to counteract plant defence responses (Kloppholz et al., 2011). In AM roots, accumulation of hydrogen peroxide (H_2O_2) has been observed around the hyphal tips attempting to penetrate a host cell and in cells containing

arbuscules, while no H_2O_2 accumulation was observed in hyphal tips growing along the middle lamella, appressoria or vesicles (Salzer et al., 1999). Recent studies provided evidence that ROS concentrations tightly control the outcome of the symbiosis. Silencing of genes involved in ROS production, such as ROP9, a small GTPase from *Medicago truncatula* (Kiirika et al., 2012) or the *Phaseolus vulgaris* NADPH oxidase RbohB (Arthikala et al., 2013), induced early hyphal colonization and enhanced root length colonization, while an enhanced accumulation of ROS in over-expressing RbohB *P. vulgaris* roots impaired AM fungal colonization (Arthikala et al., 2014). However, in *M. truncatula* it has been shown that silencing of RbohE, a NADPH oxidase isoform that is expressed in arbuscule-containing cells, induced an altered colonization pattern in the root cortex with fewer arbuscules and multiple penetration attempts (Belmondo et al., 2016). Fungal suppression of ROS-mediated defence by the secretion of ROS-scavenging enzymes, such as the superoxide dismutase (Lanfranco et al., 2005; González-Guerrero et al., 2010), or the production of antioxidant compounds, such as vitamin B6 (Benabdellah et al., 2009*a*), has been proposed to be necessary for successful colonization of the host plant by AM fungi (Lanfranco et al., 2005). In addition to the mediation of plant–fungal interactions by host-derived ROS, the endogenous production of ROS by AM fungi should be important for their normal development and adaptation to environmental stresses. In spite of the central role that gluthatione (GSH) plays as a cellular redox buffer, only one enzyme related with this metabolite, a dithiol glutaredoxin (GRX), has been characterized in an AM fungus (Benabdellah et al., 2009*b*).

Glutaredoxins (GRXs) are small ubiquitous oxidoreductases that mediate reversible reduction of the disulphide bonds formed between cysteine residues of proteins and GSH via a dithiol or monothiol mechanism. GRXs generally contain a conserved CXXC/S or CGFS active-site motif, which is involved in the reduction reaction, and the TVP and GG motifs involved in GSH binding (Lillig et al., 2008; Couturier et al., 2015). GRXs were initially classified into two groups, dithiol and monothiol, according to their active site sequence, having two or one cysteine residues in it, respectively. Nevertheless, due to the discovery of an increasing number of GRX sequences, Couturier et al. (2009) and afterwards Ströher and Millar (2012)

proposed a new classification based on sequence structure, in which non-plant GRXs were categorized into classes I and II. Class I includes GRXs containing dithiol or monothiol active-site motifs (CXXC/S), whereas class II contains all GRXs with a CGFS motif in their active site (Rouhier et al., 2009). GRXs have been shown to be involved in the maintenance and regulation of the cellular redox state and in redox-dependent signalling pathways (Foyer and Noctor, 2005). Due to the general importance of these processes, these enzymes are involved in diverse cellular processes and play an important role in defence against oxidative stress (Lillig et al., 2008). The majority of Class II GRXs characterized to date have been shown to be required for the formation of iron-sulfur clusters (Bandyopadhyay et al., 2008) or as chaperons for the transfer and delivery of iron-sulfur clusters to acceptors apoproteins (Lill et al., 2012), playing a role in iron metabolism.

Glutaredoxins have been extensively studied in *Saccharomyces cerevisiae* (Herrero et al., 2010; Luo et al., 2010) and *Schizosaccharomyces pombe* (Chung et al., 2005) and *Sinorhizobium meliloti* (Benyamina et al., 2013). In the nitrogen-fixing symbiosis established between *S. meliloti* and *Medicago* plants, two *S. meliloti* GRX proteins have been shown to be essential for optimal development and functioning of the nitrogen-fixing symbiosis, playing independent roles in deglutathionylation reactions and in the regulation of iron metabolism. In the AM fungus *R. irregularis* only a dithiol GRX, GintGRX1, displaying oxidoreductase, peroxidase and glutathione S-transferase activities has been reported (Benabdellah et al., 2009*b*). With the aim of getting further insights into the roles of GRXs in AM fungi, a genome-wide approach has been used to identify and characterize the complete set of genes encoding GRXs in the AM fungus *R. irregularis*. Our data indicate that the *R. irregularis* GRX gene family is composed of four members. Characterization of the identified genes indicates that the different *R. irregularis* isoforms play diverse roles in the fungus and that the two monothiol class II GRXs, RiGRX4 and RiGRX5, might be involved in oxidative stress protection and in the regulation of fungal iron homeostasis.

Materials and methods

Biological materials and growth conditions

Rhizophagus irregularis monoxenic cultures were established as described by St-Arnaud et al. (1996), with some modifications. Briefly, clone DC2 of carrot (*Daucus carota* L.) Ri-T DNA transformed roots were cultured with the AM fungus *R. irregularis* Schenck and Smith DAOM 197198 in two-compartment Petri dishes. Cultures were initiated in one compartment of each plate containing M medium (Chabot et al., 1992) by placing several non-mycorrhizal carrot root segments and a piece of fungal inoculum containing extraradical mycelium (ERM), fragments of mycorrhizal roots and spores. Fungal hyphae and roots were allowed to grow over to the other compartment containing the same M medium. Plates were incubated in the dark at 24 °C for 7–8 weeks until the second compartment was profusely colonized by the fungus and the roots. Then, the older compartment was removed and refilled with liquid M medium without sucrose (M-C medium) containing different iron concentrations: 0.045 mM (control), 4.5 mM or 45 mM EDTA iron(III) sodium salt. Fungal hyphae, but not roots, were allowed to grow over to this compartment (hyphal compartment). Plates were incubated in the dark at 24 °C for 2–3 additional weeks. For the oxidative stress treatments, the fungus grown in control liquid M-C medium was exposed for 0.5, 1 and 2 h to 0.1 or 1 mM H_2O_2. This was done by replacing the liquid medium of the hyphal compartment of a control plate by 15 ml of a freshly prepared liquid M-C medium supplemented with H_2O_2. The control plates received 15 ml of liquid M-C medium.

ERM from the different hyphal compartments was directly recovered under sterile conditions by using a pair of tweezers, washed with sterile water and dried on filter paper. The mycelium was immediately frozen in liquid nitrogen and stored at -80 °C until used.

To analyze intraradical gene expression, hyphae growing in the hyphal compartment were used as a source of mycorrhizal inoculum. Carrot roots were placed on top of a densely colonized hyphal compartment and

collected 15 days later. Extraradical hyphae attached to the roots were removed with forceps under a binocular microscope. Roots were then frozen in liquid N and stored at -80 °C until used. Furthermore, rice roots (*Oryza sativa* L. cv. Nipponbare) colonized by *R. irregularis* were also used. Rice plants were grown as described in Pérez-Tienda et al. (2014). Briefly, rice seedlings from seeds germinated in autoclaved vermiculite were transplanted into pots containing a sterile mixture of soil:sand:vermiculite (1:2:6, v:v:v), and plants were grown in a growth chamber with 23/18 °C day/night temperature, 60% relative humidity and 16/8 h light/dark photoperiod. Mycorrhizal inoculation was performed using a sepiolite-vermiculite-based inoculum of *R. irregularis* (10%, v/v), containing spores, hyphae and fragments of AM roots. Control plants (non-mycorrhizal) received the same proportion of the inoculum substrate and an aliquot of a filtrate (<20 μm) of the AM inoculum to provide the microbial populations accompanying *R. irregularis* but free from AM propagules. Roots were harvested 8 weeks after inoculation, gently washed under tap water to try to eliminate most of the attached fungal hyphae and spores, frozen in liquid nitrogen and stored at -80 °C until used. Mycorrhizal root colonization was estimated after trypan blue staining according to the grid-line intersect method using a stereomicroscope (Giovannetti and Mosse, 1980).

The *S. cerevisiae* strains used in this study were all isogenic derivatives of CML128, W303-1A and YPH449 wild type strains (Table 1). The *Δgrx3Δgrx4* mutant MML449, the *Δgrx5* mutant MML100 and their respective parental strains CML128 and W303-1A were kindly provided by Dr. Enrique Herrero (Departament de Ciències Mèdiques Bàsiques, Facultat de Medicina, Universitat de Lleida, Lleida, Spain). The *Δgrx6Δgrx7* yeast strain and its parental YPH449 were kindly provided by Dr. Johannes M. Herrmann (Department of Cell Biology, University of Kaiserslautern, Kaiserslautern, Germany). Strains were grown on YPD or minimal synthetic dextrose (SD) medium, supplemented with appropriate amino acids.

Table 1. ***Saccharomyces cerevisiae*** **strains used in this work.**

Strain	Relevant genotype	Reference
W303-1A	*MATa ura3–1 ade2–1 leu2–3,112 trp1–1 his3–11,15*	(Wallis et al., 1989)
CML128	*MATa leu2-3,112 ura3-52 trp1 his4 can1*^{r}	(Gallego et al., 1997)
YPH449	*MATa ura3-52 lys2-801 ade2-101 trp1-Δ63 his3-Δ200 leu2-Δ1*	(Sikorski and Hieter, 1989)
MML100	*MATa grx5*::*kanMX4* as W303-1A	(Rodríguez-Manzaneque et al., 2002)
MML449	*MATa grx3::natMX4 grx4::kanMX4* as CML128	(Pujol-Carrion et al., 2006)
Δgrx6Δgrx7	*MATa grx6::HIS3 grx7::kan* as YPH449	(Mesecke et al., 2008)
MML100 pFL61	*Δgrx5* transformed with the empty vector	This work
MML100 pFL61Sc*Grx5*	*Δgrx5* transformed with the construct pFL61*ScGrx5*	This work
MML100 pFL61*RiGRX5*	*Δgrx5* transformed with the construct pFL61*RiGRX5*	This work
MML100 pFL61*RiGRX4*	*Δgrx5* transformed with the construct pFL61*RiGRX4*	This work
MML100 pFL61*RiGRX6*	*Δgrx5* transformed with the construct pFL61*RiGRX6*	This work
MML449 pFL61	*Δgrx3Δgrx4* transformed with the empty vector	This work
MML449 pFL61*ScGrx3*	*Δgrx3Δgrx4* transformed with the construct pFL61*ScGrx3*	This work
MML449 pFL61*ScGrx4*	*Δgrx3Δgrx4* transformed with the construct pFL61*ScGrx4*	This work
MML449 pFL61*RiGRX4*	*Δgrx3Δgrx4* transformed with the construct pFL61*RiGRX4*	This work
MML449 pFL61*RiGRX5*	*Δgrx3Δgrx4* transformed with the construct pFL61*RiGRX5*	This work
MML449 pFL61*RiGRX6*	*Δgrx3Δgrx4* transformed with the construct pFL61*RiGRX6*	This work
MML449 pBL106	*Δgrx3Δgrx4* transformed with pBL106	This work
MML449 pBL106*RiGRX4*	*Δgrx3Δgrx4* transformed with the construct pBL106*RiGRX4*	This work
MML449 pBL106*RiGRX5*	*Δgrx3Δgrx4* transformed with the construct pBL106*RiGRX5*	This work
Δgrx6Δgrx7 pFL61	*Δgrx6Δgrx7* transformed with the empty vector	This work
Δgrx6Δgrx7 pMM822	*Δgrx6Δgrx7* transformed with a plasmid containing the *ScGrx6* open reading frame (Izquierdo et al., 2008)	This work
Δgrx6Δgrx7 pFL61*RiGRX6*	*Δgrx6Δgrx7* transformed with the construct pFL61*RiGRX6*	This work
Δgrx6Δgrx7 pBL106	*Δgrx6Δgrx7* transformed with pBL106	This work
Δgrx6Δgrx7 pBL106*RiGRX6*	*Δgrx6Δgrx7* transformed with the construct pBL106*RiGRX6*	This work

Nucleic acids extraction and cDNA synthesis

R. irregularis genomic DNA was extracted from ERM developed in the hyphal compartment of control plates using the DNeasy Plant Mini Kit (Qiagen), according to the manufacturer's instructions.

Total plant RNA was isolated from rice roots using the phenol/SDS method followed by LiCl precipitation as described by García-Rodríguez et al. (2007). Total fungal RNA from ERM from the different treatments of *R. irregularis* and mycorrhizal carrot roots, was extracted using the RNeasy Plant Mini Kit (QIAGEN, Maryland), following manufacturer´s instructions. DNAse treatment was performed using the RNA-free DNase set (QIAGEN, Maryland) following the manufacturer's instructions. cDNAs were obtained from 1 μg of total DNase-treated RNA in a 20 μl reaction containing 200 units of Super-Script III Reverse Transcriptase (Invitrogen) and 50 pmol oligo $(dT)_{20}$ (Invitrogen), according to the manufacturer's instructions.

Identification of **GRX** *genes in* **R. irregularis** *and sequences analyses*

Amino acid sequences of *S. cerevisiae* GRXs were retrieved from the freely accessible *S. cerevisiae* genome database (http://www.yeastgenome.org/) and used to search for orthologous sequences in the filtered model dataset of *R. irregularis* on the JGI website (http://genome.jgi.doe.gov/Gloin1/Gloin1.home.html; Tisserant et al., 2012, 2013) using Basic Local Alignment Search Tool (BLAST) algorithm (Altschul et al., 1990) via a protein BLAST. A second search was performed via a keyword search directly.

Predictions of putative transmembrane domains were made using the TMHMM Server v.2.0 (http://www.cbs.dtu.dk/services/TMHMM/) and SMART software (http://smart.embl-heidelberg.de/). Predictions of subcellular localizations were made using the TargetP 1.1 Server (http://www.cbs.dtu.dk/services/TargetP/), PSORTII (http://psort.hgc.jp/form2.html) and WoLF PSORT (http://wolfpsort.org/).

Full-length amino acid sequences were aligned with the orthologous sequences of a number of fungi representatives of distinct taxonomic groups by ClustalW (Version 2.1 (Larkin et al., 2007);

http://www.ebi.ac.uk/Tools/msa/clustalw2/). Alignments were imported into the Molecular Evolutionary Genetics Analysis (MEGA) package version 6 (Tamura et al., 2013). Phylogenetic analyses were conducted by the neighbour-joining (NJ) method, implemented in MEGA, with a pair-wise deletion of gaps and the Poisson model for distance calculation. Bootstrap analyses were carried out with 1000 replicates. The evolutionary tree was drawn to scale. Weblogo was used to generate the sequence logos of GSH binding site and active site motifs (http://weblogo.berkeley.edu/) (Crooks et al., 2004; Benyamina et al., 2013).

Gene isolation

The full-length cDNAs of *RiGRX4*, *RiGRX5* and *RiGRX6* were obtained by PCR amplification of *R. irregularis* cDNA obtained from ERM growing in control plates, using the primer pairs Grx4.fF and Grx4.fR, Grx5.fF and Grx5.fR and Grx7.fF and Grx7.fR, respectively. Sequences of the primers used are listed in Supplementary Table 1. *RiGRX4* and *RiGRX5* PCR products were cloned in the pCR2.1 vector (Invitrogen, Carlsbad, CA, USA) and *RiGRX6* in the pGEM-T Easy vector (Promega, Madison, USA).

All plasmids were amplified by transformation of E. coli following standard procedures and purified by using the Qiagen Miniprep Kit (Qiagen, Maryland, USA). All sequences and constructs were checked by sequencing before further use. Nucleotide sequences were determined by Taq polymerase cycle sequencing by using an automated DNA sequencer (ABI Prism 3130xl Genetic Analyzer, Applied Biosystems, Carlsbad, USA).

Heterologous expression and growth assays

For heterologous RiGRXs expression analyses, the full length cDNAs were cloned into the yeast expression vector pFL61 (Minet et al., 1992). To obtain pFL61-*RiGRX4*, pFL61-*RiGRX5* and pFL61-*RiGRX6*, the respective full-length cDNAs were isolated from the pCR2.1 or pGEM-T easy vector by *Not*I digestion and ligated into the *Not*I-digested pFL61 vector. The full length cDNAs of *ScGrx3*, *ScGrx4* and *ScGrx5* were also cloned into pFL61 and used as positive controls in the complementation analyses of the *Δgrx3Δgrx4* and *Δgrx5* strains.

The *S. cerevisiae* mutant strains *Δgrx3Δgrx4*, *Δgrx5* and *Δgrx6Δgrx7* were transformed with the constructs pFL61-*RiGRX4*, pFL61-*RiGRX5*, pFL61-*RiGRX6*, the empty vector (negative control), or the corresponding positive controls using a lithium acetate-based method (Schiestl and Gietz, 1989). Yeast transformants were selected on SD medium by autotrophy to uracil.

For oxidant sensitivity determination, cells from exponentially growing cultures of the transformed yeast strains were 1:10 serial diluted and spotted onto SD plates containing or not the oxidizing agents. Lysine auxotrophy assessment of the transformed *Δgrx5* strains was assayed on SD medium with or without lysine.

To test sensitivity to $CaCl_2$ of the transformed *Δgrx6Δgrx7* strains, cells grown in SD medium to exponential phase (OD_{600} = 0.6-0.8) were harvested, washed twice and resuspended in the same volume of a SD modified medium (0.2% YNB w/o amino acids and ammonium sulphate (Difco) with 76 mM NH_4Cl_2 as nitrogen source (Demaegd et al., 2013)) supplemented or not with 500 mM $CaCl_2$. Growth of the treated and untreated cells was recorded (OD_{600}) at 1 –h intervals until the stationary phase was reached. The ratio of growth values between treated and untreated cells after different periods of time was calculated and then made relative to the same ratio in the positive control (*Δgrx6Δgrx7* transformed with the *S. cerevisiae Grx6*).

Measurement of iron concentration

The *Δgrx3Δgrx4* and *Δgrx5* yeast strains transformed with either the empty vector, pFL61-*RiGRX4*, pFL61-*RiGRX5*, pFL61-*RiGRX6* or their respective positive control construct were grown in 50 ml of SD media overnight at 30 °C. Each yeast culture was washed twice, resuspended in YPD medium, diluted into 300 ml of YPD medium (OD_{600}≈0.2-0.3) and grown until an OD_{600} of 1.0 was reached. Cells were collected by centrifugation, washed with 50 mM Tris pH 7.5, resuspended in 50 mM Tris pH 7.5 containing 0.15 M NaCl and disrupted with glass beads for 10 min at 4 °C. Cell homogenates were centrifuged (7000 rpm, 4 °C, 5 min) and the supernatants used as cell extracts.

The intracellular iron content was examined with a QuantiChrom™ iron assay kit (BioAssay Systems, Hayward, CA) following the manufacturer´s instructions.

Enzyme assays

Cell extracts of the *Δgrx5* strain transformed with pFL61-*RiGRX4*, pFL61-*RiGRX5*, pFL61-*ScGrx5* or the empty vector were prepared in 0.1 M Tris pH 8.1, 2 mM EDTA and 1mM PMSF using glass beads to disrupt the cells.

Malate dehydrogenase activity was measured by following the consumption of NADH ($\varepsilon = 6.22\ mM^{-1}\ cm^{-1}$) spectrophotometrically at 340 nm (Kispal et al., 1997). Aconitase activity was assessed by measuring the absorption of converted NADPH ($\varepsilon = 6.22\ mM^{-1}\ cm^{-1}$) at 340 nm (Drapier and Hibbs Jr, 1996).

Protein content was determined by the Bio-Rad Protein Assay, using BSA as standard.

Protein localization analyses

Localization of the *R. irregularis* GRX4, GRX5 and GRX6 proteins in *S. cerevisiae* was performed with C-terminal fusions of the respective genes to the enhanced green fluorescent protein (GFP) gene in the *Δgrx3Δgrx4* or *Δgrx6Δgrx7* strains. Gene-specific primer pairs containing *Sfi*IA (GGCCATTACGGCC) and *Sfi*IB (GGCCGAGGCGGCC) overhangs (S1 Table) were used to clone the three glutaredoxin cDNAs into the *Sfi*I sites of the plasmid pBL106, a pDR196sfi vector derivative carrying *GFP* (Ellerbeck et al., 2013). The resulting plasmids pBL106-*RiGRX4* and pBL106-*RiGRX5* were used to transform the *Δgrx3Δgrx4* strain and pBL106-*RiGRX6* to transform the *Δgrx6Δgrx7* strain. Both strains were also transformed with the pBL106 empty vector. Cells were grown in CSM liquid culture to mid-logarithmic phase (OD_{600}≈0.6-0.7), washed twice and resuspended in water for direct visualization. For labeling of yeast mitochondria, MitoTracker® Red CM-H_2XRos (Molecular Probes) was added to 1 ml of a mid-logarithmic phase suspension of the *RiGRX6-GFP*-expressing *Δgrx6Δgrx7* cells (final concentration: 200 nM). Labeling was performed for 1 hour at 30 °C without

subsequent washing of cells before visualization. The fluorescence signal was visualized with a Nikon Eclipse 50i fluorescent microscope. A 510-560 nm filter was used for MitoTracker® Red CM-H_2XRos fluorescence, and GFP fusion proteins were imaged using a 450-490 nm filter. Image sets were processed and overlapped using Adobe Photoshop™.

Gene expression analyses

RiGRXs gene expression was studied by real-time RT-PCR using an iQTM5 Multicolor Real-Time PCR Detection System (Bio-Rad). Each 20 µl reaction contained 1 µl of a 1:10 dilution of the cDNA, 200 nM each primer, 10 µl of iQTM SYBR Green Supermix 2x (Bio-Rad). The PCR program consisted in a 3 min incubation at 95 °C, followed by 36 cycles of 30 s at 95 °C, 30 s at 58 °C and 30 s at 72 °C, where the fluorescence signal was measured. The specificity of the PCR amplification procedure was checked with a heat-dissociation protocol (from 58 to 95 °C) after the final cycle of the PCR. The primer sets used were GintGRXfw2 and GintGRXrev2 for *RiGRX1*; RiGrx4.qF and RiGrx4.qR for *RiGRX4*; RiGrx5.qF and RiGrx5.qR for *RiGRX5* and RiGrx7.qF and RiGrx7.qR for *RiGRX6* (S1 Table). The efficiency of the different primer sets was evaluated by performing real-time PCR on several dilutions of cDNA. Because RNA extracted from mycorrhizal roots contains plant and fungal RNAs, specificity of the primer pairs was also analyzed by PCR amplification of genomic DNA isolated from non-mycorrizal carrot roots and rice leaves and of cDNA from non-colonized carrot and rice roots. The results obtained for the different treatments were standardized to the elongation factor 1-alpha gene levels (GenBank Accession No. DQ282611), which were amplified with the primers GintEFfw and GintEFrev. RT-PCR determinations were performed on at three independent biological samples from three replicate experiments. Real-time PCR experiments were carried out three times for each biological sample, with the threshold cycle (Ct) determined in triplicate. The relative levels of transcription were calculated by using the $2^{-\Delta\Delta CT}$ method (Schmittgen and Livak, 2008), and the standard error was computed from the average of the ΔCT values for each biological sample.

Statistical analyses

Statgraphics Centurion XVI software was used for the statistical analysis of the means and standard deviation determinations. ANOVA, followed by a Fisher's LSD test ($p<0.05$) when possible, was used for the comparison of the treatments based on at least 3 biological replicates for each treatment ($n \geq 3$).

Results

Identification of three new members of the GRX family in R. irregularis

A search for putative GRX genes in the *R. irregularis* genome led to the identification of five genes encoding proteins displaying significant sequence similarity to glutaredoxins, which were named according to their orthologous in *S. cerevisiae*: *RiGRX1* (GenBank Accession No. B7ZFT1; JGI ID 350295, formerly named *GintGRX1* in Benabdellah et al. (2009*b*)), *RiGRX4* (GenBank Accession No. ESA11920; JGI ID 347595), *RiGRX5* (GenBank Accession No. ESA01501; JGI ID 337939), *RiGRX6* (GenBank Accession No. ESA04895; JGI ID 350273) and a hypothetical protein containing a GRX-like domain but whose overall sequence was closer to thioredoxins than to glutaredoxins (GenBank Accession No. ESA18464; JGI ID 344567).

The length of the nucleotide coding sequences of the four *RiGRX* genes ranged from 306 to 1002 bp. The coding exon sequences for the *RiGRX* genes were confirmed by cDNA sequencing. The number of introns in the individual *RiGRXs*, taken from the *R. irregularis* JGI database and confirmed by the comparison between the genomic sequences from JGI and the isolated coding sequences, varies from 2 to 7, and with the exception of the fourth intron of RiGRX4 which contains a non-canonical GC/AG splicing sequence, all of them were flanked by the characteristic splicing sequences GT and AG at the 5′ and 3′ ends, respectively (S1 Fig.).

RiGRX1 contains the CPYC active site typical of classical dithiol GRXs and, as previously reported by Benabdellah et al. (2009*b*) exhibits glutathione-disulfide oxidoreductase activity *in vitro*, while RiGRX4 and RiGRX5 possess the CGFS typical domain of classical monothiol GRXs (Fig. 1A). RiGRX4 is a protein of 333 amino acids that consists of one thioredoxin domain followed by two monothiol GRX domains. RiGRX4 displays higher similarity to its vertebrate homologues, also containing two GRX domains (50% identity), than to yeast Grx3 (35% identity) and Grx4 (37% identity), with one GRX domain each. RiGRX5 (167 amino acids) has a single monothiol GRX domain and is more closely related to its *Cryptococcus neoformans* homolog (49% identity) than to *S. cerevisiae* Grx5 (37% identity). RiGRX4 is predicted to be cytosolic and RiGRX5 mitochondrial. RiGRX6 encodes a protein of 273 amino acids that contains a CPYS motif at the active site, an N terminal domain of unknown function composed of 150 amino acids and a putative transmembrane domain close to the N-terminus. RiGRX6 shows the highest homology to its *Laccaria bicolor* homolog (44% identity) and is predicted to be in the secretory pathway. The *S. cerevisiae* homologs are ScGrx6 and ScGrx7, which are integral components of endoplasmic reticulum/Golgi membranes sharing sequence homology with dithiol GRXs but containing a single Cys residue at the active site.

A phylogenetic analysis of fungal GRXs revealed that RiGRX1 and RiGRX6 belong to class I GRXs and RiGRX4 and RiGRX5 to class II (Couturier et al., 2009). RiGRX1 clustered with the classical dithiol isoforms (GRX1 group) while RiGRX6 clustered with the Grx6 homologs. The GRX6 group is formed by proteins with C(P/S)(Y/H)S active-site sequences and splits in two subgroups, one clustering all the Ascomycota sequences except the *S. pombe* homolog (SpGrx3p) and the other clade grouping the Basidiomycota, Mucoromycotina and Glomeromycota homologs (Fig. 1B).

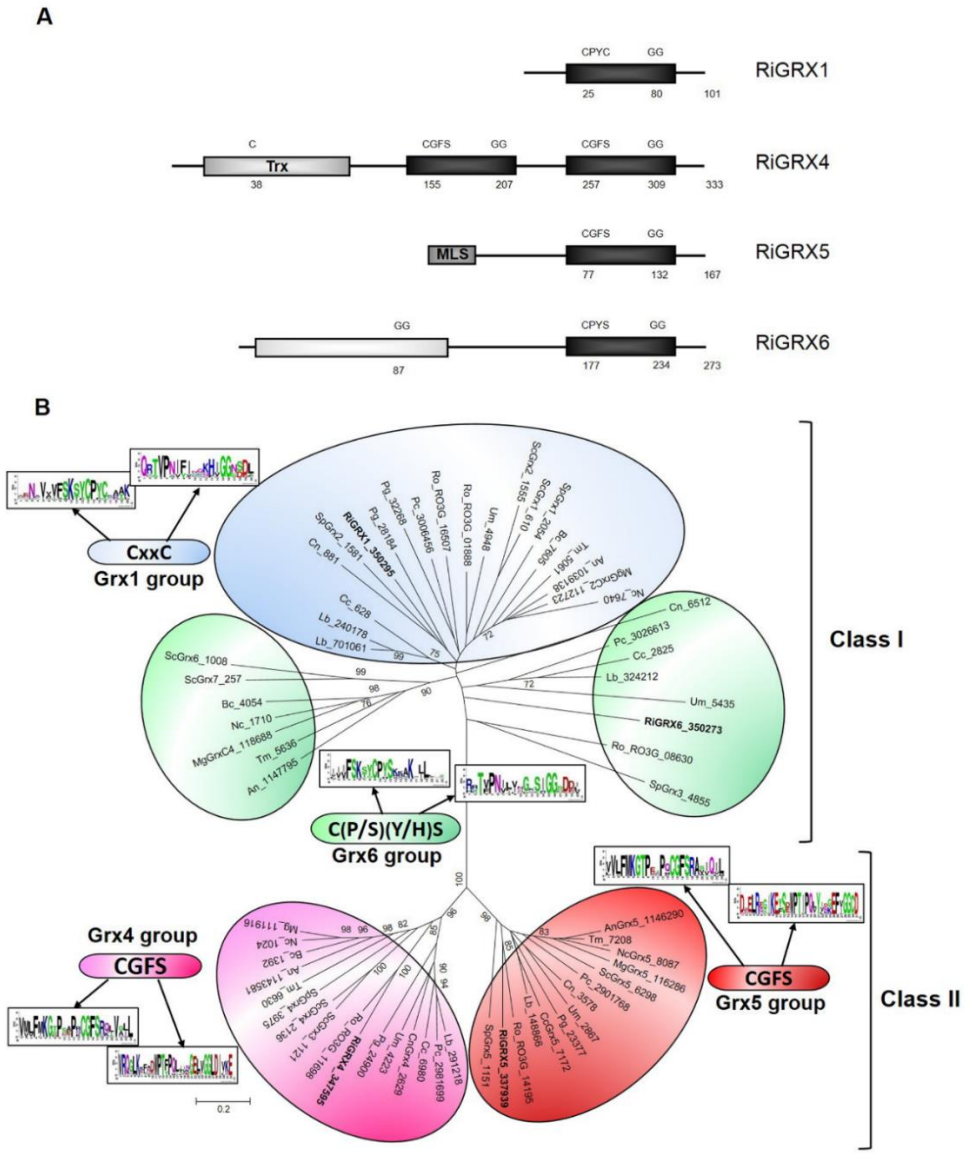

Figure 1. A. Domain organization of the *Rhizophagus irregularis* GRXs. Glutaredoxin domains are represented by black boxes. The thioredoxin-like (Trx) domain of RiGRX4, the mitochondrial location signal (MLS) of RiGRX5 and the domain of unknown function of RiGRX6 (white box) are also indicated. Numbers correspond to the position of the first cysteine in the active site in the GRX domains, the first glycine of the glutathione binding domains and the total length of the proteins. The position of the cysteine in the Trx domain of RiGRX4 is also indicated. **B. Unrooted Nieghbor-Joining tree of the GRX family in fungi.** Organisms: An, *Aspergillus niger*; Bc, *Botrytis cinerea*; Cc, *Coprinopsis cinerea*; Cn, *Cryptococcus neoformans*; Lb, *Laccaria bicolor*; Mg, *Magnaporthe grisea*; Nc, *Neurospora crassa*; Pc, *Phanerochaete chrysosporium*; Pg, *Puccinia graminis*; Ri, *Rhizophagus irregularis*; Ro, *Rhizopus oryzae*; Sc, *Saccharomyces cerevisiae*;

Sp, *Schizosaccharomyces pombe*; Tm, *Tuber melanosporum*; Um, *Ustilago maydis*. *R. irregularis* GRXs are emphasized in bold. Protein JGI identification numbers are indicated. *R. oryzae* sequences were retrieved from the Broad Institute databases (http://www.broad.mit.edu/annotation/). Bootstrap values above 70 and supporting a node are indicated.

RiGRXs *are differentially expressed in the intraradical and extraradical mycelium*

As a first step to get some insigths into the role of the different *RiGRXs* in *R. irregularis*, quantitative gene expression analysis was performed by real-time RT-PCR on ERM collected from the hyphal compartment of *R. irregularis* monoxenic cultures, on carrot mycorrhizal roots developed in a densely colonized hyphal compartment of the split Petri dishes lacking ERM and on mycorrhizal rice roots developed in pot cultures and devoid of external hyphae. Mycorrhizal colonization level of the carrot and rice roots was 10 and 25%, respectively.

RiGRX1, encoding a dithiol GRX, was the GRX isoform more highly expressed both in the ERM and in the mycorrhizal roots (IRM). Transcript levels of *RiGRX1* were 2- and 2.3-fold higher in the IRM of monoxenically grown carrot roots and of the rice mycorrhizal roots than in the ERM, respectively. Expression levels of *RiGRX6* were also higher in the IRM of carrot (3.2-fold increase) and rice (3.75-fold increase) mycorrhizal roots than in the ERM. No significant differences were observed between the expression levels of *RiGRX4* and *RiGRX5* in both fungal structures (Fig. 2).

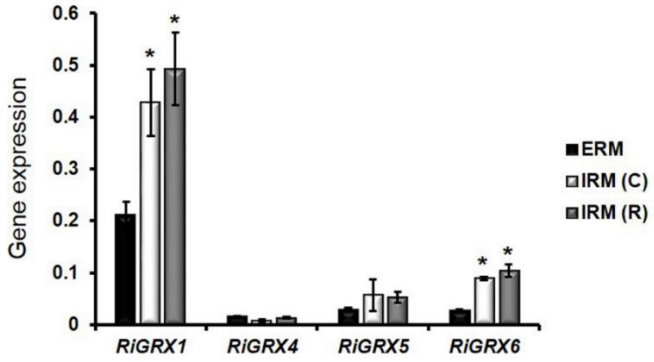

Figure 2. Relative expression of the RiGRX genes in extraradical mycelia (ERM) and intraradical (IRM) mycelia of *Rhizophagus irregularis*. *RiGRX* gene expression was assessed in ERM developed in monoxenic cultures (ERM), *R. irregularis*-colonized carrot roots grown in

monoxenic cultures and lacking ERM (IRM(C)) and *R. irregularis*-colonized rice roots grown in pot cultures and devoid of ERM (IRM(R)). Samples were normalized using the housekeeping gene *RiTEF*. Relative expression levels were calculated by the $2^{-\Delta CT}$ method. Data are means +/- standard error. Asterisks show statistically significant differences ($p<0.05$) relative to the ERM, according to the Fisher's LSD test.

RiGRXs suppress sensitivity of yeast grx *mutants to external oxidants*

Since it is not still possible to genetically manipulate AM fungi, functional analyses of the newly identified *R. irregularis GRX* genes were performed in a heterologous system. For this purpose, the *RiGRX4*, *RiGRX5* and *RiGRX6* full length cDNAs were cloned into the yeast expression vector pFL61 and tested for their ability to suppress the sensitivity of the *Δgrx3Δgrx4*, *Δgrx5* and *Δgrx6Δgrx7* disruption mutants of *S. cerevisiae* to external oxidants. In these experiments, *ScGrx3*, *ScGrx4* (functional homologs of *RiGRX4*), *ScGrx5* (homolog of *RiGRX5*) and *ScGrx6* (functional homolog of *RiGRX6*) were included as positive controls and the empty vector as negative control.

We first assessed whether RiGRX4 and RiGRX5, the two class II GRXs, could restore the inability of the *Δgrx3Δgrx4* double mutant to grow in the presence of hydrogen peroxide (Pujol-Carrion et al., 2006). The *Δgrx3Δgrx4* yeast cells transformed with the empty vector did not grow on SD media supplemented with 1 mM hydrogen peroxide. Although less efficiently than yeast Grx3 and Grx4, expression of either *RiGRX4* or *RiGRX5* in the *Δgrx3Δgrx4* mutant yeast cells suppressed their sensitivity to hydrogen peroxide (Fig. 3A). We also tested whether RiGRX4 and RiGRX5 could complement yeast Grx5 function and suppress the sensitivity of *Δgrx5* cells to menadione (Rodríguez-Manzaneque et al., 2002). Neither the empty vector- nor the *RiGRX4*-transformed *Δgrx5* mutant cells were able to grow on media supplemented with menadione. However, the *RiGRX5*-expressing mutant yeast clearly grew in the presence of menadione (Fig. 3B). Complementation of the two mutant strains by RiGRX5 suggests that in the heterologous system *RiGRX5* is not only expressed in the mitochondria but also in the cytosol. From these data it is concluded that RiGRX4 and RiGRX5 play at least in the heterologous system an *in vivo* role in oxidative stress protection.

Capability of the *R. irregularis* GRX6 to revert sensitivity of the *Δgrx6Δgrx7* deletion mutant of *S. cerevisiae* to hydrogen peroxide was also assessed (Mesecke et al., 2008). While expression of *ScGrx6* (positive control) in the *Δgrx6Δgrx7* mutant complemented its sensitivity to H_2O_2, RiGRX6 was not able to revert the mutant phenotype (data not shown). However, RiGRX6 was able to partially revert the hydrogen peroxide sensitivity of the *Δgrx3Δgrx4* mutant (Fig. 3A), which suggests that the *RiGRX6* gene product has an antioxidant activity and that it should be located in the yeast cytosol.

Since the *S. cerevisiae* Grx6 has recently been shown to be involved in redox regulation of calcium homeostasis in yeast cells (Puigpinós et al., 2015), we determined whether RiGRX6 could revert the increased sensitivity of the *Δgrx6Δgrx7* mutants to excess calcium. As shown in Fig. 3C, the *RiGRX6* expressing cells were slightly less sensitive (29%) to excess calcium than the mutant cells transformed with the empty vector.

Localization of R. irregularis *GRXs in yeast*

In an attempt to further understand the potential functions of RiGRX4, RiGRX5 and RiGRX6, localization of C-terminal GFP-tagged versions of these proteins in yeast was examined by fluorescence microscopy. For these purpose, the different *RiGRX-GFP* fusions were expressed in the *S. cerevisiae* deletion strains for their putative orthologues, except *RiGRX5-GFP* that was expressed in the *Δgrx3Δgrx4* strain due to the low viability of the *Δgrx5* transformants.

The yeast cells expressing RiGRX4-GFP fusion protein showed a general cytosolic fluorescence similar to the fluorescence of control cells expressing the soluble GFP (Fig. 4, A-C), which indicates that RiGRX4 was targeted to the cytoplasm (Fig. 4, D-F). RiGRX5-GFP was detected in the mitochondria, as determined by co-staining with the mitochondria-specific vital dye, MitoTracker® Red (Fig. 4, G-J), although a cytosolic signal was also observed in some cells (data not shown). The yeast cells expressing RiGRX6-GFP exhibited a perinuclear fluorescence pattern indicative of an ER localization (Huh et al., 2003), and an additional cytosolic fluorescence was observed in some cells (Fig. 4, K-M). Detection of RiGRX5 and RiGRX6 in the

yeast cytosol might be due to an overexpression artefact in the heterologous system.

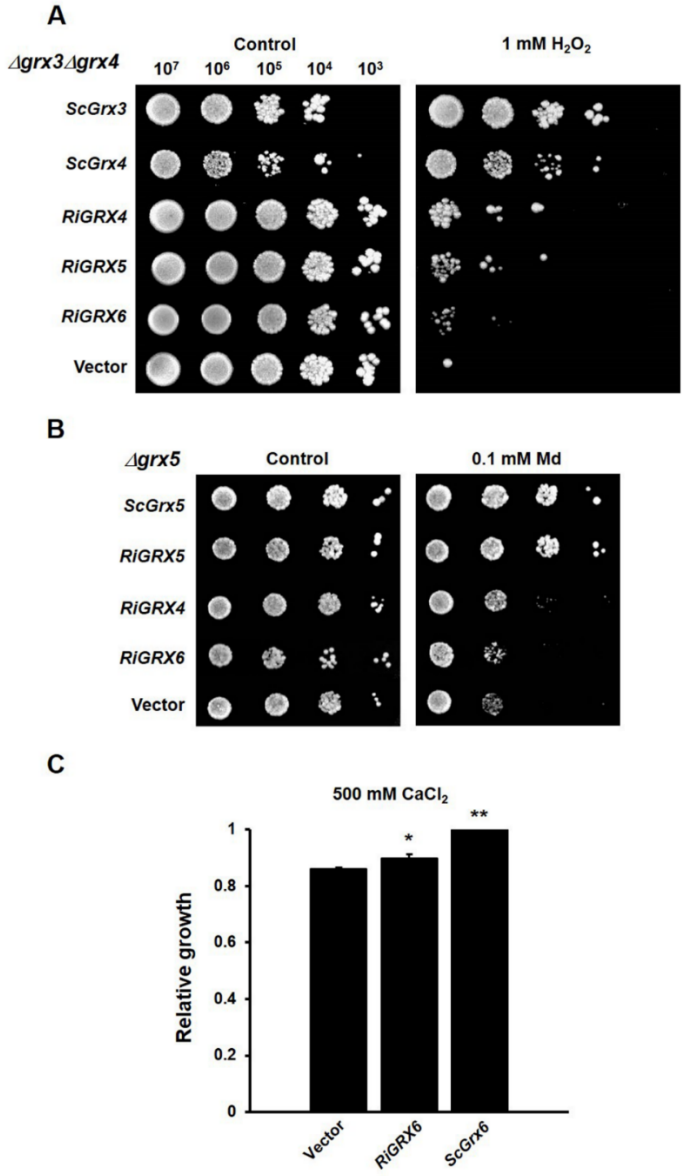

Figure 3. Complementation of the sensitivity to external oxidants of the *grx* yeast mutants by the *Rhizophagus irregularis GRX* genes. A. Effect of *RiGRX4*, *RiGRX5* and *RiGRX6* expression on the sensitivity of the *Δgrx3Δgrx4* strain to 1 mM hydrogen peroxide (H_2O_2). B. Effect of *RiGRX4*, *RiGRX5* and *RiGRX6* expression on the sensitivity of the *Δgrx5* strain to 0.1 mM menadione (Md). The photographs were taken after 3 days of growth at 30 °C. C. Effect of *RiGRX6* expression on the sensitivity of *Δgrx6Δgrx7* to 500 mM $CaCl_2$ (40 h). Data are means of three independent experiments +/- standard error and represent the growth yield ratio between

treated and untreated cultures and then made relative to this ratio in cells expressing the *Saccharomyces cerevisiae Grx6*. Asterisks show statistically significant differences ($p<0.05$) relative to the strain transformed with the empty vector, according to the Fisher's LSD test.

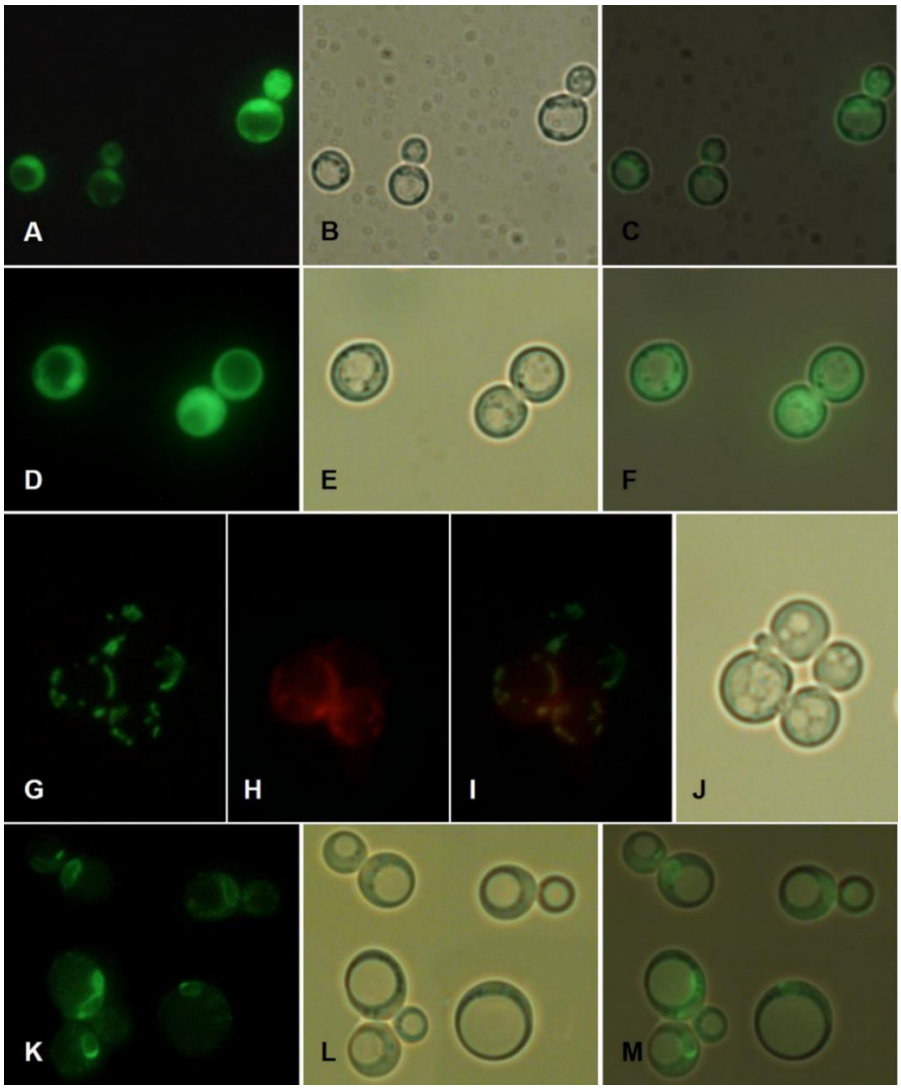

Figure 4. Localization of *Rhizophagus irregularis* GRXs in *Saccharomyces cerevisiae*. Soluble GFP (A-C) and C-terminal GFP-tagged versions of *RiGRX4* (D-F) and *RiGRX5* (G-J) were expressed in the *Δgrx3Δgrx4* cells. C-terminal GFP-tagged version of *RiGRX6* (K-M) was expressed in the *Δgrx6Δgrx7* yeast mutant cells. Cells were grown to mid-logarithmic phase and localization of fusion proteins was visualized by fluorescence microscopy (A, D, G and K). Mitochondria in the *RiGRX6-GFP* expressing cells were stained with MitoTracker® Red and visualized by fluorescence microscopy (H). Bright field (B, E, J and L) and merged (C, F, I and M) images.

RiGRX4 and RiGRX5 play a role in Fe homeostasis in yeast

Glutaredoxins with a CGFS domain in their active site have been shown to play a role in iron homeostasis. In *S. cerevisiae*, the three members of this subfamily participate in the synthesis of the iron-sulfur clusters in mitochondria (Grx5), or in signalling the iron status inside the cell for regulation of iron uptake and intracellular iron relocalization (Grx3 and Grx4). To investigate if the *R. irregularis* CGFS-type GRXs could play a role in iron homeostasis, we first determined the ability of RiGRX4 and RiGRX5, functional homologues of yeast Grx3/Grx4 and Grx5, respectively, to restore yeast Grx5 function. GRX5 deletion mutants fail to grow on lysine deficient media due to the inactivation of the mitochondrial Fe-S containing enzyme homoaconitase, an enzyme involved in lysine synthesis (Rodríguez-Manzaneque et al., 2002; Lill et al., 2012). Expression of *RiGRX5*, but not of *RiGRX4*, clearly restored lysine auxotrophy of the *Δgrx5* cells to the same extent than the *S. cerevisiae Grx5* (Fig. 5A).

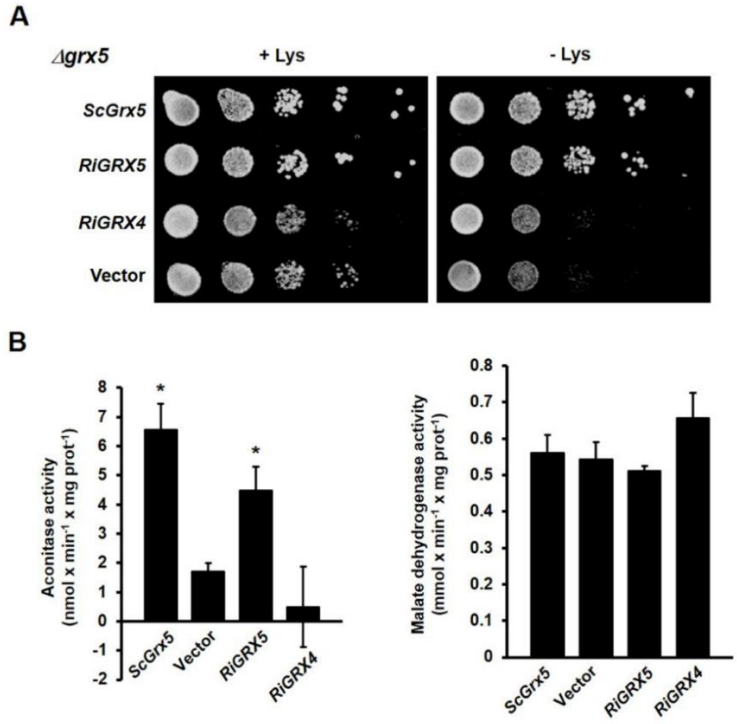

Figure 5. Analysis of the *in vivo* role of RiGRX5 in the biogenesis of Fe-S clusters in yeast. A. *Δgrx5* cells transformed with the empty vector or expressing *ScGrx5*, *RiGRX5* or *RiGRX4* were plated on SD medium with or without lysine. Plates were incubated at 30 °C for 3 days.

B. The activities of a Fe-S protein (aconitase) and a non-Fe-S protein (malate dehydrogenase) were determined in lysates of the *Δgrx5* cells transformed with the different constructs. Data are means +/- standard error. Asterisks show statistically significant differences ($p<0.05$) relative to the activities of the strain transformed with the empty vector, according to the Fisher's LSD test.

As expected, the aconitase activity was also restored in the *RiGRX5*-expressing yeast cells. However, the activity of the non Fe-S enzyme malate dehydrogenase was not affected by the expression of the *R. irregularis* CGFS-type GRXs (Fig. 5B).

Deletion of *Grx5* and *Grx3*/*Grx4* in *S. cerevisiae* also results in an increase of the intracellular Fe levels. In the *Grx5* yeast mutants, increased iron levels are a consequence of the impairment of the biogenesis of Fe-S protein complexes in the absence of the GRX (Rodríguez-Manzaneque et al., 2002). However, in the *Grx3*/*Grx4* mutants iron accumulation is the result of a constitutively activated cellular iron uptake system given that these GRXs play a central role in iron uptake regulation by interacting with the iron-responsive transcription factors Aft1 and Aft2, the major regulators of cellular iron uptake systems in yeast (Ojeda et al., 2006).

To further understand the potential functions of RiGRX4 and RiGRX5, we assayed the intracellular iron content of the *Δgrx3Δgrx4* and *Δgrx5* yeast cells expressing *RiGRX4* or *RiGRX5*. Although less efficiently than *ScGrx4*, the gene products of *RiGRX4* and *RiGRX5* significantly suppressed intracellular iron accumulation of the *Δgrx3Δgrx4* yeast cells (Fig. 6A). The decrease in iron accumulation was higher in the *RiGRX5*- (53% decrease) than in the *RiGRX4*-expressing (34% decrease) *Δgrx3Δgrx4* yeast cells. In the case of the *Δgrx5* strain, iron accumulation was suppressed in the mutant expressing *ScGrx5* and *RiGRX5* but not in the *RiGRX4*-expressing cells (Fig. 6B). All these results indicate that both RiGRX4 and RiGRX5 could have an *in vivo* role on iron homeostasis in *R. irregularis*.

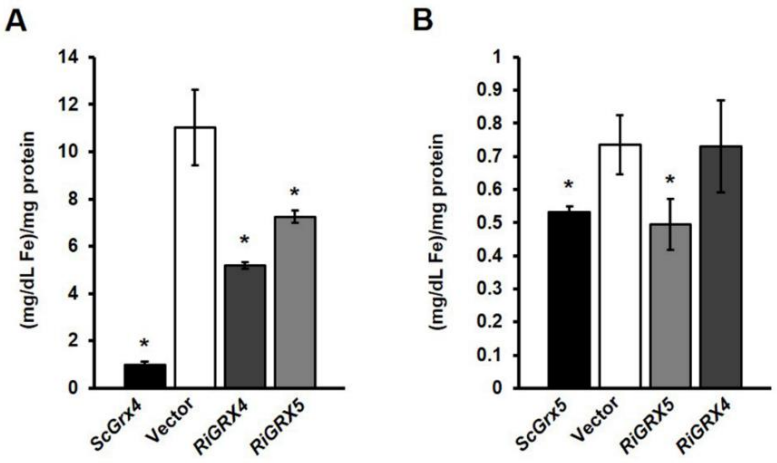

Figure 6. Analysis of the *in vivo* role of RiGRX4 and RiGRX5 in intracellular iron accumulation in *Δgrx3Δgrx4* (A) and *Δgrx5* (B) yeast mutant strains. Intracellular iron concentrations were determined in lysates of cells transformed with the empty vector or expressing *ScGrx4*, *ScGrx5*, *RiGRX4* or *RiGRX5*, with a Quantichron™ Iron Assay Kit. Data are means +/- standard error. Asterisks show statistically significant differences ($p<0.1$) relative to the values of the strain transformed with the empty vector (white columns), according to the Fisher's LSD test.

Regulation of RiGRXs *gene expression by hydrogen peroxide*

To investigate whether the RiGRXs could be involved in the response of *R. irregularis* to an oxidative stress, their gene expression was analyzed by real-time RT-PCR in the ERM that had been exposed for different periods of time to different concentrations of H_2O_2. Gene expression data are referred to the expression levels detected in mycelia from control plates. Expression of *GintPDX1*, a *R. irregularis* gene encoding a protein involved in vitamin B6 biosynthesis that is up-regulated by H_2O_2 (Benabdellah et al., 2009*a*), was also determined as a control of the H_2O_2 treatments. As expected, *GintPDX1* transcript levels increased 1 h after the addition of 1 mM H_2O_2 to the ERM. Up-regulation of *RiGRX1*, *RiGRX4* and *RiGRX5* gene expression was also observed 1 h after exposure of the fungus to 1 mM H_2O_2. However, *RiGRX6* gene expression was not significantly affected by the addition of H_2O_2 at any of the concentrations and time points analyzed (Fig. 7).

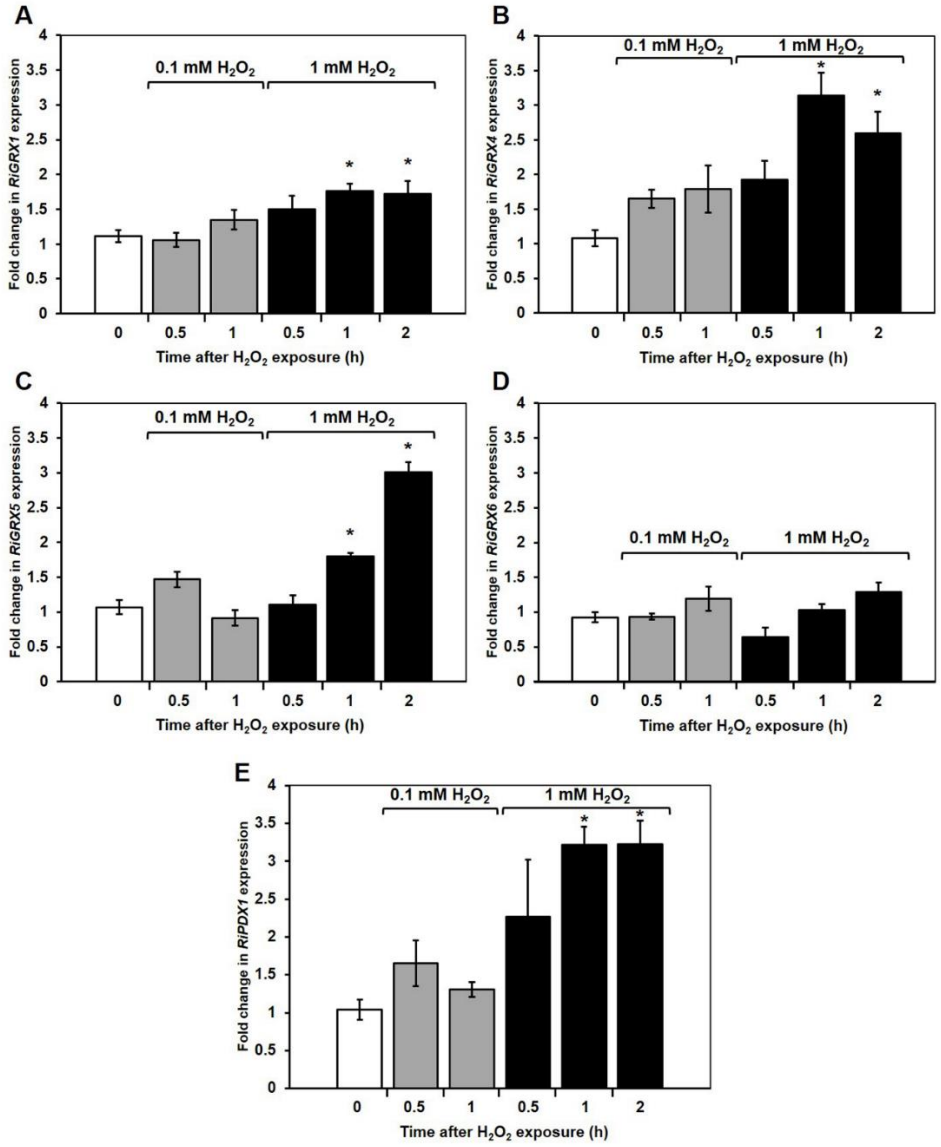

Figure 7. Effect of hydrogen peroxide on the expression of the *Rhizophagus irregularis GRX* genes. *R. irregularis* ERM grown in M-C medium was exposed for different periods of time to 0.1 mM H_2O_2 (grey columns) or 1 mM H_2O_2 (black columns). *RiGRX1* (A), *RiGRX4* (B), *RiGRX5*(C), *RiGRX6* (D) and *GintPDX1* (E) gene expression. Data were normalized using the housekeeping gene *RiTEF*. Relative expression levels were calculated by the $2^{-\Delta\Delta CT}$ method. Data are means +/- standard error. Asterisks show statistically significant differences ($p<0.05$) compared to the control value, according to the Fisher's LSD test.

RiGRX4 *expression is up-regulated by iron*

To assess if the *R. irregularis* GRXs could have an iron-related function, *RiGRXs* transcript levels were analysed in ERM grown in the presence of different iron concentrations (Fig. 8). Relative to the ERM grown in M media containing 0.045 mM Fe, development of the fungus in the presence of 45 mM Fe induced a slight but statistically significant up-regulation of *RiGRX4* gene expression. Transcript levels of *RiGRX1*, *RiGRX5* and *RiGRX6* were not significantly affected by the amount of Fe present in the culture medium.

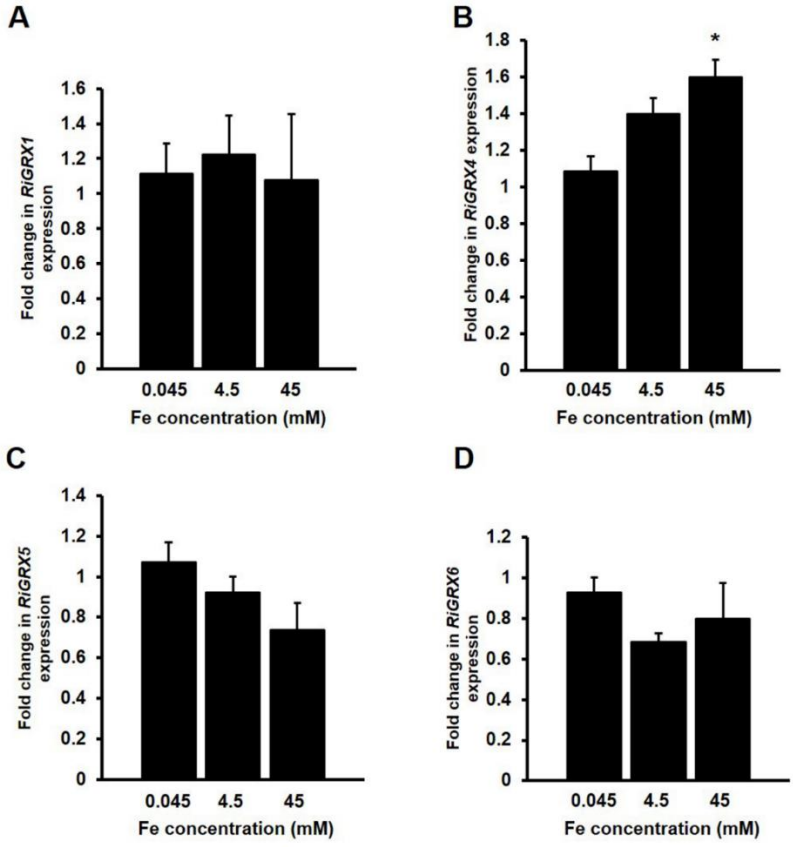

Figure 8. Effect of iron on the expression of the *Rhizophagus irregularis GRX* genes. *R. irregularis* was grown in M-C media containing 0.045 mM Fe (control) or supplemented with 4.5 mM Fe or 45 mM Fe medium for 2 weeks. *RiGRX1* (A), *RiGRX4* (B), *RiGRX5* (C) and *RiGRX6* (D) gene expression. Data were normalized using the housekeeping gene *RiTEF*. Relative expression levels were calculated by the $2^{-\Delta\Delta CT}$ method. Data are means +/- standard error. Asterisks show statistically significant differences ($p<0.05$) compared to the control value, according to the Fisher's LSD test.

Discussion

The GRX family comprises a large group of related enzymes that are ubiquitously present in different compartments of prokaryotic and eukaryotic cells. In this study, by using a wide-genome analysis of GRXs in the AM fungus *R. irregularis*, three new members of this family (RiGRX4, RiGRX5 and RiGRX6) were identified. Characterization of the newly identified genes showed that, in addition to the previously characterized cytosolic dithiol GRX (Benabdellah et al., 2009*b*), *R. irregularis* possesses three functional isoforms with a single cysteine residue in their active sites.

The *R. irregularis* GRXs are localized to different subcellular compartments. RiGRX1 and RiGRX4 were located in the cytosol, while RiGRX5 was targeted to the mitochondria and the cytosol, and RiGRX6 to the secretory pathway and the cytosol. Detection of RiGRX5 and RiGRX6 in the yeast cytosol explains why these proteins complemented the mutant phenotype of the *Δgrx3Δgrx4* strain, although expression of these proteins in the cytosol is most probably due to an artefact of the overexpression in the heterologous system. The *R. irregularis* GRX proteins were shown to suppress the mutant phenotypes of their yeast orthologs, suggesting that the biological function of this group of GRXs is evolutionary conserved. It is remarkable that RiGRX4, the *R. irregularis* GRX having a thioredoxin domain at the N-terminal end, possesses two GRX domains repeated in tandem, as it has been described for mammaliam and human GRX/PICOT proteins (Herrero and de la Torre-Ruiz, 2007; Morel et al., 2008). In contrast, in the rest of the reference fungi analyzed, except in *Rhizopus oryzeae*, these proteins contain only one GRX domain. This structure allows the binding of one or two Fe-S clusters which likely serve as redox sensors in response to redox signals for the GRX function in signal transduction and Fe-S cluster trafficking (Haunhorst et al., 2010; Mapolelo et al., 2013). RiGRX6 clustered with the monothiol class I group but in a separate group to its yeast orthologs and similarly to the characterized *S. pombe* Grx3p has an extra N-terminal region with an unknown role (Moon et al., 2005). While *S. cerevisiae* possesses two cytosolic class II GRXs (Grx3/4), *R. irregularis* has one (GRX4), similarly to *S. pombe* (Chung et al., 2005; Li and Outten, 2013). Class I GRXs come also in pairs in some organisms such as *S.*

cerevisiae, having two CxxC GRXs (Grx1/2) and being the only fungus which has two GRXs belonging to the fungal-specific Grx6/Grx7 subfamily (Morel et al., 2008; Ströher and Millar, 2012). Nevertheless, our study showed that *R. irregularis* possesses only one homolog of each group of GRXs.

The finding that all the RiGRXs were able to supress sensitivity of the yeast GRX deletion mutants to external oxidants indicates that, at least in the heterologous system, these proteins play an *in vivo* role in oxidative stress protection. Up-regulation of *RiGRX1*, *RiGRX4* and *RiGRX5* gene expression in the *R. irregularis* ERM by H_2O_2 supports the hypothesis that these proteins are involved in the regulation of fungal redox processes. Oxidative stress broadly impact cells, initiating a series of redox-dependent modifications of proteins, lipids and nucleic acids. With respect to proteins, the thiol group of the cysteine residues is a major target of ROS. Reversible post-translational modifications of cysteine, such as glutathionylation, regulate protein activity and protect the thiol group during oxidative stress from irreversible oxidation. Although class II GRXs do not display *in vitro* deglutathionylation activity (Ströher and Millar, 2012), the *S. cerevisiae* Grx5 was shown to deglutathionylate proteins *in vivo* (Shenton et al., 2002). Given that RiGRX1 was shown to perform a deglutathionylation reaction (Benabdellah et al., 2009*b*) and that function of the different types of GRXs is conserved through evolution (Ströher and Millar, 2012), our data suggest a role for RiGRX1 and RiGRX5 in regulating the glutathionylation of thiols of cytosolic and mitochondrial target proteins, respectively, to protect the fungus from the oxidative stress induced by H_2O_2. However, given that multidomain GRXs do not seem to be involved in the reduction of oxidized proteins, that yeast Grx3 and Grx4 regulate actin cytoskeleton dynamics (Pujol-Carrion and De La Torre-Ruiz, 2010) and that actin is a known target for oxidation (Farah and Amberg, 2007), it is tempting to hypothesize that RiGRX4 might be involved in the protection of the redox integrity of the actin cytoskeleton. On the other hand, the observation that RiGRX6 partially reverts the increased sensitivity of the *Δgrx6Δgrx7* mutants to excess calcium suggests that, similarly to ScGrx6, RiGRX6 might modulate intracellular calcium homeostasis in *R. irregularis*. However, further investigations are needed to confirm these hypotheses.

The ability of RiGRX4 and RiGRX5 to partially suppress iron accumulation in the *Δgrx3Δgrx4* mutant yeast and of RiGRX5 to restore the activity of the Fe-S containing protein aconitase and to suppress iron accumulation in *Δgrx5* yeast cells suggest that both proteins may be required for the biogenesis of Fe-S clusters and/or are involved in the regulation of iron homeostasis, as it has been shown for the majority of class II GRXs analysed to date (Couturier et al., 2015). Since sensitivity of the *Δgrx3Δgrx4* and *Δgrx5* cells to oxidizing agents is due to the iron-generated oxygen radicals via Fenton reaction (Rodríguez-Manzaneque et al., 2002; Pujol-Carrion et al., 2006) and since RiGRX4 and RiGRX5 reduced iron accumulation in the mutant yeasts, it is also possible that GRX4 and GRX5 protect the fungus from the oxidative damage induced by H_2O_2 by modulating iron homeostasis to control iron-generated oxygen radicals.

Gene expression data indicated that *RiGRX4* was the only *R. irregularis* GRX gene responsive to iron. In other fungi, class II or monothiol multidomain GRXs (Grx3/4) have been shown to be involved in iron uptake by interacting with iron-responsive transcription factors. In yeast under high-iron conditions, ScGrx3 and ScGrx4 interact with the transcription factors Aft1 and Aft2, excluding them from the nucleus and preventing the activation of several genes encoding proteins involved in iron uptake and distribution. Although no functional homologs of Aft1 and Aft2 have been found in the *R. irregularis* genome, a homologous sequence to the *S. pombe* iron-regulated transcription factor Fep1, which responds to high levels of iron as a negative regulator of the expression of several genes involved in iron acquisition (Labbé et al., 2013), was found. These observations suggest that the mechanisms of transcriptional regulation of iron metabolism in *R. irregularis* might be more similar to those operating in *S. pombe* and ascomycete fungi than to *S. cerevisiae* and that up-regulation of *RiGRX4* gene expression under high Fe conditions might be involved in down-regulation of the high affinity Fe uptake systems.

RiGRX4 and *RiGRX5* were found to be expressed at similar levels in the IRM and ERM. These data indicate that their encoded proteins might be required for maintaining the basal oxidative and iron metabolism of *R. irregularis*. The higher expression levels of *RiGRX1* and *RiGRX6* in the IRM

suggests that their encoded proteins might play a role in the establishment of the symbiosis, as it has been shown for the class I or dithiol SmGRX1 and class II or monothiol SmGRX2 of *Sinorhizobium meliloti* (Benyamina et al., 2013). Since RiGRX1 is a multifunctional protein that displays thiol oxidoreductase, peroxidase and glutathione-S-transferase activities (Benabdellah et al., 2009*b*), this protein should play a key role in oxidative stress protection of *R. irregularis* during its *in planta* phase, particularly through protein deglutathionylation. On the other hand, since fungal GRX6 type proteins have been proposed to be involved in redox regulation of calcium homeostasis (Puigpinós et al., 2015), it is tempting to hypothesize that RiGRX6 activity might be involved in redox regulation of the *R. irregularis* calcium pumps and transporters that have been reported to be up-regulated during mycorrhiza development (Liu et al., 2013). Unfortunately, the lack of standardized protocols for the genetic transformation in AM fungi precluded us from determining the precise *in vivo* roles of the *R. irregularis* GRXs.

In conclusion, this study shows that the AM fungus *R. irregularis* has four GRX members in its genome, and that the three monothiol GRXs identified might play a role in protection against ROS, as it was previously shown for RiGRX1. Furthermore, RiGRX4 and RiGRX5 might be involved in the regulation of iron metabolism. However, further analyses are necessary to determine the targets of RiGRXs and to fully understand the specific roles of the different GRX isoforms in *R. irregularis*.

References

Altschul SF, Gish W, Miller W, Myers EW, Lipman DJ. 1990. Basic local alignment search tool. Journal of Molecular Biology 215, 403–410. doi: 10.1016/S0022-2836(05)80360-2

Arthikala MK, Montiel J, Nava N, Santana O, Sánchez-López R, Cárdenas L, Quinto C. 2013. *PvRbohB* negatively regulates *Rhizophagus irregularis* colonization in *Phaseolus vulgaris*. Plant and Cell Physiology 54, 1391–1402. doi: 10.1093/pcp/pct089

Arthikala MK, Sánchez-López R, Nava N, Santana O, Cárdenas L, Quinto C. 2014. *RbohB*, a *Phaseolus vulgaris* NADPH oxidase gene, enhances symbiosome number, bacteroid size, and nitrogen fixation in nodules and impairs

mycorrhizal colonization. New Phytologist 202, 886–900. doi: 10.1111/nph.12714

Bandyopadhyay S, Chandramouli K, Johnson MK. 2008. Iron-sulfur cluster biosynthesis. Biochemical Society Transactions 36, 1112–1119. doi: 10.1042/BST0361112

Barea JM, Pozo MJ, López-Ráez JA, Aroca R, Ruíz-Lozano JM, Ferrol N, Azcón R, Azcón-Aguilar C. 2013. Arbuscular mycorrhizas and their significance in promoting soil-plant system sustainability against environmental stresses. In: Rodelas González MB, González-López J, editors. Beneficial plant-microbial interactions: ecology and applications. CR, USA: CRC Press. pp. 353–387.

Belmondo S, Calcagno C, Genre A, Puppo A, Pauly N, Lanfranco L. 2016. The *Medicago truncatula MtRbohE* gene is activated in arbusculated cells and is involved in root cortex colonization. Planta 243, 251–262. doi: 10.1007/s00425-015-2407-0

Benabdellah K, Azcón-Aguilar C, Valderas A, Speziga D, Fitzpatrick TB, Ferrol N. 2009*a*. *GintPDX1* encodes a protein involved in vitamin B6 biosynthesis that is up-regulated by oxidative stress in the arbuscular mycorrhizal fungus *Glomus intraradices*. New Phytologist 184, 682–693. doi: 10.1111/j.1469-8137.2009.02978.x

Benabdellah K, Merlos MÁ, Azcón-Aguilar C, Ferrol N. 2009*b*. *GintGRX1*, the first characterized glomeromycotan glutaredoxin, is a multifunctional enzyme that responds to oxidative stress. Fungal Genetics and Biology 46, 94–103. doi: 10.1016/j.fgb.2008.09.013

Benyamina SM, Baldacci-Cresp F, Couturier J, et al. 2013. Two *Sinorhizobium meliloti* glutaredoxins regulate iron metabolism and symbiotic bacteroid differentiation. Environmental Microbiology 15, 795–810. doi: 10.1111/j.1462-2920.2012.02835.x

Bonfante P, Genre A. 2015. Arbuscular mycorrhizal dialogues: do you speak `plantish´ or `fungish´? Trends in Plant Science 20, 150–154. doi: 10.1016/j.tplants.2014.12.002

Bucher M, Hause B, Krajinski F, Küster H. 2014. Through the doors of perception to function in arbuscular mycorrhizal symbioses. New Phytologist 204, 833–840. doi: 10.1111/nph.12862

Chabot S, Bécard G, Piché Y. 1992. Life cycle of *Glomus intraradix* in root organ culture. Mycologia 84, 315–321. doi: 10.2307/3760183

Chung W-H, Kim K-D, Roe J-H. 2005. Localization and function of three monothiol glutaredoxins in *Schizosaccharomyces pombe*. Biochemical and Biophysical Research Communications 330, 604–610. doi: 10.1016/j.bbrc.2005.02.183

Couturier J, Jacquot J-P, Rouhier N. 2009. Evolution and diversity of glutaredoxins in photosynthetic organisms. Cellular and Molecular Life Sciences 66, 2539–2557. doi: 10.1007/s00018-009-0054-y

Couturier J, Przybyla-Toscano J, Roret T, Didierjean C, Rouhier N. 2015. The roles of glutaredoxins ligating Fe–S clusters: Sensing, transfer or repair functions? Biochimica et Biophysica Acta 1853, 1513–1527. doi: 10.1016/j.bbamcr.2014.09.018

Crooks GE, Hon G, Chandonia J-M, Brenner SE. 2004. WebLogo: a sequence logo generator. Genome Research 14, 1188–1190. doi: 10.1101/gr.849004.1

Demaegd D, Foulquier F, Colinet A-S, Gremillon L, Legrand D, Mariot P, Peiter E, Van Schaftingen E, Matthijs G, Morsomme P. 2013. Newly characterized Golgi-localized family of proteins is involved in calcium and pH homeostasis in yeast and human cells. Proceedings of the National Academy of Sciences 110, 6859–6864. doi: 10.1073/pnas.1219871110

Drapier JC, Hibbs JB Jr. 1996. Aconitases: a class of metalloproteins highly sensitive to nitric oxide synthesis. Methods in Enzymology 296, 26–36. doi: 10.1016/S0076-6879(96)69006-5

Ellerbeck M, Schüßler A, Brucker D, Dafinger C, Loos F, Brachmann A. 2013. Characterization of three ammonium transporters of the Glomeromycotan fungus *Geosiphon pyriformis*. Eukaryot Cell 12, 1554–1562. doi: 10.1128/EC.00139-13

Farah ME, Amberg DC. 2007. Conserved actin cysteine residues are oxidative stress sensors that can regulate cell death in yeast. Molecular Biology of the Cell 18, 1359–1365. doi: 10.1091/mbc.E06–08–0718

Fester T, Hause G. 2005. Accumulation of reactive oxygen species in arbuscular mycorrhizal roots. Mycorrhiza 15, 373–379. doi: 10.1007/s00572-005-0363-4

Foyer CH, Noctor G. 2005. Redox homeostasis and antioxidant signaling: a metabolic interface between stress perception and physiological responses. The Plant Cell 17, 1866–1875. doi: 10.1105/tpc.105.033589

Gallego C, Garí E, Colomina N, Herrero E, Aldea M. 1997. The Cln3 cyclin is down-regulated by translational repression and degradation during the G_1 arrest caused by nitrogen deprivation in budding yeast. The EMBO Journal 16, 7196–7206. doi: 10.1093/emboj/16.23.7196

García-Rodríguez S, Azcón-Aguilar C, Ferrol N. 2007. Transcriptional regulation of host enzymes involved in the cleavage of sucrose during arbuscular mycorrhizal symbiosis. Physiologia Plantarum 129, 737–746. doi: 10.1111/j.1399-3054.2007.00873.x

Giovannetti M, Mosse B. 1980. An evaluation of techniques for measuring vesicular arbuscular mycorrhizal infection in roots. New Phytologist 84, 489–500. doi: 10.1111/j.1469-8137.1980.tb04556.x

González-Guerrero M, Oger E, Benabdellah K, Azcón-Aguilar C, Lanfranco L, Ferrol N. 2010. Characterization of a CuZn superoxide dismutase gene in the arbuscular mycorrhizal fungus *Glomus intraradices*. Current Genetics 56, 265–274. doi: 10.1007/s00294-010-0298-y

Gutjahr C, Paszkowski U. 2013. Multiple control levels of root system remodeling in arbuscular mycorrhizal symbiosis. Frontiers in Plant Science 4, 204. doi: 10.3389/fpls.2013.00204

Haunhorst P, Berndt C, Eitner S, Godoy JR, Lillig CH. 2010. Characterization of the human monothiol glutaredoxin 3 (PICOT) as iron-sulfur protein. Biochemical and Biophysical Research Communications 394, 372–376. doi: 10.1016/j.bbrc.2010.03.016

Herrero E, Bellí G, Casas C. 2010. Structural and functional diversity of glutaredoxins in yeast. Current Protein and Peptide Science 11, 659–668. doi: 10.2174/138920310794557637

Herrero E, de la Torre-Ruiz MA. 2007. Monothiol glutaredoxins: a common domain for multiple functions. Cellular and Molecular Life Sciences 64, 1518–1530. doi: 10.1007/s00018-007-6554-8

Huh W-K, Falvo JV, Gerke LC, Carroll AS, Howson RW, Weissman JS, O'Shea EK. 2003. Global analysis of protein localization in budding yeast. Nature. 425, 686–691. doi: 10.1038/nature02026

Izquierdo A, Casas C, Mühlenhoff U, Lillig CH, Herrero E. 2008. *Saccharomyces cerevisiae* Grx6 and Grx7 are monothiol glutaredoxins associated with the early secretory pathway. Eukaryot Cell 7, 1415–1426. doi: 10.1128/EC.00133-08

Jung SC, Martinez-Medina A, Lopez-Raez JA, Pozo MJ. 2012. Mycorrhiza-Induced Resistance and Priming of Plant Defenses. Journal of Chemical Ecology 38, 651–664. doi: 10.1007/s10886-012-0134-6

Kiirika LM, Bergmann HF, Schikowsky C, Wimmer D, Korte J, Schmitz U, Niehaus K, Colditz F. 2012. Silencing of the Rac1 GTPase *MtROP9* in *Medicago truncatula* stimulates early mycorrhizal and oomycete root colonizations but negatively affects rhizobial infection. Plant Physiology 159, 501–516. doi: 10.1104/pp.112.193706

Kispal G, Csere P, Guiard B, Lill R. 1997. The ABC transport Atm1p is required for mitochondrial iron homeostasis. FEBS Letters 418, 346–350. doi: 10.1016/S0014-5793(97)01414-2

Kloppholz S, Kuhn H, Requena N. 2011. A secreted fungal effector of *Glomus intraradices* promotes symbiotic biotrophy. Current Biology 21, 1204–1209. doi: 10.1016/j.cub.2011.06.044

Labbé S, Khan MGM, Jacques J-F. 2013. Iron uptake and regulation in *Schizosaccharomyces pombe*. Current Opinion in Microbiology 16, 669–676. doi: 10.1016/j.mib.2013.07.007

Lanfranco L, Novero M, Bonfante P. 2005. The mycorrhizal fungus *Gigaspora margarita* possesses a CuZn superoxide dismutase that is up-regulated during symbiosis with legume hosts. Plant Physiology 137, 1319–1330. doi: 10.1104/pp.104.050435

Larkin MA, Blackshields G, Brown NP, et al. 2007. Clustal W and Clustal X version 2.0. Bioinformatics 23, 2947–2948. doi: 10.1093/bioinformatics/btm404

Li H, Outten CE. 2013. Monothiol CGFS glutaredoxins and BolA-like proteins: [2Fe-2S] binding partners in iron homeostasis. Biochemistry 51, 4377–4389. doi: 10.1021/bi300393z

Lill R, Hoffmann B, Molik S, Pierik AJ, Rietzschel N, Stehling O, Uzarska MA, Webert H, Wilbrecht C, Mühlenhoff U. 2012. The role of mitochondria in cellular iron-sulfur protein biogenesis and iron metabolism. Biochimica et Biophysica Acta - Molecular Cell Research 1823, 1491–1508. doi: 10.1016/j.bbamcr.2012.05.009

Lillig CH, Berndt C, Holmgren A. 2008. Glutaredoxin systems. Biochimica et Biophysica Acta 1780, 1304–1317. doi: 10.1016/j.bbagen.2008.06.003

Lin K, Limpens E, Zhang Z, et al. 2014. Single nucleus genome sequencing reveals high similarity among nuclei of an endomycorrhizal fungus. PLoS Genetics 10, e1004078. doi: 10.1371/journal.pgen.1004078

Liu Y, Gianinazzi-Pearson V, Arnould C, Wipf D, Zhao B, van Tuinen D. 2013. Fungal genes related to calcium homeostasis and signalling are upregulated in symbiotic arbuscular mycorrhiza interactions. Fungal Biology 117, 22–31. doi: 10.1016/j.funbio.2012.11.002

Luo M, Jiang Y-L, Ma X-X, Tang Y-J, He Y-X, Yu J, Zhang R-G, Chen Y, Zhou C-Z. 2010. Structural and biochemical characterization of yeast monothiol glutaredoxin Grx6. Journal of Molecular Biology 398, 614–622. doi: 10.1016/j.jmb.2010.03.029

Mapolelo DT, Zhang B, Randeniya S, Albetel A-N, Li H, Couturier J, Outten CE, Rouhier N, Johnson MK. 2013. Monothiol glutaredoxins and A-type proteins: partners in Fe-S cluster trafficking. Dalton Transactions 42, 3107–3115. doi: 10.1039/c2dt32263c

Mesecke N, Spang A, Deponte M, Herrmann JM. 2008. A novel group of glutaredoxins in the *cis* -golgi critical for oxidative stress resistance. Molecular Biology of the Cell 19, 2673–2680. doi: 10.1091/mbc.E07

Minet M, Dufour M, Lacroute F. 1992. Complementation of *Saccharomyces cerevisiae* auxotrophic mutants by *Arabidopsis thaliana* cDNAs. The Plant Journal 2, 417–422. doi: 10.1111/j.1365-313X.1992.00417.x

Moon J-S, Lim H-W, Park E-H, Lim C-J. 2005. Characterization and regulation of the gene encoding monothiol glutaredoxin 3 in the fission yeast *Schizosaccharomyces pombe*. Molecules and Cells 20, 74–82.

Morel M, Kohler A, Martin F, Gelhaye E, Rouhier N. 2008. Comparison of the thiol-dependent antioxidant systems in the ectomycorrhizal *Laccaria bicolor* and the

saprotrophic *Phanerochaete chrysosporium*. New Phytologist 180, 391–407. doi: 10.1111/j.1469-8137.2008.02498.x

Nanda AK, Andrio E, Marino D, Pauly N, Dunand C. 2010. Reactive oxygen species during plant-microorganism early interactions. Journal Integrative Plant Biology 52, 195–204. doi: 10.1111/j.1744-7909.2010.00933.x

Ojeda L, Keller G, Muhlenhoff U, Rutherford JC, Lill R, Winge DR. 2006. Role of glutaredoxin-3 and glutaredoxin-4 in the iron regulation of the Aft1 transcriptional activator in *Saccharomyces cerevisiae*. The Journal Biological Chemistry 281, 17661–17669. doi: 10.1074/jbc.M602165200

Pérez-Tienda J, Corrêa A, Azcón-Aguilar C, Ferrol N. 2014. Transcriptional regulation of host $NH4^+$ transporters and GS/GOGAT pathway in arbuscular mycorrhizal rice roots. Plant Physiology and Biochemistry 75, 1–8. doi: 10.1016/j.plaphy.2013.11.029

Puigpinós J, Casas C, Herrero E. 2015. Altered intracellular calcium homeostasis and endoplasmic reticulum redox state in *Saccharomyces cerevisiae* cells lacking Grx6 glutaredoxin. Molecular Biology of the Cell 26, 104–116. doi: 10.1091/mbc.E14-06-1137

Pujol-Carrion N, Belli G, Herrero E, Nogues A, de la Torre-Ruiz MA. 2006. Glutaredoxins Grx3 and Grx4 regulate nuclear localisation of Aft1 and the oxidative stress response in *Saccharomyces cerevisiae*. Journal of Cell Science 119, 4554–4564. doi: 10.1242/jcs.03229

Pujol-Carrion N, De La Torre-Ruiz MA. 2010. Glutaredoxins Grx4 and Grx3 of *Saccharomyces cerevisiae* play a role in actin dynamics through their Trx domains, which contributes to oxidative stress resistance. Applied and Environmental Microbiology 76, 7826–7835. doi: 10.1128/AEM.01755-10

Requena N, Serrano E, Ocón A, Breuninger M. 2007. Plant signals and fungal perception during arbuscular mycorrhiza establishment. Phytochemistry 68, 33–40. doi: 10.1016/j.phytochem.2006.09.036

Rodríguez-Manzaneque M, Tamarit J, Belli G, Ros J, Herrero E. 2002. Grx5 is a mitochondrial glutaredoxin required for the activity of iron/sulfur enzymes. Molecular Biology of the Cell 13, 1109–1121. doi: 10.1091/mbc.01–10–0517

Rouhier N, Couturier J, Johnson MK, Jacquot J-P. 2009. Glutaredoxins: roles in iron homeostasis. Trends in Biochemical Sciences 35, 43–52. doi: 10.1016/j.tibs.2009.08.005

Salzer P, Corbière H, Boller T. 1999. Hydrogen peroxide accumulation in *Medicago truncatula* roots colonized by the arbuscular mycorrhiza-forming fungus *Glomus intraradices*. Planta 208, 319–325. doi: 10.1007/s004250050565

Schiestl RH, Gietz RD. 1989. High efficiency transformation of intact cells using single stranded nucleic acids as a carrier. Current Genetics 16, 339–346. doi: 10.1007/BF00340712

Schmittgen TD, Livak KJ. 2008. Analyzing real-time PCR data by the comparative C_T method. Nature Protocols 3, 1101–1108. doi: 10.1038/nprot.2008.73

Shenton D, Perrone G, Quinn KA, Dawes IW, Grant CM. 2002. Regulation of protein S-thiolation by glutaredoxin 5 in the yeast *Saccharomyces cerevisiae*. Journal of Biological Chemistry 277, 16853–16859. doi: 10.1074/jbc.M200559200

Sikorski RS, Hieter P. 1989. A system of shuttle vectors and yeast host strains designed for efficient manipulation of DNA in *Saccharomyces cerevisiae*. Genetics 122, 19–27.

Smith SE, Read DJ. 2008. *Mycorrhizal Symbiosis*. London: Academic Press.

St-Arnaud M, Hamel C, Vimard B, Caron M, Fortin JA. 1996. Enhanced hyphal growth and spore production of the arbuscular mycorrhizal fungus *Glomus intraradices* in an *in vitro* system in the absence of host roots. Mycological Research 100, 328–332. doi: 10.1016/S0953-7562(96)80164-X

Ströher E, Millar AH. 2012. The biological roles of glutaredoxins. Biochemical Journal 446, 333–348. doi: 10.1042/BJ20112131

Tamura K, Stecher G, Peterson D, Filipski A, Kumar S. 2013. MEGA6: Molecular evolutionary genetics analysis version 6.0. Molecular Biology and Evolution 30, 2725–2729. doi: 10.1093/molbev/mst197

Tisserant E, Kohler A, Dozolme-Seddas P, et al. 2012. The transcriptome of the arbuscular mycorrhizal fungus *Glomus intraradices* (DAOM 197198) reveals functional tradeoffs in an obligate symbiont. New Phytologist 193, 755–769. doi: 10.1111/j.1469-8137.2011.03948.x

Tisserant E, Malbreil M, Kuo A, et al. 2013. Genome of an arbuscular mycorrhizal fungus provides insight into the oldest plant symbiosis. Proceedings of the National Academy of Sciences 110, 20117–20122. doi: 10.1073/pnas.1313452110

Wallis JW, Chrebet G, Brodsky G, Rolfe M, Rothstein R. 1989. A hyper-recombination mutation in *S. cerevisiae* identifies a novel eukaryotic topoisomerase. Cell 58, 409–419. doi: 10.1016/0092-8674(89)90855-6

Supporting Information

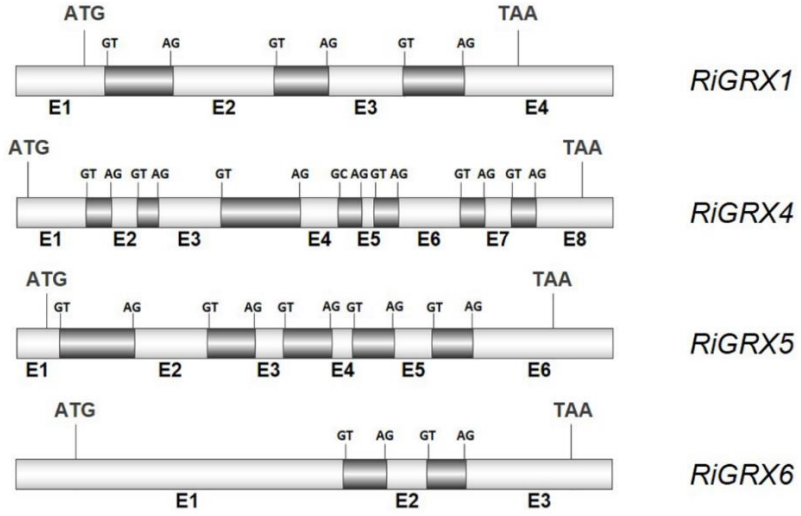

S1 Figure. Exon/intron organization of the *Rhizophagus irregularis GRX* genes. Exon (E) and introns are represented by white and black boxes, respectively. The intron flanking sequences and the start and stop codons are indicated.

S1 Table. Oligonucleotides used in this study. Overhangs are underlined (*Not*I (continuous lines) or *Sfi*I (dashed lines) restriction sites).

Primer	Sequence 5' - 3'
ScGRX3f	ATGTGTTCTTTTCAGGTTCCATCTG
ScGRX3r	TTAAGATTGGAGAGCATGCTGCAA
ScGRX4f	ATGACTGTGGTTGAAATAAAAAGC
ScGRX4r	TTACTGTAGAGCATGTTGGAAATA
ScGRX5f	ATGTTTCTCCCAAAATTCAATCC
ScGRX5r	TCAACGATCTTTGGTTTCTTCTTC
Grx4.fF	GCGGCCGCATGGACAGCAACTTG
Grx4.fR	GCGGCCGCTCAAATTGATTTCTCTAA
Grx5.fF	GCGGCCGCATGAGCTTACGATCATTA
Grx5.fR	GCGGCCGCTTAATTTTCCTCCTGTTC
Grx7.fF	ATGTCTAAAGCGGCGATCTTACC
Grx7.fR	TTATAAAGATGGTCGAAAAATTTCGTG
GintGRXfw2	GAAGATTCCGAAGGAAGAGC
GintGRXrev2	CAACGTGTTGACCCTTGATA
RiGrx4.qF	GATTTTTGGGCAACATGGGC
RiGrx4.qR	CGGGGAATTTCTCAGCCTCAATCT
RiGrx5.qF	GCGCAAGGTTTGGATTTCT
RiGrx5.qR	AGGGACTGTTGGCCATTGT
RiGrx7.qF	TGGGAGAAGGAGGTGAAGAA
RiGrx7.qR	CCAATGCTTCCTCGAAACG
GintPDXfw	CTGGAGATCCTGCTAAAAGAGC
GintPDXrev	CCAAGATCCTCCGATACTTCG
GintEFfw	GCTATTTTGATCATTGCCGCC
GintEFrev	TCATTAAAACGTTCTTCCGACC
RiGRX4-sfi-F	CAAGGCCATTACGGCCATGGACAGCAACTTGATAGAACTTAC
RiGRX4-sfi-R	GATGGCCGAGGCGGCCGAAATTGATTTCTCTAAAGCAAACATGG
RiGRX5-sfi-F	CAAGGCCATTACGGCCATGAGCTTACGATCATTAACACGTC
RiGRX5-sfi-R	GATGGCCGAGGCGGCCGATTTTTCCTCCTGTTCTAATTCATTTTTAG
RiGRX6-sfi-F	CAAGGCCATTACGGCCATGTCTAAAGCGGCGATCTTAC
RiGRX6-sfi-R	GATGGCCGAGGCGGCCGATAAAGATGGTCGAAAAATTTCGTG

DISCUSSION

This chapter integrates the whole set of results achieved in the different chapters of this PhD thesis, as a way to give a global overview of our contributions to the understanding of the mechanisms of Fe homeostasis in the arbuscular mycorrhizal (AM) fungus *Rhizophagus irregularis*. As in other organisms, Fe homeostasis in mycorrhizal fungi must be achieved by the coordinated action of a series of processes that control the acquisition of the metal from the soil by the extraradical mycelium (ERM), its use and storage in the different subcellular compartments, translocation of the metal from the extraradical to the intraradical mycelium (IRM) and subsequent transfer to the host plant. All these processes require the action of proteins that transport Fe through the plasma membrane of the different structures the fungus develops both outside and inside the root as well as its subcellular membranes. Hence, it was decided in this PhD thesis to identify and characterize the transport systems operating in AM fungi, in order to study the mechanisms of Fe homeostasis in these organisms.

The consideration that some fungi use a reductive pathway of Fe uptake while others use a strategy based on the production of siderophores led us to determine which strategy AM fungi use to solubilize and take up Fe from the soil. Identification of *RiFTR1* and *RiFTR2* in the genome of *R. irregularis*, two orthologues of the permease that mediates Fe uptake through the reductive pathway in other fungi, indicated that AM fungi have a reductive pathway of Fe uptake. It is a high-affinity Fe transport system in which, in order to increase metal solubility, Fe^{3+} is first reduced to Fe^{2+} by the action of a ferric reductase. Afterwards, Fe^{2+} is taken up by the concerted action of a ferroxidase and a permease that form a protein complex in the plasma membrane, the OFet complex, which gives its name to the gene family (Stearman et al., 1996).

The existence of a ferric reductase activity inducible by Fe deficient conditions has been shown biochemically in the ERM of *R. irregularis*. In addition, a gene encoding a potential ferric reductase, *RiFRE1*, has been identified in its genome, whose expression is repressed under high Fe conditions. This expression pattern is similar to the ferric reductase genes from other fungi, such as *Candida albicans* and *Aspergillus nidulans* genes (Dancis et al., 1992; Knight et al., 2002; Oberegger et al., 2002).

Considering that OFet transporters pump Fe into the cytoplasm, either from the outside or from the lumen of intracellular organelles, in order to determine the specific function of the proteins encoded by *RiFTR1* and *RiFTR2* and since there is currently no methodologies to genetically modify AM fungi, the *RiFTR1* and *RiFTR2* genes were functionally analyzed in a heterologous system. These analyses demonstrated that *RiFTR1* encodes a high-affinity Fe transporter located in the plasma membrane. Unfortunately, functionality of RiFTR2 could not be demonstrated because it was located in the endoplasmic reticulum in the heterologous system. The observation that *RiFTR1* expression in the ERM presented a typical pattern of a high-affinity transporter, that is, activation under Fe deficient conditions and inhibition under toxicity conditions together with the functional analyses performed in yeast indicate that RiFTR1 is involved in the Fe uptake by the ERM. Although the function of RiFTR2 could not be determined, considering that the majority of fungi have two Fe permeases, one in the plasma membrane and the other in the vacuole (Urbanowski and Piper, 1999; Park et al., 2007; Ziegler et al., 2011), it is expected that the protein encoded by *RiFTR2* is located in the tonoplast, being, therefore, involved in mobilization of the vacuolar Fe reserves, which would justify that the expression of this gene is inhibited when the ERM develops in the presence of high Fe conditions.

The observation that *RiFTR1* expression levels were much higher both in the *in vitro* cultured mycorrhizal carrot roots and *in vivo* cultured maize roots than in the ERM indicates that RiFTR1 is also involved in the maintenance of Fe homeostasis in the fungal structures developed inside the root. Due to RiFTR1 transports Fe into the fungus, this protein is not responsible for the transport of Fe from the fungus to the apoplast of the symbiotic interface that is developed in arbuscule-colonized cells for its later uptake by the host plant. As described for P and N transporters (Balestrini et al., 2007; Pérez-Tienda et al., 2011), the fact that *RiFTR1* is expressed in IRM suggests that the fungus exerts some control over the amount of Fe it transfers to the plant. Although the mechanisms involved in the Fe uptake by the plant *via* the mycorrhizal pathway are currently unknown, it has been observed that the Fe transporters *MtNRAMP1* and *MtNRAMP3* are overexpressed in arbuscule-colonized cortical cells in *Medicago truncatula* (Hogekamp y Kuster,

2013). These results suggest that the plant and the fungus compete for Fe present at the symbiotic interface to fulfill their metabolic needs. In addition, given that an accumulation of Fe in the interfacial apoplast would lead to the formation of reactive oxygen species, the fact that Fe transporters of both symbionts are induced in the symbiotic interface suggests that the maintenance of Fe homeostasis in the symbiotic interface may be essential for the establishment of the symbiosis. The observation that the expression of *RiFTR2*, which encodes a putative vacuolar Fe transporter, increases in the IRM under Fe-limiting conditions, supports this hypothesis.

Identification of the ferroxidases acting in a coordinated way with the RiFTR1 and RiFTR2 permeases has been more complicated since these proteins belong to the family of multicopper oxidases (MCOs), and nine candidates have been found in the *R. irregularis* genome. Although fungal MCOs are phylogenetically distributed according to the subfamily to which they belong and not according to taxonomic criteria, the nine MCOs of *R. irregularis* clustered in the clade of the proteins that have ferroxidase/laccase activity and none of them clustered in the clade of *sensu stricto* ferroxidases. Since on the basis of the *in silico* studies the nine RiMCOs can have ferroxidase activity and in order to try to identify the isoform that cooperates with RiFTR1 in Fe uptake from the soil, transcriptional regulation of the ERM-expressed *RiMCOs* by Fe was analyzed. These analyses revealed that *RiMCO1* was the only *RiMCO* exhibiting an expression pattern similar to *RiFTR1*, suggesting that it could be involved in Fe transport, a fact that was demonstrated by its functional characterization in yeast. However, it cannot be ruled out that some other member of the RiMCO family also has ferroxidase activity. Characterization of these genes will be the aim of future studies.

Inspection of the *R. irregularis* genome indicates that it does not contain *Sid1*/*SidA* orthologs, genes that encode a protein involved in the biosynthesis of hydroxamates, the main fungal siderophores. The absence of a *Sid1*/*SidA* ortholog in a fungal genome is generally taken as strong evidence that no siderophore production takes place (Haas et al., 2008). Therefore, it is likely that *R. irregularis* does not use this Fe uptake system. Nevertheless, a gene encoding a putative siderophore aerobactin biosynthetic protein was found in the *R. irregularis* genome. Irrespective of the ability of AM fungi to produce

siderophores, *R. irregularis* has several homologues to *SIT* genes (siderophore-iron transporters) in its genome, indicating that, as in other fungi, *R. irregularis* could take advantage of the siderophores produced by other soil microorganisms, securing in such manner their own Fe needs.

In addition to the OFet transporters, three genes potentially encoding VIT transporters (*RiCCC1-3*) which facilitate transport of Fe/Mn from the cytosol to the vacuole; a CDF transporter, *RiMMT1*, involved in the transport of Fe to the mitochondria, and several members of the NRAMP family (*RiSMFs*) that facilitate the transport of several divalent metals into the cytosol, have been identified in the *R. irregularis* genome.

Even though in this PhD thesis only the fungal transporters involved in Fe uptake from the soil have been characterized, taking into account the role that the fungal vacuoles play in the translocation of nutrients from the ERM to the IRM and the Fe transporters present in mycorrhizal fungi, the following model is proposed for the transport of this micronutrient through the mycorrhizal pathway in a mycorrhizal root: First, the Fe^{3+} present in the soil solution is reduced to Fe^{2+} by the action of the ferric reductase RiFRE1 located in the plasma membrane of the ERM and Fe^{2+} is then transported into the cytosol through the protein complex RiFTR1-RiMCO1. Once in the cytosol and to avoid its toxicity, Fe must be bound to a chaperone or a chelator and transported either into the mitochondria, the organelle that uses most of the cellular Fe, by the CDF transporter RiMMT1 or into the vacuole by one of the identified VIT transporters (RiCCC1-3). The iron accumulated into the vacuoles must be stabilized by the polyphosphate that accumulates in the AM fungal vacuoles and, these vacuoles would transport the metal from the ERM to the IRM. Once in the IRM and more specifically in the arbuscules, Fe must be released to the cytosol by the action of either the vacuolar permease RiFTR2 or the NRAMP transporter RiSMF3 and later transferred to the apoplast of the symbiotic interface, either as free Fe or bound to some organic compound through an unidentified transporter. Although the plant transporters responsible for the Fe uptake present at the symbiotic interface have not been yet identified, this transport could be mediated either by a NRAMP transporter or by an oligopeptide transporter, as it has been recently suggested (Kobae et al., 2014). (Fig. 1).

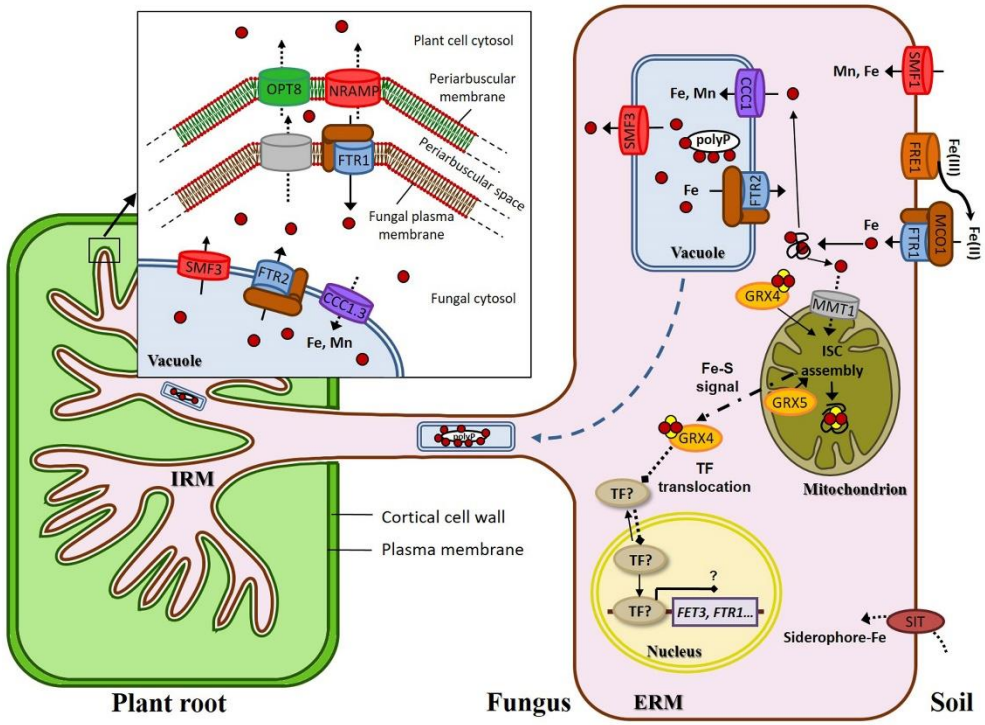

Figure 1. Proposed model of Fe homeostasis mechanisms in *Rhizophagus irregularis*. Discontinuous arrows refer to transporters whose transcript levels in the ERM have not been determined yet. Glutaredoxins are in light orange; putative NRAMP family members in red; the oxidase-dependent Fe^{2+} transporter (OFeT) family members in brown (ferroxidases) and blue (permeases); cation diffusion facilitators (CDFs) in gray, NRAMPs in red and VITs in purple. Red and yellow circles symbolize Fe-S clusters. ISC, Fe/S cluster; TF, transcription factor.

The consideration that in other organisms glutaredoxins play a fundamental role in the regulation of Fe homeostasis, led us to characterize these proteins in *R. irregularis*. Of the three glutaredoxins characterized in this PhD thesis, RiGRX4 and RiGRX5 appear to be involved in the regulation of Fe homeostasis in *R. irregularis*. RiGRX4 is homologous to the *S. cerevisiae* monothiol glutaredoxins ScGRX3 and ScGRX4 that act as Fe chaperons transporting cytosolic Fe to the Fe-dependent enzymes and to the different cellular organelles, thanks to their ability to bind labile iron-sulfur (Fe-S) clusters (Mühlenhoff et al., 2010; Lill et al., 2012). Moreover, ScGRX3 and ScGRX4 regulate Fe transport systems by interacting with Aft1 and Aft2 transcription factors that control Fe homeostasis. Aft1 and Aft2 are constitutively expressed in the cytoplasm, but under low Fe concentrations

they locate in the nucleus acting as transcriptional activators of the genes of the high-affinity system. Under high Fe conditions, ScGRX3 and ScGRX4 interact with Aft1/2 excluding them from the nucleus and preventing the activation of the high-affinity Fe uptake systems (Kumánovics et al., 2008; Outten and Albetel, 2013). In fact, the absence of GRX3 and GRX4 leads to a Fe accumulation in *S. cerevisiae*. The observations that RiGRX4 reverted this phenotype and that high Fe concentrations up-regulate *RiGRX4* expression suggest that, as in *S. cerevisiae*, RiGRX4 is involved in the regulation of Fe homeostasis by inhibiting high-affinity Fe uptake systems. On the other hand, functional analysis of RiGRX5 in yeast showed that this glutaredoxin is involved in the synthesis of Fe-S clusters in the mitochondria and, therefore, in regulation of Fe homeostasis in *R. irregularis*. Further analyses are needed to test whether this is also the case under *in vivo* conditions in *R. irregularis*.

The work carried out in this PhD thesis represents a first step in the understanding of the mechanisms of Fe homeostasis in mycorrhizal fungi and of those involved in Fe uptake by the mycorrhizal pathway. The in-depth knowledge of these mechanisms is essential to understand the potential of AM fungi in the development of crop biofortification strategies and in the phytoremediation of contaminated soils.

CONCLUSIONS

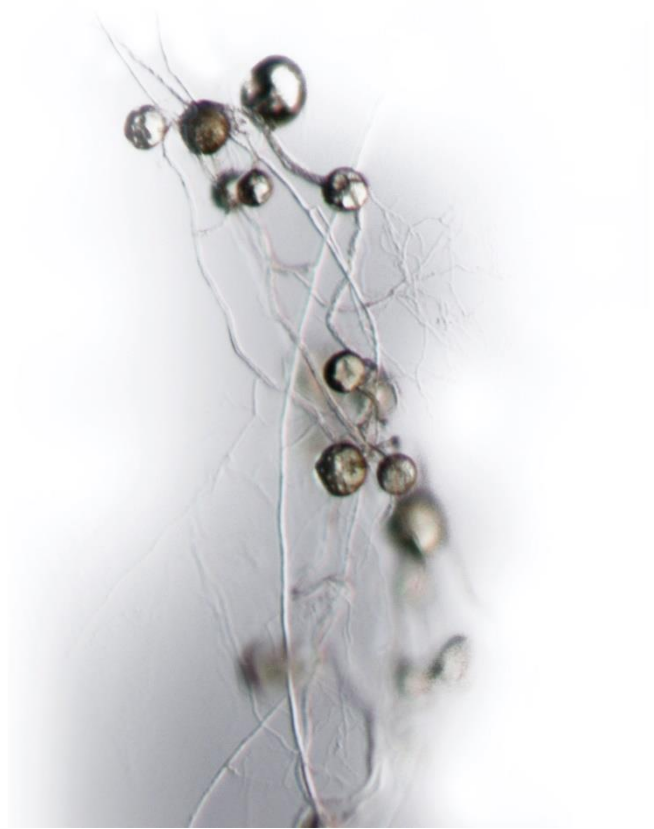

1. The arbuscular mycorrhizal fungus *Rhizophagus irregularis* has 12 open reading frames in its genome, which potentially encode iron transporters belonging to the siderophore-iron transporter (SIT), oxidase-dependent Fe^{2+} transporter (OFet), vacuolar iron transporter (VIT), cation diffusion facilitator (CDF) and natural resistance-associated macrophage protein (NRAMP) families.

2. The *Rhizophagus irregularis* extraradical mycelium possesses a surface ferric reductase activity that is induced by iron deficiency. This protein is putatively encoded by *RiFRE1*.

3. *Rhizophagus irregularis* has two genes potentially encoding iron permeases in it is genome, *RiFTR1* and *RiFTR2*. *RiFTR1* encodes a plasma membrane high-affinity iron transporter that plays a role in iron acquisition under iron-limiting conditions. RiFTR2 function could not be determined, but it might encode a tonoplast-localized iron permease.

4. In the *Rhizophagus irregularis* intraradical mycelium, *RiFTR1* is highly expressed and *RiFTR2* is up-regulated under low iron conditions, indicating that RiFTR1 and RiFTR2 are involved in iron homeostasis during the *in planta* phase of the fungus.

5. *Rhizophagus irregularis* possesses at least nine genes (*RiMCO1-9*) putatively encoding multicopper oxidases in its genome, all belonging to the ferroxidase/laccase group. The *RiMCO* genes are differentially expressed in the intraradical and extradical mycelium. *RiMCO1* was the only *MCO* gene displaying an expression pattern typical of a high-affinity iron transport system and encodes a protein with ferroxidase activity that is highly expressed in the extraradical mycelium. RiMCO1 might be the ferroxidase partner of the iron permease RiFTR1 that mediates the high-affinity ferroxidation/permeation iron uptake pathway at the extraradical mycelium.

6. The *Rhizophagus irregularis* glutaredoxin gene family is composed of four members, two belonging to class I GRXs (*RiGRX1* and *RiGRX6*) and two to class II (*RiGRX4* and *RiGRX5*). While the four *R. irregularis* GRXs play a role in oxidative stress protection, the glutaredoxins monothiol RiGRX4 and RiGRX5 are also involved in the regulation of fungal iron homeostasis.

CONCLUSIONES

1. El hongo micorrícico arbuscular *Rhizophagus irregularis* tiene 12 marcos abiertos de lectura en el genoma, que codifican potencialmente transportadores de hierro pertenecientes a las familias de transportadores de sideróforo-hierro (SIT), transportadores de Fe^{2+} dependientes de oxidasa (OFet), transportadores de hierro vacuolares (VIT), facilitadores de la difusión de cationes (CDF) y proteínas de macrófagos asociados a la resistencia natural (NRAMP).

2. El micelio extrarradical de *Rhizophagus irregularis* posee una actividad reductasa férrica superficial que se induce por la deficiencia de hierro. Esta proteína está codificada putativamente por *RiFRE1*.

3. *Rhizophagus irregularis* tiene en el genoma dos genes que codifican potencialmente permeasas de hierro, *RiFTR1* y *RiFTR2*. *RiFTR1* codifica un transportador de hierro de membrana plasmática de alta afinidad con un papel en la adquisición de hierro bajo condiciones limitantes de hierro. La función de RiFTR2 no pudo ser determinada, pero podría codificar una permeasa de hierro localizada en el tonoplasto.

4. En el micelio intrarradical de *Rhizophagus irregularis*, *RiFTR1* se expresa abundantemente y *RiFTR2* se regula al alza bajo condiciones limitantes de hierro, lo que indica que RiFTR1 y RiFTR2 están implicados en la homeostasis de hierro durante la fase *in planta* del hongo.

5. *Rhizophagus irregularis* tiene al menos nueve genes en su genoma (*RiMCO1*-9) que codifican putativamente oxidasas multicobre, todas del grupo de ferroxidasas/lacasas. Los genes *RiMCO* se expresan diferencialmente en el micelio intrarradical y extrarradical. *RiMCO1* fue el único gen *MCO* que mostró un patron típico de un sistema de transporte de hierro de alta afinidad, y codifica una proteína con actividad ferroxidasa que se expresa abundantemente en el micelio extrarradical. RiMCO1 podría ser el compañero ferroxidasa de la permeasa de hierro RiFTR1 que media la vía de absorción de hierro de ferroxidación/permeación en el micelio extrarradical.

6. La familia génica de las glutarredoxinas de *Rhizophagus irregularis* está compuesta por cuatro miembros, dos que pertenecen a las GRXs de clase I (*RiGRX1* y *RiGRX6*) y dos a la clase II (*RiGRX4* y *RiGRX5*). Mientras que las cuatro GRXs de *R. irregularis* tienen un papel en la protección frente al estrés oxidativo, las glutarredoxinas monotioles RiGRX4 y RiGRX5 también están implicadas en la regulación de la homeostasis de hierro del hongo.

GENERAL BIBLIOGRAPHY

Al Agely A, Sylvia DM, Ma LQ. 2005. Mycorrhizae increase arsenic uptake by the hyperaccumulator chinese brake fern (*Pteris vittata* L.). Journal of Environmental Quality 34, 2181–2186. doi: 10.2134/jeq2004.0411

Aguilera P, Borie F, Seguel A, Cornejo P. 2011. Fluorescence detection of aluminum in arbuscular mycorrhizal fungal structures and glomalin using confocal laser scanning microscopy. Soil Biology and Biochemistry 43, 2427–2431. doi: 10.1016/j.soilbio.2011.09.001

Akiyama K, Matsuzaki K, Hayashi H. 2005. Plant sesquiterpenes induce hyphal branching in arbuscular mycorrhizal fungi. Nature 435, 824–827. doi: 10.1038/nature03608

Aloui A, Recorbet G, Gollotte A, Robert F, Valot B, Gianinazzi-Pearson V, Aschi-Smiti S, Dumas-Gaudot E. 2009. On the mechanisms of cadmium stress alleviation in *Medicago truncatula* by arbuscular mycorrhizal symbiosis: a root proteomic study. Proteomics 9, 420–433. doi: 10.1002/pmic.200800336

Aloui A, Recorbet G, Robert F, Schoefs B, Bertrand M, Henry C, Gianinazzi-Pearson V, Dumas-Gaudot E, Aschi-Smiti S. 2011. Arbuscular mycorrhizal symbiosis elicits shoot proteome changes that are modified during cadmium stress alleviation in *Medicago truncatula*. BMC Plant Biology 11, 75. doi: 10.1186/1471-2229-11-75

Angelard C, Tanner CJ, Fontanillas P, Niculita-Hirzel H, Masclaux F, Sanders IR. 2014. Rapid genotypic change and plasticity in arbuscular mycorrhizal fungi is caused by a host shift and enhanced by segregation. The ISME Journal 8, 284–294. doi: 10.1038/ismej.2013.154

Aroca R, Bago A, Sutka M, Paz JA, Cano C, Amodeo G, Ruiz-Lozano JM. 2009. Expression analysis of the first arbuscular mycorrhizal fungi aquaporin described reveals concerted gene expression between salt-stressed and nonstressed mycelium. Molecular Plant-Microbe Interactions 22, 1169–1178. doi: 10.1094/MPMI-22-9-1169

Aroca R, Porcel R, Ruiz-Lozano JM. 2007. How does arbuscular mycorrhizal symbiosis regulate root hydraulic properties and plasma membrane aquaporins in *Phaseolus vulgaris* under drought, cold or salinity stresses? New Phytologist 173, 808–816. doi: 10.1111/j.1469-8137.2006.01961.x

Audet P, Charest C. 2008. Allocation plasticity and plant–metal partitioning: Meta-analytical perspectives in phytoremediation. Environmental Pollution 156, 290–296. doi: 10.1016/j.envpol.2008.02.010

Azcón-Aguilar C, Barea JM. 1997. Arbuscular mycorrhizas and biological control of soil-borne plant pathogens – an overview of the mechanisms involved. Mycorrhiza 6, 457–464. doi: 10.1007/s005720050147

Bago B, Pfeffer PE, Shachar-hill Y. 2000. Carbon metabolism and transport in arbuscular mycorrhizas. Plant Physiology 124, 949–957. doi: 10.1104/pp.124.3.949

Bago B, Vierheilig H, Piché Y, Azcón-Aguilar C. 1996. Nitrate depletion and pH changes induced by the extraradical mycelium of the arbuscular mycorrhizal fungus *Glomus intraradices* grown in monoxenic culture. New Phytologist 133, 273–280. doi: 10.1111/j.1469-8137.1996.tb01894.x

Balestrini R, Gómez-Ariza J, Lanfranco L, Bonfante P. 2007. Laser microdissection reveals that transcripts for five plant and one fungal phosphate transporter genes are contemporaneously present in arbusculated cells. Molecular Plant-Microbe Interactions 20, 1055–1062. doi: 10.1094/MPMI-20-9-1055

Barea JM. 1991. Vesicular-arbuscular mycorrhizae as modifiers of soil fertility. In: Stewart BA, ed. *Advances in Soil Science*: 15. New York: Springer, 1–40. doi: 10.1007/978-1-4612-3030-4_1

Barea J-M, Azcón-Aguilar C. 2013. Evolution, Biology and ecological effects of arbuscular mycorrhiza. In: AF Camisão and CC Pedroso [eds.]. In: *Symbiosis: Evolution, Biology and ecological effects*. Nova Science Publishers, Inc. pp. 1-34.

Bárzana G, Aroca R, Bienert GP, Chaumont F, Ruiz-Lozano JM. 2014. New insights into the regulation of aquaporins by the arbuscular mycorrhizal symbiosis in maize plants under drought stress and possible implications for plant performance. Molecular Plant-Microbe Interactions 27, 349–363. doi: 10.1094/MPMI-09-13-0268-R

Benabdellah K, Azcón-Aguilar C, Valderas A, Speziga D, Fitzpatrick TB, Ferrol N. 2009*a*. *GintPDX1* encodes a protein involved in vitamin B6 biosynthesis that is up-regulated by oxidative stress in the arbuscular mycorrhizal fungus *Glomus intraradices*. New Phytologist 184, 682–693. doi: 10.1111/j.1469-8137.2009.02978.x

Benabdellah K, Merlos M-A, Azcón-Aguilar C, Ferrol N. 2009*b*. *GintGRX1*, the first characterized glomeromycotan glutaredoxin, is a multifunctional enzyme that responds to oxidative stress. Fungal Genetics and Biology 46, 94–103. doi: 10.1016/j.fgb.2008.09.013

Benedetto A, Magurno F, Bonfante P, Lanfranco L. 2005. Expression profiles of a phosphate transporter gene (*GmosPT*) from the endomycorrhizal fungus *Glomus mosseae*. Mycorrhiza 15, 620–627. doi: 10.1007/s00572-005-0006-9

Benedito VA, Li H, Dai X, et al. 2010. Genomic inventory and transcriptional analysis of *Medicago truncatula* transporters. Plant Physiology 152, 1716–1730. doi: 10.1104/pp.109.148684

Berruti A, Lumini E, Balestrini R, Bianciotto V. 2016. Arbuscular mycorrhizal fungi as natural biofertilizers: Let's benefit from past successes. Frontiers in Microbiology 6, 1559. doi: 10.3389/fmicb.2015.01559

Besserer A, Bécard G, Jauneau A, Roux C, Séjalon-Delmas N. 2008. GR24, a synthetic analog of strigolactones, stimulates the mitosis and growth of the arbuscular mycorrhizal fungus *Gigaspora rosea* by boosting its energy metabolism. Plant Physiology 148, 402–413. doi: 10.1104/pp.108.121400

Besserer A, Puech-Pagès V, Kiefer P, Gomez-Roldan V, Jauneau A, Roy S, Portais J-C, Roux C, Bécard G, Séjalon-Delmas N. 2006. Strigolactones stimulate arbuscular mycorrhizal fungi by activating mitochondria. PLoS Biology 4, e226. doi: 10.1371/journal.pbio.0040226

Bever JD, Wang M. 2005. Arbuscular mycorrhizal fungi: hyphal fusion and multigenomic structure. Nature 433, E3–E4. doi: 10.1038/nature03294

Bianciotto V, Lumini E, Bonfante P, Vandamme P. (2003). '*Candidatus* Glomeribacter gigasporarum' gen. nov., sp. nov., an endosymbiont of arbuscular mycorrhizal fungi. International Journal of Systematic and Evolutionary Microbiology 53, 121–124. doi: 10.1099/ijs.0.02382-0

Bonfante P, Desirò A. 2015. Arbuscular mycorrhizas: the lives of beneficial fungi and their plant hosts. *In*: B. Lugtenberg (ed). *Principles of Plant-Microbe Interactions*. Springer International Publishing Switzerland, pp. 235–245. doi: 10.1007/978-3-319-08575-3

Bonfante P, Genre A. 2010. Mechanisms underlying beneficial plant-fungus interactions in mycorrhizal symbiosis. Nature Communications 1, 1–11. doi: 10.1038/ncomms1046

Bonfante P, Genre A. 2015. Arbuscular mycorrhizal dialogues: do you speak 'plantish' or 'fungish'? Trends in Plant Science 20, 150–154. doi: 10.1016/j.tplants.2014.12.002

Boon E, Halary S, Bapteste E, Hijri M. 2015. Studying genome heterogeneity within the arbuscular mycorrhizal fungal cytoplasm. Genome Biology and Evolution 7, 505–521. doi: 10.1093/gbe/evv002

Breuillin-Sessoms F, Floss DS, Gomez SK, et al. 2015. Suppression of arbuscule degeneration in *Medicago truncatula phosphate transporter4* mutants is dependent on the ammonium transporter 2 family protein AMT2;3. The Plant Cell 27, 1352–1366. doi: 10.1105/tpc.114.131144

Brundrett MC. 2009. Mycorrhizal associations and other means of nutrition of vascular plants: understanding the global diversity of host plants by resolving conflicting information and developing reliable means of diagnosis. Plant and Soil 320, 37–77. doi: 10.1007/s11104-008-9877-9

Bucher M. 2007. Functional biology of plant phosphate uptake at root and mycorrhiza interfaces. New Phytologist 173, 11–26. doi: 10.1111/j.1469-8137.2006.01935.x

Bürkert B, Robson A. 1994. ^{65}Zn uptake in subterranean clover (*Trifolium subterraneum* L.) by three vesicular-arbuscular mycorrhizal fungi in a root-free sandy soil. Soil Biology and Biochemistry 26, 1117–1124. doi: 10.1016/0038-0717(94)90133-3

Cabral L, Soares CRFS, Giachini AJ, Siqueira JO. 2015. Arbuscular mycorrhizal fungi in phytoremediation of contaminated areas by trace elements: mechanisms and major benefits of their applications. World Journal of Microbiology and Biotechnology 31, 1655–1664. doi: 10.1007/s11274-015-1918-y

Calabrese S, Pérez-tienda J, Ellerbeck M, et al. 2016. GintAMT3 – a low-affinity ammonium transporter of the arbuscular mycorrhizal *Rhizophagus irregularis*. Frontiers in Plant Science 7, 679. doi: 10.3389/fpls.2016.00679

Cappellazzo G, Lanfranco L, Fitz M, Wipf D, Bonfante P. 2008. Characterization of an amino acid permease from the endomycorrhizal Fungus *Glomus mosseae*. Plant Physiology 147, 429–437. doi: 10.1104/pp.108.117820

Caris C, Hördt W, Hawkins H-J, Römheld V, George E. 1998. Studies of iron transport by arbuscular mycorrhizal hyphae from soil to peanut and sorghum plants. Mycorrhiza 8, 35–39. doi: 10.1007/s005720050208

Carvalho LM, Caçador I, Martins-Louçao MA. 2006. Arbuscular mycorrhizal fungi enhance root cadmium and copper accumulation in the roots of the salt marsh plant *Aster tripolium* L. Plant and Soil 285, 161–169. doi: 10.1007/s11104-006-9001-y

Casieri L, Ait Lahmidi N, Doidy J, et al. 2013. Biotrophic transportome in mutualistic plant-fungal interactions. Mycorrhiza 23, 597–625. doi: 10.1007/s00572-013-0496-9

Cavagnaro TR. 2008. The role of arbuscular mycorrhizas in improving plant zinc nutrition under low soil zinc concentrations: a review. Plant and Soil 304, 315–325. doi: 10.1007/s11104-008-9559-7

Cavagnaro TR. 2014. Arbuscular mycorrhizas and their role in plant zinc nutrition. In: Solaiman, MZ, Abbott, KL, Varma, A, eds. *Mycorrhizal fungi: use in sustainable agriculture and land restoration*. Heidelberg: Springer, 189–200. doi: 10.1007/978-3-662-45370-4_11

Chabot S, Bécard G, Piché Y. 1992. Life cycle of *Glomus intraradix* in root organ culture. Mycologia 84, 315–321. doi: 10.2307/3760183

Chaney RL, Malik M, Li YM, Brown SL, Brewer EP, Angle JS, Baker AJ. 1997. Phytoremediation of soil metals. Current Opinion in Biotechnology 8, 279–284. doi: 10.1016/S0958-1669(97)80004-3

Chen BD, Li XL, Tao HQ, Christie P, Wong MH. 2003. The role of arbuscular mycorrhiza in zinc uptake by red clover growing in a calcareous soil spiked with various quantities of zinc. Chemosphere 50, 839–846. doi: 10.1016/S0045-6535(02)00228-X

Chen XW, Wu FY, Li H, Chan WF, Wu C, Wu SC, Wong MH. 2013. Phosphate transporters expression in rice (*Oryza sativa* L.) associated with arbuscular mycorrhizal fungi (AMF) colonization under different levels of arsenate stress. Environmental and Experimental Botany 87, 92–99. doi: 10.1016/j.envexpbot.2012.08.002

Chen X, Wu C, Tang J, Hu S. 2005. Arbuscular mycorrhizae enhance metal lead uptake and growth of host plants under a sand culture experiment. Chemosphere 60, 665–671. doi: 10.1016/j.chemosphere.2005.01.029

Christophersen HM, Smith AF, Smith SE. 2012. Unraveling the influence of arbuscular mycorrhizal colonization on arsenic tolerance in *Medicago*: *Glomus mosseae* is more effective than *G. intraradices*, associated with lower expression of root epidermal Pi transporter genes. Frontiers in Physiology 3, 91. doi: 10.3389/fphys.2012.00091

Cicatelli A, Lingua G, Todeschini V, Biondi S, Torrigiani P, Castiglione S. 2010. Arbuscular mycorrhizal fungi restore normal growth in a white poplar clone grown on heavy metal-contaminated soil, and this is associated with upregulation of foliar metallothionein and polyamine biosynthetic gene expression. Annals of Botany 106, 791–802. doi: 10.1093/aob/mcq170

Cicatelli A, Lingua G, Todeschini V, Biondi S, Torrigiani P, Castiglione S. 2012. Arbuscular mycorrhizal fungi modulate the leaf transcriptome of a *Populus alba* L. clone grown on a zinc and copper-contaminated soil. Environmental and Experimental Botany 75, 25–35. doi: 10.1016/j.envexpbot.2011.08.012

Cooper KM, Tinker PB. 1978. Translocation and transfer of nutrients in vesicular-arbuscular mycorrhizas. New Phytologist 81, 43–52. doi: 10.1111/j.1469-8137.1978.tb01602.x

Cornejo P, Meier S, Borie G, Rillig MC, Borie F. 2008. Glomalin-related soil protein in a Mediterranean ecosystem affected by a copper smelter and its contribution to Cu and Zn sequestration. Science of the Total Environment 406, 154–160. doi: 10.1016/j.scitotenv.2008.07.045

Cornejo P, Pérez-Tienda J, Meier S, Valderas A, Borie F, Azcón-Aguilar C, Ferrol N. 2013. Copper compartmentalization in spores as a survival strategy of arbuscular mycorrhizal fungi in Cu-polluted environments. Soil Biology and Biochemistry 57, 925–928. doi: 10.1016/j.soilbio.2012.10.031

Corradi N, Brachmann A. 2017. Fungal mating in the most widespread plant symbionts? Trends in Plant Science 22, 175–183. doi: 10.1016/j.tplants.2016.10.010

Corrêa A, Cruz C, Pérez-Tienda J, Ferrol N. 2014. Shedding light onto nutrient responses of arbuscular mycorrhizal plants: nutrient interactions may lead to

unpredicted outcomes of the symbiosis. Plant Science 221-222, 29–41. doi: 10.1016/j.plantsci.2014.01.009

Cox G, Moran KJ, Sanders F, Nockolds C, Tinker PB. 1980. Translocation and transfer of nutrients in vesicular-arbuscular mycorrhizas. III. Polyphosphate granules and phosphorus translocation. New Phytologist 84, 649–659. doi: 10.1111/j.1469-8137.1980.tb04778.x

Croll D, Giovannetti M, Koch AM, Sbrana C, Ehinger M, Lammers PJ, Sanders IR. 2009. Nonself vegetative fusion and genetic exchange in the arbuscular mycorrhizal fungus *Glomus intraradices*. New Phytologist 181, 924–937. doi: 10.1111/j.1469-8137.2008.02726.x

Cruz C, Egsgaard H, Trujillo C, Ambus P, Requena N, Martins-Loução MA, Jakobsen I. 2007. Enzymatic evidence for the key role of arginine in nitrogen translocation by arbuscular mycorrhizal fungi. Plant Physiology 144, 782–792. doi: 10.1104/pp.106.090522

Dabrowska G, Hrynkiewicz K, Trejgell A. 2012. Do arbuscular mycorrhizal fungi affect metallothionein *Mt2* expression in *Brassica napus* L. roots? Acta Biologica Cracoviensia Series Botanica 54, 34–39. doi: 10.2478/v10182-012-0003-1

DalCorso G, Manara A, Furini A. 2013. An overview of heavy metal challenge in plants: from roots to shoots. Metallomics 5, 1117–1132. doi: 10.1039/c3mt00038a

Dancis A, Roman DG, Anderson GJ, Hinnebusch AG, Klausner RD. 1992. Ferric reductase of *Saccharomyces cerevisiae*: molecular characterization, role in iron uptake, and transcriptional control by iron. Proceedings of the National Academy of Sciences 89, 3869–3873. doi: 10.1073/pnas.89.9.3869

de Andrade SAL, da Silveira APD, Jorge RA, de Abreu MF. 2008. Cadmium accumulation in sunflower plants influenced by arbuscular mycorrhiza. International Journal of Phytoremediation 10, 1–13. doi: 10.1080/15226510701827002

de Souza LA, de Andrade SAL, de Souza SCR, Schiavinato MA. 2012. Arbuscular mycorrhiza confers Pb tolerance in *Calopogonium mucunoides*. Acta Physiologiae Plantarum 34, 523–531. doi: 10.1007/s11738-011-0849-y

Degola F, Fattorini L, Bona E, Sprimuto CT, Argese E, Berta G, di Toppi LS. 2015. The symbiosis between *Nicotiana tabacum* and the endomycorrhizal fungus *Funneliformis mosseae* increases the plant glutathione level and decreases leaf cadmium and root arsenic contents. Plant Physiology and Biochemistry 92, 11–18. doi: 10.1016/j.plaphy.2015.04.001

Denton B. 2007. Advances in phytoremediation of heavy metals using plant growth promoting bacteria and fungi. Basic Biotechnology 3, 1–5.

Desirò A, Salvioli A, Ngonkeu EL, Mondo SJ, Epis S, Faccio A, Kaech A, Pawlowska TE, Bonfante P. 2014. Detection of a novel intracellular microbiome hosted in arbuscular mycorrhizal fungi. The ISME Journal 8, 257–270. doi: 10.1038/ismej.2013.151

Eivazi F, Weir CC. 1989. Phosphorus and mycorrhizal interaction on uptake of P and trace elements by maize. Fertilizer Research 21, 19–22. doi: 10.1007/BF01054731

Estrada B, Aroca R, Barea JM, Ruiz-Lozano JM. 2013*a*. Native arbuscular mycorrhizal fungi isolated from a saline habitat improved maize antioxidant systems and plant tolerance to salinity. Plant Science 201–202, 42–51. doi: 10.1016/j.plantsci.2012.11.009

Estrada B, Aroca R, Maathuis FJM, Barea JM, Ruiz-Lozano JM. 2013*b*. Arbuscular mycorrhizal fungi native from a Mediterranean saline area enhance maize tolerance to salinity through improved ion homeostasis. Plant, Cell & Environment 36, 1771–1782. doi: 10.1111/pce.12082

Facelli E, Smith SE, Facelli JM, Christophersen HM, Smith FA. 2010. Underground friends or enemies: model plants help to unravel direct and indirect effects of arbuscular mycorrhizal fungi on plant competition. New Phytologist 185, 1050–1061. doi: 10.1111/j.1469-8137.2009.03162.x

Frank AB. 1885. Ueber die auf Wurzelsymbiose beruhende Ernährung gewisser Bäume durch unterirdische Pilze. Berichte der Deutschen Botanischen Gesellschaft 3, 128-145. doi: 10.1111/j.1438-8677.1885.tb04240.x

Galli U, Schüepp H, Brunold C. 1994. Heavy metal binding by mycorrhizal fungi. Physiologia Plantarum 92, 364–368. doi: 10.1111/j.1399-3054.1994.tb05349.x

García-Rodríguez S, Azcón-Aguilar C, Ferrol N. 2007. Transcriptional regulation of host enzymes involved in the cleavage of sucrose during arbuscular

mycorrhizal symbiosis. Physiologia Plantarum 129, 737–746. doi: 10.1111/j.1399-3054.2007.00873.x

Garg N, Aggarwal N. 2012. Effect of mycorrhizal inoculations on heavy metal uptake and stress alleviation of *Cajanus cajan* (L.) Millsp. genotypes grown in cadmium and lead contaminated soils. Plant Growth Regulation 66, 9–26. doi: 10.1007/s10725-011-9624-8

Garg N, Kaur H. 2013. Response of antioxidant enzymes, phytochelatins and glutathione production towards Cd and Zn stresses in *Cajanus cajan* (L.) Millsp. genotypes colonized by arbuscular mycorrhizal fungi. Journal of Agronomy and Crop Science 199, 118–133. doi: 10.1111/j.1439-037X.2012.00533.x

Gaude N, Bortfeld S, Duensing N, Lohse M, Krajinski F. 2012. Arbuscule-containing and non-colonized cortical cells of mycorrhizal roots undergo extensive and specific reprogramming during arbuscular mycorrhizal development. The Plant Journal 69, 510–528. doi: 10.1111/j.1365-313X.2011.04810.x

Genre A, Chabaud M, Balzergue C, et al. 2013. Short-chain chitin oligomers from arbuscular mycorrhizal fungi trigger nuclear Ca^{2+} spiking in *Medicago truncatula* roots and their production is enhanced by strigolactone. New Phytologist 198, 190-202. doi: 10.1111/nph.12146

Genre A, Chabaud M, Faccio A, Barker DG, Bonfante P. 2008. Prepenetration apparatus assembly precedes and predicts the colonization patterns of arbuscular mycorrhizal fungi within the root cortex of both *Medicago truncatula* and *Daucus carota*. The Plant Cell 20, 1407–1420. doi: 10.1105/tpc.108.059014

Genre A, Chabaud M, Timmers T, Bonfante P, Barker DG. 2005. Arbuscular mycorrhizal fungi elicit a novel intracellular apparatus in *Medicago truncatula* root epidermal cells before infection. The Plant Cell 17, 3489–3499. doi: 10.1105/tpc.105.035410

Genre A, Ivanov S, Fendrych M, Faccio A, Zársky V, Bisseling T, Bonfante P. 2012. Multiple exocytotic markers accumulate at the sites of perifungal membrane biogenesis in arbuscular mycorrhizas. Plant and Cell Physiology 53, 244–255. doi: 10.1093/pcp/pcr170

Gil-Cardeza ML, Ferri A, Cornejo P, Gomez E. 2014. Distribution of chromium species in a Cr-polluted soil: Presence of Cr(III) in glomalin related protein fraction.

Science of the Total Environment 493, 828–833. doi: 10.1016/j.scitotenv.2014.06.080

Göhre V, Paszkowski U. 2006. Contribution of the arbuscular mycorrhizal symbiosis to heavy metal phytoremediation. Planta 223, 1115–1122. doi: 10.1007/s00425-006-0225-0

Goicoechea N, Garmendia I, Sánchez-Díaz M, Aguirreolea J. 2010. Arbuscular mycorrhizal fungi (AMF) as bioprotector agents against wilt induced by *Verticillium* spp. in pepper: a review. Spanish Journal of Agricultural Research 8, S25–S42. doi: 10.5424/sjar/201008S1-5300

Gomez SK, Javot H, Deewatthanawong P, Torres-Jerez I, Tang Y, Blancaflor EB, Udvardi MK, Harrison MJ. 2009. *Medicago truncatula* and *Glomus intraradices* gene expression in cortical cells harboring arbuscules in the arbuscular mycorrhizal symbiosis. BMC Plant Biology 9, 10. doi: 10.1186/1471-2229-9-10

González-Chávez MC, Carrillo-González R, Wright SF, Nichols KA. 2004. The role of glomalin, a protein produced by arbuscular mycorrhizal fungi, in sequestering potentially toxic elements. Environmental Pollution 130, 317–323. doi: 10.1016/j.envpol.2004.01.004

Gonzalez-Chavez C, D'Haen J, Vangronsveld J, Dodd JC. 2002. Copper sorption and accumulation by the extraradical mycelium of different *Glomus* spp. (arbuscular mycorrhizal fungi) isolated from the same polluted soil. Plant and Soil 240, 287–297. doi: 10.1023/A:1015794622592

González-Chávez MCA, Miller B, Maldonado-Mendoza IE, Scheckel K, Carrillo-González R. 2014. Localization and speciation of arsenic in *Glomus intraradices* by synchrotron radiation spectroscopic analysis. Fungal Biology 118, 444–452. doi: 10.1016/j.funbio.2014.03.002

González-Chávez MCA, Ortega-Larrocea MP, Carrillo-González R, López-Meyer M, Xoconostle-Cázares B, Gomez SK, Harrison MJ, Figueroa-López AM, Maldonado-Mendoza IE. 2011. Arsenate induces the expression of fungal genes involved in As transport in arbuscular mycorrhiza. Fungal Biology 115, 1197–1209. doi: 10.1016/j.funbio.2011.08.005

González-Guerrero M, Azcón-Aguilar C, Mooney M, Valderas A, MacDiarmid CW, Eide DJ, Ferrol N. 2005. Characterization of a *Glomus intraradices* gene encoding a putative Zn transporter of the cation diffusion facilitator family. Fungal Genetics and Biology 42, 130–140. doi: 10.1016/j.fgb.2004.10.007

González-Guerrero M, Benabdellah K, Valderas A, Azcón-Aguilar C, Ferrol N. 2010*a*. *GintABC1* encodes a putative ABC transporter of the MRP subfamily induced by Cu, Cd, and oxidative stress in *Glomus intraradices*. Mycorrhiza 20, 137–146. doi: 10.1007/s00572-009-0273-y

González-Guerrero M, Cano C, Azcón-Aguilar C, Ferrol N. 2007. *GintMT1* encodes a functional metallothionein in Glomus intraradices that responds to oxidative stress. Mycorrhiza 17, 327–335. doi: 10.1007/s00572-007-0108-7

González-Guerrero M, Melville LH, Ferrol N, Lott JNA, Azcón-Aguilar C, Peterson RL. 2008. Ultrastructural localization of heavy metals in the extraradical mycelium and spores of the arbuscular mycorrhizal fungus *Glomus intraradices*. Canadian Journal of Microbiology 54, 103–110. doi: 10.1139/w07-119

González-Guerrero M, Oger E, Benabdellah K, Azcón-Aguilar C, Lanfranco L, Ferrol N. 2010*b*. Characterization of a CuZn superoxide dismutase gene in the arbuscular mycorrhizal fungus *Glomus intraradices*. Current Genetics 56, 265–274. doi: 10.1007/s00294-010-0298-y

Goto BT, Silva GA, De Assis DMA, et al. 2012. *Intraornatosporaceae* (*Gigasporales*), a new family with two new genera and two new species. Mycotaxon 119, 117–132. doi: 10.5248/119.117

Govindarajulu M, Pfeffer PE, Jin H, Abubaker J, Douds DD, Allen JW, Bücking H, Lammers PJ, Shachar-Hill Y. 2005. Nitrogen transfer in the arbuscular mycorrhizal symbiosis. Nature 435, 819–823. doi: 10.1038/nature03610

Guerrieri E, Lingua G, Digilio MC, Massa N, Berta G. 2004. Do interactions between plant roots and the rhizosphere affect parasitoid behaviour? Ecological Entomology 29, 753–756. doi: 10.1111/j.0307-6946.2004.00644.x

Guether M, Balestrini R, Hannah M, He J, Udvardi MK, Bonfante P. 2009. Genome-wide reprogramming of regulatory networks, transport, cell wall and membrane biogenesis during arbuscular mycorrhizal symbiosis in *Lotus japonicus*. New Phytologist 182, 200–212. doi: 10.1111/j.1469-8137.2008.02725.x

Haas H, Eisendle M, Turgeon BG. 2008. Siderophores in fungal physiology and virulence. Annual Review of Phytopathology 46, 149–187. doi: 10.1146/annurev.phyto.45.062806.094338

Hall JL. 2002. Cellular mechanisms for heavy metal detoxification and tolerance. Journal of Experimental Botany 53, 1–11. doi: 10.1093/jexbot/53.366.1

Halliwell B, Gutteridge JMC. 1989. *Free radicals in biology and medicine*. Clarendon, UK: Oxford University Press.

Handa Y, Nishide H, Takeda N, Suzuki Y, Kawaguchi M, Saito K. 2015. RNA-seq transcriptional profiling of an arbuscular mycorrhiza provides insights into regulated and coordinated gene expression in *Lotus japonicus* and *Rhizophagus irregularis*. Plant and Cell Physiology 56, 1490-1511. doi: 10.1093/pcp/pcv071

Harrison MJ. 1999. Molecular and cellular aspects of the arbuscular mycorrhizal symbiosis. Annual Review of Plant Physiology and Plant Molecular Biology 50, 361–389. doi: 10.1146/annurev.arplant.50.1.361

Harrison MJ, van Buuren ML. 1995. A phosphate transporter from the mycorrhizal fungus *Glomus versiforme*. Nature 378, 626–629. doi: 10.1038/378626a0

Harrison MJ, Dewbre GR, Liu J. 2002. A phosphate transporter from *Medicago truncatula* involved in the acquisiton of phosphate released by arbuscular mycorrhizal fungi. The Plant Cell 14, 2413–2429. doi: 10.1105/tpc.004861

Hause B, Fester T. 2005. Molecular and cell biology of arbuscular mycorrhizal symbiosis. Planta 221, 184–196. doi: 10.1007/s00425-004-1436-x

Hawkins H-J, Johansen A, George E. 2000. Uptake and transport of organic and inorganic nitrogen by arbuscular mycorrhizal fungi. Plant and Soil 226, 275–285. doi: 10.1023/A:1026500810385

He X, Nara K. 2007. Element biofortification: can mycorrhizas potentially offer a more effective and sustainable pathway to curb human malnutrition? Trends in Plant Science 12, 331–333. doi: 10.1016/j.tplants.2007.06.008

Heggo A, Angle JS, Chaney RL. 1990. Effects of vesicular-arbuscular mycorrhizal fungi on heavy metal uptake by soybeans. Soil Biology and Biochemistry 22, 865–869. doi: 10.1016/0038-0717(90)90169-Z

Helber N, Requena N. 2008. Expression of the fluorescence markers DsRed and GFP fused to a nuclear localization signal in the arbuscular mycorrhizal fungus *Glomus intraradices*. New Phytologist 177, 537–548. doi: 10.1111/j.1469-8137.2007.02257.x

Helber N, Wippel K, Sauer N, Schaarschmidt S, Hause B, Requena N. 2011. A versatile monosaccharide transporter that operates in the arbuscular mycorrhizal fungus *Glomus* sp is crucial for the symbiotic relationship with plants. The Plant Cell 23, 3812–3823. doi: 10.1105/tpc.111.089813

Hijikata N, Murase M, Tani C, Ohtomo R, Osaki M, Ezawa T. 2010. Polyphosphate has a central role in the rapid and massive accumulation of phosphorus in extraradical mycelium of an arbuscular mycorrhizal fungus. New Phytologist 186, 285–289. doi: 10.1111/j.1469-8137.2009.03168.x

Hildebrandt U, Kaldorf M, Bothe H. 1999. The zinc violet and its colonization by arbuscular mycorrhizal fungi. Journal of Plant Physiology 154, 709–717. doi: 10.1016/S0176-1617(99)80249-1

Hildebrandt U, Regvar M, Bothe H. 2007. Arbuscular mycorrhiza and heavy metal tolerance. Phytochemistry 68, 139–146. doi: 10.1016/j.phytochem.2006.09.023

Hodge A, Fitter AH. 2010. Substantial nitrogen acquisition by arbuscular mycorrhizal fungi from organic material has implications for N cycling. Proceedings of the National Academy of Sciences 107, 13754–13759. doi: 10.1073/pnas.1005874107

Hogekamp C, Arndt D, Pereira PA, Becker JD, Hohnjec N, Küster H. 2011. Laser microdissection unravels cell-type-specific transcription in arbuscular mycorrhizal roots, including CAAT-box transcription factor gene expression correlating with fungal contact and spread. Plant Physiology 157, 2023–2043. doi: 10.1104/pp.111.186635

Hogekamp C, Küster H. 2013. A roadmap of cell-type specific gene expression during sequential stages of the arbuscular mycorrhiza symbiosis. BMC Genomics 14, 306. doi: 10.1186/1471-2164-14-306

Hosny M, Gianinazzi-Pearson V, Dulieu H. 1998. Nuclear DNA content of 11 fungal species in Glomales. Genome 41, 422–428. doi: 10.1139/g98-038

Ivanov S, Fedorova EE, Limpens E, De Mita S, Genre A, Bonfante P, Bisseling T. 2012. *Rhizobium*–legume symbiosis shares an exocytotic pathway required for arbuscule formation. Proceedings of the National Academy of Sciences 109, 8316–8321. doi: 10.1073/pnas.1200407109

Jansa J, Mozafar A, Frossard E. 2003. Long-distance transport of P and Zn through the hyphae of an arbuscular mycorrhizal fungus in symbiosis with maize. Agronomie 23, 481–488. doi: 10.1051/agro:2003013

Jany J-L, Pawlowska TE. 2010. Multinucleate spores contribute to evolutionary longevity of asexual Glomeromycota. The American Naturalist 175, 424–435. doi: 10.1086/650725

Javot H, Pumplin N, Harrison MJ. 2007. Phosphate in the arbuscular mycorrhizal symbiosis: transport properties and regulatory roles. Plant, Cell and Environment 30, 310–322. doi: 10.1111/j.1365-3040.2006.01617.x

Jeffries P, Barea JM. 2012. Arbuscular mycorrhiza- a key component of sustainable plant-soil ecosystems. In B Hock (Ed.). *The mycota*. Berlin, Heidelberg, Springer-Verlag, pp. 51-75.

Jeffries P, Gianinazzi S, Perotto S, Turnau K, Barea J-M. 2003. The contribution of arbuscular mycorrhizal fungi in sustainable maintenance of plant health and soil fertility. Biology and Fertility of Soils 37, 1–16. doi: 10.1007/s00374-002-0546-5

Jiang Q-Y, Zhuo F, Long S-H, Zhao H-D, Yang D-J, Ye Z-H, Li S-S, Jing Y-X. 2016. Can arbuscular mycorrhizal fungi reduce Cd uptake and alleviate Cd toxicity of *Lonicera japonica* grown in Cd-added soils? Scientific Reports 6, 21805. doi: 10.1038/srep21805

Jin H, Liu J, Liu J, Huang X. 2012. Forms of nitrogen uptake, translocation, and transfer via arbuscular mycorrhizal fungi: A review. Science China. Life Sciences 55, 474–482. doi: 10.1007/s11427-012-4330-y

Jin H, Pfeffer PE, Douds DD, Piotrowski E, Lammers PJ, Shachar-Hill Y. 2005. The uptake, metabolism, transport and transfer of nitrogen in an arbuscular mycorrhizal symbiosis. New Phytologist 168, 687–696. doi: 10.1111/j.1469-8137.2005.01536.x

Joner EJ, Briones R, Leyval C. 2000. Metal-binding capacity of arbuscular mycorrhizal mycelium. Plant and Soil 226, 227–234. doi: 10.1023/A:1026565701391

Joner EJ, Leyval C. 1997. Uptake of ^{109}Cd by roots and hyphae of a *Glomus mosseae*/*Trifolium subterraneum* mycorrhiza from soil amended with high and low concentrations of cadmium. New Phytologist 135, 353–360. doi: 10.1046/j.1469-8137.1997.00633.x

Joner EJ, Leyval C. 2001. Time-course of heavy metal uptake in maize and clover as affected by root density and different mycorrhizal inoculation regimes. Biology and Fertility of Soils 33, 351–357. doi: 10.1007/s003740000331

Jung SC, Martinez-Medina A, Lopez-Raez JA, Pozo MJ. 2012. Mycorrhiza-induced resistance and priming of plant defenses. Journal of Chemical Ecology 38, 651–664. doi: 10.1007/s10886-012-0134-6

Kaldorf M, Kuhn AJ, Schröder WH, Hildebrandt U, Bothe H. 1999. Selective element deposits in maize colonized by a heavy metal tolerance conferring arbuscular mycorrhizal fungus. Journal of Plant Physiology 154, 718–728. doi: 10.1016/S0176-1617(99)80250-8

Kikuchi Y, Hijikata N, Ohtomo R, Handa Y, Kawaguchi M, Saito K, Masuta C, Ezawa T. 2016. Aquaporin-mediated long-distance polyphosphate translocation directed towards the host in arbuscular mycorrhizal symbiosis: application of virus-induced gene silencing. New Phytologist 211, 1202–1208. doi: 10.1111/nph.14016

Kim SA, Guerinot ML. 2007. Mining iron: Iron uptake and transport in plants. FEBS Letters 581, 2273–2280. doi: 10.1016/j.febslet.2007.04.043

Kiranmayi P, Vijaya RK, Santyasyamala M, Nagamrutha M. 2014. Genome-wide identification of transition metal ion transporters in *Oryza sativa*. Journal of Rice Research 2, 124. doi: 10.4172/jrr.1000124

Knight SAB, Lesuisse E, Stearman R, Klausner RD, Dancis A. 2002. Reductive iron uptake by *Candida albicans*: role of copper, iron and the *TUP1* regulator. Microbiology 148, 29–40. doi: 10.1099/00221287-148-1-29

Kobae Y, Tamura Y, Takai S, Banba M, Hata S. 2010. Localized expression of arbuscular mycorrhiza-inducible ammonium transporters in soybean. Plant and Cell Physiology 51, 1411–1415. doi: 10.1093/pcp/pcq099

Kobae Y, Tomioka R, Tanoi K, Kobayashi NI, Ohmori Y, Nishida S, Fujiwara T. 2014. Selective induction of putative iron transporters, *OPT8a* and *OPT8b*, in maize by mycorrhizal colonization. Soil Science and Plant Nutrition 60, 843–847. doi: 10.1080/00380768.2014.949854

Koegel S, Lahmidi NA, Arnould C, Chatagnier O, Walder F, Ineichen K, Boller T, Wipf D, Wiemken A, Courty P-E. 2013. The family of ammonium transporters (AMT) in *Sorghum bicolor*: two AMT members are induced locally, but not

systemically in roots colonized by arbuscular mycorrhizal fungi. New Phytologist 198, 853–865. doi: 10.1111/nph.12199

Koltai H. 2014. Receptors, repressors, PINs: a playground for strigolactone signaling. Trends in Plant Science 19, 727–733. doi: 10.1016/j.tplants.2014.06.008

Kosuta S, Chabaud M, Lougnon G, Gough C, Dénarié J, Barker DG, Bécard G. 2003. A diffusible factor from arbuscular mycorrhizal fungi induces symbiosis-specific *MtENOD11* expression in roots of *Medicago truncatula*. Plant Physiology 131, 952–962. doi: 10.1104/pp.011882

Kothari SK, Marschner H, Römheld V. 1991. Contribution of the VA mycorrhizal hyphae in acquisition of phosphorus and zinc by maize grown in a calcareous soil. Plant and Soil 131, 177–185. doi: 10.1007/BF00009447

Kumánovics A, Chen OS, Li L, et al. 2008. Identification of *FRA1* and *FRA2* as genes involved in regulating the yeast iron regulon in response to decreased mitochondrial iron-sulfur cluster synthesis. The Journal of Biological Chemistry 283, 10276-10286. doi: 10.1074/jbc.M801160200

Kumar P, Lucini L, Rouphael Y, Cardarelli M, Kalunke RM, Colla G. 2015. Insight into the role of grafting and arbuscular mycorrhiza on cadmium stress tolerance in tomato. Frontiers in Plant Science 6, 477. doi: 10.3389/fpls.2015.00477

Lambert DH, Weidensaul TC. 1991. Element uptake by mycorrhizal soybean from sewage-sludge-treated soil. Soil Science Society of America Journal 55, 393–398. doi: 10.2136/sssaj1991.03615995005500020017x

Lanfranco L, Bolchi A, Ros EC, Ottonello S, Bonfante P. 2002. Differential expression of a metallothionein gene during the presymbiotic versus the symbiotic phase of an arbuscular mycorrhizal fungus. Plant Physiology 130, 58–67. doi: 10.1104/pp.003525

Larkin MA, Blackshields G, Brown NP, et al. 2007. Clustal W and Clustal X version 2.0. Bioinformatics 23, 2947–2948. doi: 10.1093/bioinformatics/btm404

Lee Y-J, George E. 2005. Contribution of mycorrhizal hyphae to the uptake of metal cations by cucumber plants at two levels of phosphorus supply. Plant and Soil 278, 361–370. doi: 10.1007/s11104-005-0373-1

Lee J, Young JPW. 2009. The mitochondrial genome sequence of the arbuscular mycorrhizal fungus *Glomus intraradices* isolate 494 and implications for the

phylogenetic placement of *Glomus*. New Phytologist 183, 200–211. doi: 10.1111/j.1469-8137.2009.02834.x

Lehmann A, Rillig MC. 2015. Arbuscular mycorrhizal contribution to copper, manganese and iron nutrient concentrations in crops – A meta-analysis. Soil Biology and Biochemistry 81, 147–158. doi: 10.1016/j.soilbio.2014.11.013

Li T, Hu YJ, Hao Z-P, Li H, Wang Y-S, Chen B-D. 2013. First cloning and characterization of two functional aquaporin genes from an arbuscular mycorrhizal fungus *Glomus intraradices*. New Phytologist 197, 617–630. doi: 10.1111/nph.12011

Li X, Christie P. 2001. Changes in soil solution Zn and pH and uptake of Zn by arbuscular mycorrhizal red clover in Zn-contaminated soil. Chemosphere 42, 201–207. doi: 10.1016/S0045-6535(00)00126-0

Li X-L, Marschner H, George E. 1991. Acquisition of phosphorus and copper by VA-mycorrhizal hyphae and root-to-shoot transport in white clover. Plant and Soil 136, 49–57. doi: 10.1007/BF02465219

Li ZS, Szczypka M, Lu YP, Thiele DJ, Rea PA. 1996. The yeast cadmium factor protein (YCF1) is a vacuolar glutathione S-conjugate pump. Journal of Biological Chemistry 271, 6509–6517. doi: 10.1074/jbc.271.11.6509

Lill R, Hoffmann B, Molik S, Pierik AJ, Rietzschel N, Stehling O, Uzarska MA, Webert H, Wilbrecht C, Mühlenhoff U. 2012. The role of mitochondria in cellular iron-sulfur protein biogenesis and iron metabolism. Biochimica et Biophysica Acta 1823, 1491–1508. doi:10.1016/j.bbamcr.2012.05.009

Lin K, Limpens E, Zhang Z, et al. 2014. Single nucleus genome sequencing reveals high similarity among nuclei of an endomycorrhizal fungus. PLoS genetics 10, e1004078. doi: 10.1371/journal.pgen.1004078

Lingua G, Bona E, Todeschini V, Cattaneo C, Marsano F, Berta G, Cavaletto M. 2012. Effects of heavy metals and arbuscular mycorrhiza on the leaf proteome of a selected poplar clone: a time course analysis. PLoS ONE 7, e38662. doi: 10.1371/journal.pone.0038662

Lingua G, Franchin C, Todeschini V, Castiglione S, Biondi S, Burlando B, Parravicini V, Torrigiani P, Berta G. 2008. Arbuscular mycorrhizal fungi differentially affect the response to high zinc concentrations of two registered poplar

clones. Environmental Pollution 153, 137–147. doi: 10.1016/j.envpol.2007.07.012

Liu A, Hamel C, Hamilton RI, Ma BL, Smith DL. 2000. Acquisition of Cu, Zn, Mn and Fe by mycorrhizal maize (*Zea mays* L.) grown in soil at different P and micronutrient levels. Mycorrhiza 9, 331–336. doi: 10.1007/s005720050277

Liu Y, Steenkamp ET, Brinkmann H, Forget L, Philippe H, Lang BF. 2009. Phylogenomic analyses predict sistergroup relationship of nucleariids and Fungi and paraphyly of zygomycetes with significant support. BMC Evolutionary Biology 9, 272. doi: 10.1186/1471-2148-9-272

Liu H, Trieu AT, Blaylock LA, Harrison MJ. 1998. Cloning and characterization of two phosphate transporters from *Medicago truncatula* roots: regulation in response to phosphate and to colonization by arbuscular mycorrhizal (AM) fungi. Molecular Plant-Microbe Interactions 11, 14–22. doi: 10.1094/MPMI.1998.11.1.14

Liu Y, Zhu YG, Chen BD, Christie P, Li XL. 2005. Influence of the arbuscular mycorrhizal fungus *Glomus mosseae* on uptake of arsenate by the As hyperaccumulator fern *Pteris vittata* L. Mycorrhiza 15, 187–192. doi: 10.1007/s00572-004-0320-7

López-Pedrosa A, González-Guerrero M, Valderas A, Azcón-Aguilar C, Ferrol N. 2006. *GintAMT1* encodes a functional high-affinity ammonium transporter that is expressed in the extraradical mycelium of *Glomus intraradices*. Fungal Genetics and Biology 43, 102–110. doi: 10.1016/j.fgb.2005.10.005

Mäder P, Vierheilig H, Streitwolf-Engel R, Boller T, Frey B, Christie P, Wiemken A. 2000. Transport of ^{15}N from a soil compartment separated by a polytetrafluoroethylene membrane to plant roots via the hyphae of arbuscular mycorrhizal fungi. New Phytologist 146, 155–161. doi: 10.1046/j.1469-8137.2000.00615.x

Maillet F, Poinsot V, André O, et al. 2011. Fungal lipochitooligosaccharide symbiotic signals in arbuscular mycorrhiza. Nature 469, 58–64. doi: 10.1038/nature09622

Malbreil M, Tisserant E, Martin F, Roux C. 2014. Genomics of arbuscular mycorrhizal fungi: out of the shadows. In: *Advances in Botanical Research* 70, pp. 259–290. doi: 10.1016/B978-0-12-397940-7.00009-4

Maldonado-Mendoza IE, Dewbre GR, Harrison MJ. 2001. A phosphate transporter gene from the extra-radical mycelilum of an arbuscular mycorrhizal fungus *Glomus intraradices* is regulated in response to phosphate in the environment. Molecular Plant-Microbe Interactions 14, 1140–1148. doi: 10.1094/MPMI.2001.14.10.1140

Manck-Götzenberger J, Requena N. 2016. *Arbuscular mycorrhiza* symbiosis induces a major transcriptional reprogramming of the potato *SWEET* sugar transporter family. Frontiers in Plant Science 7, 487. doi: 10.3389/fpls.2016.00487

Manjunath A, Habte M. 1988. Development of vesicular-arbuscular mycorrhizal infection and the uptake of immobile nutrients in *Leucaena leucocephala*. Plant and Soil 106, 97–103. doi: 10.1007/BF02371200

Marschner H, Dell B. 1994. Nutrient uptake in mycorrhizal symbiosis. Plant and Soil 159, 89–102. doi: 10.1007/BF00000098

Martin F, Tuskan GA, DiFazio SP, Lammers P, Newcombe G, Podila GK. 2004. Symbiotic sequencing for the *Populus* mesocosm. New Phytologist 161, 330–335. doi: 10.1111/j.1469-8137.2004.00982.x

Mäser P, Thomine S, Schroeder JI, et al. 2001. Phylogenetic relationships within cation transporter families of *Arabidopsis*. Plant Physiology 126, 1646–1667. doi: 10.1104/pp.126.4.1646

Meier S, Azcón R, Cartes P, Borie F, Cornejo P. 2011. Alleviation of Cu toxicity in *Oenothera picensis* by copper-adapted arbuscular mycorrhizal fungi and treated agrowaste residue. Applied Soil Ecology 48, 117–124. doi: 10.1016/j.apsoil.2011.04.005

Meier S, Borie F, Bolan N, Cornejo P. 2012. Phytoremediation of metal-polluted soils by arbuscular mycorrhizal fungi. Critical Reviews in Environmental Science and Technology 42, 741–775. doi: 10.1080/10643389.2010.528518

Minet M, Dufour M, Lacroute F. 1992. Complementation of *Saccharomyces cerevisiae* auxotrophic mutants by *Arabidopsis thaliana* cDNAs. The Plant Journal 2, 417–422. doi: 10.1046/j.1365-313X.1992.t01-38-00999.x

Moscatiello R, Sello S, Novero M, Negro A, Bonfante P, Navazio L. 2014. The intracellular delivery of TAT-aequorin reveals calcium- mediated sensing of environmental and symbiotic signals by the arbuscular mycorrhizal fungus *Gigaspora margarita*. New Phytologist 203, 1012–1020. doi: 10.1111/nph.12849

Mühlenhoff U, Molik S, Godoy JR, et al. 2010. Cytosolic monothiol glutaredoxins function in intracellular iron sensing and trafficking via their bound iron-sulfur cluster. Cell Metabolism 12, 373–385. doi: 10.1016/j.cmet.2010.08.001

Nadal M, Paszkowski U. 2013. Polyphony in the rhizosphere: presymbiotic communication in arbuscular mycorrhizal symbiosis. Current Opinion in Plant Biology 16, 473-479. doi: 10.1016/j.pbi.2013.06.005

Nagahashi G, Douds DD Jr. 2011. The effects of hydroxy fatty acids on the hyphal branching of germinated spores of AM fungi. Fungal Biology 115, 351–358. doi: 10.1016/j.funbio.2011.01.006

Nagahashi G, Douds DD, Ferhatoglu Y (2010) Functional categories of root exudate compounds and their relevance to AM fungal growth. *In*: H. Koltai and Y.Kapulnik [eds.]. *Arbuscular Mycorrhizas: Physiology and Function*. Springer, The Netherlands, pp. 33-56. doi: 10.1007/978-90-481-9489-6

Nayuki K, Chen B, Ohtomo R, Kuga Y. 2014. Cellular imaging of cadmium in resin sections of arbuscular mycorrhizas using synchrotron micro X-ray fluorescence. Microbes and Environments 29, 60–66. doi: 10.1264/jsme2.ME13093

Oberegger H, Schoeser M, Zadra I, Schrettl M, Parson W, Haas H. 2002. Regulation of *freA*, *acoA*, *lysF*, and *cycA* expression by iron availability in *Aspergillus nidulans*. Applied and Environmental Microbiology 68, 5769–5772. doi: 10.1128/AEM.68.11.5769-5772.2002

Oehl F, Sieverding E, Palenzuela J, Ineichen K, Alves da Silva G. 2011. Advances in *Glomeromycota* taxonomy and classification. IMA Fungus 2, 191–199. doi: 10.5598/imafungus.2011.02.02.10

Öpik M, Zobel M, Cantero JJ, et al. 2013. Global sampling of plant roots expands the described molecular diversity of arbuscular mycorrhizal fungi. Mycorrhiza 23, 411–430. doi: 10.1007/s00572-013-0482-2

Outten CE, Albetel A-N. 2013. Iron sensing and regulation in *Saccharomyces cerevisiae*: Ironing out the mechanistic details. Current Opinion in Microbiology 16, 662–668. doi: 10.1016/j.mib.2013.07.020

Ouziad F, Hildebrandt U, Schmelzer E, Bothe H. 2005. Differential gene expressions in arbuscular mycorrhizal-colonized tomato grown under heavy metal stress. Journal of Plant Physiology 162, 634–649. doi: 10.1016/j.jplph.2004.09.014

Pallara G, Todeschini V, Lingua G, Camussi A, Racchi ML. 2013. Transcript analysis of stress defence genes in a white poplar clone inoculated with the arbuscular mycorrhizal fungus *Glomus mosseae* and grown on a polluted soil. Plant Physiology and Biochemistry 63, 131–139. doi: 10.1016/j.plaphy.2012.11.016

Palmer C, Guerinot ML. 2009. A question of balance: Facing the challenges of Cu, Fe and Zn homeostasis. Nature Chemical Biology 5, 333–340. doi: 10.1038/nchembio.166

Park Y-S, Kim J-H, Cho J-H, Chang H-I, Kim S-W, Paik H-D, Kang C-W, Kim T-H, Sung H-C, Yun C-W. 2007. Physical and functional interaction of FgFtr1-FgFet1 and FgFtr2-FgFet2 is required for iron uptake in *Fusarium graminearum*. The Biochemical Journal 408, 97–104. doi: 10.1042/BJ20070450

Parniske M. 2008. Arbuscular mycorrhiza: the mother of plant root endosymbioses. Nature Reviews. Microbiology 6, 763-775. doi: 10.1038/nrmicro1987

Pawlowska TE. 2005. Genetic processes in arbuscular mycorrhizal fungi. FEMS Microbiology Letters 251, 185–192. doi: 10.1016/j.femsle.2005.08.007

Pawlowska TE, Taylor JW. 2004. Organization of genetic variation in individuals of arbuscular mycorrhizal fungi. Nature 427, 733–737. doi: 10.1038/nature02290

Pellegrino E, Bedini S. 2014. Enhancing ecosystem services in sustainable agriculture: Biofertilization and biofortification of chickpea (*Cicer arietinum* L.) by arbuscular mycorrhizal fungi. Soil Biology and Biochemistry 68, 429–439. doi: 10.1016/j.soilbio.2013.09.030

Pérez-Tienda J, Corrêa A, Azcón-Aguilar C, Ferrol N. 2014. Transcriptional regulation of host NH_4^+ transporters and GS/GOGAT pathway in arbuscular mycorrhizal rice roots. Plant Physiology and Biochemistry 75, 1–8. doi: 10.1016/j.plaphy.2013.11.029

Pérez-Tienda J, Testillano PS, Balestrini R, Fiorilli V, Azcón-Aguilar C, Ferrol N. 2011. GintAMT2, a new member of the ammonium transporter family in the arbuscular mycorrhizal fungus *Glomus intraradices*. Fungal Genetics and Biology 48, 1044–1055. doi: 10.1016/j.fgb.2011.08.003

Perrier N, Amir H, Colin F. 2006. Occurrence of mycorrhizal symbioses in the metal-rich lateritic soils of the Koniambo Massif, New Caledonia. Mycorrhiza 16, 449–458. doi: 10.1007/s00572-006-0057-6

Pfeffer PE, Douds Jr DD, Bécard G, Shachar-Hill Y. 1999. Carbon uptake and the metabolism and transport of lipids in an arbuscular mycorrhiza. Plant Physiology 120, 587–598. doi: 10.1104/pp.120.2.587

Pongrac P, Sonjak S, Vogel-Mikuš K, Kump P, Necemer M, Regvar M. 2009. Roots of metal hyperaccumulating population of *Thlaspi praecox* (Brassicaceae) harbour arbuscular mycorrhizal and other fungi under experimental conditions. International Journal of Phytoremediation 11, 347–359. doi: 10.1080/15226510802565527

Porcel R, Aroca R, Azcon R, Ruiz-Lozano JM. 2016. Regulation of cation transporter genes by the arbuscular mycorrhizal symbiosis in rice plants subjected to salinity suggests improved salt tolerance due to reduced Na^+ root-to-shoot distribution. Mycorrhiza 26, 673–684. doi: 10.1007/s00572-016-0704-5

Porcel R, Aroca R, Ruiz-Lozano JM. 2012. Salinity stress alleviation using arbuscular mycorrhizal fungi. A review. Agronomy for Sustainable Development 32, 181–200. doi: 10.1007/s13593-011-0029-x

Pozo MJ, Azcón-Aguilar C. 2007. Unraveling mycorrhiza-induced resistance. Current Opinion in Plant Biology 10, 393–398. doi: 10.1016/j.pbi.2007.05.004

Pozo MJ, Verhage A, García-Andrade J, García JM, Azcón-Aguilar C. 2009. Priming plant defence against pathogens by arbuscular mycorrhizal fungi. *In:* C. Azcón-Aguilar, J.M. Barea, S. Gianinazzi and V. Gianinazzi-Pearson [eds.]. *Mycorrhizas Functional Processes and Ecological Impact*. Springer-Verlag, Berlín, Heidelberg. pp. 123-135. doi: 10.1007/978-3-540-87978-7

Pozo MJ, Jung SC, López-Ráez JA, Azcón-Aguílar C. 2010. Impact of arbuscular mycorrhizal symbiosis on plant response to biotic stress: The role of plant defence mechanisms. *In:* H. Koltai and Y.Kapulnik [eds.]. *Arbuscular Mycorrhizas: Physiology and Function*. Springer, The Netherlands, pp. 193-207. doi: 10.1007/978-90-481-9489-6_9

Puig S, Peñarrubia L. 2009. Placing metal micronutrients in context: transport and distribution in plants. Current Opinion in Plant Biology 12, 299–306. doi: 10.1016/j.pbi.2009.04.008

Redecker D, Kodner R, Graham LE. 2000. Glomalean fungi from the Ordovician. Science 289, 1920–1921. doi: 10.1126/science.289.5486.1920

Redecker D, Schüßler A, Stockinger H, Stürmer SL, Morton JB, Walker C. 2013. An evidence-based consensus for the classification of arbuscular mycorrhizal fungi (*Glomeromycota*). Mycorrhiza 23, 515–531. doi: 10.1007/s00572-013-0486-y

Regvar M, Vogel K, Irgel N, Wraber T, Hildebrandt U, Wilde P, Bothe H. 2003. Colonization of pennycresses (*Thlaspi* spp.) of the Brassicaceae by arbuscular mycorrhizal fungi. Journal of Plant Physiology 160, 615–626. doi: 10.1078/0176-1617-00988

Rentsch D, Laloi M, Rouhara I, Schmelzer E, Delrot S, Frommer WB. 1995. *NTR1* encodes a high affinity oligopeptide transporter in *Arabidopsis*. FEBS Letters 370, 264–268. doi: 10.1016/0014-5793(95)00853-2

Repetto O, Bestel-Corre G, Dumas-Gaudot E, Berta G, Gianinazzi-Pearson V, Gianinazzi S. 2003. Targeted proteomics to identify cadmium-induced protein modifications in *Glomus mosseae*-inoculated pea roots. New Phytologist 157, 555–567. doi: 10.1046/j.1469-8137.2003.00682.x

Riley R, Charron P, Idnurm A, Farinelli L, Dalpé Y, Martin F, Corradi N. 2014. Extreme diversification of the mating type–high-mobility group (*MATA-HMG*) gene family in a plant-associated arbuscular mycorrhizal fungus. New Phytologist 201, 254–268. doi: 10.1111/nph.12462

Riley R, Corradi N. 2013. Searching for clues of sexual reproduction in the genomes of arbuscular mycorrhizal fungi. Fungal Ecology 6, 44–49. doi: 10.1016/j.funeco.2012.01.010

Rivera-Becerril F, van Tuinen D, Martin-Laurent F, Metwally A, Dietz K-J, Gianinazzi S, Gianinazzi-Pearson V. 2005. Molecular changes in *Pisum sativum* L. roots during arbuscular mycorrhiza buffering of cadmium stress. Mycorrhiza 16, 51–60. doi: 10.1007/s00572-005-0016-7

Ropars J, Corradi N. 2015. Homokaryotic vs heterokaryotic mycelium in arbuscular mycorrhizal fungi: different techniques, different results? New Phytologist 208, 638–641. doi: 10.1111/nph.13448

Ropars J, Toro KS, Noel J, et al. 2016. Evidence for the sexual origin of heterokaryosis in arbuscular mycorrhizal fungi. Nature Microbiology 1, 16033. doi: 10.1038/nmicrobiol.2016.33

Ruíz-Lozano JM, Perálvarez MdC, Aroca R, Azcón R. 2011. The application of a treated sugar beet waste residue to soil modifies the responses of mycorrhizal and non mycorrhizal lettuce plants to drought stress. Plant and Soil 346, 153. doi: 10.1007/s11104-011-0805-z

Ruiz-Sánchez M, Aroca R, Muñoz Y, Polón R, Ruiz-Lozano JM. 2010. The arbuscular mycorrhizal symbiosis enhances the photosynthetic efficiency and the antioxidative response of rice plants subjected to drought stress. Journal of Plant Physiology 167, 862–869. doi: 10.1016/j.jplph.2010.01.018

Ruth B, Khalvati M, Schmidhalter U. 2011. Quantification of mycorrhizal water uptake via high-resolution on-line water content sensors. Plant and Soil 342, 459–468. doi: 10.1007/s11104-010-0709-3

Ruyter-Spira C, Al-Babili S, van der Krol S, Bouwmeester H. 2013. The biology of strigolactones. Trends in Plant Science 18, 72–83. doi: 10.1016/j.tplants.2012.10.003

Ryan MH, Angus JF. 2003. Arbuscular mycorrhizae in wheat and field pea crops on a low P soil: increased Zn-uptake but no increase in P-uptake or yield. Plant and Soil 250, 225–239. doi: 10.1023/A:1022839930134

Salvioli A, Ghignone S, Novero M, Navazio L, Venice F, Bagnaresi P, Bonfante P. 2016. Symbiosis with an endobacterium increases the fitness of a mycorrhizal fungus, raising its bioenergetic potential. The ISME Journal 10, 130–144. doi: 10.1038/ismej.2015.91

Sanders IR. 1999. Evolutionary genetics: No sex please, we're fungi. Nature 399, 737–739. doi: 10.1038/21544

Schiestl RH, Gietz RD. 1989. High efficiency transformation of intact yeast cells using single stranded nucleic acids as a carrier. Current Genetics 16, 339–346. doi: 10.1007/BF00340712

Schmittgen TD, Livak KJ. 2008. Analyzing real-time PCR data by the comparative C_T method. Nature Protocols 3, 1101–1108. doi: 10.1038/nprot.2008.73

Schüßler A, Walker C. 2010. *The Glomeromycota: a species list with new families and new genera*. Gloucester, UK: The Royal Botanic Garden Edinburgh, The Royal Botanic Garden Kew, Botanische St.

Schüßler A, Schwarzott D, Walker C. 2001. A new fungal phylum, the *Glomeromycota*: phylogeny and evolution. Mycological Research 105, 1413–1421. doi: 10.1017/S0953756201005196

Sędzielewska KA, Fuchs J, Temsch EM, Baronoian K, Watzke R, Kunze G. 2011. Estimation of the *Glomus intraradices* nuclear DNA content. New Phytologist 192, 794–797. doi: 10.1111/j.1469-8137.2011.03937.x

Shachar-Hill Y, Pfeffer PE, Douds D, Osman SF, Doner LW, Ratcliffe RG. 1995. Partitioning of intermediary carbon metabolism in vesicular-arbuscular mycorrhizal leek. Plant Physiology 108, 7–15. doi: 10.1104/pp.108.1.7

Sheikh-Assadi M, Khandan-Mirkohi A, Alemardan A, Moreno-Jiménez E. 2015. Mycorrhizal *Limonium sinuatum* (L.) mill. enhances accumulation of lead and cadmium. International Journal of Phytoremediation 17, 556–562. doi: 10.1080/15226514.2014.922928

Sheng M, Tang M, Zhang F, Huang Y. 2011. Influence of arbuscular mycorrhiza on organic solutes in maize leaves under salt stress. Mycorrhiza 21, 423–430. doi: 10.1007/s00572-010-0353-z

Shine AM, Shakya VP, Idnurm A. 2015. Phytochelatin synthase is required for tolerating metal toxicity in a basidiomycete yeast and is a conserved factor involved in metal homeostasis in fungi. Fungal Biology and Biotechnology 2, 1–21. doi: 10.1186/s40694-015-0013-3

Sieh D, Watanabe M, Devers EA, Brueckner F, Hoefgen R, Krajinski F. 2013. The arbuscular mycorrhizal symbiosis influences sulfur starvation responses of *Medicago truncatula*. New Phytologist 197, 606–616. doi: 10.1111/nph.12034

Smith SE, Facelli E, Pope S, Smith FA. 2010. Plant performance in stressful environments: interpreting new and established knowledge of the roles of arbuscular mycorrhizas. Plant Soil 326, 3-20. doi: 10.1007/s11104-009-9981-5

Smith SE, Read DJ. 2008. *Mycorrhizal symbiosis* (Third edition). London: Academic Press.

Smith SE, Smith FA. 2012. Fresh perspectives on the roles of arbuscular mycorrhizal fungi in plant nutrition and growth. Mycologia 104, 1–13. doi: 10.3852/11-229

Smith SE, Smith FA, Jakobsen I. 2004. Functional diversity in arbuscular mycorrhizal (AM) symbioses: the contribution of the mycorrhizal P uptake pathway is not

correlated with mycorrhizal responses in growth or total P uptake. New Phytologist 162, 511–524. doi: 10.1111/j.1469-8137.2004.01039.x

Solaiman MZ, Saito M. 1997. Use of sugars by intraradical hyphae of arbuscular mycorrhizal fungi revealed by radiorespirometry. New Phytologist 136, 533–538. doi: 10.1046/j.1469-8137.1997.00757.x

St-Arnaud M, Hamel C, Vimard B, Caron M, Fortin JA. 1996. Enhanced hyphal growth and spore production of the arbuscular mycorrhizal fungus *Glomus intraradices* in an *in vitro* system in the absence of host roots. Mycological Research 100, 328–332. doi: 10.1016/S0953-7562(96)80164-X

Stearman R, Yuan DS, Yamaguchi-iwai Y, Klausner RD, Dancis A. 1996. A permease-oxidase complex involved in high-affinity iron uptake in yeast. Science 271, 1552–1557. doi: 10.1126/science.271.5255.1552

Stürmer SL. 2012. A history of the taxonomy and systematics of arbuscular mycorrhizal fungi belonging to the phylum Glomeromycota. Mycorrhiza 22, 247–258. doi: 10.1007/s00572-012-0432-4

Subramanian KS, Balakrishnan N, Senthil N. 2013. Mycorrhizal symbiosis to increase the grain micronutrient content in maize. Australian Journal of Crop Science 7, 900–910.

Tamura K, Stecher G, Peterson D, Filipski A, Kumar S. 2013. MEGA6: Molecular evolutionary genetics analysis version 6.0. Molecular Biology and Evolution 30, 2725–2729. doi: 10.1093/molbev/mst197

Tang N, San Clemente H, Roy S, Bécard G, Zhao B, Roux C. 2016. A survey of the gene repertoire of *Gigaspora rosea* unravels conserved features among Glomeromycota for obligate biotrophy. Frontiers in Microbiology 7, 233. doi: 10.3389/fmicb.2016.00233

Thompson JP. 1990. Soil sterilization methods to show VA-mycorrhizae aid P and Zn nutrition of wheat in vertisols. Soil Biology and Biochemistry 22, 229–240. doi: 10.1016/0038-0717(90)90092-E

Tian C, Kasiborski B, Koul R, Lammers PJ, Bücking H, Shachar-Hill Y. 2010. Regulation of the nitrogen transfer pathway in the arbuscular mycorrhizal symbiosis: gene characterization and the coordination of expression with nitrogen flux. Plant Physiology 153, 1175–1187. doi: 10.1104/pp.110.156430

Tisserant E, Kohler A, Dozolme-Seddas P, et al. 2012. The transcriptome of the arbuscular mycorrhizal fungus *Glomus intraradices* (DAOM 197198) reveals functional tradeoffs in an obligate symbiont. New Phytologist 193, 755–769. doi: 10.1111/j.1469-8137.2011.03948.x

Tisserant E, Malbreil M, Kuo A, et al. 2013. Genome of an arbuscular mycorrhizal fungus provides insight into the oldest plant symbiosis. Proceedings of the National Academy of Sciences 110, 20117–20122. doi: 10.1073/pnas.1313452110

Toussaint J-P, St-Arnaud M, Charest C. 2004. Nitrogen transfer and assimilation between the arbuscular mycorrhizal fungus *Glomus intraradices* Schenck & Smith and Ri T-DNA roots of *Daucus carota* L. in an *in vitro* compartmented system. Canadian Journal of Microbiology 50, 251–260. doi: 10.1139/w04-009

Tsuzuki S, Handa Y, Takeda N, Kawaguchi M. 2016. Strigolactone-induced putative secreted protein 1 is required for the establishment of symbiosis by the arbuscular mycorrhizal fungus *Rhizophagus irregularis*. Molecular Plant-Microbe Interactions 29, 277–286. doi: 10.1094/MPMI-10-15-0234-R

Tulasne LR, Tulasne C. 1845. Fungi nonnulli hypogaei, novi minus cogniti. Giornale Botanico Italiano 2, 35–63.

Tullio M, Pierandrei F, Salerno A, Rea E. 2003. Tolerance to cadmium of vesicular arbuscular mycorrhizae spores isolated from a cadmium-polluted and unpolluted soil. Biology and Fertility of Soils 37, 211–214. doi: 10.1007/s00374-003-0580-y

Turnau K. 1998. Heavy metal content and localization in mycorrhizal *Euphorbia cyparissias* from zinc wastes in southern Poland. Acta Societatis Botanicorum Poloniae 67, 105–113.

Turnau K, Kottke I, Oberwinkler F. 1993. Element localization in mycorrhizal roots of *Pteridium aquilinum* (L.) Kuhn collected from experimental plots treated with cadmium dust. New Phytologist 123, 313–324. doi: 10.1111/j.1469-8137.1993.tb03741.x

Turnau K, Mesjasz-Przybyłowicz J. 2003. Arbuscular mycorrhiza of *Berkheya coddii* and other Ni-hyperaccumulating members of Asteraceae from ultramafic soils in South Africa. Mycorrhiza 13, 185–190. doi: 10.1007/s00572-002-0213-6

Ultra VU, Tanaka S, Sakurai K, Iwasaki K. 2007. Effects of arbuscular mycorrhiza and phosphorus application on arsenic toxicity in sunflower (*Helianthus annuus* L.) and on the transformation of arsenic in the rhizosphere. Plant and Soil 290, 29–41. doi: 10.1007/s11104-006-9087-2

Urbanowski JL, Piper RC. 1999. The iron transporter Fth1p forms a complex with the Fet5 iron oxidase and resides on the vacuolar membrane. The Journal of Biological Chemistry 274, 38061–38070. doi: 10.1074/jbc.274.53.38061

Vasconcelos MW, Li GW, Lubkowitz MA, Grusak MA. 2008. Characterization of the PT clade of oligopeptide transporters in rice. The Plant Genome 1, 77–88. doi: 10.3835/plantgenome2007.10.0540

Vatansever R, Ozyigit II, Filiz E. 2016. Genome-Wide identification and comparative analysis of copper transporter genes in plants. Interdisciplinary Sciences: Computational Life Sciences, 1–14. doi: 10.1007/s12539-016-0150-2

Viehweger K. 2014. How plants cope with heavy metals. Botanical Studies 55, 1–12. doi: 10.1186/1999-3110-55-35

Vogel-Mikuš K, Drobne D, Regvar M. 2005. Zn, Cd and Pb accumulation and arbuscular mycorrhizal colonisation of pennycress *Thlaspi praecox* Wulf. (Brassicaceae) from the vicinity of a lead mine and smelter in Slovenia. Environmental Pollution 133, 233–242. doi: 10.1016/j.envpol.2004.06.021

Walder F, Brulé D, Koegel S, Wiemken A, Boller T, Courty P-E. 2015. Plant phosphorus acquisition in a common mycorrhizal network: regulation of phosphate transporter genes of the Pht1 family in sorghum and flax. New Phytologist 205, 1632–1645. doi: 10.1111/nph.13292

Waschke A, Sieh D, Tamasloukht M, Fischer K, Mann P, Franken P. 2006. Identification of heavy metal-induced genes encoding glutathione S-transferases in the arbuscular mycorrhizal fungus *Glomus intraradices*. Mycorrhiza 17, 1–10. doi: 10.1007/s00572-006-0075-4

Watts-Williams SJ, Cavagnaro TR. 2014. Nutrient interactions and arbuscular mycorrhizas: a meta-analysis of a mycorrhiza-defective mutant and wild-type tomato genotype pair. Plant and Soil 384, 79–92. doi: 10.1007/s11104-014-2140-7

Watts-Williams SJ, Patti AF, Cavagnaro TR. 2013. Arbuscular mycorrhizas are beneficial under both deficient and toxic soil zinc conditions. Plant and Soil 371, 299–312. doi: 10.1007/s11104-013-1670-8

Watts-Williams SJ, Smith FA, McLaughlin MJ, Patti AF, Cavagnaro TR. 2015. How important is the mycorrhizal pathway for plant Zn uptake? Plant and Soil 390, 157–166. doi: 10.1007/s11104-014-2374-4

Wewer V, Brands M, Dörmann P. 2014. Fatty acid synthesis and lipid metabolism in the obligate biotrophic fungus *Rhizophagus irregularis* during mycorrhization of *Lotus japonicus*. The Plant Journal 79, 398–412. doi: 10.1111/tpj.12566

White PJ, Broadley MR. 2009. Biofortification of crops with seven mineral elements often lacking in human diets–iron, zinc, copper, calcium, magnesium, selenium and iodine. New Phytologist 182, 49–84. doi: 10.1111/j.1469-8137.2008.02738.x

Wintz H, Fox T, Wu Y-Y, Feng V, Chen W, Chang H-S, Zhu T, Vulpe C. 2003. Expression profiles of *Arabidopsis thaliana* in mineral deficiencies reveal novel transporters involved in metal homeostasis. Journal of Biological Chemistry 278, 47644–47653. doi: 10.1074/jbc.M309338200

Wright SF, Upadhyaya A. 1996. Extraction of an abundant and unusual protein from soil and comparison with hyphal protein of arbuscular mycorrhizal fungi. Soil Science 161, 575–586. doi: 10.1097/00010694-199609000-00003

Wu S, Zhang X, Chen B, Wu Z, Li T, Hu Y, Sun Y, Wang Y. 2016. Chromium immobilization by extraradical mycelium of arbuscular mycorrhiza contributes to plant chromium tolerance. Environmental and Experimental Botany 122, 10–18. doi: 10.1016/j.envexpbot.2015.08.006

Yao Q, Yang R, Long L, Zhu H. 2014. Phosphate application enhances the resistance of arbuscular mycorrhizae in clover plants to cadmium *via* polyphosphate accumulation in fungal hyphae. Environmental and Experimental Botany 108, 63–70. doi: 10.1016/j.envexpbot.2013.11.007

Young JPW. 2015. Genome diversity in arbuscular mycorrhizal fungi. Current Opinion in Plant Biology 26, 113–119. doi: 10.1016/j.pbi.2015.06.005

Zhou X, Li S, Zhao Q, Liu X, Zhang S, Sun C, Fan Y, Zhang C, Chen R. 2013. Genome-wide identification, classification and expression profiling of nicotianamine

synthase (NAS) gene family in maize. BMC Genomics 14, 238. doi: 10.1186/1471-2164-14-238

Ziegler L, Terzulli A, Gaur R, McCarthy R, Kosman DJ. 2011. Functional characterization of the ferroxidase, permease high-affinity iron transport complex from *Candida albicans*. Molecular Microbiology 81, 473–485. doi: 10.1111/j.1365-2958.2011.07704.x